Final Design Review Report

Constructive Interference Inducer for an Overtopping Ocean Wave Energy Device

Submitted to:
Professor Guillermo Paniagua Perez

Submitted by:
Colton Doherty
Jack Burke
Matt Pugsley
Odette Kuehn
Cyrus Blackmore
Amanda Mudd

April 27, 2021

Contents

Executive Summary 3
Appendix A: Team Members and Organization Structure 9
Appendix B: Charter 10
Appendix C: Business Case & Project Budget 11
Market Research 11
Business Case Focused on Scaled Down Testing Rig 13
Appendix D: Network Diagram and Project Schedule 18
Appendix E: Risk Mitigation 21
Appendix F: Sketches & Design Development 22
Preliminary Design 22
Overall Assembly 25
Overtopping Device 26
Wave Gates 38
Wave Deflectors 40
Appendix G: Mechanical CAD 43
CDR CAD 43
Whole Assembly 44
Frame 48
Overtopping Device 48
Wave Gates 50
Wave Deflectors 51
Wiring 53
Appendix H: Engineering Analysis 54
Principal Analysis 54
Flow Sensor Research & Calculations 60
Static Analysis on Overtopping Device Reservoirs 62
Frame Length Dimension Calculation 63
Motor Torque Requirement Calculation 65
Force of Waves Calculation 67
Internal Stress on Wave Gate/Deflector Plate 70
Force on Rack and Pinion Gear Teeth 71

Iterative Design Spreadsheet 72
Appendix I: Mechanical CAE 74
Input Conditions for FEA 74
SolidWorks FEA 77
Displacement Analysis from FEA Results 83
Dimensional Analysis for Wave Parameters 86
CFD Software & Process 88
CFD Results 90
Future CFD & Testing 95
Appendix J: Electronic Schematics and Controls 96
Appendix K: Manufacturing Drawings & Process 101
Bar Cuts 101
Water Jet Cuts 101
Critical Fits and Tolerances 102
Assembly Steps 104
Manufacturing Drawings 106
Appendix L: Validation Plan & Results 164
Appendix M: What was learned from the prototypes and validation 166
Low-fidelity Prototype 166
Mid-Fidelity Prototype 167
High-Fidelity Prototype and Testing 168
Appendix N: List of Standards Referenced 169
Appendix O: Sources 170
Appendix P: Acknowledgments 173

Executive Summary

US ocean wave energy has the potential to provide 64% of total US energy consumption (U.S. Energy Information Administration, 2020). Currently, there is no single well accepted design for wave energy converters (WECs) because many existing designs are not economically viable and do not produce consistent energy. Existing types of WECs including point absorbers, oscillating water columns, and overtopping devices. In overtopping devices, waves run up the ramps and fall into reservoirs to drive a turbine. Current overtopping devices are not economically viable due to their low efficiencies.

The proposed design, Figure 1, is a scaled-down test rig focused on increasing wave height at the reservoirs of an overtopping WEC through constructive interference to improve efficiency and power output. The innovative features of the design include wave deflectors and gates that orient reflected waves from the overtopping device and incoming waves together to achieve constructive interference, shown by the wave path in Figure 4. This test rig will be used in wave pools to determine the optimal geometry of the innovative features based on the specific full-scale device location wave parameters. Test rig wave gates and deflectors can be adjusted to determine configurations that produce the highest efficiency; however, once employed in a full-scale overtopping device, these features will be stationary in the geometry determined by the test rig.

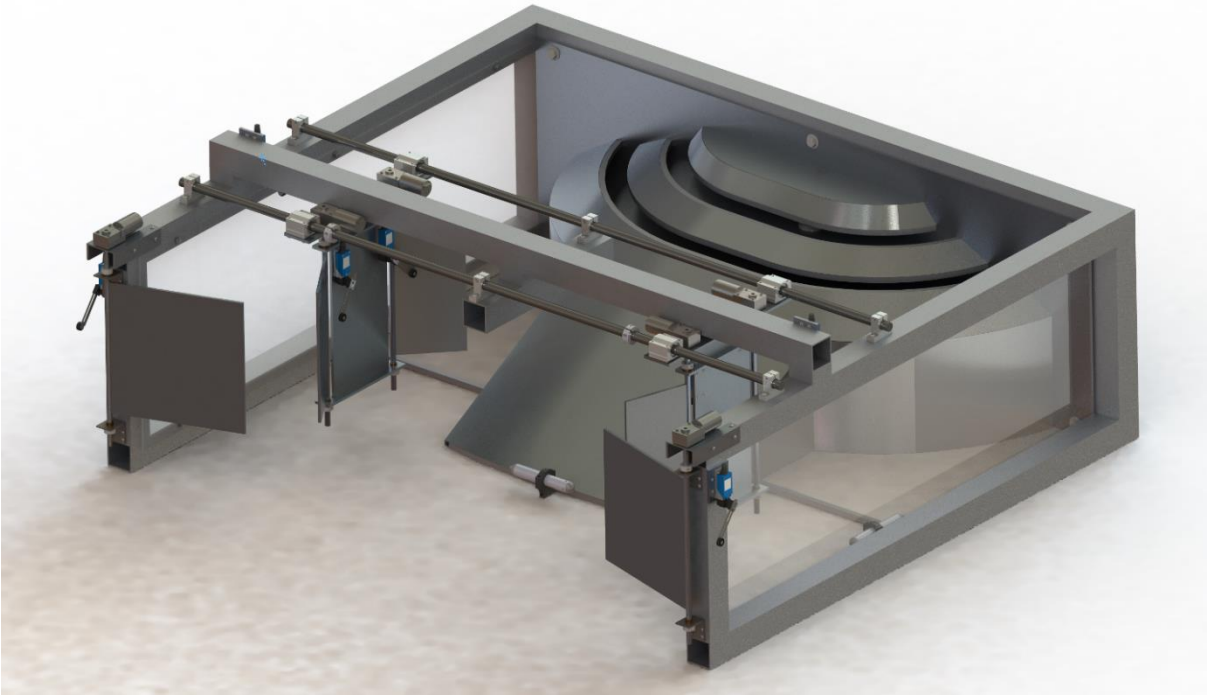

Figure 1: Overtopping Test Rig – Isometric View

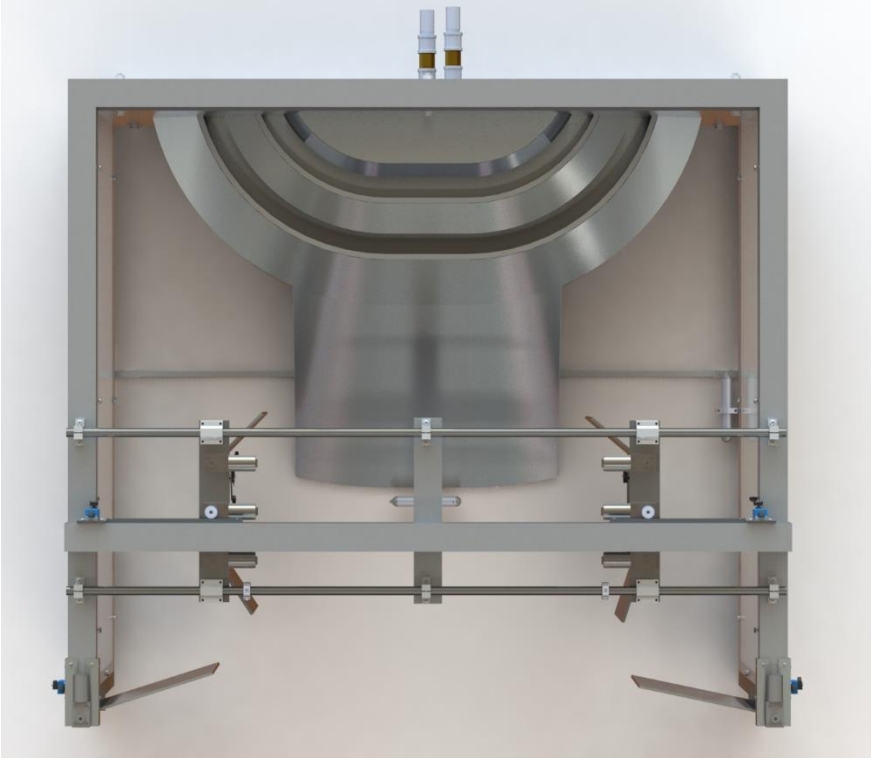

Figure 2: Overtopping Test Rig - Top View

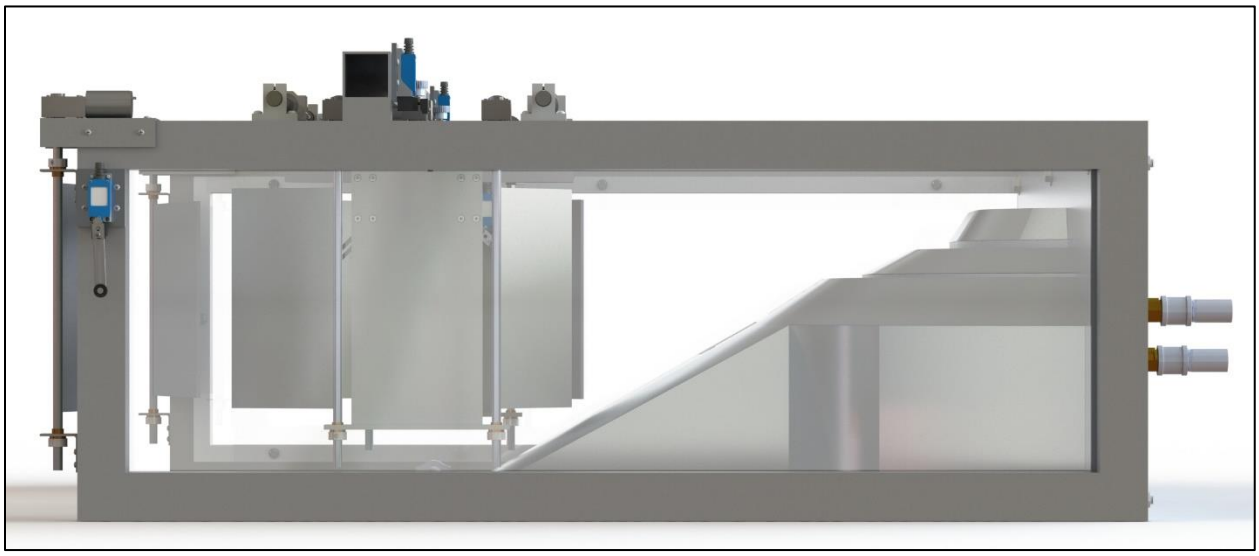

Figure 3: Overtopping Test – Side View

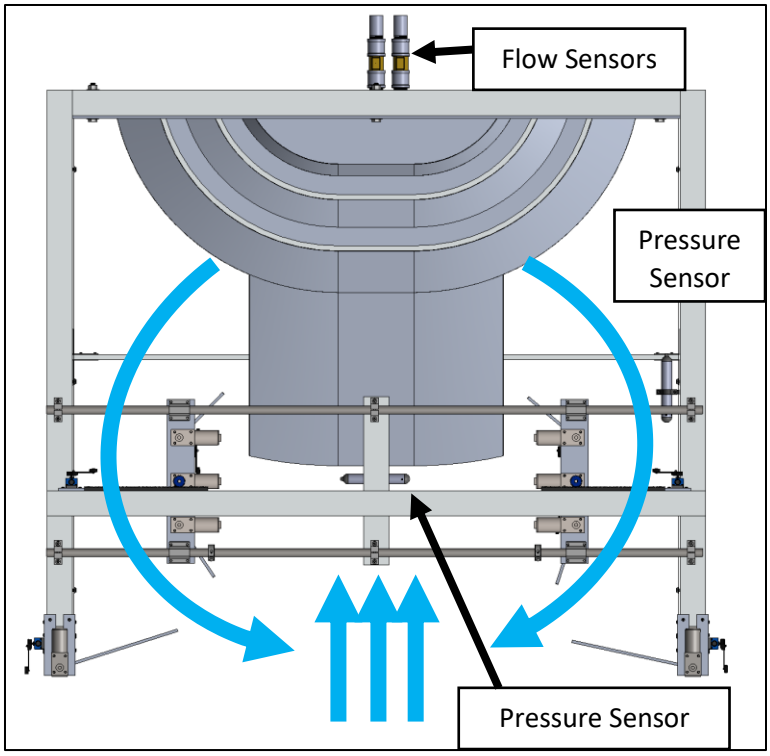

Figure 4: Wave Path

Full-scale overtopping device dimensions were determined based on the wave climate characteristics at various Pacific Northwest locations (Appendix F.) These dimensions were scaled 1:32 for experimentation in the Burke Lab at the Lyles School of Civil Engineering. The wave gates and deflectors were designed around these dimensions (Appendices F & G.) The wave gate subassembly consists of adjustable plates that focus reflected waves together to achieve higher amplitude. The specific wave parameters achieved are dependent on the angle of the wave gate adjusted by a worm gear motor (WGM). The wave deflector subassembly consists of two deflector plates per side with adjustable angles. The deflector sides translate linearly by a rack and pinion system controlled by WGMs. The final design dimensions and weights are listed in Table 1. The design is controlled utilizing a National Instruments myRIO system detailed in Appendix J. The complete wiring schematic is seen in Figure 5.

Important Parameters	**Value**
Total Width	5.34ft
Total Height	2.10ft
Total Length with Retracted Wave Gates	5.41ft
Total Length with Extended Wave Gates	6.35ft
Total Weight	203lb

Frame Weight	66.6lb
Overtopping Weight	49.0lb
Wave Deflector Weight	58.9lb
Wave Gate Weight	7.0lb

Table 1: Device Dimensions and Weights

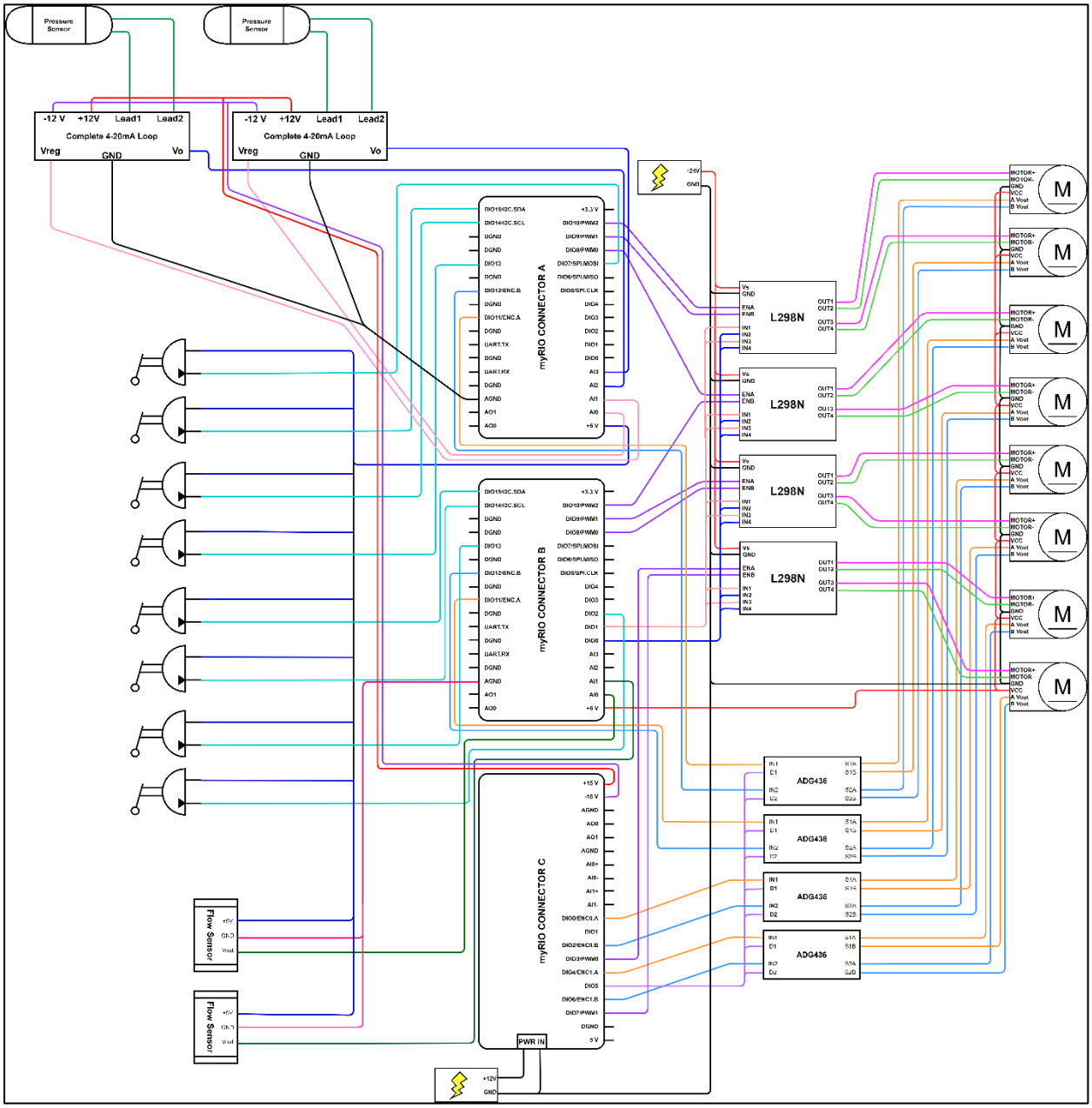

Figure 5: Device Wiring Schematic

Engineering analysis, FEA, and CFD were performed on the device to validate performance and structural integrity (Appendices H & I.) The key results from these studies are seen in Figure 6 and Figure 7.

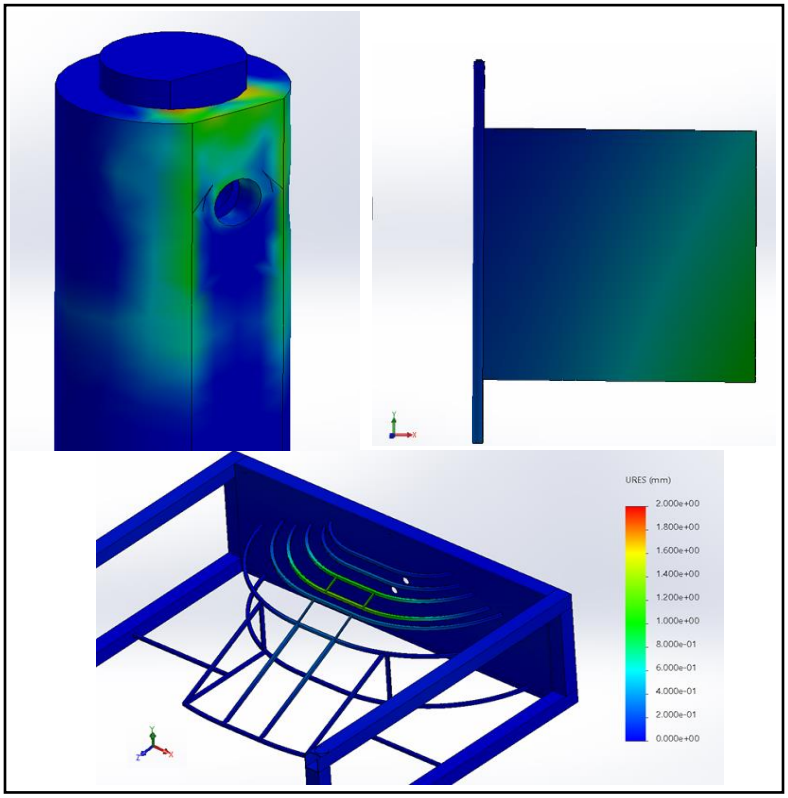

Figure 6: FEA of Device

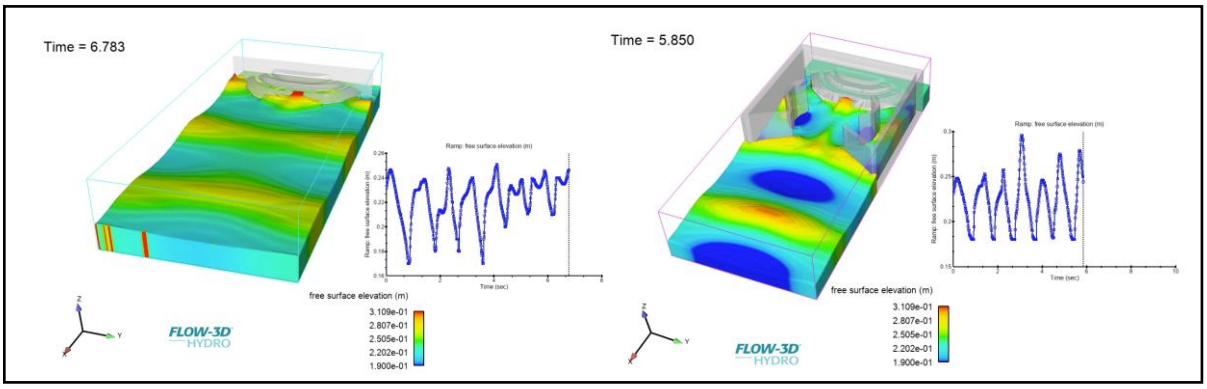

Figure 7: CFD Simulation Results

The test rig prototype is estimated to cost $5470 as seen in Table 2. The resultant data from simulations and testing will be marketed towards research groups and wave energy companies for the addition of the optimal wave deflector and gate configurations to their respective overtopping designs at the desired locations. Although the deflector and gate addition will add lifetime cost to the WEC, the associated yearly profit increase makes this economically viable shown in Figure 8: Lifetime Cost vs. Yearly Profit Increase.

Totals	
Total Purchased Parts ($)	4574.15
Total Custom Manufactured Parts ($)	670
Total Assembly Cost ($)	225
Total Cost Student Manufactured ($)	4574.15
Total Cost Outsourced Fabrication ($)	5469.15

Table 2: Total Cost of Device

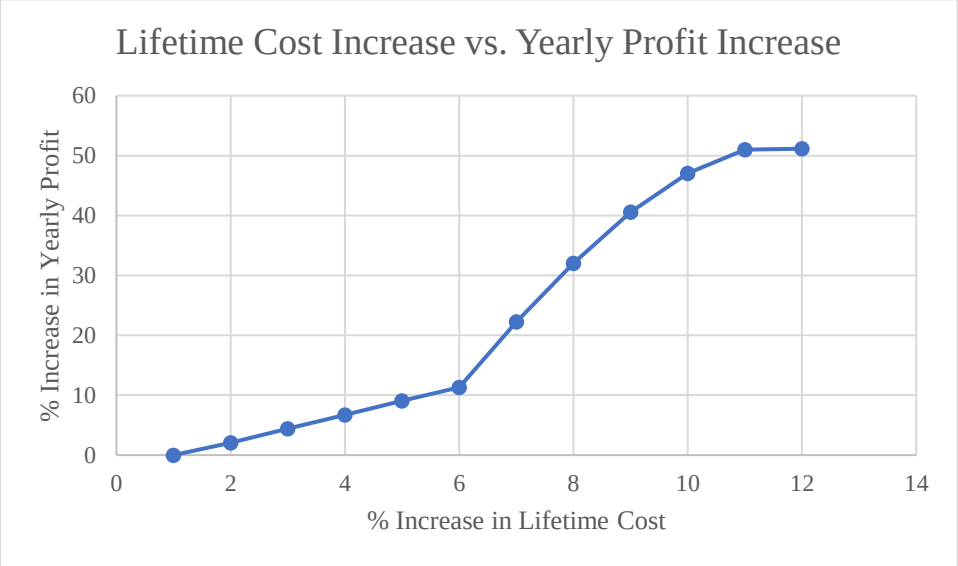

Figure 8: Lifetime Cost vs. Yearly Profit Increase

Appendix A: Team Members and Organization Structure

Below are the Coastal Current team members and their corresponding roles and contact information.

Figure 9: Team Photo - left to right: Colton Doherty, Matt Pugsley, Odette Kuehn, Cyrus Blackmore, Amanda Mudd, Jack Burke

Team Member	**Role**	**Phone**	**Email**
Colton Doherty	Project Manager	(636)-698-4493	doherty6@purdue.edu
Jack Burke	Buyer	(615)-232-4347	burke140@purdue.edu
Odette Kuehn	Manufacturing Manager	(574)-400-3724	okuehn@purdue.edu
Matt Pugsley	Chief Engineer	(816)-489-5985	mpugsley@purdue.edu
Amanda Mudd	Business Manager/Customer Eyes	(847)-302-7128	mudd3@purdue.edu
Cy Blackmore	Validation Lead	(314)-608-3010	cblackm@purdue.edu

Table 3: Team Organization Structure

Appendix B: Charter

Below is the team charter for Coastal Current. The charter outlines the mission and accomplishments of Coastal Current.

PURDUE UNIVERSITY
Mechanical Engineering

ME 463 Senior Design

Project Title:	Design of Constructive Interference Inducer for Overtopping Ocean Wave Energy Device
Team Name:	Coastal Current
Team Members:	Colton Doherty, Jack Burke, Odette Kuehn, Matt Pugsley, Cy Blackmore, Amanda Mudd

Vision Statement: Improve the efficinecy of an overtopping wave energy converter in an economically beneficial, safe, and environmentally conscious way through implementing constructie inerference between incoming and reflective waves

Problem Statement (Current State)

Ocean waves have large energy generation potential that has yet to be harnessed efficiently. The proposed design is to improve the efficiency of an overtopping wave device in an economically beneficial, safe, and environmentally conscious way. This will be done through implementing wave constructive interference to maximize the overtopping wave.

Business / Society Benefit (Future State)

Ocean wave energy in the US alone has the capability to produce 2640 TWh/year, 2/3rds of US yearly energy use. Optimizing ocean wave energy will lead to more affordable and sustainable electricity as no fuel is purchased and much less pollution is produced compared to traditional fossil fuels and natrual gases.

Project Scope

IN Scope	OUT of Scope
Constructive interference of waves	Optimal overtopping reservoir geometry
Modularity of water channels	Multi-stage turbine
Virtual Test Rig Prototype	Generator
Detailed CFD Analysis	Test rig wave generator
Detailed FEA Analysis	Full scale prototype
Verification and testing plan of prototype if to be built in the future	

Key Milestones

PDR: Preliminary Prototype
CDR: Heavily refined design mechanisms, Materials and proper dimensions chosen, Full design CAD model and assembly simulations
FDR: Generated manufacturing drawings for all components, controls scheme, CAD wiring, FEA and CFD analysis, refined business case

Key Assumptions & Risks

Key Assumptions: scaled prototype and CAD models accurately reflect the actual device, testing device will accurately represent ocean wave motion.
Key Risks: lack of experience, COVID exposure, differentiaion between theoretical calculations and model performance

Team Members & Roles

Colton Doherty: Project Manager
Jack Burke: Buyer
Odette Kuehn: Manufacturing Manager
Matt Pugsley: Chief Engineer
Amanda Mudd: Business Manager/Customer Eyes
Cy Blackmore: Validation Lead

Key Resources Required

Zoom/Webex/Slack communication, Solidworks, Ocean wave simulator, sketching software, Microsoft Project

Version: 2

Last Updated: 04/26/2021

Figure 10: Coastal Current Team Charter

Appendix C: Business Case & Project Budget

Market Research

In the United States alone, the total available wave energy is estimated to be 2,640 TW/year, 64% of the annual US electricity generation (Hagerman, 2011). Wave energy has tremendous potential to power the world; however, no technology robust, reliable, and efficient enough has been widely accepted. Harnessing wave energy has proven far more difficult than other renewable energy sources, such as solar and wind, due to the larger expense of operating in the ocean, hostile saltwater environment, and complexity of wave motion (Levitan, 2014). Unlike wind energy, which simply depends on the speed of the wind, wave energy depends on the height, period, and directionality of the waves. Devices that currently exist to harness wave energy do not possess a capacity for generating electricity that is competitive with established renewable energy devices such as solar, wind, or hydroelectric. Current existing solutions include, but not limited to, point absorbers, attenuators, rotating mass, oscillating water column, and overtopping devices, detailed in Table 4 (EMEC, n.d.).

Device	Image
Point absorber – utilizes the relative motion between the buoyant feature and base to produce electrical power.	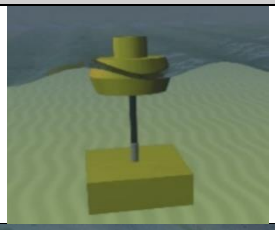
Attenuators – floating device parallel to waves which utilize relative motion of two arms.	
Rotating Mass – rotation is used to capture energy from movement of device in waves,	
Oscillating Water Column – utilizes rise and fall of tides to compress and decompress air to flow through turbine.	
Overtopping – captures water from breaking waves in a reservoir to pass through a low-head turbine.	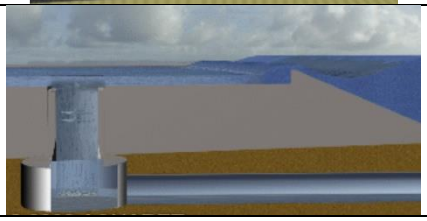

Table 4: Types of Wave Power Devices

Various companies have further developed the concepts listed in Table 4: Types of Wave Power DevicesTable 4 and some even deployed prototypes, including Wavestar's buoy point absorber, WavEnergy's overtopping device, and LIMPET's oscillating water column. Located in Denmark, the Wavestar wave energy conversion (WEC) device converts the kinetic motion of the waves into power utilizing a complex hydraulic system. As waves pass the system, the hydraulic system is driven by the vertical movement of 20 large buoys connected to a base with a long arm. This design is well established and has been in operation for several years. While the Wavestar operates nearly 20 km from shore, other notable designs such as the WAVEnergy Sea-wave Slot- cone Generator (SSG) and the Oscillating Water Column (OWC) take advantage of waves closer to shore. Onshore and near shore devices decrease the likelihood of energy lost from transporting to land as well as decreases the risk and difficulty of maintenance. The SSG overtopping device employs a multi-stage turbine to convert the potential energy of water from reservoirs filled by incoming waves. Multiple reservoirs at differing heights ensures water capture at varying wave amplitudes. An OWC operates such that as incident waves occur the volume of water enclosed in a chamber oscillates and the resultant airflow drives a turbine.

An investigation on the feasibility of deployment of the SSG and OWC devices in various locations was conducted and conclusions on net production and economic investment were presented (Lacasa, 2019). Table 5 shows that the initial investment for the deployment of either the SSG or OWC for a capacity of one MW is substantially larger than any other form of electricity generation. This is because of the very large infrastructure of each device and complexity of building in an ocean environment. However, when compared to existing WEC technology, the acreage required per MW is substantially larger for any of the existing forms of renewable energy (Stevens, 2017). If the initial investment cost per MW and energy efficiency of ocean wave energy technology decreases, ocean wave energy will be a competitive renewable energy source, helping solve the current climate crisis.

	Renewable			**Non-Renewables**			**Current Designs**		
Energy Source	Solar	Wind	Hydroelectric	Nuclear	Coal	Natural Gas	Wavestar	WAVEnergy SSG	OWC
Land Footprint (acre/MW)	70.6	43.5	315.2	12.71	12.21	12.41	1.23	1.97	2.02
Green House Gas Emissions (kg CO2/kwh)	0.046	0.012	0.004	0.029	0.64	0.181	0.047	NEI	NEI
Energy Capacity (MW)	3.40E-04	3	15140	582	650	237	1	0.209	0.203
Expected Lifespan (years)	25	25	100	40	46	22	20	20	20
Construction Cost (million$/MW)	1.4	1.3	3.5	6.8	3.66	0.71	3.88	119.62	93.60
Variable Cost ($/MWh)	25	20	10.8	23.73	36.66	28.33	NEI	NEI	NEI

Table 5: Energy Source Data (Stevens, 2017) (U.S. Energy Information Administration, 2021) (U.S Energy Information Administration, 2019) (Dalton, Madden, & Daly , 2014) (O'Connor,

Lewis, & Dalton) (Lacasa, 2019) (Tesla, n.d.) (Areva Inc. , 2014) (World Nuclear Association , 2011)

The three most utilized renewable energy technologies (excluding biomass) are solar, wind, and hydroelectric energy conversion systems. (U.S. Energy Information Administration, 2020) Collectively, these sources produce just over 6 percent the energy consumed in the United States. These sources only produce greenhouse gas emissions during their beginning of life and end of life stages including manufacturing and decommission. Due to no emissions during operation, renewable energy sources produce significantly less CO2 than nonrenewable energy sources. Many of the effects of climate change are already visible around the globe. These effects are expected to continue to manifest if action is not taken to control greenhouse gas emissions and mitigate environmental damage. As global temperatures rise, we are expected to experience more frequent draught and heat waves as well as displacement from coasts due to sea level rise. Changes in climate and precipitation patterns will strain agricultural practices. (NASA, 2021). More than 75 percent of U.S. greenhouse gas emissions comes from fossil fuel combustion. (U.S. Energy Information Administration , 2020). One of the most practical and impactful ways to combat this is to invest in the implementation of clean energy.

Marketability of a product is determined by its ability to meet the requirements of a customer. Customer requirements were defined based on the desirable qualities of current designs of WECs, other forms of operational renewable energy technologies, and effect on the environment and local inhabitants. To promote function and longevity, an energy device must be able to generate consistent electricity that is transmittable to the grid, resist corrosion and damage from its environment, and be feasible to construct and maintain. To avoid negative environmental impact, the product must minimize environmental disturbance and lifetime greenhouse gas emissions. To be economically viable and safe, the product must produce enough energy to justify cost, consider location and aesthetics so as not to devalue property, and be safe to install and maintain. Specific to wave energy converters, a customer would require the device be effective at differing tide depths and resistant to and usable in unpredictable weather and ocean conditions.

The proposed test rig will utilize constructive interference to increase the efficiency of an overtopping type of wave energy converter. The principles of wave reflection and onsetting waves will be used to passively redirect outgoing waves towards the apparatus to join with incoming waves and increase amplitude and manipulate the period. This concept of constructive interference has yet to be applied to WECs; therefore, innovation is possible. Current overtopping designs are feasible, but not viable for large scale energy production because of their low efficiency and cost. The proposed design aims at improving the efficiency with onsetting waves and therefore making overtopping energy wave devices much more viable.

Business Case Focused on Scaled Down Testing Rig

The product to be sold to consumers will be the data for the optimal configuration of wave deflectors and gates based on the overtopping design and the desired location provided by the customer. The service our company will provide is the manufacturing of a scaled down test

rig that will be used for physical testing to design a deflector and gate configuration to be added on and increase overtopping efficiency by increasing significant wave height. The test rig proposed will be scaled down from the full-scale device to a size large enough to create constructive interference with simulated waves and small enough that it could fit in a wave pool. The proposed scale was determined based on the wave pool housed at the Burke Laboratory in the Lyles School of Civil Engineering. The Purdue Towing Tank is 150 ft long, 11ft wide and 5 ft deep (School of Civil Engineering, Purdue University, n.d.). The overall dimensions for the test rig are approximately 4.2’ wide x 5’ long and 1.4’ tall. The scale of the device is also constrained by weight so that it can be transported and safely mounted. This design is easily scalable to fit in different wave pools as desired by potential future partners.

Additionally, the test rig will house motors, actuators, and sensors that will control the deflectors and gates, as well as store and present flow data to the user. This will make the test rig easy to install and use for any researcher. The device will be mounted in a wave simulation pool and will require inputs for the desired positions and orientations of wave deflectors according to the desired testing plan. CFD simulations will be conducted in the next stage of the project to better inform physical testing. The goal of these simulations would be to find the theoretical optimal configurations for creating constructive interference and increasing efficiency to be verified with the physical test model.

The test rig is currently expected to cost approximately $5470 from the Bill of Materials shown in Figure 12Figure 13 and the total estimated cost from Table 6. For the size, scope, and potential value of this project, this is a reasonable budget. The overall goal of employing the test rig is to research the effects of the wave deflectors on achieving constructive interference. The price of the data to the customer includes the manufacturing of the test rig and the plans for the configuration and construction of the stationary wave deflectors and wave gates. The price is determined based on the expected efficiency increase validated by the physical simulations. It is estimated that a larger increase in efficiency will require more time and more simulations and therefore, should cost more. There is capability to decrease the cost of the rig through design changes, finding new suppliers, and ordering stock materials in large quantities instead of in individual parts.

The construction cost of the overtopping device is consistent for each case. However, the overall construction increases with efficiency to account for the potential increase in prices or necessarily number of turbines to keep up with the expected increase in water that overtops. As shown in *Table 7: Client Costs and Profits*, the projected wave deflector and gate cost is also kept consistent. As previously mentioned, the data cost increases with efficiency to account for the amount of time and simulations that will likely be required for a greater efficiency increase. The lifetime cost increase and the yearly profit increase are compared to the case for which deflectors and gates are not installed and the overtopping device performs without them. Profit increases are calculated based on the cost of energy to the producer and the anticipated yearly output of energy in kilowatt hours. The increase in lifetime cost versus the yearly profit increase is plotted in Figure 13Figure 13: Lifetime Cost vs. Yearly Profit Increase. This shows that with

relatively small increases in efficiency and lifetime cost, the yearly profit increases make the product economically viable.

Type Key	
A	Assembly
C	Custom Manufactured
P	Purchased

Figure 11: Type Key for Bill of Materials

Element	Item No.	Part No.	Type	Part Name	Total Units	Line Total Cost ($)	Price per Part ($)
Gates	42	G1	P	Shaft Collar	12	66	66
	43	G2	P	Sleeve Bearing	12	22.8	22.8
	44	G3	P	Worm Gear Motor	2	40.6	40.6
	45	G4	P	Corner Bracket	4	31.56	31.56
	46	G5	P	D-Shaft	2	9.54	9.54
	47	G6	P	Gate Plate	1	134.14	134.14
	48	G7	P	Motor Mounting Plate	1	13.76	13.76
	49	G8	P	M4 Fasteners	2	13.84	0.2768
	50	G9	P	4-40 thread fasteners	1	4.45	0.0445
	51	G10	C	Shaft cut and Mill	2	40	40
	52	G11	C	Holes in Brackets	2	10	10
	53	G12	C	Wave gate cuts	2	20	20
	54	G13	C	Weld plate/shaft	2	30	30
	55	G14	C	Motor mount cut	2	20	20
	56	G15	A	Assembly wave gates	1	25	25
Controls	57	C1	P	Waterproof Limit Switch	2	39.98	7.996
	58	C2	C	Limit Switch Mount	4	0	0
	59	C3	P	Flat Head M5 Fasteners	1	7.76	0.1552
	60	C4	P	12 V Battery	1	37.99	37.99
	61	C5	P	Electronics Box	1	9.25	9.25
	62	C6	P	4-20mA Reciever	2	22.42	22.42
	63	C7	P	Capacitors	1	18.75	18.75
	64	C8	P	Soldering Boards	1	13.99	13.99
	65	C9	P	Wiring	1	34.98	34.98
	60	C10	P	Resistors	1	11.99	11.99
	61	C11	P	Transmitter	2	20.34	20.34
	62	C12	P	Motor Controller	4	27.56	27.56
	60	C13	P	Switch	4	31.68	31.68
	61	C14	P	Diode	1	0.1	0.1
	62	C15	P	24 V Battery	1	36.99	36.99
Welding	63	W1	P	0.047" Aluminum Weld Filler	1	18.48	18.48
	64	!2	P	0.03" Aluminum Weld Filler Material	1	19.83	19.83

Figure 12: Bill of Materials

Element	Item No.	Part No.	Type	Part Name	Total Units	Line Total Cost ($)	Price per Part ($)
Overtopping Device	1	E1	P	Back Plate	1	175.74	175.74
	2	E2	P	.5" 6ft Square Hollow Bar	8	120	120
	3	E3	P	.25" 3ft Square Hollow Bar	1	0	0
	4	E4	P	Sheet Metal	1	136.8	136.8
	5	E5	P	Silicone Sealant	10	39.5	39.5
	6	E6	P	Flowmeter	2	37.98	18.99
	7	E7	P	Brass 90deg Elbow, 1" NPT	2	38.18	38.18
	8	E8	P	Brass Connector, 1" NPT	4	70.44	70.44
	9	E9	P	Brass Pipe, 6" Long, 1" NPT	2	34.86	34.86
	10	E10	P	Brass Pipe, 3" Long, 1" NPT	2	22.06	22.06
	11	E11	P	Aluminum Weld-On Tank Bung, 1" NPT	2	55.86	55.86
	12	E12	P	Brass Pipe, fully threaded connector, 1" NPT	2	10.92	10.92
	13	E13	P	Liquid-Level Sensor	2	1129.56	1129.56
	14	E14	P	Liquid-Level Sensor Mount	2	39.98	39.98
	15	E15	C	Sheet Metal Cutouts	1	0	0
	16	E16	C	Skeleton Bar Cuts	1	100	100
	17	E17	C	Skeleton Bar Bends	1	100	100
	18	E18	C	Welding	1	300	300
Frame	19	W1	P	2.5" x .2.5" x 6' Square Bar	7	620.76	620.76
	20	W2	P	2.5" x .2.5" x 2' Square Bar	1	37.25	37.25
	20	W3	P	Clear Walls	1	76.95	76.95
	21	W4	P	Fasteners for Plexiglass	1	10.11	0.4044
	22	W5	P	Fasteners for Plexiglass	1	7.11	0.0711
	23	W6	P	Square Brackets for Overtopping	4	6.96	6.96
	24	W7	P	Fasteners for Brackets	2	1.96	0.245
	25	W8	P	Fasteners for Brackets	1	2.45	0.049
	26	W9	P	Fasteners for Brackets	1	0.98	0.245
	27	W10	P	Fasteners for Back Plate	1	37.17	1.4868
	28	W11	P	Fasteners for Back Plate	1	8.16	0.3264
	29	W12	P	Fasteners for Back Plate	1	9.25	1.541666667
	30	W13	C	Bar Cuts	1	50	50
	31	W14	A	Frame Welding	1	200	200
Deflectors	32	D1	P	Shaft Support	6	213.9	213.9
	33	D2	P	Linear Bearing	4	349.24	349.24
	34	D7	P	Worm Gear Motor	8	162.4	162.4
	35	D8	P	Gear Rack	2	9.26	9.26
	36	D9	P	Gear	1	18.07	18.07
	37	D10	P	Two Piece Shaft Collar	1	11.28	5.64
	38	D11	P	D-Shaft	4	19.08	19.08
	39	D13	P	M6 Fasteners	1	7.52	0.3008
	40	D15	P	Welded Base and 2 Deflector Plate	1	134.14	134.14
	41	D16	P	4 Deflector Shafts	2	267.8	267.8

Figure 12: Bill of Materials Continued

Totals	
Total Purchased Parts ($)	4574.15
Total Custom Manufactured Parts ($)	670
Total Assembly Cost ($)	225
Total Cost Student Manufactured ($)	4574.15
Total Cost Outsourced Fabrication ($)	5469.15

Table 6: Total Cost of Scaled Prototype

	Overtopping Construction Cost ($)	Deflector and Gate Cost ($)	Data Price ($)	Total Upfront Cost ($)	Lifetime Cost Increase (%)	Breakeven (Years)	Yearly Profit Increase (%)
Without Deflectors	6073996.03	NA	NA	6073996.03	0	8.77	0
5% Efficiency Increase	6103200.268	60167.52	148533.9128	6311901.7	6.742136245	8.30	11.31712275
10% Efficiency Increase	6131579.681	60167.52	381968.5795	6573715.78	14.29456713	7.93	22.23883347
15% Efficiency Incresase	6158858.591	60167.52	725838.2775	6944864.389	23.73755549	7.75	32.04321707
20% Efficiency Increase	6185846.517	60167.52	1241277.678	7487291.715	36.23995098	7.77	40.54941688
25% Efficiency Incresae	6211883.307	60167.52	1970523.45	8242574.277	52.45475966	8.00	47.04925041
30% Efficiency Increase	6237724.124	60167.52	3015453.717	9313345.36	74.26763824	8.48	51.01206955

Table 7: Client Costs and Profits

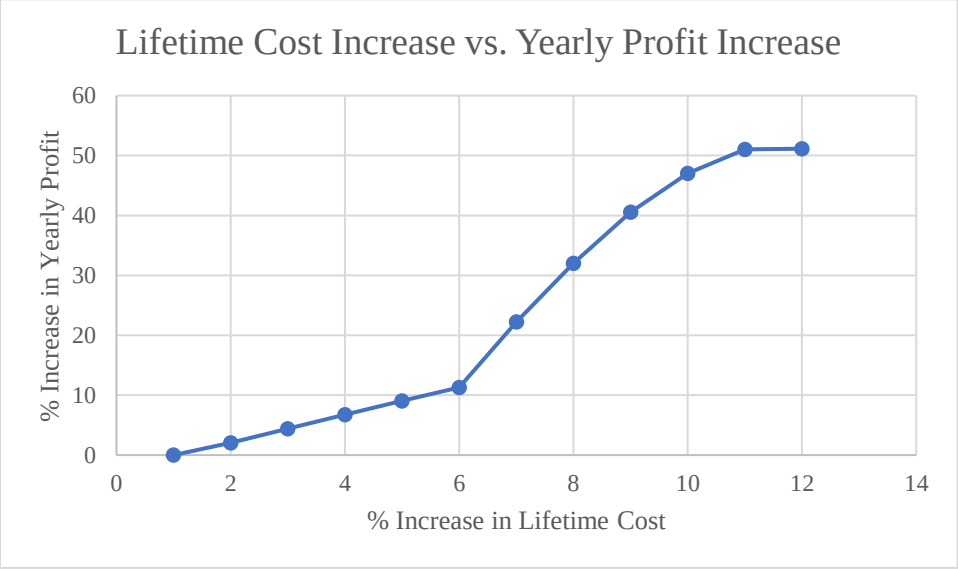

Figure 13: Lifetime Cost vs. Yearly Profit Increase

Appendix D: Network Diagram and Project Schedule

Figure 14 shows an overall network diagram which outlines the tasks to be completed through each phase of the project. An additional network diagram for the CAD components was also made to guide the team in completing all components, seen in Figure 15. These tasks were put into a project schedule shown in Figure 16 using Microsoft Project.

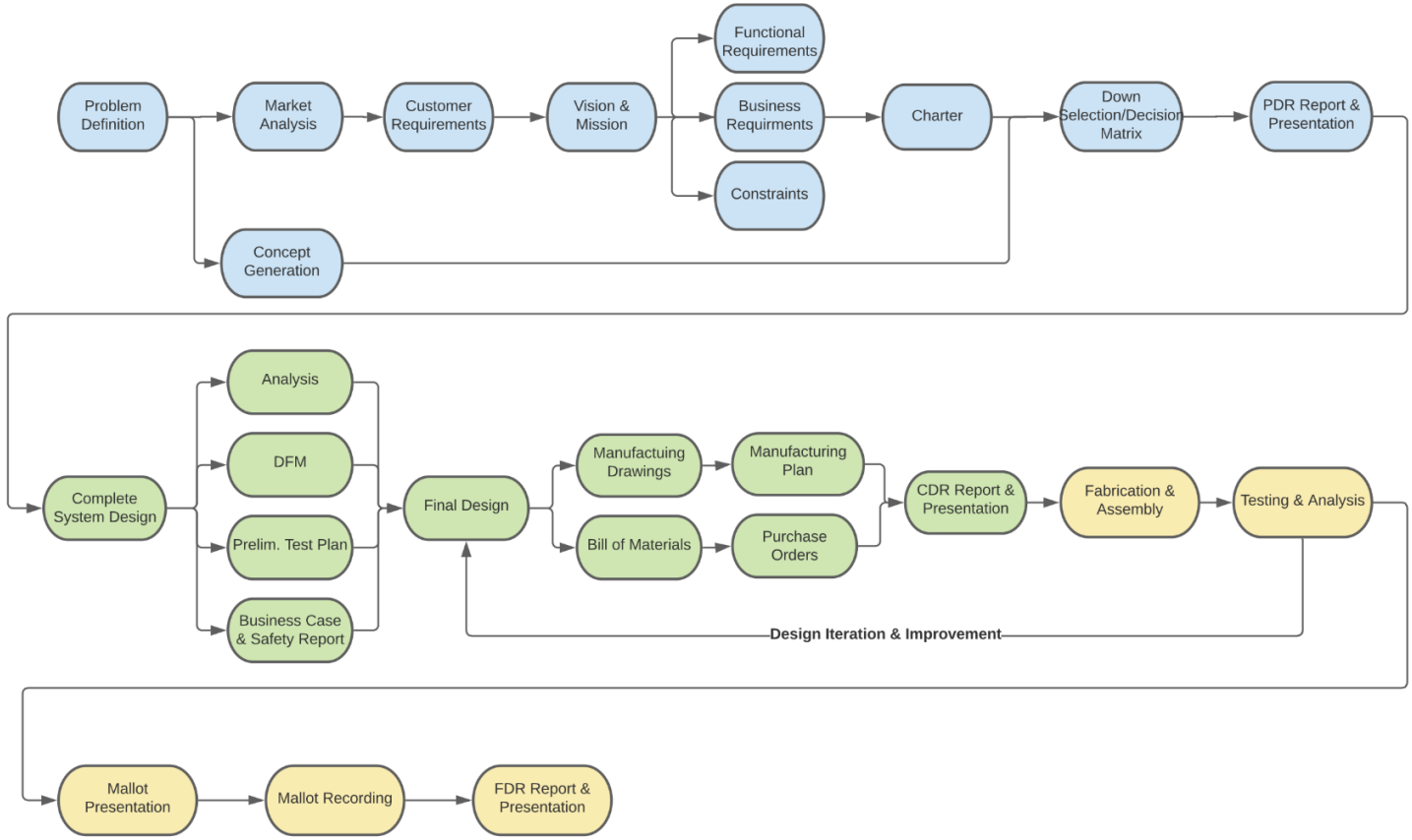

Figure 14: Overall Network Diagram

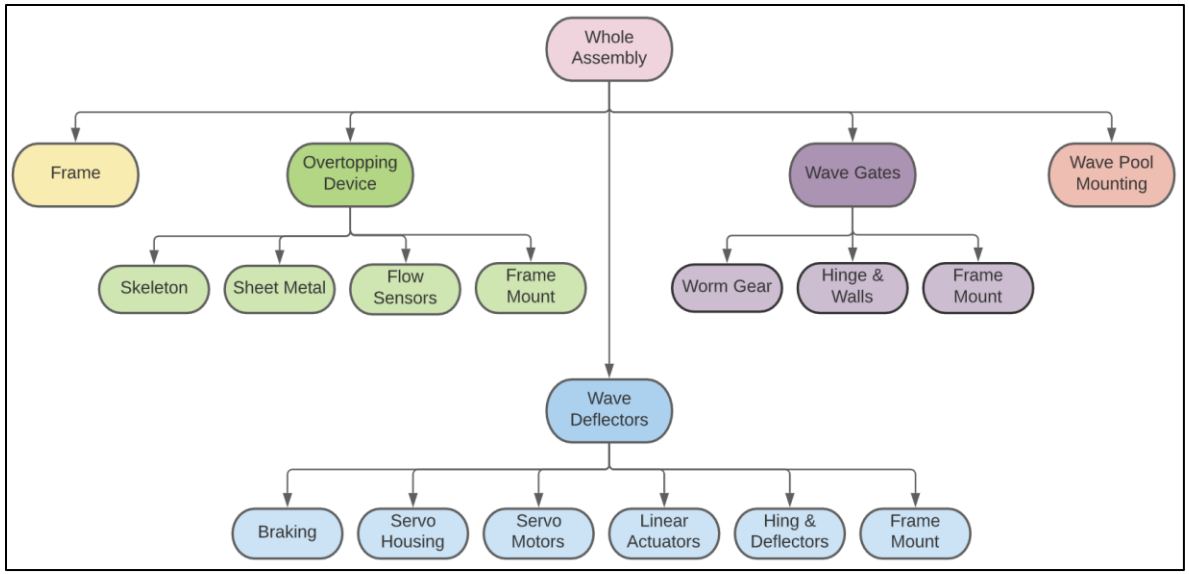

Figure 15: Mechanical CAD Network Diagram

	% Comple	Task Mode	Task Name	Duration	Start	Finish
1	**100%**		**Problem Definition & Concept Review**	**24 days**	**Tue 1/19/21**	**Thu 2/11/21**
2	100%		WBS, Network Diagram, Schedule	2 days	Tue 1/19/21	Wed 1/20/21
3	100%		Market Analysis	8 days	Thu 1/21/21	Thu 1/28/21
4	100%		Patent/Existing Solutions Research	8 days	Thu 1/21/21	Thu 1/28/21
5	100%		Design Idea Generation	10 days	Thu 1/21/21	Sat 1/30/21
6	100%		Customer & Functional Requirement	1 day	Thu 1/28/21	Fri 1/29/21
7	100%		Vission & Mission	1 day	Fri 1/29/21	Fri 1/29/21
8	100%		Concept Down Selection	3 days	Sun 1/31/21	Tue 2/2/21
9	100%		Charter	2 days	Wed 2/3/21	Thu 2/4/21
10	100%		Design Sketching	4 days	Wed 2/3/21	Sat 2/6/21
11	100%		Preliminary Risk Register	2 days	Sun 2/7/21	Mon 2/8/21
12	100%		Low-Fidelity Prototype	3 days	Sun 2/7/21	Tue 2/9/21
13	100%		Create PDR Presentation	5 days	Sun 2/7/21	Thu 2/11/21
14	100%		PDR Presentation	0 days	Thu 2/11/21	Thu 2/11/21
15	100%		PDR Written Report	7 days	Fri 2/5/21	Thu 2/11/21
16	**100%**		**Critical Design Review**	**28 days**	**Fri 2/12/21**	**Thu 3/11/21**
30	**100%**		**Final Design Review**	**47 days**	**Fri 3/12/21**	**Tue 4/27/21**
44	100%		**Mallot Competition**	**33 days**	**Fri 3/12/21**	**Tue 4/13/21**

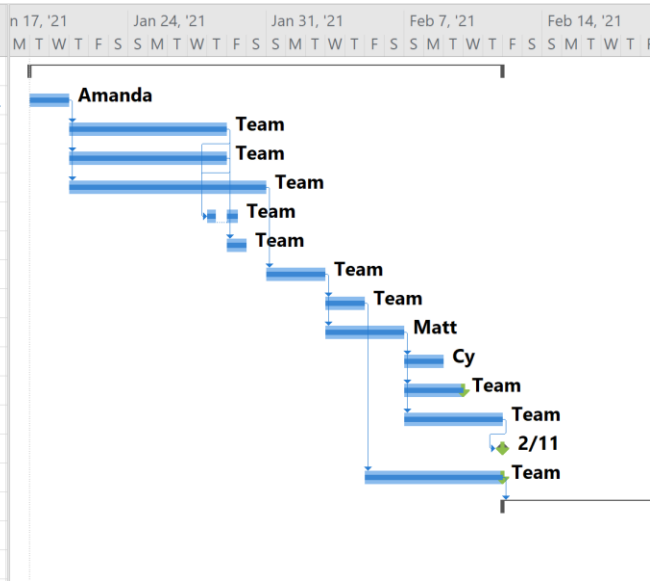

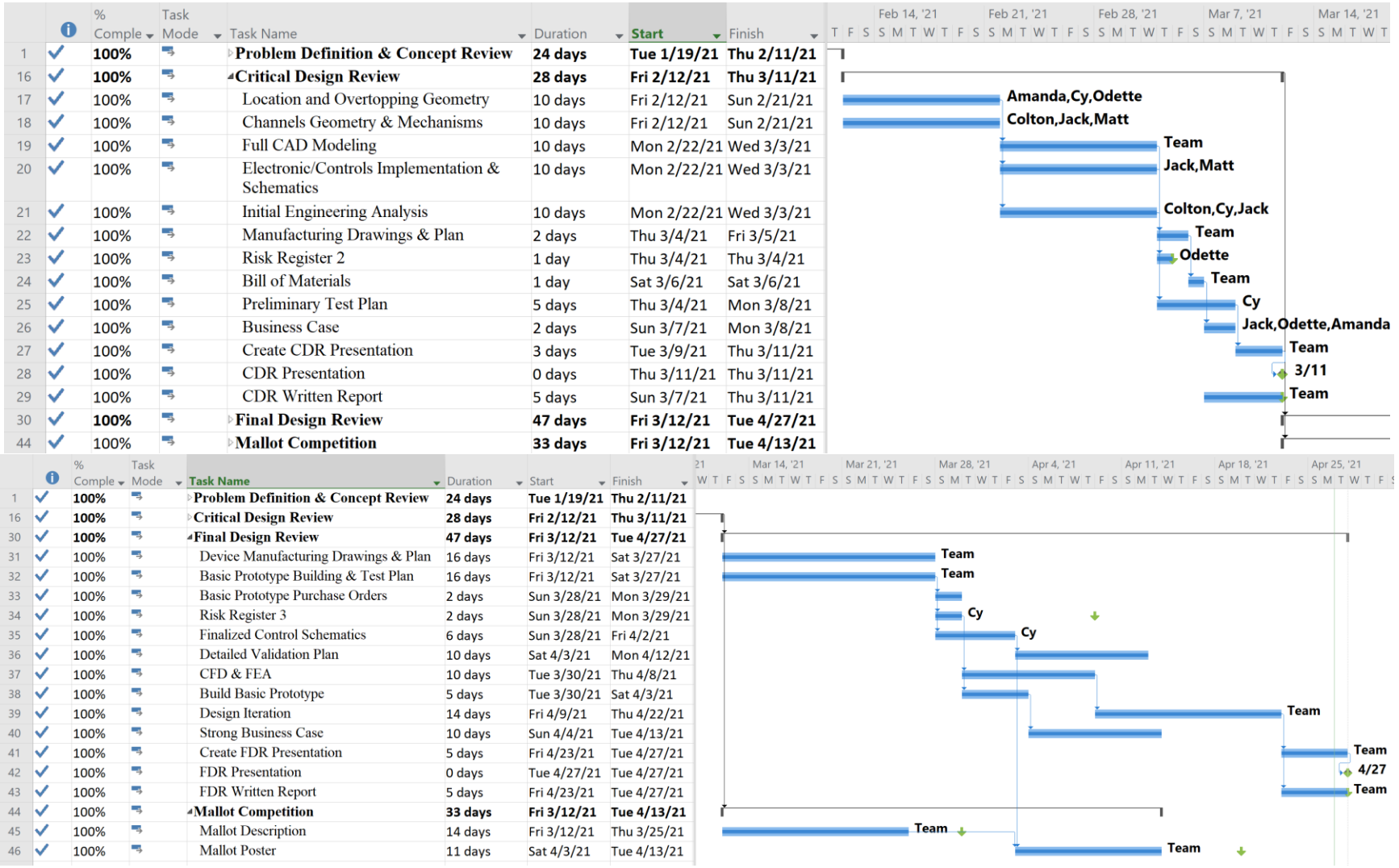

		% Comple	Task Mode	Task Name	Duration	Start	Finish
1	✓	100%		**Problem Definition & Concept Review**	**24 days**	**Tue 1/19/21**	**Thu 2/11/21**
16	✓	100%		**Critical Design Review**	**28 days**	**Fri 2/12/21**	**Thu 3/11/21**
17	✓	100%		Location and Overtopping Geometry	10 days	Fri 2/12/21	Sun 2/21/21
18	✓	100%		Channels Geometry & Mechanisms	10 days	Fri 2/12/21	Sun 2/21/21
19	✓	100%		Full CAD Modeling	10 days	Mon 2/22/21	Wed 3/3/21
20	✓	100%		Electronic/Controls Implementation & Schematics	10 days	Mon 2/22/21	Wed 3/3/21
21	✓	100%		Initial Engineering Analysis	10 days	Mon 2/22/21	Wed 3/3/21
22	✓	100%		Manufacturing Drawings & Plan	2 days	Thu 3/4/21	Fri 3/5/21
23	✓	100%		Risk Register 2	1 day	Thu 3/4/21	Thu 3/4/21
24	✓	100%		Bill of Materials	1 day	Sat 3/6/21	Sat 3/6/21
25	✓	100%		Preliminary Test Plan	5 days	Thu 3/4/21	Mon 3/8/21
26	✓	100%		Business Case	2 days	Sun 3/7/21	Mon 3/8/21
27	✓	100%		Create CDR Presentation	3 days	Tue 3/9/21	Thu 3/11/21
28	✓	100%		CDR Presentation	0 days	Thu 3/11/21	Thu 3/11/21
29	✓	100%		CDR Written Report	5 days	Sun 3/7/21	Thu 3/11/21
30	✓	**100%**		**Final Design Review**	**47 days**	**Fri 3/12/21**	**Tue 4/27/21**
44	✓	100%		**Mallot Competition**	**33 days**	**Fri 3/12/21**	**Tue 4/13/21**

		% Comple	Task Mode	Task Name	Duration	Start	Finish
1	✓	**100%**		**Problem Definition & Concept Review**	**24 days**	**Tue 1/19/21**	**Thu 2/11/21**
16	✓	**100%**		**Critical Design Review**	**28 days**	**Fri 2/12/21**	**Thu 3/11/21**
30	✓	**100%**		**Final Design Review**	**47 days**	**Fri 3/12/21**	**Tue 4/27/21**
31	✓	100%		Device Manufacturing Drawings & Plan	16 days	Fri 3/12/21	Sat 3/27/21
32	✓	100%		Basic Prototype Building & Test Plan	16 days	Fri 3/12/21	Sat 3/27/21
33	✓	100%		Basic Prototype Purchase Orders	2 days	Sun 3/28/21	Mon 3/29/21
34	✓	100%		Risk Register 3	2 days	Sun 3/28/21	Mon 3/29/21
35	✓	100%		Finalized Control Schematics	6 days	Sun 3/28/21	Fri 4/2/21
36	✓	100%		Detailed Validation Plan	10 days	Sat 4/3/21	Mon 4/12/21
37	✓	100%		CFD & FEA	10 days	Tue 3/30/21	Thu 4/8/21
38	✓	100%		Build Basic Prototype	5 days	Tue 3/30/21	Sat 4/3/21
39	✓	100%		Design Iteration	14 days	Fri 4/9/21	Thu 4/22/21
40	✓	100%		Strong Business Case	10 days	Sun 4/4/21	Tue 4/13/21
41	✓	100%		Create FDR Presentation	5 days	Fri 4/23/21	Tue 4/27/21
42	✓	100%		FDR Presentation	0 days	Tue 4/27/21	Tue 4/27/21
43	✓	100%		FDR Written Report	5 days	Fri 4/23/21	Tue 4/27/21
44	✓	100%		**Mallot Competition**	**33 days**	**Fri 3/12/21**	**Tue 4/13/21**
45	✓	100%		Mallot Description	14 days	Fri 3/12/21	Thu 3/25/21
46	✓	100%		Mallot Poster	11 days	Sat 4/3/21	Tue 4/13/21

Figure 16: Project Schedule

Appendix E: Risk Mitigation

The risk register below outlines anticipated risks and their mitigations. For example, the team anticipated that access to a wave pool for physical testing would not be possible. Further, creating a functional prototype would be out of the scope of the class due to both time and cost constraints. Instead, a detailed CAD model was created. CFD and FEA analysis were performed instead of physical testing. The risk register allowed the team to identify the most potent risks and mitigate them before encountering problems.

1. IDENTIFICATION						2. CURRENT ASSESSMENT			3. TREATMENT		4. RESIDUAL ASSESSMENT			5. REVIEW, CONTROL, COMMUNICATE	
ID	RAISED BY	DATE RAISED	CAUSE (IF…)	EFFECT (THEN…)	RISK OWNER	P	I	Current Risk Score	STRATEGY	TREATMENT DESCRIPTION	P	I	Residual Risk Score	Commentary	Last Updated
	The originator of the risk	*When the risk was first identified*	*If **uncertain event** occurs due to (or because of) specified **root cause(s).** Tip: ask "why, why, why…" to drill down to root cause*	*then the **ultimate impact** to our objectives are. Tip: ask "so what, so what, …"*	*Single named owner*	*Probability of the event occurring*	*'Worst' impact*	*Calculated risk score*	*Select overall approach to treatment (Mitigate or Accept)*	*Summary of the treatment responses (actions, controls, fallbacks) that treat the risk.*	*Probability of the event occurring*	*'Worst' impact*	*Calculated risk score*	*Any additional notes, comments or actions*	*Enter the last review or update date for the risk*
1	Cy	5-Feb-21	Project not completed on time due to large scope	Incomplete project; bad grades	Colton	M	H	15	Mitigate	Scope of final deliverable changed from physical model to CAD model only	L	H	11	Less probable that the project won't be completed on time	5-Feb-21
2	Cy	5-Feb-21	COVID exposure	One or more team members will not be able to meet in person	Colton	M	L	5	Accept	Quarantined team member can meet with team and professor virtually	M	L	5		5-Feb-21
3	Cy	6-Feb-21	Budget is exceeded	Final prototype will not be completed	Jack	M	H	15	Mitigate	Additional Funding could possibly be aquired to be manufactured in the future	L	M	6	Since Prototype is now virtual, this is less of an immediate concern, design will be iterated to reduce price	9-Mar-21
4	Cy	6-Feb-21	Team members are not aware of their responsibilities or team direction	Team members can't be productive and deadlines are missed	Amanda	H	M	14	Mitigate	Meeting minutes are kept to record delegations to individual team members	L	M	6	Team members will complete almost all of thier tasks on time, so the project will not be delayed.	6-Feb-21
5	Cy	8-Feb-21	Access to a wave pool is not possible	Physical testing must be done eslewhere or not at all	Cy	M	M	10	Mitigate	Must decide whether to build a testing pool or to test using CFD exculsively	M	L	5		8-Feb-21
6	Cy	9-Feb-21	Team members lack the specialized skills needed to perform in their roles	Project will be delayed while skills are learned	Colton	L	L	1	Accept	Team members can learn skills quickly. Other team members can pick up slack.	L	L	1		9-Feb-21
7	Cy	9-Feb-21	Articulating plate adjustment system fails	System will be less effective until maintenance is performed	Pugsley	L	M	6	Mitigate	System must be designed with ease of maintenance in mind	L	M	6	The final product can still break, but it will be fixed more quickly.	9-Feb-21
8	Cy	23-Feb-21	CFD testing cannot demonstrate constructive interference in waves	Constructive interference must be physically demonstrated	Cy	M	M	10	Mitigate	A simple experiment must be performed in a wave pool to show that constructive interference is possible.	L	M	6	This is the best we can do to demonstrate our design concept.	23-Feb-21
9	Cy	9-Mar-21	Wires are not properly insulated against water	Electrical shortages can occur	Pugsley	M	H	15	Mitigate	All wires will be coated and heat shrink added to their terminations.	L	H	11	There will always be some risk of electrical shortage with water nearby.	9-Mar-21
10	Cy	10-Mar-21	Flowmeters are not water-resistant enough to maintain function when submerged/soaked	Electrical shortage and/or loss of data measurement and microprocessor shortage	Cy	L	H	11	Mitigate	A clear waterproof box will be built to enclose the flowmeters	L	M	6	The risk of electrical shortage still exists but shock should be confined to the water in the box.	10-Mar-21
11	Colton	1-Mar-21	Back drive of geared motors breaks the motors and induces motion	The deflector or wave gates will be rotated by the waves and possibly casue more damage	Colton	M	L	5	Accept				#N/A		1-Mar-21
12	Colton	3-Mar-21	Motors could stall or burn out	Motors will need to be replaced, no other damage should occur	Colton	L	L	1	Accept		L	L	1		3-Mar-21
13	Colton	5-Mar-21	Wave Deflector or Gate Plates could yield from the waves and fail	Shaft and Plate will need to be replaced	Colton	M	M	10	Mitigate	Proper Engineering Analysis of the plates will be used to determine dimensions and materials that provide sufficent factor of safety	L	M	6		5-Mar-21

Table 8: Risk Register

Appendix F: Sketches & Design Development

Preliminary Design

Design selection began with several brainstormed concepts for generating power from ocean waves that were narrowed down to four concepts based on practicality, shown in Figure 17. A decision matrix was used to compare these four designs, shown in Figure 18, and eliminate two design ideas, designs 3 and 4. After extensive research into both concepts, a turbine-driven overtopping reservoir device modeled after the patented design shown in Figure 19 was selected (United Kingdom Patent No. GB2536071A, 2016). Current overtopping designs waste a large amount of energy on the wave-to-crest portion of the power generation. The wave-to-crest efficiency is the loss of potential power from the incoming ocean wave to the total power that enters the overtopping system. Loss of power results from backwash; the water that does not make it into the reservoir recedes and destructively interferes with the next incoming wave. Traditional overtopping devices operate at ~40% wave-to-crest efficiency (Vicinanza, 2012).

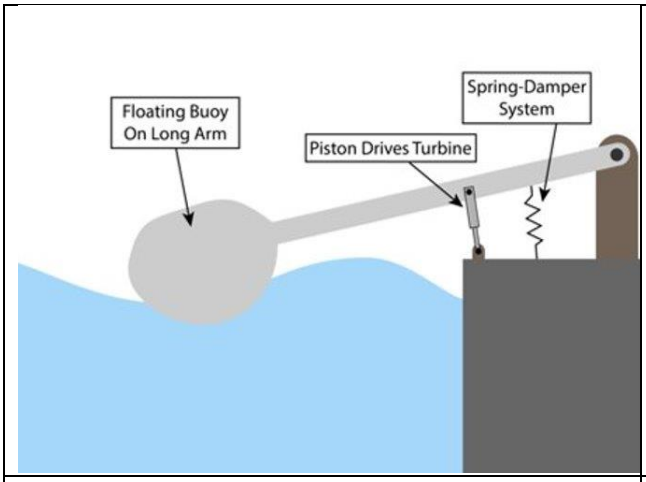

Concept 1: Buoy and Rotating Mass

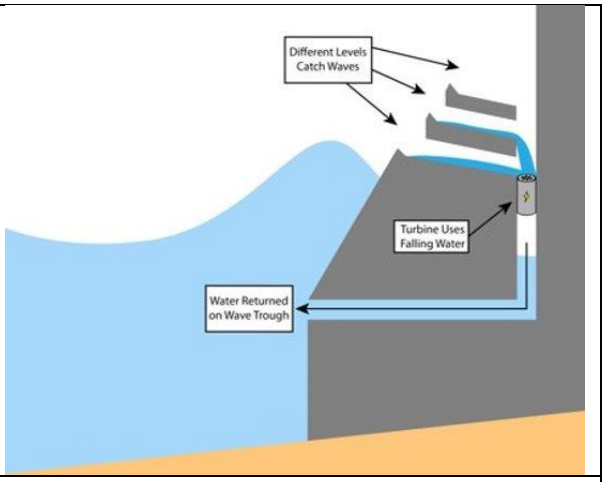

Concept 2: Overtopping

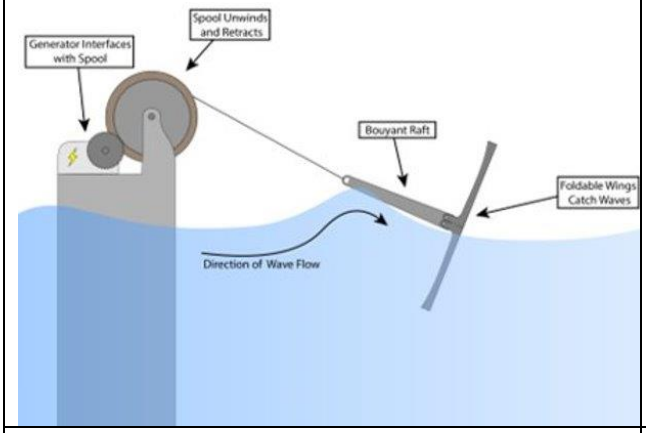

Concept 3: Umbrella

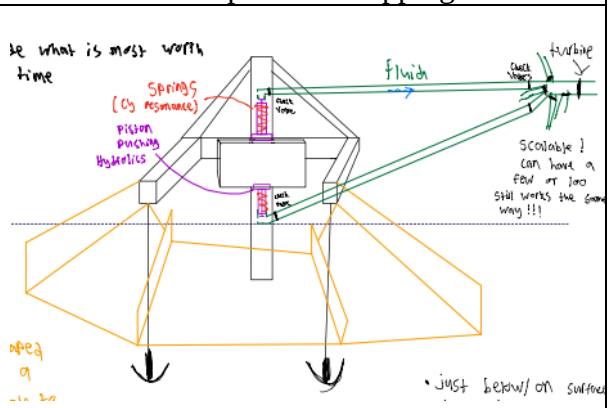

Concept 4: Buoy and Constructive Interference

Figure 17: Designs Included in Decision Matrix

Customer Requirement	Weight	1	2	3	4	Datum
Generates consistent electricity	5	1	1	-1	1	0
Usable at different tides	1	0	-1	0	0	0
Resistant to corrosion & environment	3	1	-1	-1	-1	0
Economically Beneficial - $24/MWh	5	1	1	1	1	0
Ease of maintentance	4	0	1	0	0	0
Ease of construction	3	-1	-1	-1	-1	0
Minimal marine life harm	3	0	0	-1	0	0
Value of Coastal Property	2	-1	-1	0	0	0
Safety to Humans	3	0	0	-1	0	0
Total -		2	4	5	2	0
Total +		3	3	1	2	0
Unweighted Total		1	-1	-4	0	0
Weighted Total		3	1	-7	-1	0

Concept	Description
1	Buoy & Rotating Mass
2	Overtopping
3	Umbrella
4	Buoy & Constructive Interference

Datum	Description
5	Basic point buoy system

Scores	
1	Better
0	Same
-1	Worse

Figure 18: Weighted decision matrix

The proposed design focuses on increasing overall and wave-to-crest efficiency through implementing constructive interference between the incoming waves and waves reflected off the overtopping device. The preliminary design sketch is shown in Figure 20 and Figure 21. In theory, the waves reflected from the ramp due to backwash would be redirected to combine with incoming waves, creating taller waves, more energy generation, and better wave to crest efficiency. Figure 20 shows rotatable wave deflectors that can be anchored anywhere along 80/20 rails. The “gates” at the front of the device are rotatable, and adjustable ramps are attached that allow the period and amplitude of redirected waves to be adjusted. The final deliverable will be a scaled down version of the overtopping device in a test rig in which the angle and position of wave deflectors and ramps are variable. This test rig will simulate waves and measure the effect of the deflectors and ramps on constructive interference and energy conversion efficiency. The final goal of the project is to identify the optimal configuration to be implemented into a full-scale WEC.

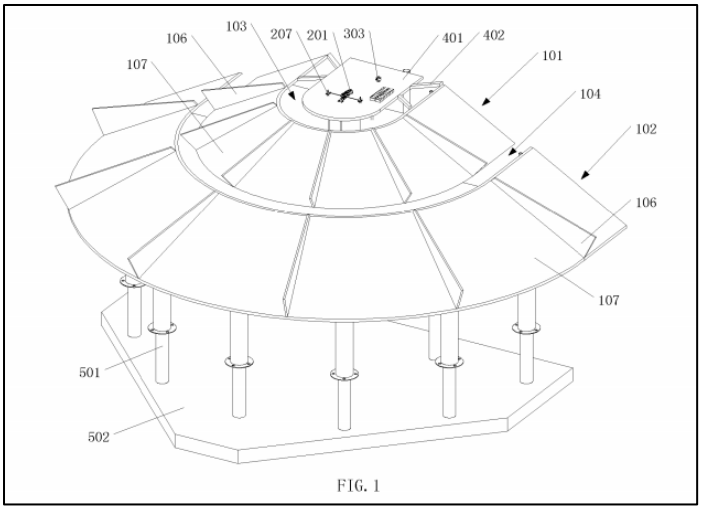

Figure 19: Patented Overtopping Device

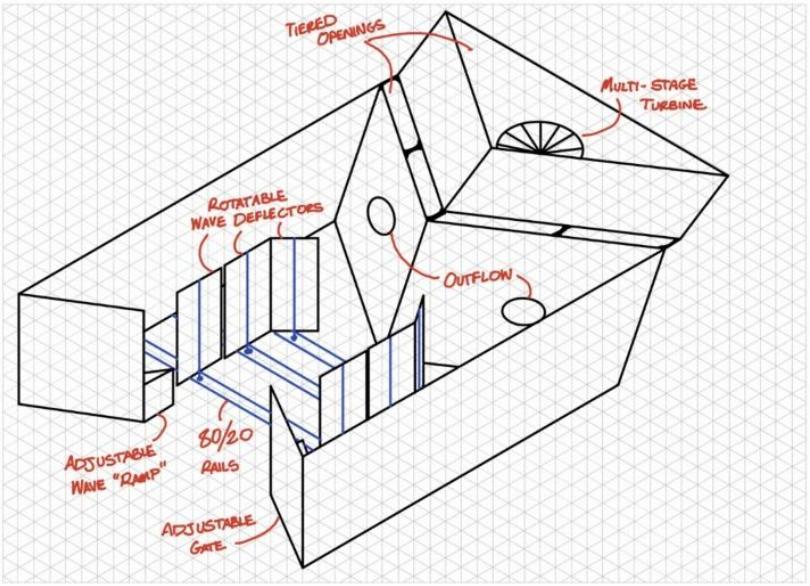

Figure 20: Preliminary Overtopping Design

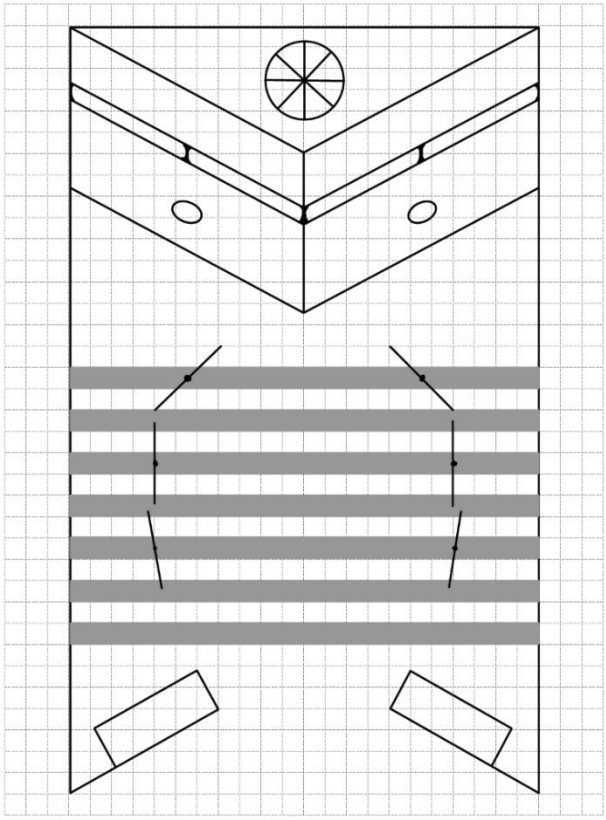

Figure 21: Preliminary Design Top View

Overall Assembly

From the preliminary design, a more developed concept and sketch was derived. The developed concept consisted of 4 subassemblies: Frame (black), Overtopping Device (purple), Wave Gates (green), and Wave Deflectors (orange). The sketch below shows the developed overall assembly concept.

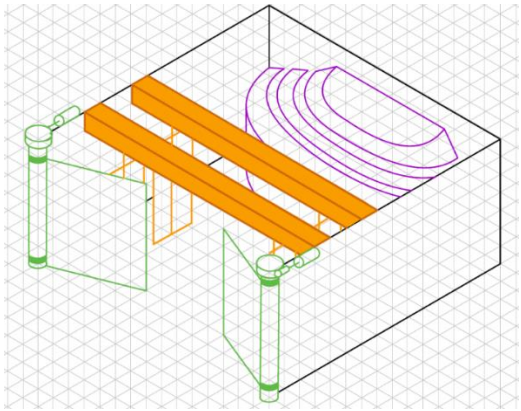

Figure 22: Developed Overall Assembly Sketch

There is no additional design development for the frame since the sketch above shows its shape and it has no additional functions.

Overtopping Device

US West Coast Tide Height Analysis

Research shows that as tide height variance increases, efficiency of a stationary overtopping device decreases. We would like to position an overtopping device where the tide does not change much – ideally less than 1.84m, which is the average tidal variance at the Port of Garibaldi, OR where an overtopping device was planned to be constructed. This would have been incorporated into a jetty reconstruction project. This location and four others on the US West Coast were studied to determine tide height variance. Generally, moving farther north on the US Pacific coast will mean a larger tidal variance. The equation describing tidal variance as a function of north latitude is:

Equation 1

$$Avg.Tidal\ Variance\ (m) = 16.72 * N.Latitude\ (degrees) + 15.843$$

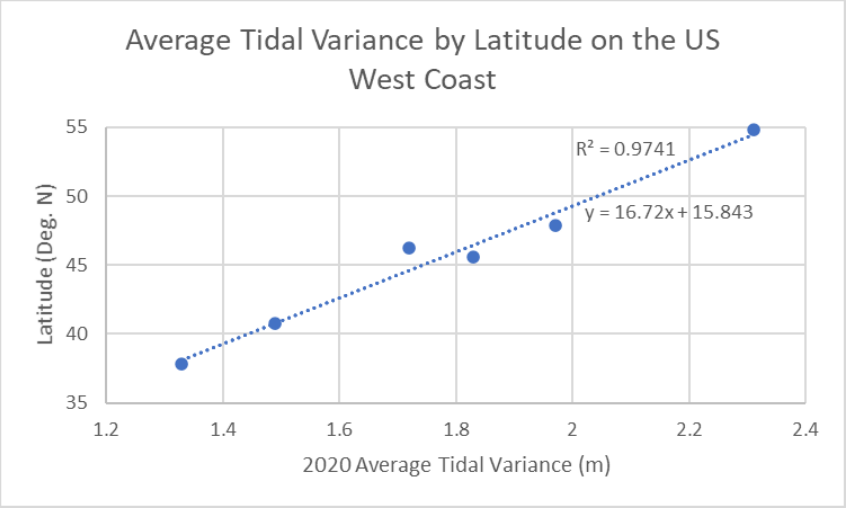

Figure 23: Average Tidal Variance by North Latitude on the US West Coast

North Jetty, Tillamook Bay, OR			Point Bonita, San Francisco, CA			North Spit, Humboldt Bay, CA		
Year 2020	Tide Height (cm)		Year 2020	Tide Height (cm)		Year 2020	Tide Height (cm)	
Overall	Average	131	Overall	Average	102	Overall	Average	113
	Median	142		Median	113		Median	124
	St. Dev.	101		St. Dev.	75		St. Dev.	84
High Tide	Average	223	High Tide	Average	168	High Tide	Average	188
	Median	221		Median	167		Median	186
	St. Dev.	31		St. Dev.	23		St. Dev.	29
Low Tide	Average	40	Low Tide	Average	35	Low Tide	Average	38
	Median	37		Median	34		Median	38
	St. Dev.	52		St. Dev.	42		St. Dev.	47
Tide Deviation	Average	183	Tide Deviation	Average	133	Tide Deviation	Average	149
	Median	184		Median	133		Median	148

Columbia R. Entr., N. Jetty, OR			La Push, WA		
Year 2020	Tide Height (cm)		Year 2020	Tide Height (cm)	
Overall	Average	126	Overall	Average	141
	Median	129		Median	147
	St. Dev.	94		St. Dev.	109
High Tide	Average	212	High Tide	Average	239
	Median	212		Median	239
	St. Dev.	30		St. Dev.	35
Low Tide	Average	40	Low Tide	Average	42
	Median	35		Median	41
	St. Dev.	46		St. Dev.	55
Tide Deviation	Average	172	Tide Deviation	Average	197
	Median	177		Median	198

Figure 24: Tide Height Statistics at Five Locations on the US West Coast

Point Bonita, San Francisco, CA	**North Spit, Humboldt Bay, CA**	**Columbia River Entrance, North Jetty, OR**	**La Push, WA**
This location on the coastline, while probably protected by law due to its vicinity to the city, should be a good indication of conditions on the sea-facing coast near San Francisco. Tidal range is desirable at 1.33m.	This spot is in northern CA close to OR. The narrow spit forms a natural breakwater protecting the bay, an ideal location to add an overtopping device facing the open sea.	This data is meant to predict coastal tide data near the Columbia River entrance on the border between OR and WA.	This data is meant to predict coastal tide data in northern WA near the border with Canada.

Table 9: Descriptions of Tide Height Study Locations

Location and Wave Climate Analysis

The wave climate of a location is the distribution and probably of the characteristics that describe the sea state. The wave power, significant wave height, and average period of waves are used to determine device dimensions best suited for that location and estimate the power output per year. The average wave power for a period of time is calculated using Equation 2 (B.G. Reguero, 2015) where P is the wave power in units of watts per meter, c_g is the group velocity of the wave in units of meters per second, and $S(f)$ is the sea state as a function of frequency.

Equation 2

$$P = \rho g \int c_g(f) \cdot S(f) df$$

The group velocity is calculated using Equation 3 (B.G. Reguero, 2015) where k is the wave number, h is the mean water depth, T is the period of the wave, and L is the wavelength. The relation between wave number and wavelength is given by Equation 4. The dispersion equation relating wavelength and period of a wave defined by Equation 5. In order to isolate k from the dispersion equation Guo's Approximation Equation 6 (Fenton, 2006) used. Equation 3

$$c_g = \frac{1}{2}\left(1 + \frac{2kh}{\sinh(2kh)}\right)\frac{L}{T}$$

Equation 3

$$c_g = \frac{1}{2}\left(1 + \frac{2kh}{\sinh(2kh)}\right)\frac{L}{T}$$

Equation 4

$$k = \frac{2\pi}{L}$$

Equation 5

$$\left(\frac{2\pi}{T}\right)^2 = gktanh(kh)$$

Equation 6

$$k = \frac{\sigma^2}{g}\left(\left(1 - e^{-\left(\sigma\sqrt{h/g}\right)}\right)^{5/2}\right)^{-2/5}$$

The spectral wave density data for each location is extracted from the National Data Buoy Center (Historical NDBC Data, 2020) for the year 2020 and imported into a MATLAB script shown in Figure 25. The spectral density means at each frequency are calculated for the entire time period which is one year. In order to account for the probability of occurrence of each sea state in the wave climate parameters the zeroth, first, and second order statistical moments are calculated using Equation 7 where n is the order number. From this significant wave height can be determined for the location data set using Equation 8 (National Data Buoy Center, 2018). Once determined, these parameters will be used to finalize a location and determine device dimensions and estimates for yearly output power. The output parameters based on spectral wave density data for the year 2020 at various locations are shown in Table 10.

Equation 7

$$m_n = \sum_{f_i}^{f_f} S(f) \times d(f) \times f^n$$

Equation 8

$$H_s = 4 \times \sqrt{m_0}$$

Figure 25: Wave Power Calculations MATLAB Script

```
%Wave Power Calculations - Irregular Waves
%Last Updated: 2/23/2021 Time 5:37pm

%water depth and angle of direction of wave kept constant for now to
%simplify
%Format and Define Constants
format short
clear;
clc;
rho = 997; %density of water (kg/m^3)
alpha = 0.538;
g = 9.81; %gravity constant (kg*m/s^2)

%Initialize Based on Location and Buoy data
buoylocation = "West Oregon 275NM NW west of Coos Bay, OR";%---- MUST
 BE UPDATED BASED ON STATION LOCATION
coast_location = 'Floras Creek Outlet, OR'; %---- MUST BE UPDATED
 BASED ON STATION LOCATION
h = 3455; %water depth at buoy (m) ---- MUST BE UPDATED BASED ON
 STATION LOCATION
h2 = 19; %water depth closer to shore (m) ---- MUST BE UPDATED BASED
 ON LOCATION
lat = 42.6; %Latitude ---- MUST BE UPDATED BASED ON STATION LOCATION

%Load Data for Spectral Density and assign to variables
filename = '46002.txt';
    dataimport = importdata(filename); %Station Spectral Density Year
 2020
    data = dataimport.data(:,:);
    sz = size(data); %output vector is matrix size [m,n]
freq = data(1,1:sz(2)); %frequency bins
S = data(2:sz(1),1:sz(2)); %matrix of spectral densities
    sz2 = size(S); %[m,n] vector of size of spectral density matrix
time = [1:1:sz2(1)]; %time vector - unit step in hours

%Calculate Spectral Density Means at each frequency
for count = 1:sz2(2) %until the amount of frequency bins is reached
    Sf(count) = mean(S(:,count)); %averages values over the whole year
 of spectral density at a single frequency
end

%Calculate probability of sea state occurance
for count = [1,1:sz(2)]
    n(count)=nnz(S(:,count));
    fn(count) = n(count)/sz2(1); %how often these sea  states occur
 for each frequency
end
%Calculate frequency bin size
for count = 1:sz2(2);
    if count == 1;
        ft(count) = freq(count);
    else
```

```
        ft(count) = freq(count)-freq(count-1); %bin sizes
    end
end
%END

%Calculate Order Moments of Wave Spectrum
for n = 1:3 % 0 1 and 2 order moments
    for count = 1:sz2(2) %until the amount of frequency bins is
 reached
        if count == 1
            m_s(count) =
 (freq(count)^(n-1))*Sf(count)*(freq(count));%k=count value of moment
 series - for first frequency-- bin size is itself
        else
            m_s(count) = (freq(count)^(n-1))*Sf(count)*(freq(count)-
freq(count-1));%k=count value of moment series; size of frequency bin
 is f(k)-f(k-1)
        end
    end
    m(n) = sum(m_s); %vector of moments
end

%Zero Order Moment: area under spectral curve
%First Order Moment: Mean
%Second Order Moment: Sample Variance
m0 = m(1);
m1 = m(2);
m2 = m(3);

%Calculate Wave Constants at Buoy Location
Hm0 = 4.004*sqrt(m0); %Wave Height of m0
T = 1./freq; %wave period
Tm = mean(T); %mean period
sig = (2*pi())./T;
k = ((sig.^2)./g).*(((1-exp(-((sig.*sqrt(h/
g)).^(5/2))))).^(-2/5));%calculates a vector of wavenumbers for each
 frequency based on Guo's approximation (deeper wave--smaller wave
 number)
L = (2*pi())./k; %vector of wave lengths for each frequency
Te = Tm*alpha; %energy period
Hs = 4*sqrt(m0); %significant wave height
pd = sqrt(m0/m2);%dominant/peak wave period

%Average Wavelength
 BWLA = mean(L.*fn);%(m)

for count = 1:length(T);
cg(count) = (1/2)*(1+((2*k(count)*h)/(sinh(2*k(count)*h))))*(L(count)/
T(count)); %group velocity
end

%Wave Power Calculations at Buoy Location
for count = 1:sz2(2); %until the amount of frequency bins is reached
        if count == 1;
```

```
            P1(count) = cg(count)*Sf(count)*(freq(count));%k=count
 value of moment series - for first frequency-- bin size is itself
        else
            P1(count) = cg(count)*Sf(count)*(freq(count)-
freq(count-1));%k=count value of moment series, frequency bin is f(k)-
f(k-1)
        end
        PwB = rho*g*sum(P1); % average wave power (W/m)
end

%Calculate Wave Constants at Coastal Location
Hm0C = 4.004*sqrt(m0); %Wave Height of m0
TC = 1./freq; %wave period
TmC = mean(TC); %mean period
sigC = (2*pi())./TC;
kC = ((sigC.^2)./g).*(((1-exp(-((sigC.*sqrt(h2/
g)).^(5/2))))).^(-2/5)); %calculates a vector of wavenumbers for each
 frequency based on Guo's approximation
LC = (2*pi())./kC; %vector of wave lengths for each frequency
TeC = TmC*alpha; %energy period
HsC = 4*sqrt(m0); %significant wave height
pdC = sqrt(m0/m2);%dominant/peak wave period

%Average Period
CPA = mean(TC.*fn)%(s)

%Average Wavelength
CWLA = mean(LC.*fn);%(m)

for count = 1:length(TC);
cgC(count) = (1/2)*(1+((2*kC(count)*h2)/
(sinh(2*kC(count)*h2))))*(LC(count)/TC(count)); %group velocity
end

%Average Group Velocity
CGVA = mean(cgC.*fn)%(m/s)

%Wave Distance Traveled Over One Period
wdt = CPA*CGVA %(m)

%Wave Power Calculations at Coastal Location
for count = 1:sz2(2); %until the amount of frequency bins is reached
        if count == 1;
            P1(count) = cgC(count)*Sf(count)*(freq(count));%k=count
 value of moment series - for first frequency-- bin size is itself
        else
            P1(count) = cgC(count)*Sf(count)*(freq(count)-
freq(count-1));%k=count value of moment series, frequency bin is f(k)-
f(k-1)
        end
        PwC = rho*g*sum(P1); % average wave power (W/m)
end
```

```
% Coastal Location: Ocean Shores - Aberdeen,WA
% Station Number: 46041.txt
% Latitude at Buoy Location: 4.720000e+01
%
% Water Depth at Buoy (m): 128
% Average Wave Power at Buoy(Year 2020) (W/m) : 3.444377e+04
% Significant Wave Height at Buoy (m): 2.628835e+00
% Dominant Wave Period at Buoy (s): 7.757314e+00
% Average Wave Length at Buoy (m): 8.245447e+01
%
% Water Depth near shore (m): 2.010000e+01
% Average Wave Power at Coast(Year 2020) (W/m) : 3.673159e+04
% Significant Wave Height at Coast (m): 2.628835e+00
% Dominant Wave Period at Coast (s): 7.757314e+00
% Average Wave Length at Coast (m): 5.802747e+01

% Buoy Location:Grays Reef - 40NM Southeast of Savannah, GA
% Coastal Location: Ossabaw Island, GA
% Station Number: 41008.txt
% Latitude at Buoy Location: 3.140000e+01
%
% Water Depth at Buoy (m): 16
% Average Wave Power at Buoy(Year 2020) (W/m) : 3.873130e+03
% Significant Wave Height at Buoy (m): 1.082801e+00
% Dominant Wave Period at Buoy (s): 4.930776e+00
% Average Wave Length at Buoy (m): 4.255882e+01
%
% Water Depth near shore (m): 1
% Average Wave Power at Coast(Year 2020) (W/m) : 2.082766e+03
% Significant Wave Height at Coast (m): 1.082801e+00
% Dominant Wave Period at Coast (s): 4.930776e+00
% Average Wave Length at Coast (m): 1.422966e+01

% Buoy Location:Stonewall Bank - 20NM West of Newport,OR
% Coastal Location: Yaquina Head - Newport,OR
% Station Number: 46050.txt
% Latitude at Buoy Location: 4.420000e+01
%
% Water Depth at Buoy (m): 160
% Average Wave Power at Buoy(Year 2020) (W/m) : 3.288363e+04
% Significant Wave Height at Buoy (m): 2.595997e+00
% Dominant Wave Period at Buoy (s): 7.625684e+00
% Average Wave Length at Buoy (m): 8.345933e+01
%
% Water Depth near shore (m): 1.828000e+01
% Average Wave Power at Coast(Year 2020) (W/m) : 3.503283e+04
% Significant Wave Height at Coast (m): 2.595997e+00
% Dominant Wave Period at Coast (s): 7.625684e+00
% Average Wave Length at Coast (m): 5.631873e+01

% Buoy Location:18NM West of San Francisco, CA
% Coastal Location: Bolinas Point, CA
% Station Number: 46026.txt
% Latitude at Buoy Location: 3.775000e+01
```

```
%
% Water Depth at Buoy (m): 5.490000e+01
% Average Wave Power at Buoy(Year 2020) (W/m) : 1.865436e+04
% Significant Wave Height at Buoy (m): 1.910010e+00
% Dominant Wave Period at Buoy (s): 7.021763e+00
% Average Wave Length at Buoy (m): 7.880560e+01
%
% Water Depth near shore (m): 22
% Average Wave Power at Coast(Year 2020) (W/m) : 1.850897e+04
% Significant Wave Height at Coast (m): 1.910010e+00
% Dominant Wave Period at Coast (s): 7.021763e+00
% Average Wave Length at Coast (m): 6.266323e+01


% Buoy Location:Santa Maria 21NM NW of Point Arguello, CA
% Coastal Location: Rocky Point - Point Arguello, CA
% Station Number: 46011.txt
% Latitude at Buoy Location: 3.490000e+01
%
% Water Depth at Buoy (m): 4.648000e+02
% Average Wave Power at Buoy(Year 2020) (W/m) : 2.127240e+04
% Significant Wave Height at Buoy (m): 2.093388e+00
% Dominant Wave Period at Buoy (s): 7.350626e+00
% Average Wave Length at Buoy (m): 9.388351e+01
%
% Water Depth near shore (m): 2.010000e+01
% Average Wave Power at Coast(Year 2020) (W/m) : 2.282231e+04
% Significant Wave Height at Coast (m): 2.093388e+00
% Dominant Wave Period at Coast (s): 7.350626e+00
% Average Wave Length at Coast (m): 6.197034e+01


CPA =

    6.0079


CGVA =

    4.8225


wdt =

   28.9730

Buoy Location:West Oregon 275NM NW west of Coos Bay, OR
Coastal Location: Floras Creek Outlet, OR
Station Number: 46002.txt
Latitude at Buoy Location: 4.260000e+01

Water Depth at Buoy (m): 3455
Average Wave Power at Buoy(Year 2020) (W/m) : 7.009968e+04
Significant Wave Height at Buoy (m): 3.685372e+00
```



```
Dominant Wave Period at Buoy (s): 8.290531e+00
Average Wave Length at Buoy (m): 9.544170e+01

Water Depth near shore (m): 19
Average Wave Power at Coast(Year 2020) (W/m) : 7.470079e+04
Significant Wave Height at Coast (m): 3.685372e+00
Dominant Wave Period at Coast (s): 8.290531e+00
Average Wave Length at Coast (m): 6.161151e+01
```

Published with MATLAB® R2020a

Location	Latitude (°)	Water Depth (m)	Significant Wave Height (m)	Dominant Wave Period (s)	Average Wave Power (W/m)
Western Gulf of Alaska - Kodiak, AK	42.5	38.7	2.92	7.44	43040
West Oregon - Coos Bay, OR	42.65	19	3.68	8.29	74700
Cape Elizabeth - Aberdeen, WA	47.2	20.1	2.63	7.76	36730
Stonewall Bank - Newport, OR	44.2	18.3	2.6	7.63	35033
West of San Francisco, CA	37.75	22	1.91	7.02	18509
Rocky Point - Point Arguello, CA	34.9	20.1	2.09	7.35	22822

Table 10: Wave Climate Parameters Based on Location (Year 2020)

The location and wave climate research were used to determine the optimal geometry by calculating the corresponding hydraulic efficiency of the device. This is because the optimal geometry, the geometry that results in the highest efficiency and overtopping discharge, for an overtopping device is highly dependent on the wave and tide climate. The main wave climate parameters that effect overtopping is the significant wave height, water level, wave peak, and wave period (Vicinanza, 2012). The most important geometry feature is the crest freeboard of the reservoirs, the vertical distance from the mean water level to the reservoir height. Due to this, the existing equations for calculating the overtopping discharge for reservoir m q_m are heavily dependent on the crest freeboards $R_{c,m}$ and significant wave height H_s. Equation 9 is used to calculate the overtopping discharge of reservoir m (Kofoed, 2002).

Equation 9

$$q_m(z_1, z_2) = \lambda_{d_r}\sqrt{gH_s^3}\frac{A}{B}e^{C\frac{R_{c,m}}{H_s}}\left(e^{B\frac{z_2}{H_s}} - e^{B\frac{z_1}{H_s}}\right)$$

Where:

$q_m(z_1, z_2)$ = Overtopping discharge of reservoir m per unit width ($m^3/s/m$)

λ_{d_r} = Correction factor describing the influence of limited draught on the average overtopping discharge

g = Acceleration due to gravity $\frac{m}{s^2}$

H_s = Significant wave height (m)

A = 0.37

B = -4.5

C = 3.5

$R_{c,m}$ = Reservoir crest freeboard (m)

z_2 = Upper reservoir boundary (m) ($R_{c,1}$ for reservoir 1, $R_{c,2}$ for reservoir 2)

z_1 = lower reservoir boundary (m) ($R_{c,2}$ for reservoir 2, $2 * R_{c,2}$ for reservoir 2)

Variables $A, B,$ and C are taken from previous linear regression analysis based on the significant wave height (Kofoed, 2002) To significantly simplify calculations, it is assumed that the draught correction factor λ_{d_r} is 1. The corresponding energy in overtopping for each reservoir m is calculated with Equation 10.

Equation 10

$$P_m = q_m z_1 \rho_w g$$

Where:

P_m = Energy in overtopping for reservoir m (W/m)

ρ_w = Water density (kg/m^3)

Incorporating the turbine efficiency, the total energy for a single wave state is calculated with Equation 11. The hydraulic efficiency is then calculated with Equation 12.

Equation 11

$$P(H_s) = P_m \eta_{turb}$$

Where:

$P(H_s)$ = Total overtopping power per unit length (W/m)

η_{turb} = Turbine efficiency (%)

Equation 12

$$\eta_{hydr} = \frac{P}{P_{wave}}$$

Where:

η_{hydr} = Hydraulic efficiency (%)

P = Total overtopping power per unit length (W/m)

P_{wave} = Power of incoming wave per unit length (W/m)

As the final design test rig will not have a turbine in the overtopping device, only a flow sensor, it is assumed that the turbine efficiency is equal to 1. It was found in previous research

from Kofoed that a reasonable $h_{l,m}$ value, the horizontal distance of the reservoir openings, is 1.2m for various wave states (Kofoed, 2002). Additionally, it was found that a good $R_{c,1}$ value is 2.3m with a $\triangle z$ of 1.33m for a corresponding significant wave height of 2.5m, close to the average of the significant wave heights at the research location (Kofoed, 2002). An appropriate draught value d_r is 0.325 the total depth at the location, and so 8m was determined to be a good choice for the draught at the chosen locations. These dimensions were used to calculate the hydraulic the efficiency and power capacity at each researched location, seen in Figure 26. Koefed determined an approximate 6.25% reduction of the hydraulic efficiency is experienced for every meter of tidal variance, which was incorporated in the calculations as well.

Geometry	
Slope Angle (deg)	35
Reservoir 1 Crest Freeboard Rc1 (m)	2.3
Reservoir 2 Crest Freeboard Rc2 (m)	3.63
z1	2.3
z2	3.63
z3	7.26
Device frontal width (m)	20
dr	8

Calculations						
Location	San Fransisco	Western Gulf of Alaska	Cape Elizabeth	Stonewall Bank	Santa Maria Point	Coos Bay,OR
Latitude (degrees N)	37.75	42.5	47.2	44.2	34.9	42.65
Average Tidal Variance (m)	1.31	1.59	1.88	1.70	1.14	1.60
Tidal Reduction Factor	0.918	0.900	0.883	0.894	0.929	0.900
Water Depth (near coast) (m)	22	38.7	20.1	18.28	20.1	19
Significant Wave Height Hs (m)	1.91	2.915	2.63	2.6	2.09	3.685
Pwave (W/m)	18508	43042	36730	35030	22822	74700
q1 (m3/s/m)	0.195010028	0.507536282	0.411036073	0.401153613	0.244115338	0.783586884
q2 (m3/s/m)	0.101602175	0.367586152	0.2757143	0.266765489	0.136951568	0.672166459
P1 based on Rc1 (W/m)	4488.011481	11680.57196	9459.691052	9232.253547	5618.133848	18033.67228
P2 based on Rc2 (W/m)	3690.445603	13351.65021	10014.63432	9689.591092	4974.424134	24414.77025
nturb1	1	1	1	1	1	1
nturb2	1	1	1	1	1	1
Ptot (W/m)	7509	22538	17192	16916	9838	38195
nhydr (hydraulic efficiency)	0.4057	0.5236	0.4681	0.4829	0.4311	0.5113
Power Capacity (kW)	150	451	344	338	197	764
Power per year (MWh)	1315.53	3948.64	3011.98	2963.71	1723.62	6691.74

Figure 26: Hydraulic Efficiency and Power Capacity at Chosen Locations

With these dimensions, it is seen that the power capacity and hydraulic efficiency at every location is very comparable to existing implemented designs. With Coastal Current's proposed design that introduces constructive interference, the power capacity and hydraulic efficiency will increase and add value not seen in existing implemented designs. Once these calculations were completed to determine the proper crest freeboard and total width dimensions, all other preliminary dimensions were determined, shown in Table 11 below.

Dimension	Description	Value
h	Water depth at toe of structure	20m
C_r	Device crest Level	1.5*Rc2
R_{c1}	Reservoir 1 crest level	2.3m
R_{c2}	Reservoir 2 crest level	3.63m
D_r	Ramp draught	-8.00m
α	Ramp angle	30°
Θ_1	Front angle 1	35°
Θ_2	Front angle 2	35°
d_T	Turbine Diameter	4.0m
HD1	Horizontal distance between reservoir 1 and 2	1.20m

HD2	Horizontal distance between reservoir 2 and device crest level	1.20m
R_{w1}	Horizontal distance from reservoir 1 front to device back	9.585m
R_{w2}	Horizontal distance from reservoir 2 front to device back	7
T	Overtopping base length	23.71m
w_b	Overtopping back width	10m
w_f	Overtopping front ramp width	6m
H_c	Channel wall height	Approximately 2.3m above water

Table 11: Preliminary Overtopping Dimensions

After determining the preliminary dimensions for the overtopping device shown in Table 11, a solid part model was created in SolidWorks to ensure these dimensions were appropriate. However, it was obvious that the width proportions were incorrect, and the device would not function correctly. Changes were made to widen the back width w_b in proportion to the other dimensions. The front ramp width w_f was cut down from the sides, allowing the wave deflectors to move closer to the body of the overtopping device while still allowing incoming waves to run up the ramp. This also reduced the overall length of the full overtopping assembly, lessening its projection into the ocean and the associated construction costs.

To fit the entire prototype assembly in the Lyles Wave Pool at Purdue, the overtopping device needed to be scaled down significantly from its full-size dimensions. The back width w_b needed to be less than 11ft, so the scale was based on this dimension. The initial scale was chosen to be 1:8 so that w_b became 2.5m or about 8ft. However, this would have made the prototype large and difficult to assemble in the wave pool. The scale was decreased until it reached 1:32. At this scale, the overtopping device could be built more easily from smaller size, less costly materials. It could also be small and light enough to manufacture in a single piece and transport with only two people.

Dimension	Description	Full Size (meters/degrees)	Scaled Down for Wave Pool (m)	Scaled Down for Wave Pool (ft)
h	Water depth at toe of structure	20	0.625	2.050525
C_r	Device crest Level	5.44	0.170	0.5577428
R_{c1}	Reservoir 1 crest freeboard	2.304	0.072	0.23622048
R_{c2}	Reservoir 2 crest freeboard	3.632	0.114	0.37237534
D_r	Ramp draught	-8	-0.250	-0.82021
α	Ramp angle	30	30.000	30
Θ_1	Front angle 1	35	35.000	35
Θ_2	Front angle 2	35	35.000	35
d_T	Turbine Diameter	4	0.125	0.410105
HD1	Horizontal distance between reservoir 1 and 2	1.2	0.0375	0.1230315
HD2	Horizontal distance between reservoir 2 and device crest level	1.2	0.0375	0.1230315
R_{w1}	Horizontal distance from reservoir 1 front to device back	12.48	0.390	1.2795276
Ht	Total Device height	13.44	0.500	1.3779528
R_{w2}	Horizontal distance from reservoir 2 front to device back	7.008	0.219	0.71850396
T	Overtopping base length	28.112	0.879	2.88221794
w_b	Overtopping back width	40.8	1.275	4.183071
Wr	Overtopping Ramp width	20	0.625	2.050525
tw	wall thickness	0.4	0.0125	0.0410105
w_f	Overtopping front width	6	0.1875	0.6151575
H_c	Channel wall height	2.304	0.072	0.23622048
R	Curve radius	17.9104	0.560	1.836286148

Table 12: Final Prototype Dimensions at 1:32 Scale

Wave Gates

The original idea for the wave deflectors was to use servo motors to easily control the angle of the wave gates. However, we recognized that the wave gates would be holding a single position for extended amounts of time and the gate would be subjected to the forces of waves. If a servo motor would be used it would either need to be left on for an extended amount time and be constantly auto updating or be implemented with a solenoid break to resist back drive when power is not supplied to servo motor. We recognized that a worm gear and encoder could be

used to go to an assigned angular position and then turn off because a worm gear is self-locking and does not allow back drive.

The figure below shows the decision matrix used to decide between using a DC motor with an encoder and worm gear vs servo motor with solenoid brake.

[x indicates better option]	**Weight (1-5)**	***Servo Motor with Solenoid Break***	***DC Motor with encoder and Worm Gear***
Engineering Requirement			
Price	5		x
Ease of Preventing Backdrive	5		x
Controllability	1	x	
Robustness	4	x	
Ease of Controls Implementation	2	x	
Score		7	10

Figure 27: Decision Matrix for Wave Gate Mechanism Actuator

The figure below shows a sketch of the initial design of the wave gate mechanism. The sketch below uses a separate motor with a worm gear system. The actual CAD implements a motor with built in worm gear box.

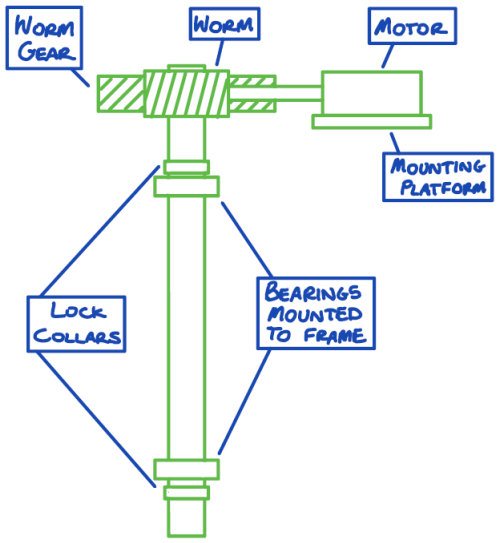

Figure 28: Sketch of Wave Gate Assembly Concept

Also, after further analysis it was determined that the controllable ramps at the bottom of the wave gates were not necessary. The proposed purpose of the ramps was to be able to control the period of reflecting waves in order to improve the chance of constructive interference. However, due to research and analysis it was decided that the shape and position of the wave gates and deflectors could possibly control the wave periods through drag on the walls and due to

the complexity of wave reflection it is unlikely the ramps would be able to accurately adjust the reflecting wave periods. Finally, due time constraints, we thought it was better to focus on the more critical systems.

Wave Deflectors

Initially, it was planned to have the deflectors use a peg board like system. This system would entail manual adjustment and locking of the wave deflectors. The system would also require users to take manual measurements. The sketch below shows this initial concept.

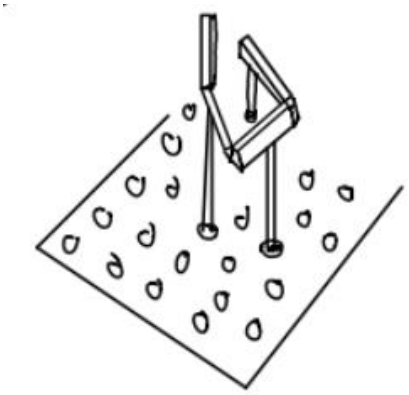

Figure 29: Initial Concept for Wave Deflectors

However, it was decided the wave deflectors should also be controllable and actuated. This was decided because of two major factors. First, the prototype was determined to be virtual, giving us more time to develop the design since time will not need to be spent on manufacturing. Second, many test wave pools, including the one here at Purdue, our constructed in a manner where the device cannot be easily accessed while in the pool so to manually adjust certain shapes the entire device would have to be removed from the wave pool.

Due to these reasons, concepts were developed to how to acuate the wave deflectors. The first concept that was investigated was a design involving point movement of 3 plates with angle and distance control from the edges of the frame. This would have been implemented with 3 rack and pinion assemblies with angular control through servos. A preliminary sketch of this design can be found in Figure 30: Wave Deflectors Design Idea Figure 30. It was decided that while this design provides incredible control of the exact position of the wave deflectors, that this would be too difficult to implement in a real-world system.

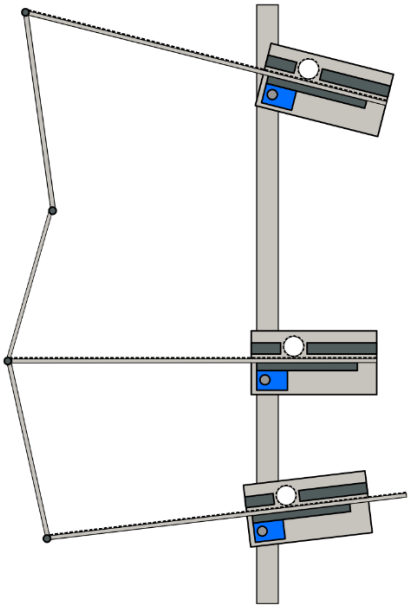

Figure 30: Wave Deflectors Design Idea 2

The next concept that was proposed was a 5-bar mechanism that would be able to control the exact position of 2 larger wave deflection walls. The advantage of this design is that all relative orientations of the wave deflectors can be achieved with only 2 actuators. A basic conceptual sketch of this idea can be seen below. This design was discarded due to the complexity of supporting the mechanism and the inability to make channel width adjustments without changing the angle of at least one deflector wall.

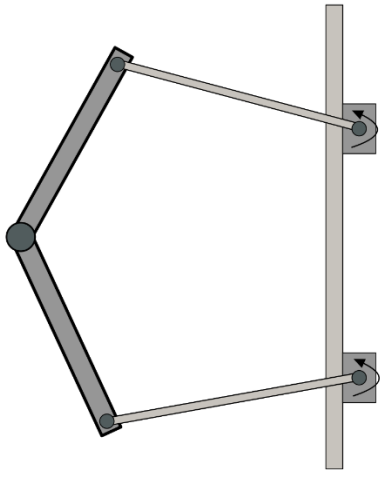

Figure 31: Wave Deflectors Design Idea 3

The design that was eventually decided upon for the Critical Design Review phase made slight compromises for deflector maneuverability but was designed to be very robust and to

provide the test cases that were deemed important for the validation of the reflection design. This mechanism involves a linear actuator to change the width of the reflection channels directly by translating a fixed angle center wave deflector. Attached to this center deflector are 2 motors to change inlet and outlet reflectors for the channels. A concept sketch for this design is pictured in Figure 32. This concept was then employed in SolidWorks for the virtual prototype and presented for the mid-fidelity prototype, seen in Figure 33.

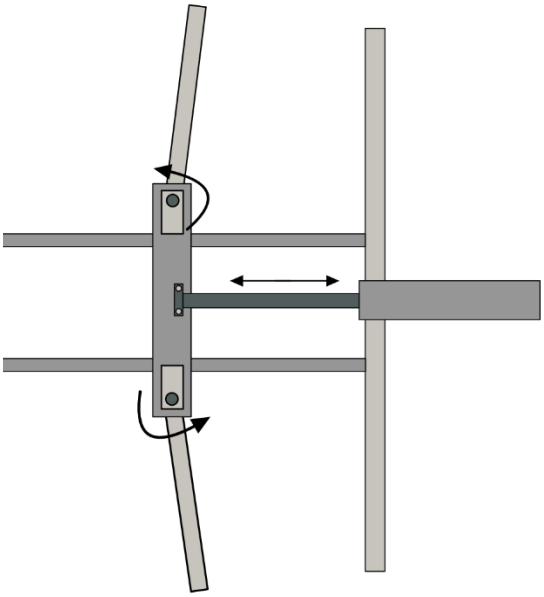

Figure 32: Concept Sketch of CDR Wave Deflector Actuators

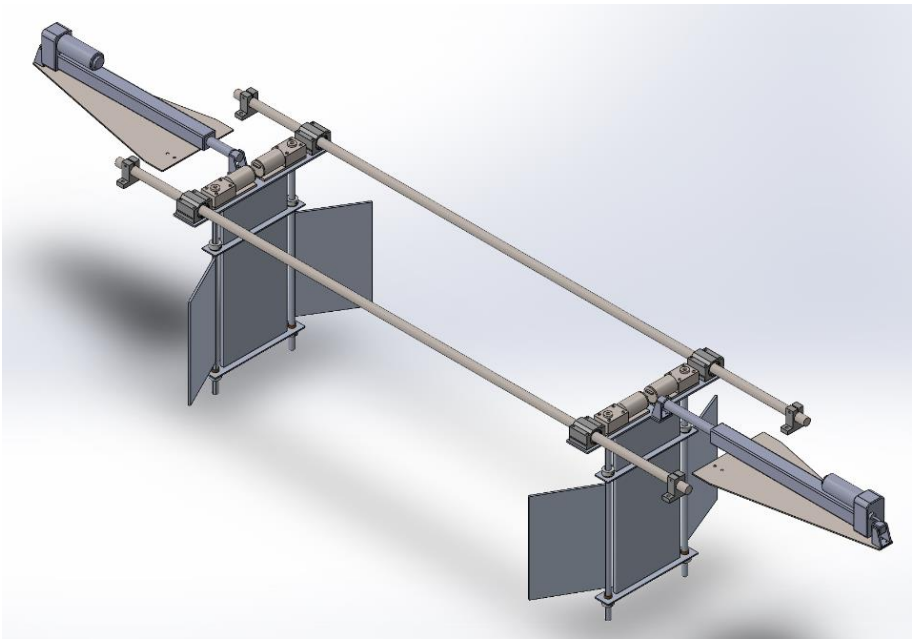

Figure 33: CDR Wave Deflectors

For the final design, the linear actuators were replaced with a rack and pinion system. The rack was made stationary by mounting to a square bar that ran across the center of the device. The pinion was attached to another worm gear of the same type used for the deflectors. This change was made because the linear actuators were extremely expensive at around $600 per unit. The extremely large price was due to the linear actuators' ability to output high amounts of force, but our design only required translational motion with very little required force output. The change also allowed all the systems to use the same actuator and limit switch which greatly simplified the controls process. Although the rack and pinion design does have some drawbacks regarding assembly process and its higher dependence on tolerances and deflections, further design improvement and engineering analysis could mitigate these drawbacks. The pros of the simplified controls and cost savings of almost $1000 outweighed the drawbacks.

Appendix G: Mechanical CAD

CDR CAD

Many key developments were made from the preliminary design to the Critical Design Review (CDR) design. The materials, mechanisms, and dimensions were determined for each of the four subsystems and then implemented in a 3D CAD model using SolidWorks, seen in Figure 34 and Figure 35. During the Final Design Review (FDR) phase, multiple changes and developments were made to the CDR design to improve the structural integrity, improve the measurement and control systems, reduce cost, and achieve a high-fidelity prototype, explained in further detail below.

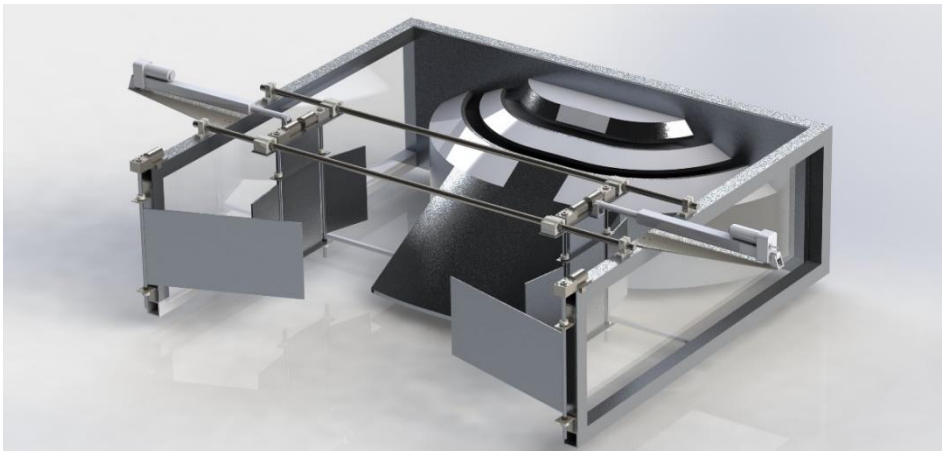

Figure 34: CDR Design - Isometric

Figure 35: CDR Design - Top View

Whole Assembly

The final design is seen below in Figure 36, Figure 37, Figure 38, and Figure 39. The design consists of four subassemblies: the frame, overtopping device, wave gate, and wave deflectors. Each subassembly plays a crucial role in the function of the test rig, explained in further detail in the following subsections. As seen, many design changes were made from the CDR design to the final design.

First, the linear actuation of the deflector sides was changed to a rack and pinion design, making the actuation much more cost effective and simplified, explained more in Appendix F – Wave Deflectors. Second, the height of the wave deflector plates was changed to change the wave parameters more effectively. Third, pressure sensors were added to the front of the overtopping device and side of the frame to measure the wave parameters of the overtopping and reflected waves, explained further in Appendix L. Fourth, flow sensors were added to each reservoir to measure the flow through the overtopping device, explained further in Appendix L. Fifth, the wave gate plate length was decreased to limit the amount of deflection that occurs, explained further in Appendix I – SolidWorks FEA. Finally, lots of development was made on the wiring and controls of the design, with the wires implemented in the SolidWorks model, explained more in Appendix J. Along with these crucial changes, the model was finalized by adding all fasteners, material properties, and photo rendering appearances to achieve a high-fidelity virtual prototype.

The full assembly without the controls components and wiring so that the mechanical components are easily visible is seen in Figure 36, Figure 37, and Figure 38 below. The full assembly with the controls and wiring is seen in Figure 39 and further explained in Appendix J. The overall dimensions and weight of the device are summarized in Figure 40 and Table 13.

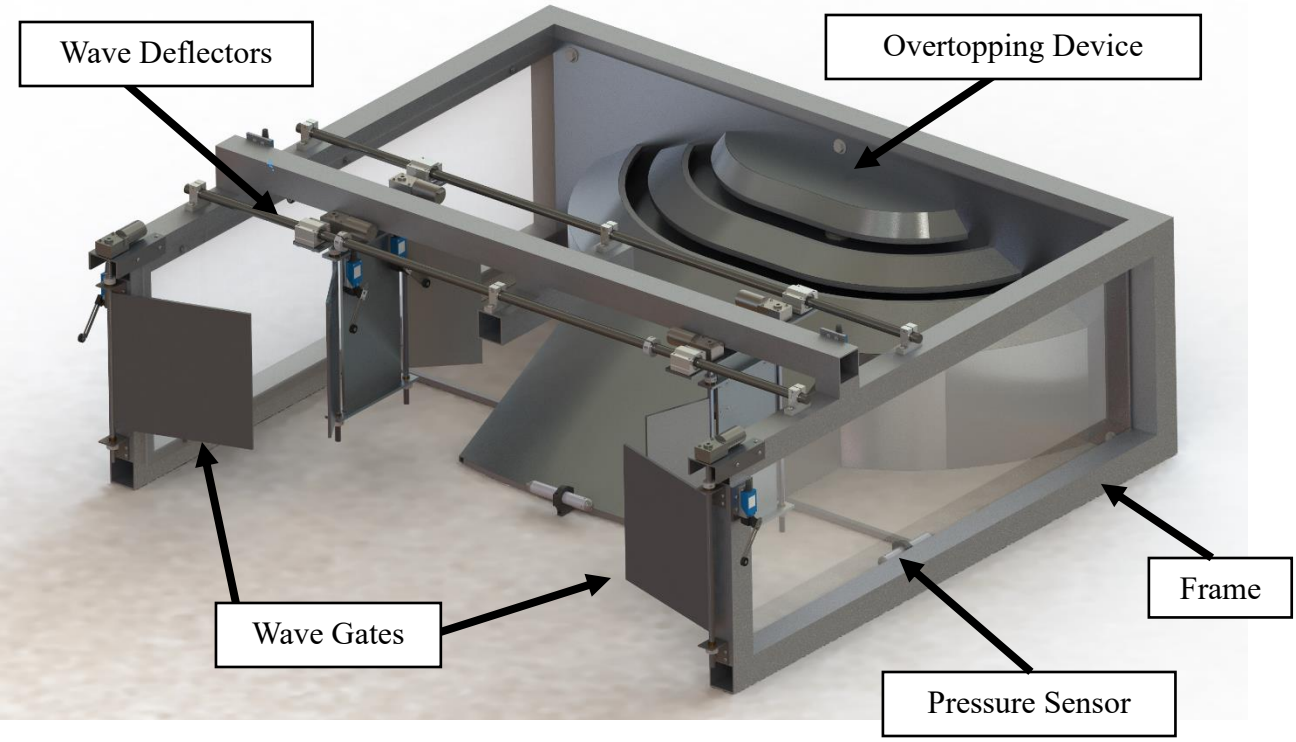

Figure 36: Whole Test Rig Assembly- Isometric View

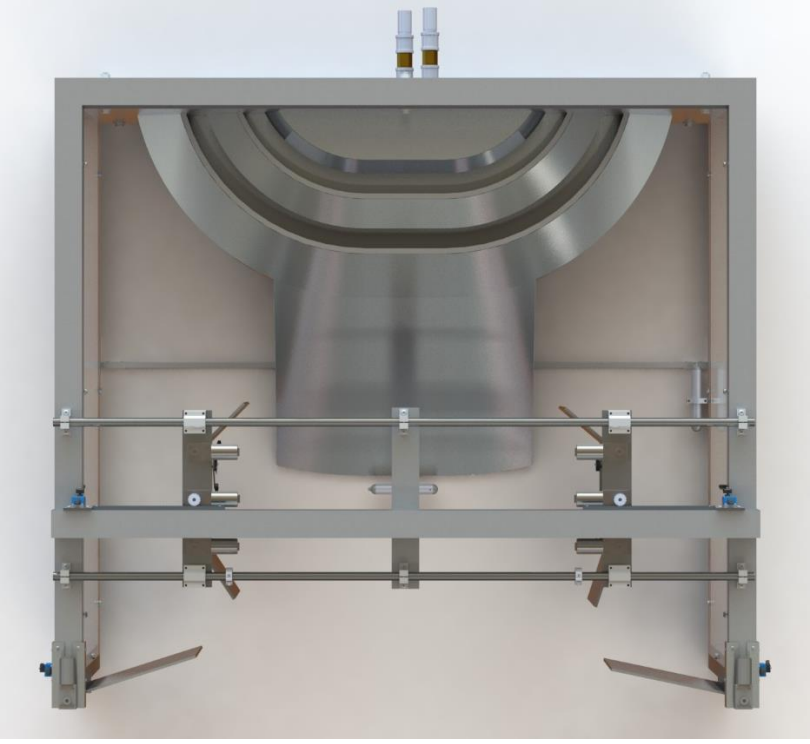

Figure 37: Whole Test Rig Assembly - Top View

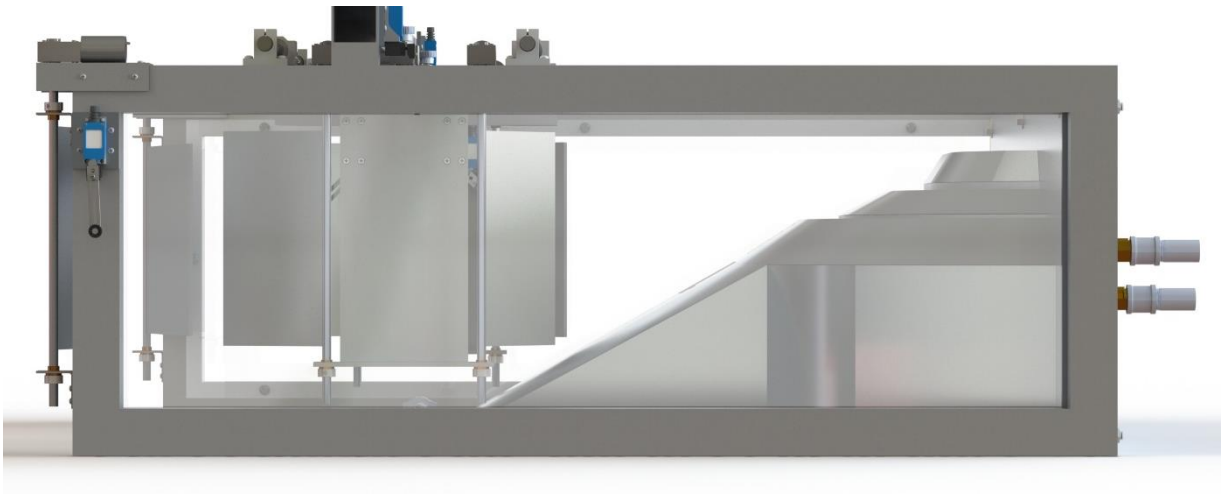

Figure 38: Whole Assembly - Side View

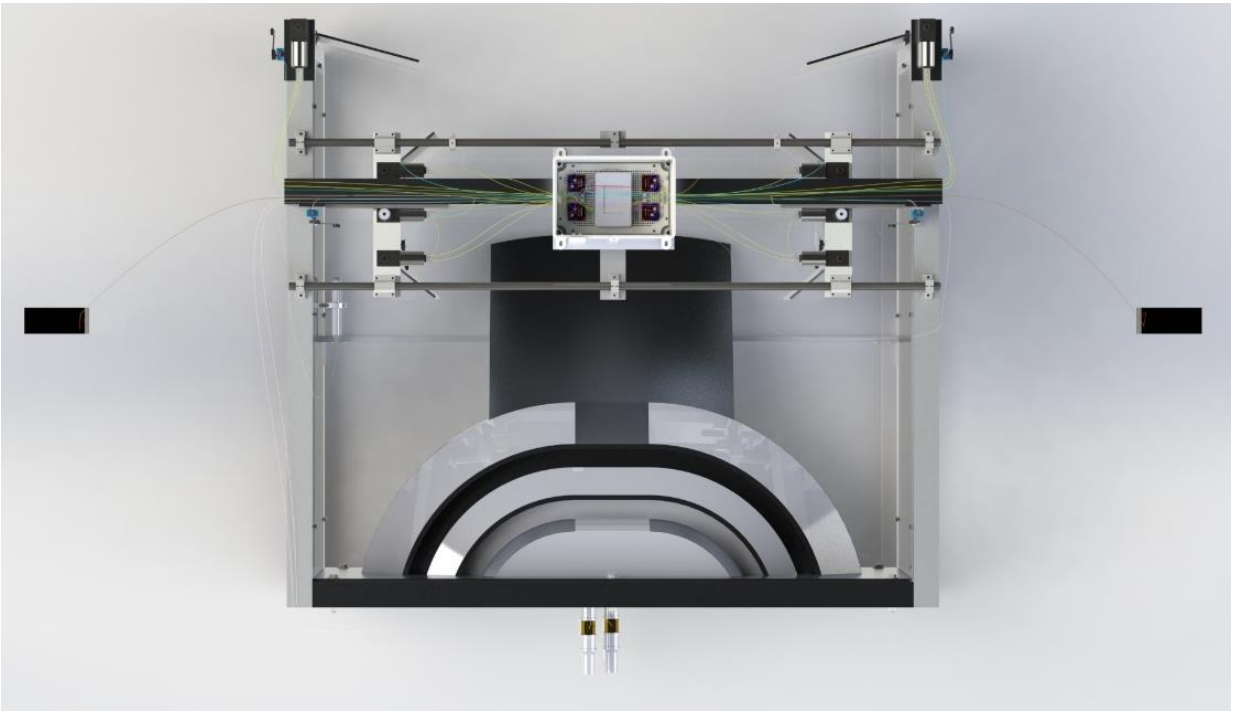

Figure 39: Whole Assembly with Wiring and Controls

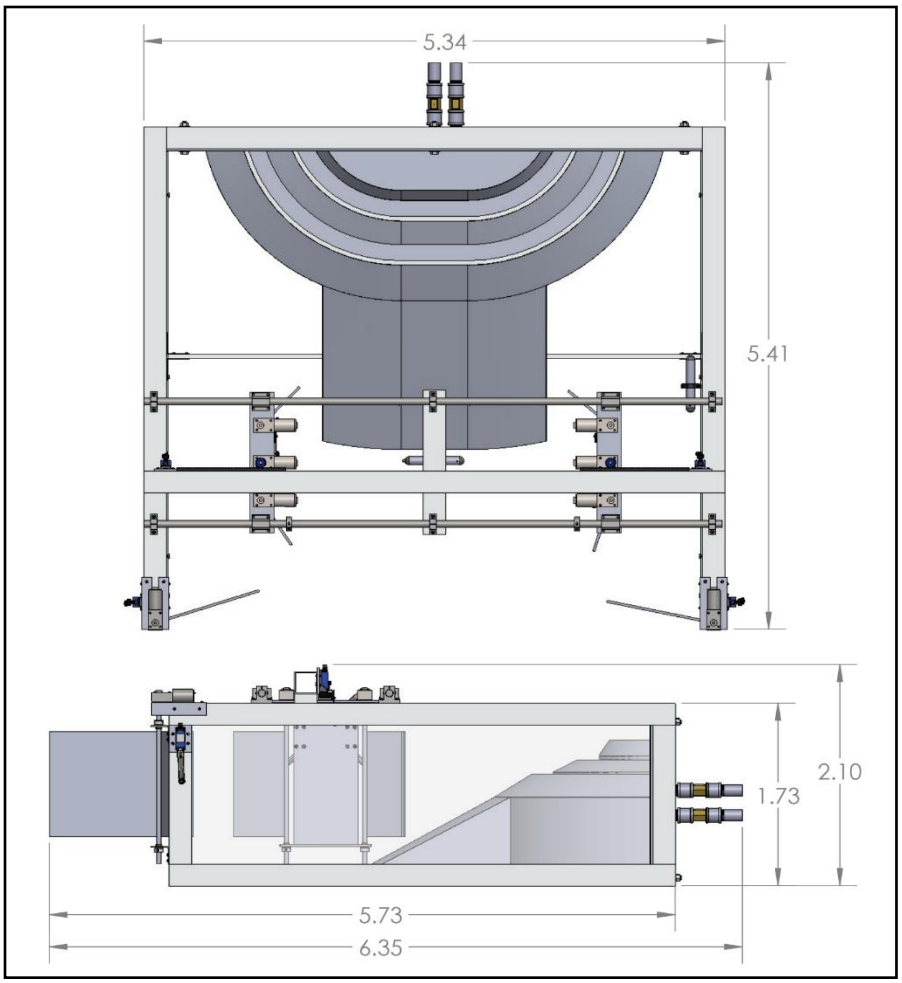

Figure 40: Test Rig Dimensions

Important Parameters	**Value**
Total Width	5.34ft
Total Height	2.10ft
Total Length with Retracted Wave Gates	5.41ft
Total Length with Extended Wave Gates	6.35ft
Total Weight	203lb
Frame Weight	66.6lb
Overtopping Weight	49.0lb
Wave Deflector Weight	58.9lb
Wave Gate Weight	7.0lb

Table 13: Overall Dimensions and Weight of Device

Frame

The frame, seen in Figure 41, is what the three other subassemblies are mounted to and provides structural support. It is made of 2.5” square 6061-aluminum bar from McMaster Carr. This bar is cut and then welded together. The sides of the frame are 1/8” thick acrylic plates secured by bolts and washers.

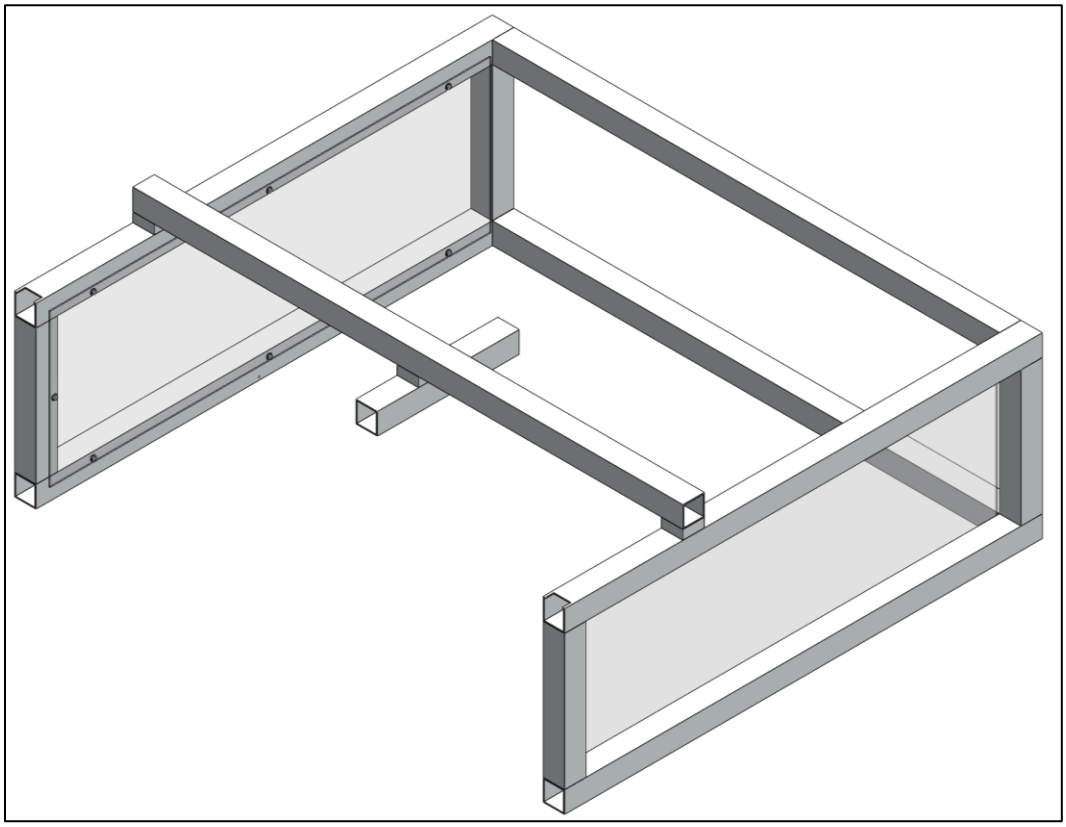

Figure 41: Device Frame

Overtopping Device

The overtopping device, shown in Figure 43, is constructed by welding sheet metal walls to a skeleton frame. The skeleton frame, shown in Figure 42**Error! Reference source not found.**, is made of 0.5” square 6061-aluminum bar from McMaster Carr while the sheet metal is 0.04” thick 3003-aluminum. The skeleton bars and sheet metal parts are cut and bent to the appropriate geometry and then welded together with 4043-aluminum filler material. The entire assembly is then welded to a 6061-aluminum backplate that will be mounted to the frame (Figure 41). These materials were chosen as they are corrosion resistant and weldable. Additionally, the 6061 is very strong which makes it a suitable choice for the skeleton and back plate, while 3003 is more lightweight making it more suitable for the sheet metal walls. While fiberglass or carbon fiber shells were considered in place of sheet metal as robust, waterproof plating options, they

were discarded due to their higher costs and difficult assembly. Both of these methods require forms to be constructed and would be more suitable for mass production.

A pressure sensor that measures the wave parameters is mounted to the front of the skeleton frame. Two flow sensors welded to each reservoir measure the flow through the reservoirs. The choice and details of these sensors is further explained in Appendix L. Fasteners chosen to secure the overtopping device to the frame were all stainless steel for corrosion resistance. In back, four ½" bolts will hold the backplate to the frame. Holes will be drilled all the way through the frame and these bolts will be secured with nuts on the other side. These bolts are large because the overtopping device is heavy and mostly supported from the back, so the fasteners need to be strong. To secure the protruding bars near the front of the overtopping device to the frame, #6 flathead machine screws were chosen. These countersunk screws will fit into the countersinks in the brackets and screw into threaded holes on the frame. Because the screws are smaller and too short to go all the way through the frame, threaded holes are necessary.

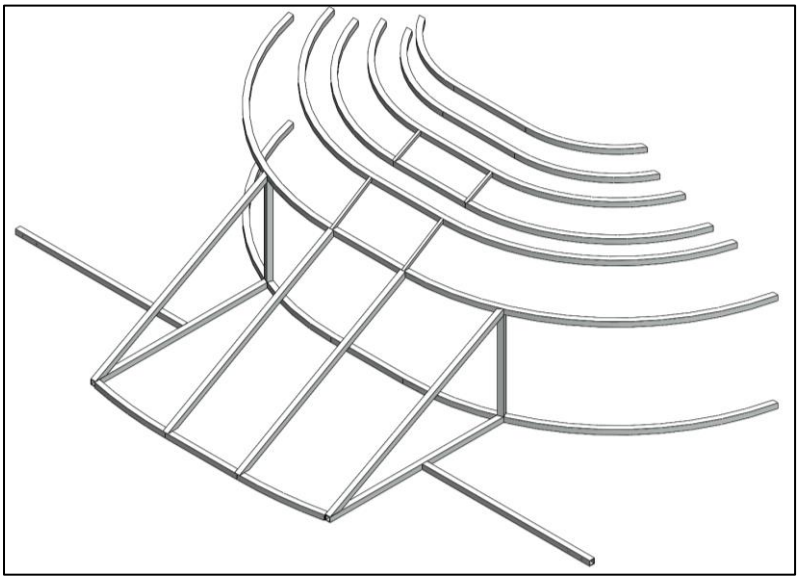

Figure 42: Overtopping Device Bar Stock Skeleton

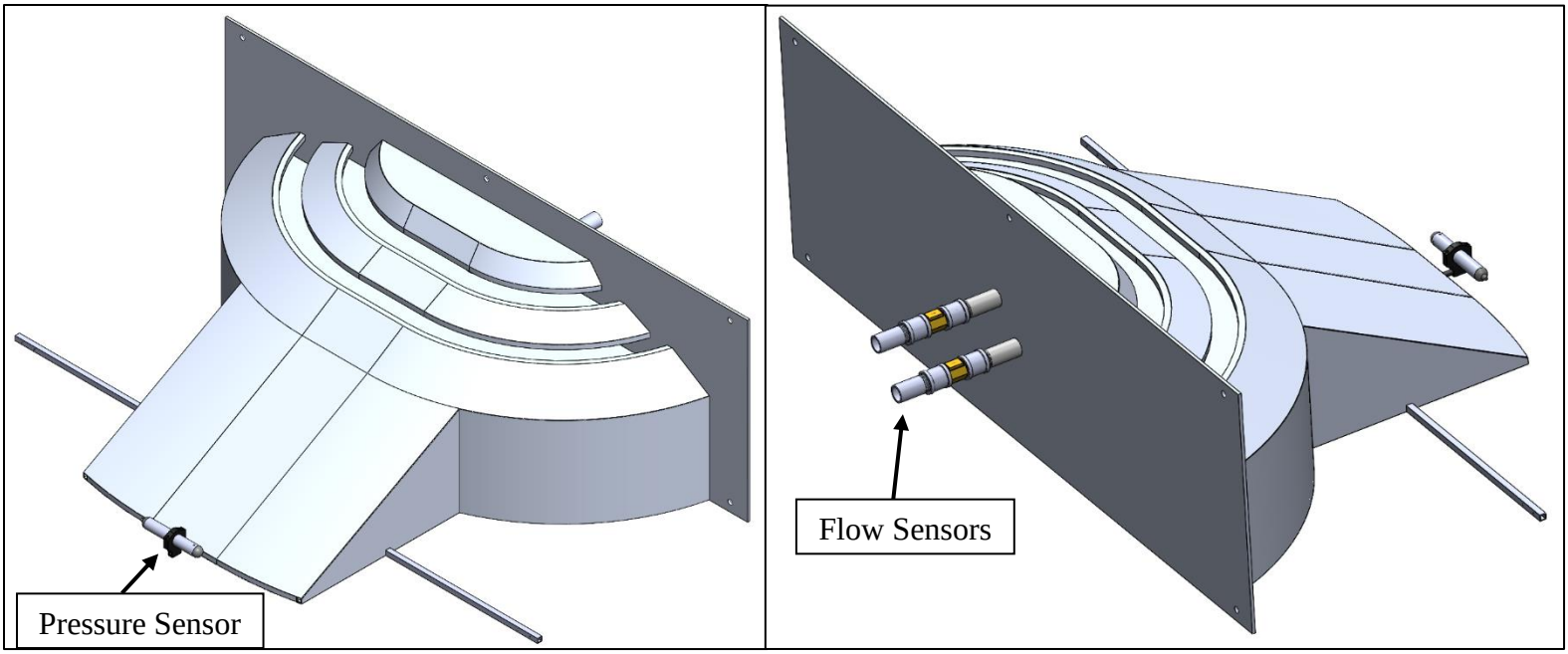

Figure 43: Overtopping Device Assembly with Sheet Metal

Wave Gates

The wave gate subassembly consists of an adjustable plate that focuses or squishes the reflected waves together to achieve a higher amplitude. The specific wave amplitude and parameters achieved are dependent on the angle of the wave gate, which is adjusted by a worm gear motor. The worm gear motor was chosen as it can lock in a desired angular position to resist the force of waves hitting the against it. The wave gates are assembled by welding a 0.25” thick 6061 aluminum plate to a 6061 aluminum D-shaft. There is a bushing, shaft collar, and L-bracket above and below the plate to hold the shaft in place and mount to the frame. The shaft is secured to the motor by a set screw going through the flats of the D-Shaft and Motor output shaft. The motor is secured to a mounting platen which is then secured to the frame. Aluminum 6061 was chosen for the mounting plate, gate, and shaft for its water resistance, weldability, and machinability. The bushing and shaft collar material were chosen to be water resistant and avoid binding as the shaft rotates. This design can be seen in Figure 44.

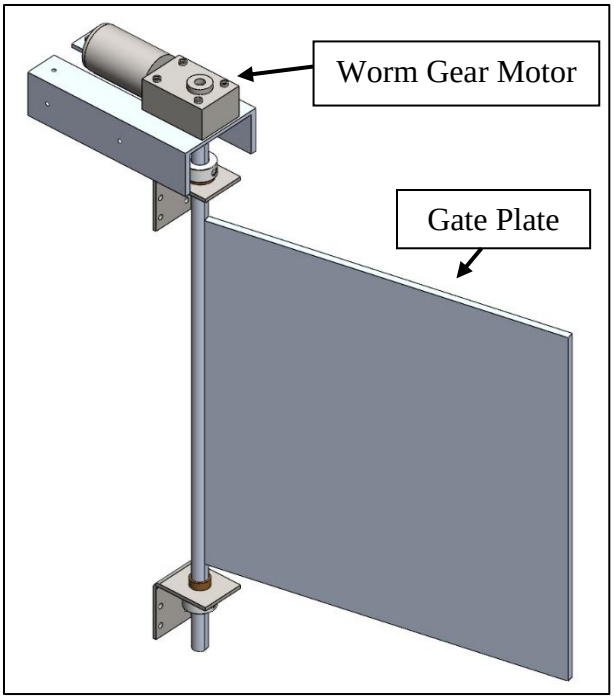

Figure 44: Wave Gate Assembly

Wave Deflectors

Like the wave gates, the wave deflectors are 0.25” thick 6061 aluminum plates welded to 6061 D-shafts and controlled by worm gear motors. There are two deflector plates per deflector side, connected by a 6061-aluminum welded base. The shafts are secured by the same bushings and shaft collars as in the wave gates. A rack and pinion assembly translate the wave deflector sides in and out on a pair of carbon steel support shafts supported by waterproof linear bearings. The rack is mounted to the frame support bar while the pinion is driven by a third worm geared DC motor. The two limit switches are mounted to the wave deflector base and help control the angular position of the deflector plates by marking the zero position. The rack and pinion are made from acetal and nylon respectively to be cost effective and corrosion resistant, but still meeting design requirements. Carbon steel was chosen for the support shafts because it is very strong, cost effective, and its poor corrosion resistance is negligible as the shafts are not constantly submerged in water. An image of a single deflector side is seen in Figure 45 below with the full assembly seen in Figure 46.

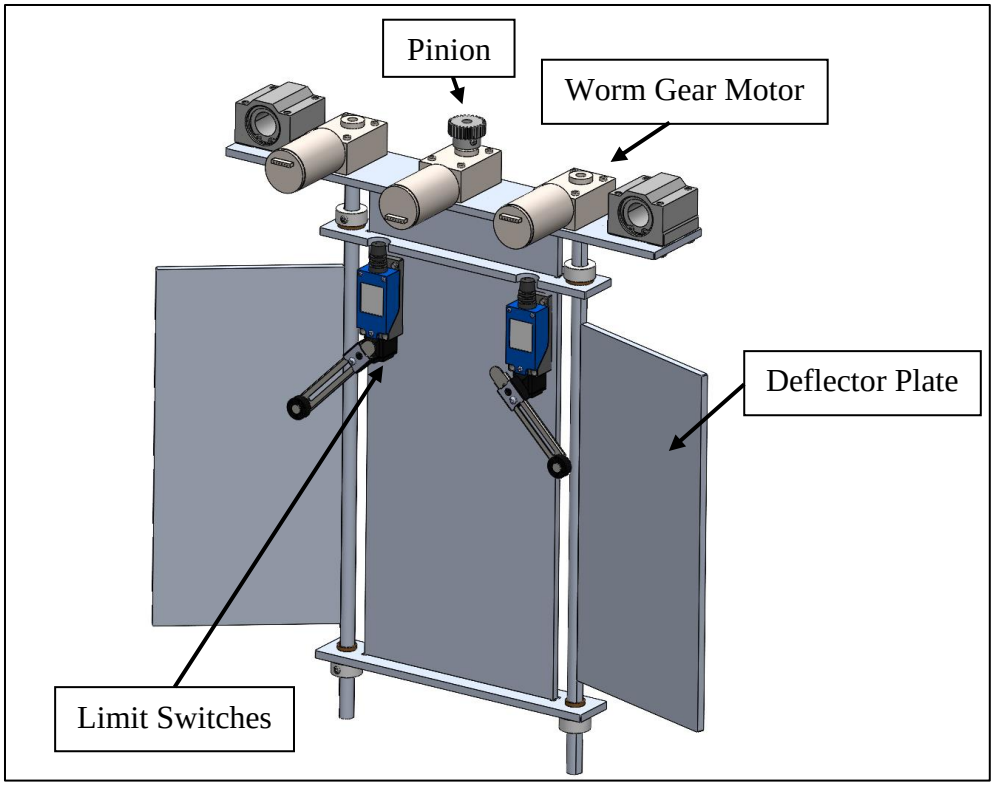

Figure 45: Wave Deflector Side

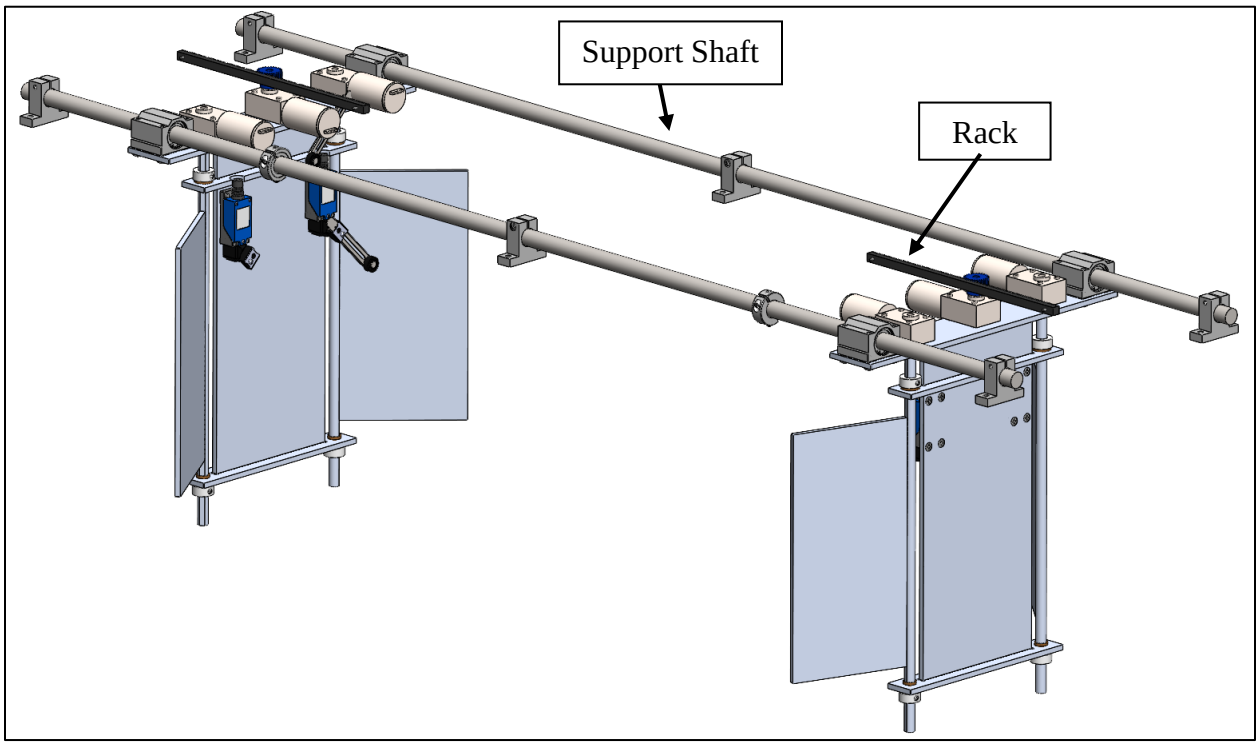

Figure 46: Wave Deflector Assembly

Wiring

The wiring configuration in Figure 89: Full Device Wiring Diagram is modeled in three dimensions using SolidWorks 2020 Electrical Routing. The wiring assembly is shown in its configuration for use in the overall assembly in Figure 47 and Figure 48. The colored wires aid in distinguishing the wire and cable routes. Yellow cables correspond to the worm gear motor routes, the green cables to the limit switches, the white cables to the flow and pressure sensors, and the brown cables to batteries. The electronic box mounted on the deflector support beam, Figure 49: Open Electronics Box Close-Up, houses the myRIO, motor controllers, switches, and the 4-20mA current loop for the pressure sensors. This box will have holes on the left and right sides to allow cables in and provide some protection against water exposure. The batteries are shown in Figure 47: Wiring Assembly Isometric View to the sides of the assembly and would be outside of the water when the assembly is mounted in the wave pool to reduce water exposure.

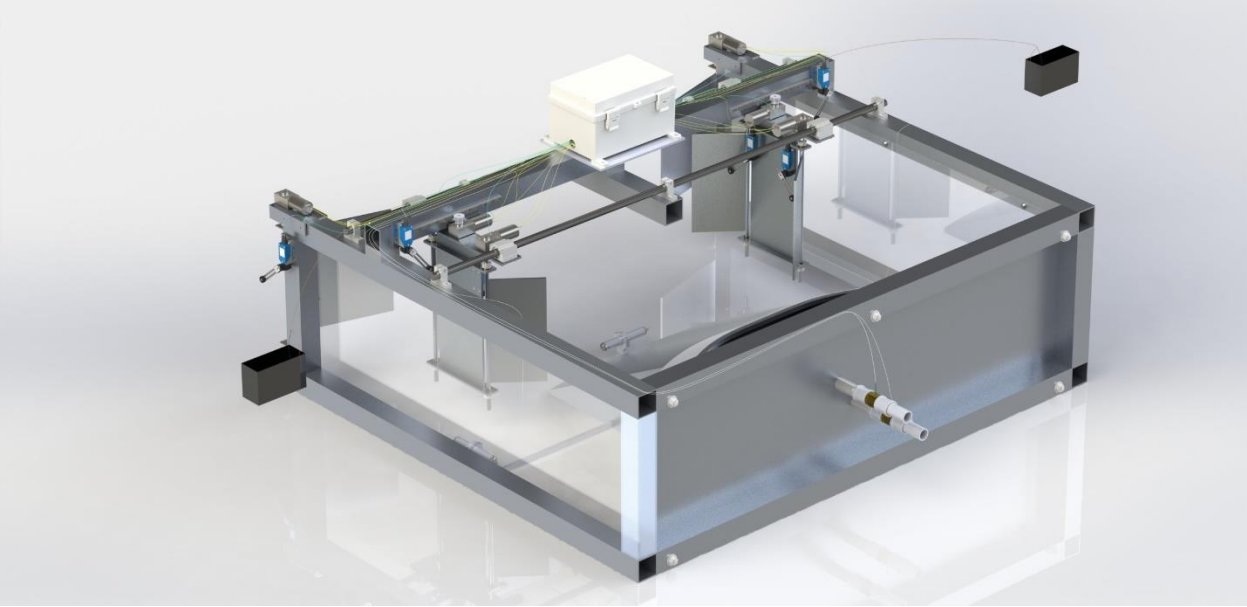

Figure 47: Wiring Assembly Isometric View

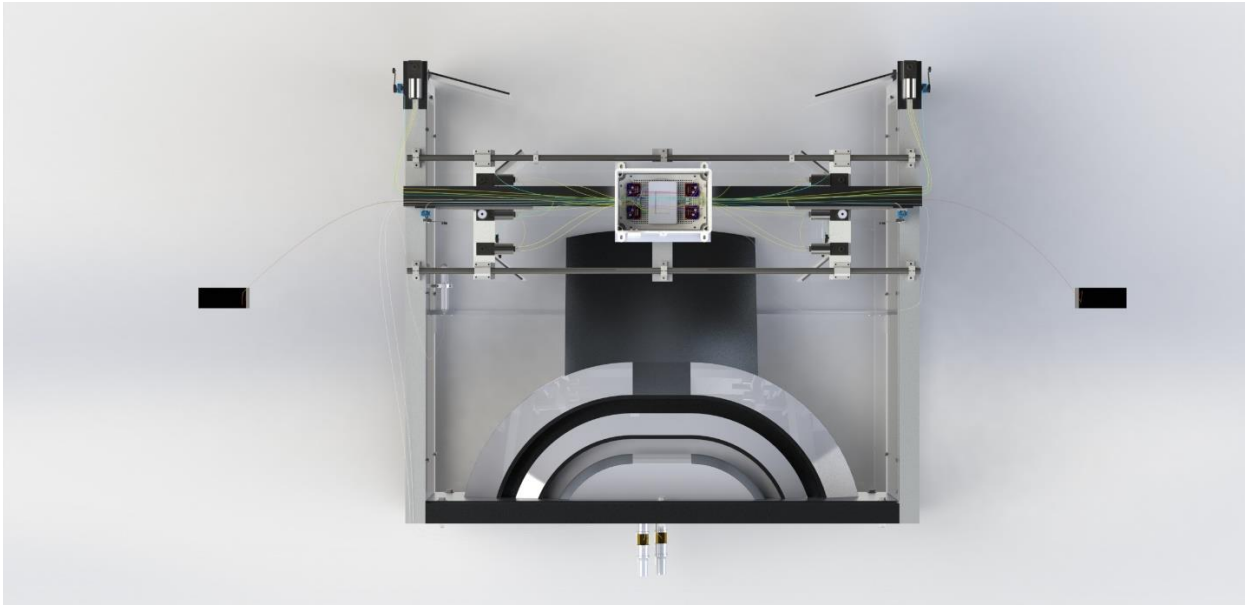

Figure 48: Wiring Assembly Top View

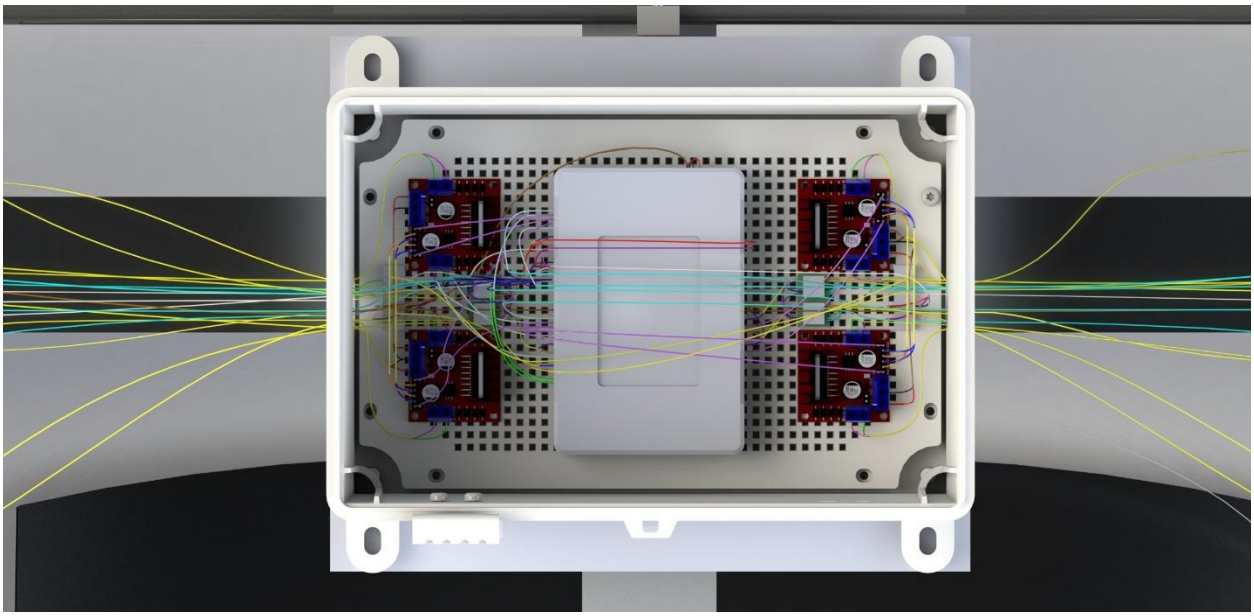

Figure 49: Open Electronics Box Close-Up

Appendix H: Engineering Analysis

Principal Analysis

The first analysis of the design calculates the potential power increase provided by constructive interference. Equation 13 is an equation approximating the power (in kW/m – it is independent of the width of the wave) for an idealized ocean wave, where the idealized ocean wave is treated as a sine wave. In the equation, P is power, H is the total height of the wave from trough to crest (twice the amplitude), and t is the period of the wave. For our calculations, we

looked at a reflected wave that is 45° out of phase with the same period and half the amplitude. The amplitude was assumed to be half of the incoming wave since approximately 50% of the wave is deflected from the overtopping device. The period was assumed to be the same for both the incoming wave and reflected wave because that is the most important assumption to our project. It is important to keep the period of the incoming wave and reflected wave the same otherwise there will be random constructive/destructive interference, which is no better than current solutions. We plan to control the period of the wave through the ramp angle. Next, a 45° out of phase wave was chosen. This was the choice because 0° out of phase would be perfectly constructive, 180° would be perfectly destructive, and 90° out of phase is what we considered to be average ocean conditions that has little impact on wave height. Since our goal is to achieve perfect constructive interference, we went with a conservative estimate of 50% between perfectly constructive interference and average ocean conditions, leading to the 45° phase angle. With these assumptions, it was shown that the power would increase 95.7%, nearly double the original power of the wave.

Equation 13

$$P = H^2 t$$

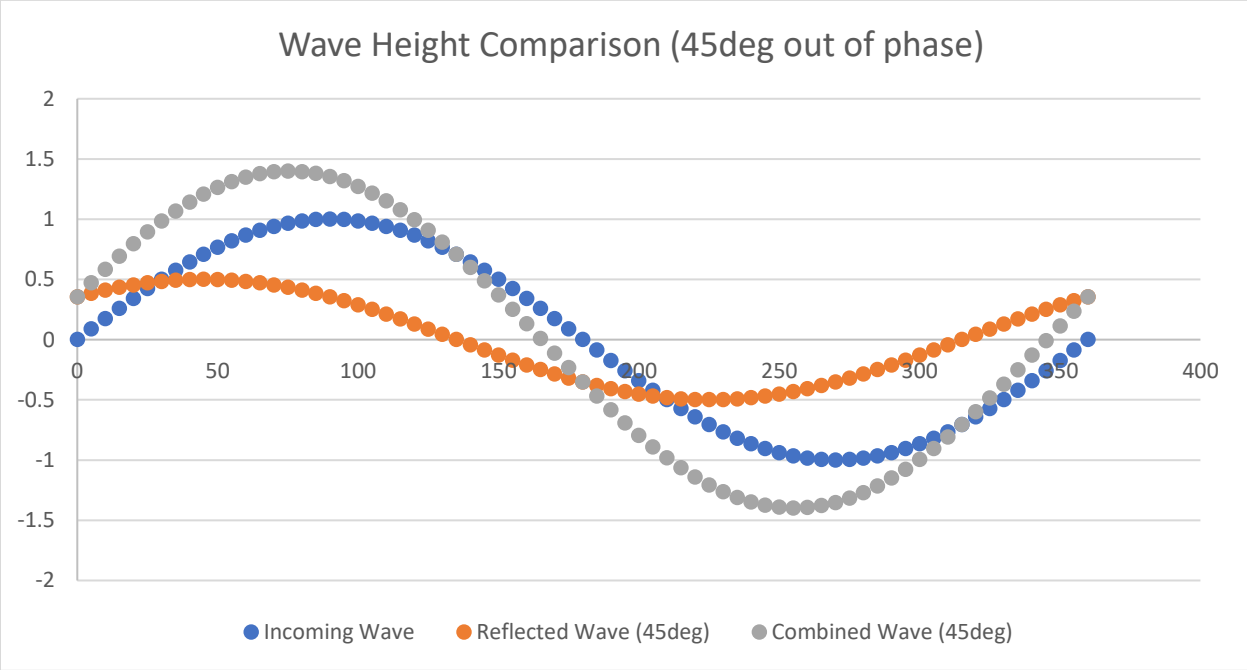

Figure 50: Wave Height Comparison between an incoming ocean wave and a reflected wave that is 45 degrees out of phase

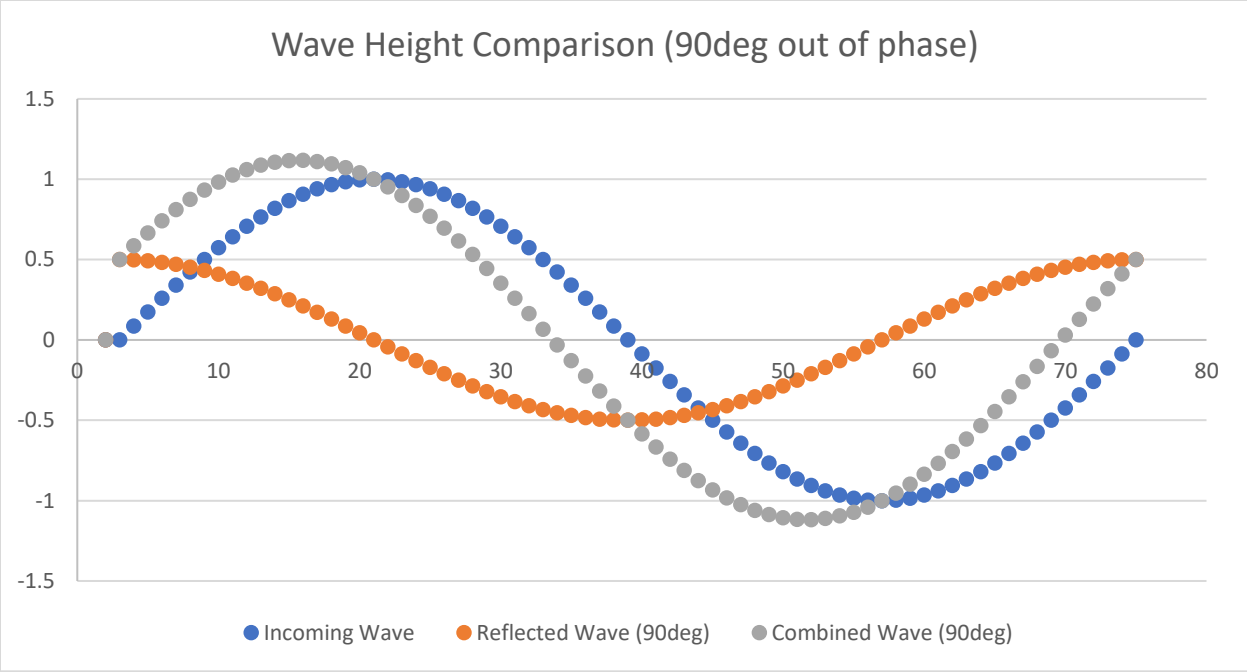

Figure 51: Wave Height Comparison between an incoming ocean wave and a reflected wave that is 90 degrees out of phase

This next analysis examines a motion path of waves. In the figure below the dotted line represents a discretized or vectorized portion of the wave entering the device and the arrows represent its direction. Although the angles of the deflectors are arbitrary, the figure shows some important key features. Firstly, it is known that when a wave reflects, it reflects at angle so that the angle of incidence is equal to angle of reflection and the figure below follows that rule. This means that changing the locations and angles of the deflectors will change the way in which the waves bounce and the resulting intersection/interference points. The interference points are shown in green and purple; the green circles are where 2 vectors interfere and the purple circles are where 3 vectors interfere. When modifying the angle and location of the deflectors, the goal will be to ensure ideal locations of the interference points. The ideal locations of these points are still unknown but our prediction at this current time is that the best location to provide maximum efficiency would be at the reservoir wall or just before it.

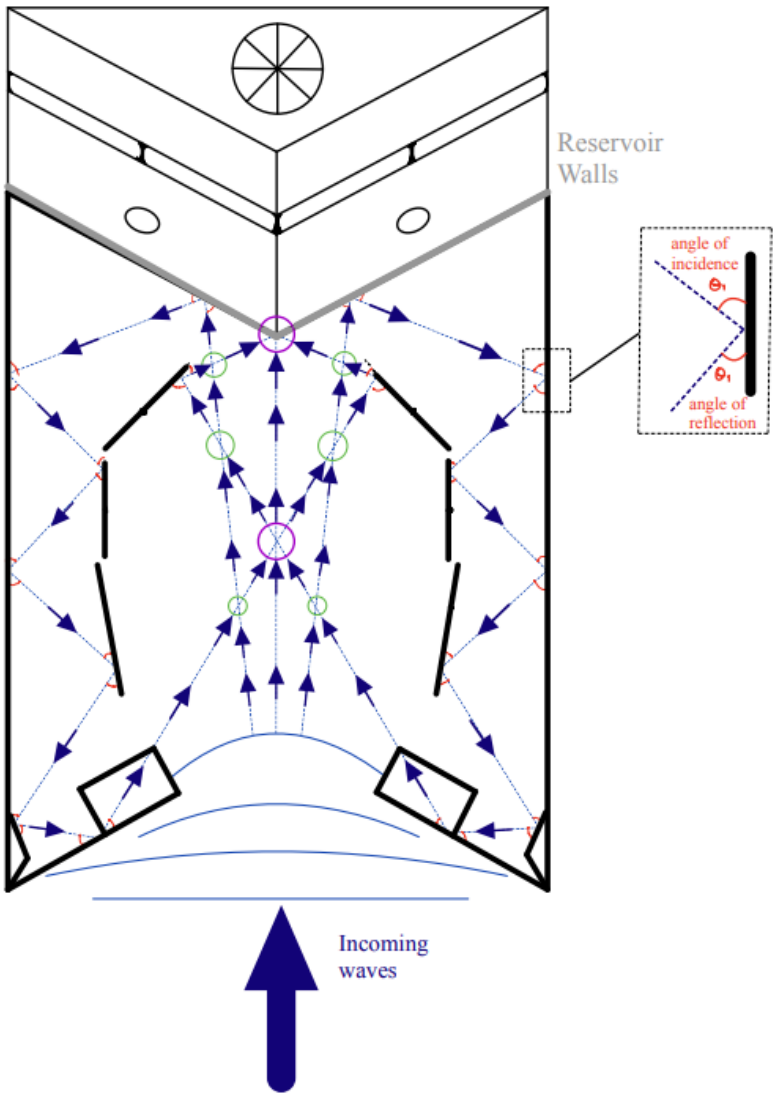

Figure 52: Motion Path Analysis of Discretized Wave

The next figure shows a quick analysis to prove our assumption that when the angle of a deflector changes it will cause the exit angle of the reflecting vector to change by the same amount the deflector angle was changed. In the figure below the angle of the deflector is represented by ϕ, the angle of incident and reflection is represented by Θ, and the exit angle is represented by ϕ.

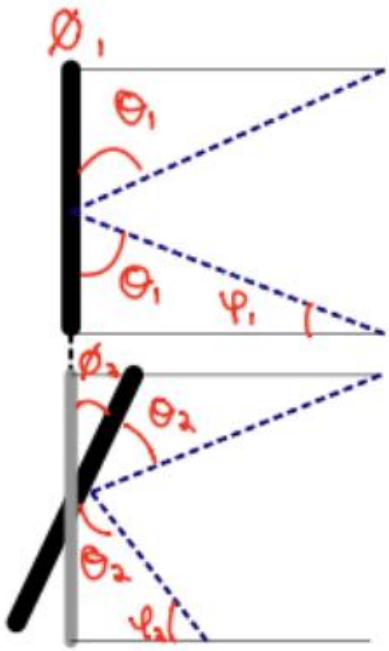

$$\varphi_1 = 90 - \theta_1$$
$$\varphi_2 = 90 - \theta_2$$
$$\theta_2 = \theta_1 - (\phi_2 - \phi_1)$$
$$\varphi_2 = 90 - (\theta_1 - \phi_2)$$
$$\varphi_2 - \varphi_1 = 90 - (\theta_1 - \phi_2) - (90 - \theta_1)$$
$$\varphi_2 - \varphi_1 = \phi_2$$

Figure 53: Proof of Relationship Between Angle of Deflector and Exit Angle

The wave deflectors and their shafts will be a critical design component of this project. The wave deflectors and their shafts will have to withstand forces exerted on them by the reflecting waves. The most likely failure mode would be the failure of the shaft due to a bending moment. The shaft must also fit into the rails so that they can be adjustable. This means that the shaft widths/diameters must be within a range where they are large enough to not break, but small enough to fit within the rails. This requires an analysis of the forces felt by the wave reflectors and the associated internal bending moment on the shaft. The figure below shows a rudimentary free body diagram of the wave deflectors. In this analysis there are many assumptions: the fluid static forces on either side of the deflector (F_{S1} and F_{S2}) are assumed to be equal, the torsion applied about the z-axis is ignored, and it is assumed the internal bending moment will have the only significant effects on the shafts potential yielding and failure.

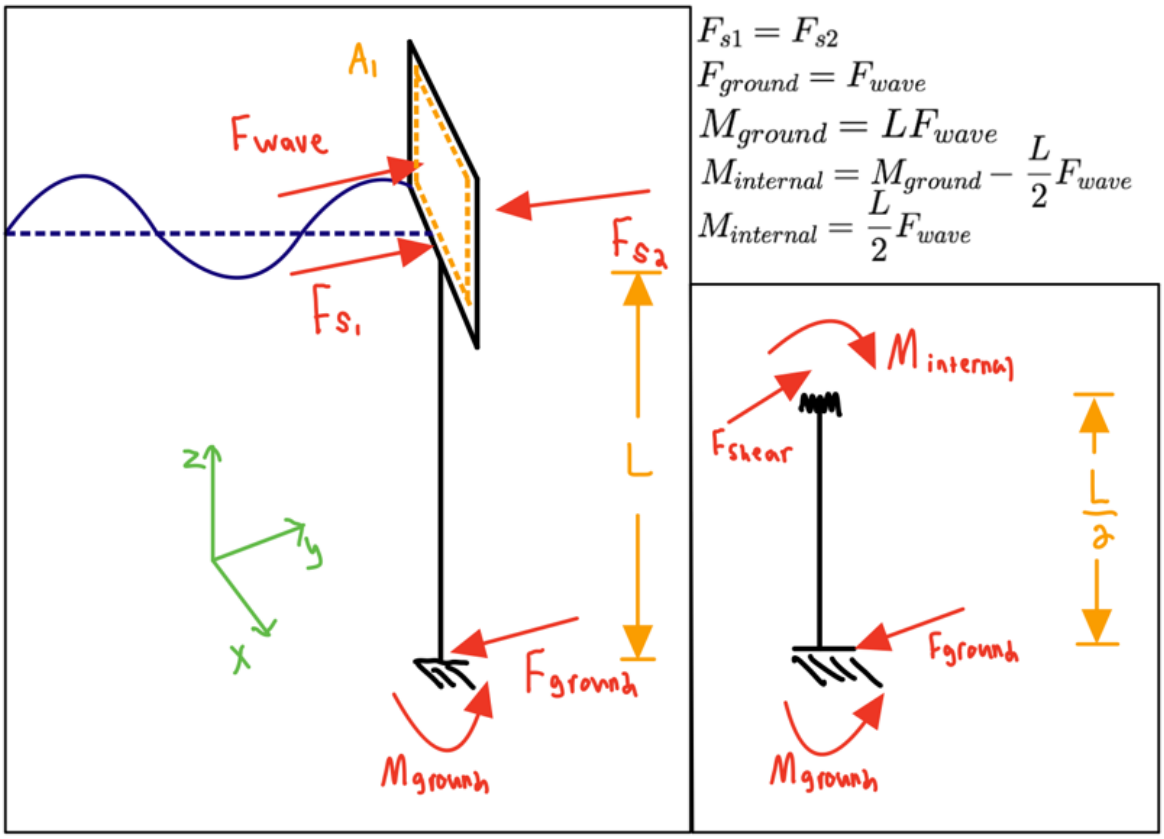

Figure 54: FBD of Wave Deflectors

As seen in the figure above the internal moment felt by the shaft, which will eventually be used to find the axial stress, is dependent on the length of the shaft and the force of the wave. Acquiring the force of the wave is a complicated task. Future plans for calculations include using the area of the surface reflector exposed to the wave (A_1) and the horizontal local acceleration of the water particles to calculate an estimate for the horizontal force of the wave. The local horizontal acceleration can be derived using a first order wave approximation and the continuity equation. This derivation and its resulting force will be shown in analysis in future reports. The figure below summarizes how ocean water particles have a horizontal acceleration.

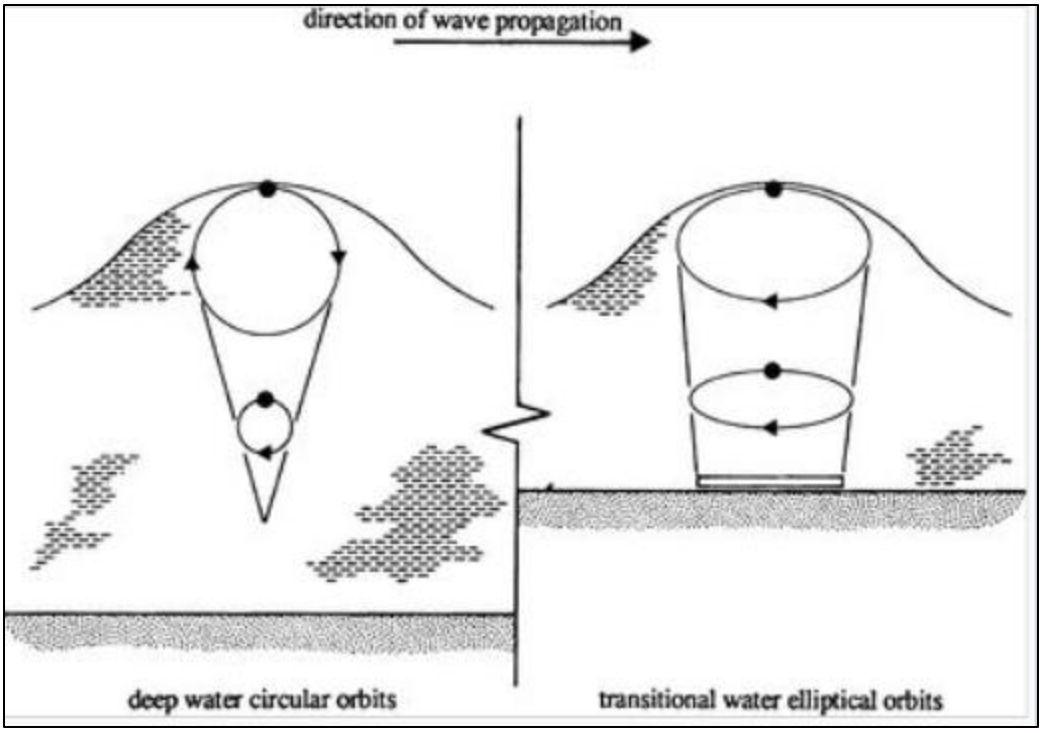

Figure 55: Water Particle Orbits From (Shallow-water Wave Thoery, n.d.)

Previous experimentation and analysis have shown that as a wave approaches shore, its amplitude increases, and its period decreases. This phenomenon will be used by the wave ramps to control the period of reflecting waves to improve the chance of constructive interference occurring. The figure below shows the basics of the phenomenon and will be investigated further in the future.

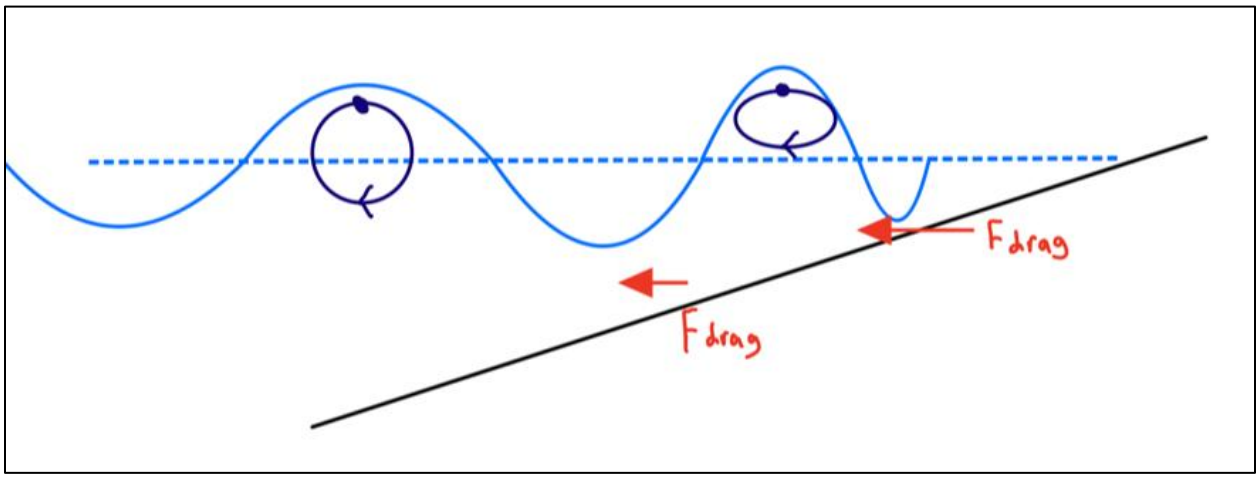

Figure 56: Wave Behavior in Relation to Shore

Flow Sensor Research & Calculations

The upper reservoir (denoted 1) is roughly calculated to hold 2.6 L of water maximum. To find the velocity of water from the outlet of the reservoir, consider the reservoir half full (above average conditions). Bernoulli's Equation can be rearranged to solve for this velocity:

Equation 14

$$v_{1,max} = \sqrt{2gh} = 0.634\,{}^{m}/_{s}$$

Where v is velocity, $g = 9.81\,{}^{m}/_{s^2}$ is gravitational acceleration, and $h_1 = 0.0205m$ is the height of the water. Volumetric flow rate can be calculated by multiplying velocity by the area of the hole with diameter $d = 0.125m$. This comes out to

Equation 15

$$\dot{V}_{1,max} = v_{1,max}A = \tfrac{1}{4} * \pi * d^2 * v_{1,max} = 0.00778\,{}^{m^3}/_{s} = 467\,{}^{L}/_{min}.$$

For the lower reservoir (denoted 2), the volumetric flow rate through the flowmeter includes the flow rate from the upper reservoir as well. Here, $h = 0.036m$. Then

Equation 16

$$v_{2,max} = \sqrt{2gh} = 0.840\,{}^{m}/_{s}$$

Thus,

Equation 17

$$\dot{V}_{2,max} = (v_{1,max} + v_{2,max})A = \frac{1}{4} * \pi * d^2 * (v_{1,max} + v_{2,max}) = 0.01809\,{}^{m^3}/_{s} = 1085\,{}^{L}/_{min}$$

Although the maximum unrestricted flow rate through the bottom reservoir outlet is 1085 L/min, flowmeters of this capacity are expensive, and output piping will be smaller than 125mm. Also, in reality, the turbine would create resistance for the water so that it could not flow as quickly out of each reservoir. The reservoir outlets will neck down to 1" (25.4mm) tubing, making the maximum flow rates effectively.

Equation 18

$$\dot{V}_{1,max} = v_{1,max}A_{tube} = \frac{1}{4} * \pi * {d_{tube}}^2 * v_{1,max} = 0.000321\,{}^{m^3}/_{s} = 19.3\,{}^{L}/_{min}$$

And

Equation 19

$$\dot{V}_{2,max} = (v_{1,max} + v_{2,max})A_{tube} = \frac{1}{4} * \pi * {d_{tube}}^2 * (v_{1,max} + v_{2,max}) = 0.000747\,{}^{m^3}/_{s} = 44.8\,{}^{L}/_{min}$$

Thus, the flowmeter chosen should have a maximum flow rate higher than 44.8 L/min and a minimum flow rate of close to 0 L/min for cases of low or inconsistent flow. The flowmeters chosen are 1" NPT DIGITEN flowmeters, 2-50 L/min for both reservoirs. These also have DC voltage outputs so their data can be exported and analyzed for research purposes.

Static Analysis on Overtopping Device Reservoirs

The static analysis performed considers both reservoirs completely full, the highest-stress scenario for our materials. Note that $\rho_{water} = 997 \frac{kg}{m^3}$.

Reservoir 1 (Lower):

Equation 20

$$V_1 = 0.0657m * \left(\frac{\pi * 0.444m^2}{2} + \frac{1}{2} * \frac{\pi * (0.52m^2 - 0.444m^2)}{2} \right) = 0.0241m^3$$

Equation 21

$$m_1 = V_1 \rho_{water} = 24.03kg$$

Force exerted downwards by the water:

Equation 22

$$F_1 = m_1 g = 235.7N$$

Static analysis on this section would require FEA, as the skeleton structure is supporting the weight of the water in a more complex manner. However, I would assume that Reservoir 1's attachment method is much stronger than Reservoir 2's because it is supported in both front and back. While more analysis is needed, I am confident this section will support the weight of a full reservoir.

Reservoir 2 (Upper):

Equation 23

$$V_2 = 0.0352m * \left(\frac{\pi * 0.316m^2}{2} + \frac{1}{2} * \frac{\pi * (0.384m^2 - 0.316m^2)}{2} \right) = 0.00684m^3$$

Equation 24

$$m_2 = V_2 \rho_{water} = 6.82kg$$

Force exerted downwards by the water:

Equation 25

$$F_2 = m_2 g = 66.9N$$

Moment exerted on four total welds to frame:

Equation 26

$$M_2 = F_2 x_2 = 6.69Nm$$

Each weld will experience a moment of

Equation 27

$$M_{w,2} = \frac{1}{4} M_2 = 1.673Nm$$

The welded area for each bar is its cross-sectional area, $A_{bar} = 3.78 * 10^{-5}\ m^2$. The area moment of inertia for the hollow square bar is:

Equation 28

$$I = \frac{(outside\ width)^4 - (inside\ width)^4}{12} = \frac{(0.5\ in)^4 - (0.375\ in)^4}{12} = 3.56 * 10^{-3}\ in^4$$
$$= 1.52 * 10^{-9}\ m^4$$

Thus the total stress carried by each weld due to bending is

Equation 29

$$\sigma_{w,2} = \frac{M_{w,2} * y}{I} = 6.99MPa$$

To account for the welded connection, a factor of safety of 2 can be applied, making the maximum bending stress effectively 13.98 MPa. The yield strength of 6061 aluminum is 276 MPa. Factors of safety for the welded connections are:

Equation 30

$$\frac{\sigma_{max}}{\sigma_{weld}} = \frac{276\ MPa}{13.98\ MPa} = 19.74$$

Frame Length Dimension Calculation

The width and height of the frame was determined by the dimensions of the overtopping device dimensions which were found from the analysis above in . However, the length of the frame is not determined by the overtopping dimensions. The length of the frame is constrained to be relatively proportional to the other dimensions to allow the device to be manufacturable. Also, this length dimension would determine how far out into the ocean the deflectors and gates would be in the full scaled device so it must not be excessively long due to the increased construction costs of building structures in deeper ocean. The length of the scaled down prototype was determined using scaled down wave parameters from a potential location, Coos Bay, Or. For the possibility of constructive interference to occur, the waves being channeled must travel a total of

one wave period, if the travel distance is less, it would be impossible for constructive interference occur because there would be no point time where the peaks could possibly combine. Figure 57 below shows the calculations for finding the approximate length dimension of the frame.

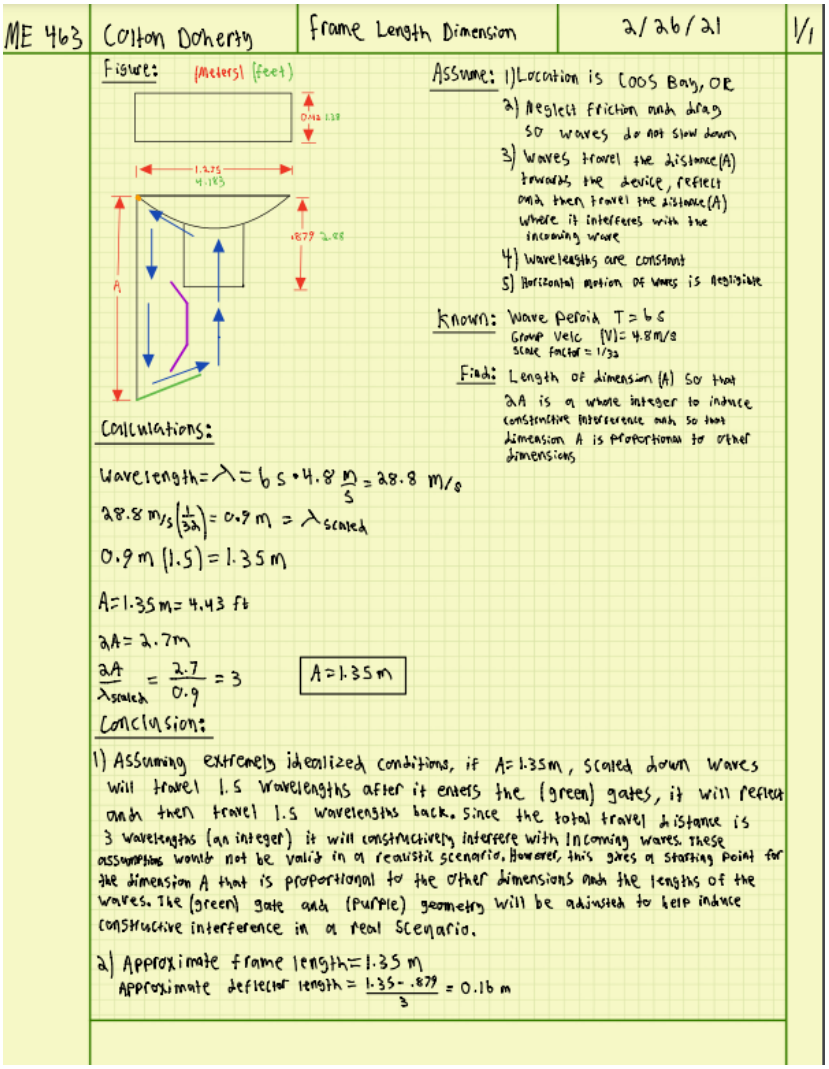

Figure 57: Approximate Calculation of Frame Length Dimension

The average wave conditions were obtained from the analysis [see Table 10: Wave Climate Parameters Based on Location (Year 2020)]. From those conditions and the scale factor, the scaled down wave period was found. To allow space for the wave deflectors and to ensure that waves being deflected and rechanneled would travel at least more than one wavelength, the estimated length of the frame was decided to be 1.5 wavelengths. In extremely idealized conditions this would mean reflected and rechanneled waves would travel 3 wave periods, which allows the possibility for constructive interference. Also, since it is much greater than 1, it accounts for the large amount of uncertainty due to the extremely idealized conditions. This analysis is extremely idealized and in no way guarantees the occurrence of constructive interference, but it provided a methodical way to estimate the length of the dimension and ensure

general proportionality to the actual waves and the possibility of constructive interference. The initial length dimension was determined to be 1.35 meters. From this value, the approximate deflector length of 0.16m was also obtained by dividing it by 3.

Motor Torque Requirement Calculation

Figure 58 shown below calculates a rough estimate for the torque requirement of the motors to move the wave gate and wave deflector plates. The analysis considers inertial forces of the plates and the drag of the plates in the water, it does not account for friction or other external forces.

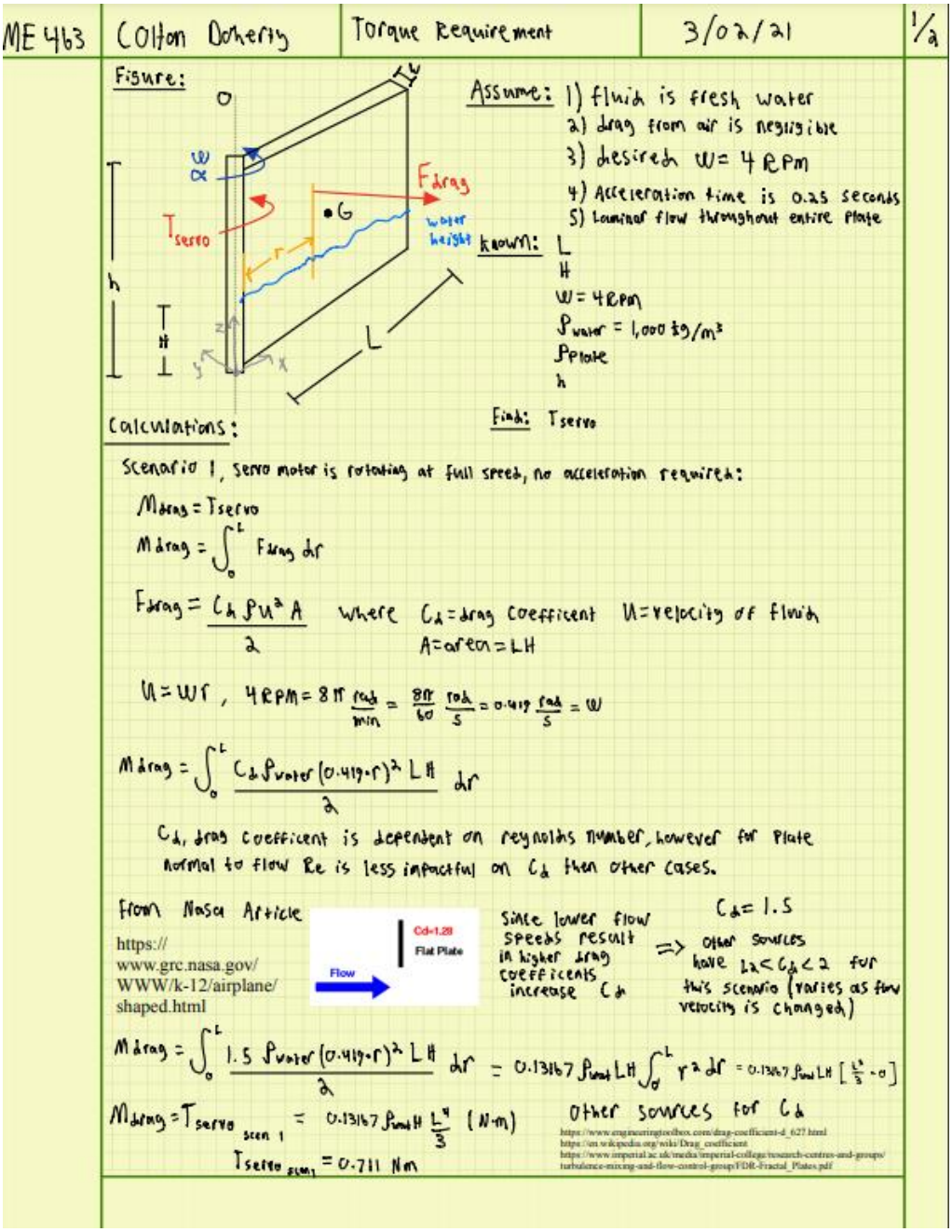

ME 463 | Colton Doherty | Torque Requirement | 3/02/21 | 2/2

Scenario 2, Servo motor is accelerating (inertial forces must be overcome)

Note: To be conservative the drag force from Scenario 1 will be used although the actual drag force would be lower due to a slower rotational velocity.

$$\Sigma M_o = I_o \alpha$$

$$\Sigma M_o = T_{servo} - M_{drag}$$

$$\alpha = \frac{\omega_f - \omega_i}{t_{accel}} = \frac{4\,rpm - 0\,rpm}{0.25\,sec} = \frac{0.419\,\frac{rad}{s}}{0.25\,s} = 1.676\,\frac{rad}{s^2}$$

$$I_o = I_G + m d_{oo}^2$$

$$m = \rho_{plate} L W h$$

$$d_{oo} = \frac{L}{2}$$

$$I_o = I_G + \rho_{plate} L W h \left(\frac{L}{2}\right)^2$$

$$I_G = \frac{1}{12} m L^2 + \frac{1}{12} \rho_{plate} L W h L^2$$

$$I_o = \frac{1}{12} \rho_{plate} L W h L^2 + \rho_{plate} L W h \left(\frac{L}{2}\right)^2$$

$$I_o = \rho_{plate} \left[\frac{1}{12} W h L^3 + L^3 W h \frac{1}{4}\right]$$

$$I_o = \rho_{plate} W h L^3 \frac{1}{3}$$

$$1.676\,\frac{rad}{s^2} \cdot \rho_{plate} W h L^3 \frac{1}{3} = T_{servo} - M_{drag}$$

$$T_{servo} = 1.676\,\frac{rad}{s^2} \cdot \rho_{plate} W h L^3 \frac{1}{3} + 0.13167\,\rho_{water} H \frac{L^4}{3}$$

$$T_{servo} = L^3 \frac{1}{3}\left[1.676\,W h\,\rho_{plate} + 0.13167\,L H \rho_{water}\right]$$

Conclusion: Assuming idealized conditions the equation $T_{servo} = L^3 \frac{1}{3}\left[1.676\,W h\,\rho_{plate} + 0.13167\,L H \rho_{water}\right]$ provides a rough estimate for the Torque requirement of motors to rotate the wave deflectors and wave gates in water. This value does not account for friction between the shaft and the bushing / shaft collar and bushing so a large FS will be used when selecting motors, preliminary FS = 3

If $H = 0.125m$ $h = 0.250m$ $W = .01\,m$ $L = 0.3m$ $\rho_{plate} = \rho_{steel} = 8{,}000\,kg/m^3$

$$T_{motor} = L^3 \frac{1}{3}\left[1.676\,W h\,\rho_{plate} + 0.13167\,L H \rho_{water}\right] = 0.28\,Nm$$

Figure 58: Calculation of Motor Torque Requirement

The calculations above use an experimentally determined drag coefficient from NASA (Hall, 2015). A rough estimate for the torque requirement using approximate dimensions is 0.28Nm. Equation 31 shown below can be used to calculate the approximate Torque requirement for future iterations with slightly modified dimensions.

Equation 31

$$T = L^3 \frac{1}{3}[1.676Wh\rho_{plate} + 0.13167LHh\rho_{plate}] \text{ (all standard metric units)}$$

Force of Waves Calculation

The calculations below shown in Figure 59 approximate the horizontal force exerted by the waves on the wave deflectors and wave gates. The calculations assume wave conditions from Coors, Or [see Table 10: Wave Climate Parameters Based on Location (Year 2020)]

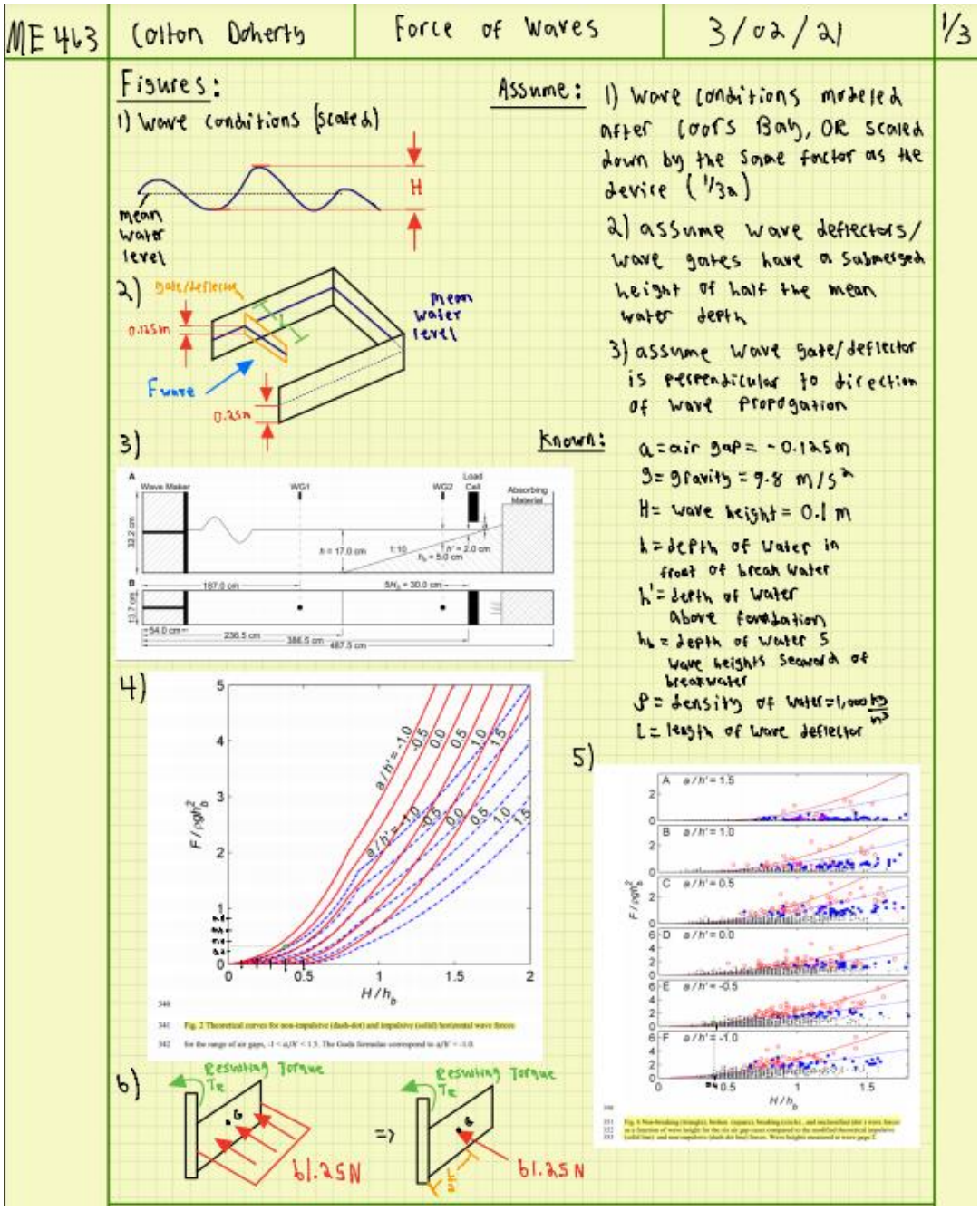

ME 463	Colton Doherty	Force of Waves	3/02/21	2/3

Find: F' = Horizontal force of wave per unit length (L)

Calculations:

From wave condition assumptions and the simple geometry of the test rig
$\Rightarrow h = 0.250\,m$, $h_b = 0.250\,m$, $a = -0.125\,m$, $h' = 0.250\,m$

$$\frac{H}{h_b} = \frac{0.1\,m}{0.250\,m} = 0.4$$

$$\frac{a}{h'} = \frac{-0.125\,m}{0.250\,m} = -0.5$$

$$\frac{F'}{\rho g h^2} = \frac{F'}{1000\,\frac{kg}{m^3}\,9.8\,m/s^2\,(0.25m)^2} = \frac{F'}{612.5\,\frac{kg}{s^2}} = \frac{F'}{612.5\,\frac{N}{m}}$$

from the fourth Figure above, theoretical curve for impulsive forces and $\frac{H}{h_b} = 0.4$, $\frac{a}{h'} = -0.5 \Rightarrow \frac{F'}{\rho g h^2} = \frac{F'}{612.5\,\frac{N}{m}} \approx 0.25$ Note: The experimental results from figure (5) support these values

$$F' \approx 0.25 \cdot 612.5\,\frac{N}{m} = 153.125\,\frac{N}{m}$$

If we assume a wave gate/deflector length of $L = 0.375$

$$\Rightarrow F = F' \cdot L = 153.125\,\frac{N}{m} \cdot 0.375 = 57.422\,\frac{N}{m}$$

From figure (6) and its associated load condition assumptions

$$T_R = F \cdot \frac{L}{2} = 57.42\,N \cdot \frac{0.375}{2} = 10.77\,Nm$$

Conclusion: A rough, and most likely large over-estimate, for the max possible Back force and back torque on the wave gates or deflectors is and respectively

The nondimensionalized values for our situation are lower than the values this study calculated so calculated results may not be completely accurate but a large FS will be used to account for this.

FS = 0.75 Driven factor of safety (teeth should be able to take the load much higher than driven

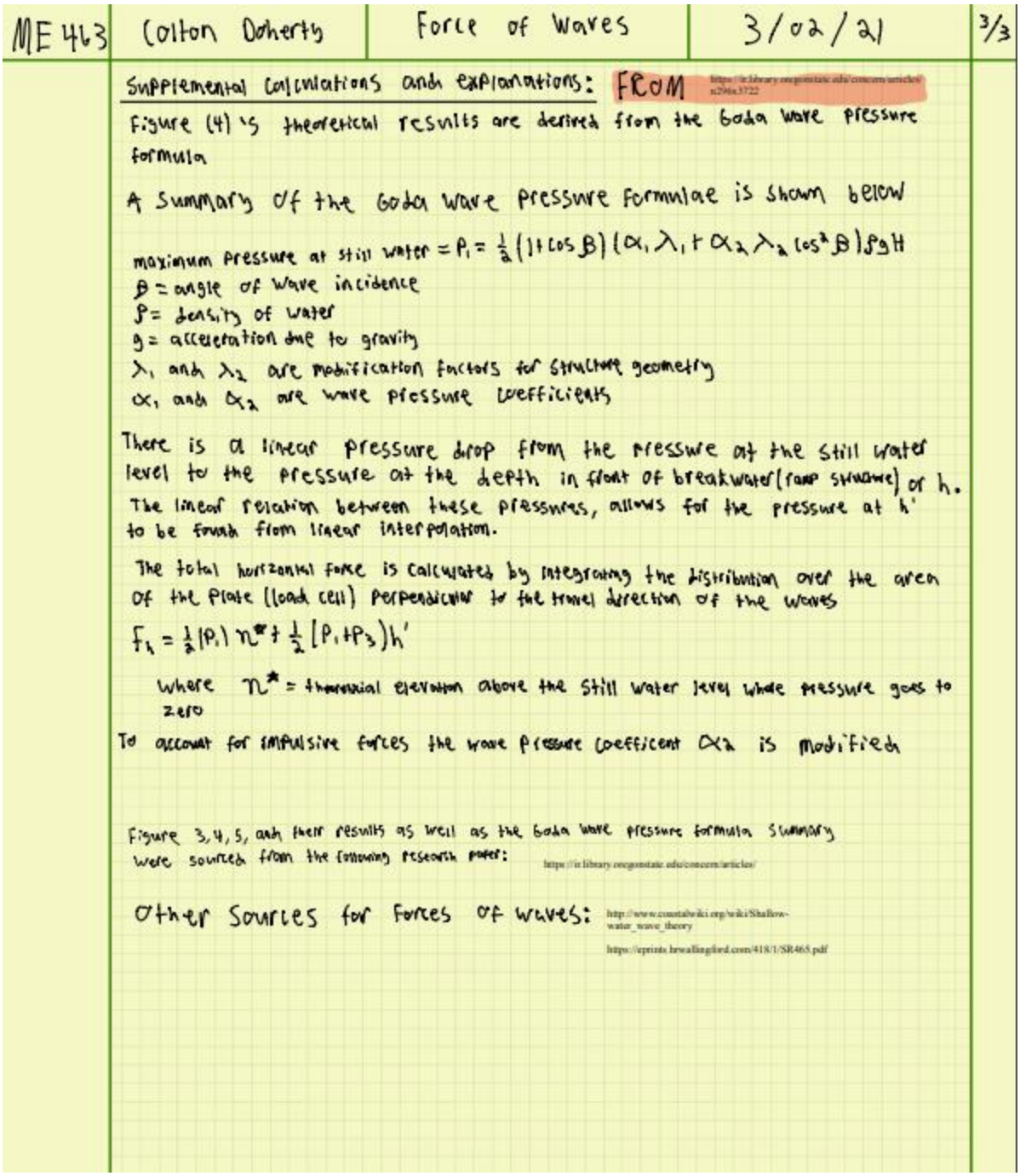

Figure 59: Horizontal Force of Waves Calculation

The calculations above in Figure 59 reference a research paper that references experimental results and the Goda Pressure Distribution applied to ocean waves (Dane M. Wiebe, 2014). The experimental setup used in the paper is similar to the worst-case scenario being analyzed in the calculations above. The paper contained non-dimensionalized values of force plotted against non-dimensionalized values for wave height for both experimental results and theoretical results. Our conditions fall in their theoretically calculated range and has a

slightly lower non-dimensionalized force that occurred in their experimental cases. Due to this, the non-dimensionalized force value for our analyzed condition was extracted from the theoretical curve (labeled figure 4 in calculations). This value is to be used with caution due to the uncertainty of the calculation. The extracted non-dimensionalized force value was then converted to a value with dimensions (units) by multiplying by the appropriate geometric dimensions. The geometric dimensions used were for a wave gate plate with a significant submerged height to account for uncertainty and to allow for the value to be used in later iterations with relative confidence without having to recalculate the force value if a dimension is changed slightly. The estimated force per unit length was found to be 153.125 Newtons per meter. If a wave gate length dimension of 0.3 m is used, the estimated worse case force on the wave gate is 60 Newtons. This equates to about 12lb which is reasonable considering the scaled down waves are assumed to have a height of about 0.1 meters. The back torque applied to the shaft can then be calculated using Equation 32 shown below.

Equation 32

$$T_{back} = 153.125\frac{L^2}{2}$$

Equation 32 can be used with relative confidence as the length of the wave gate/deflector plate is iterated. This equation can be used to determine the back torque that the worm gear must be able to withstand as well as be used to determine the internal stress on the wave plate.

Internal Stress on Wave Gate/Deflector Plate

Equation 32 can be used to estimate the internal stresses felt by the wave gate/deflector plate if the plate is assumed to be in pure bending. That assumption allows the normal stress due to bending be estimated using the following hand calculations and equation shown in Figure 60.

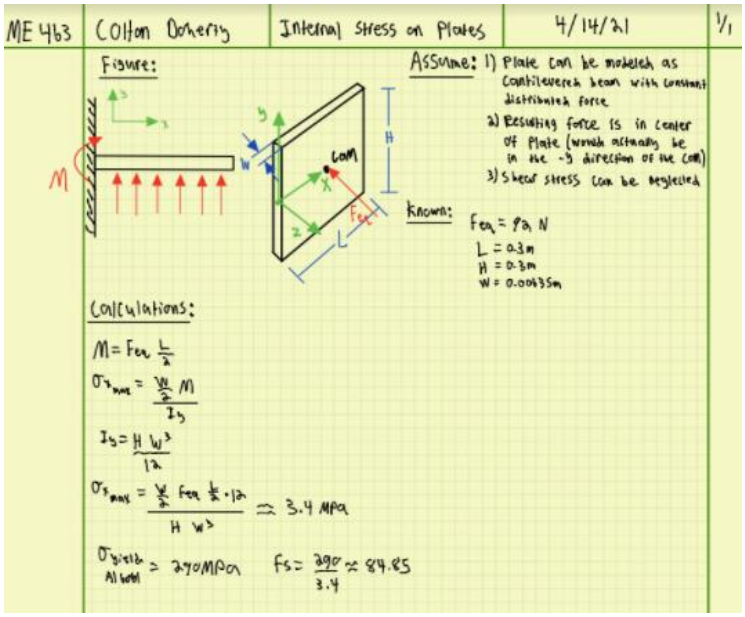

Figure 60: Hand Calculations of Internal Stress on Plates

The calculations in Figure 60 can be generalized for other dimensions using Equation 33 shown below.

Equation 33

$$\sigma = \frac{T_{back} * \frac{w}{2}}{\frac{L * (\frac{w}{2})^3}{12}}, where\ w = width\ of\ plate\ and\ L = length\ of\ plate$$

Force on Rack and Pinion Gear Teeth

Hand calculations were performed to see if the plastic rack and pinion would fail. The calculations shown in Figure 61 below use the worst-case scenario of the full force of the waves and assuming assembly is perpendicular to the direction of travel of the waves. The deflector assembly would then transfer the load from the pinion teeth to the rack. Even with this worst-case scenario an acceptable factory of safety was calculated using the plastic rack and pinion. Note, the calculations shown in Figure 61 use calculations from Figure 58 and Figure 59.

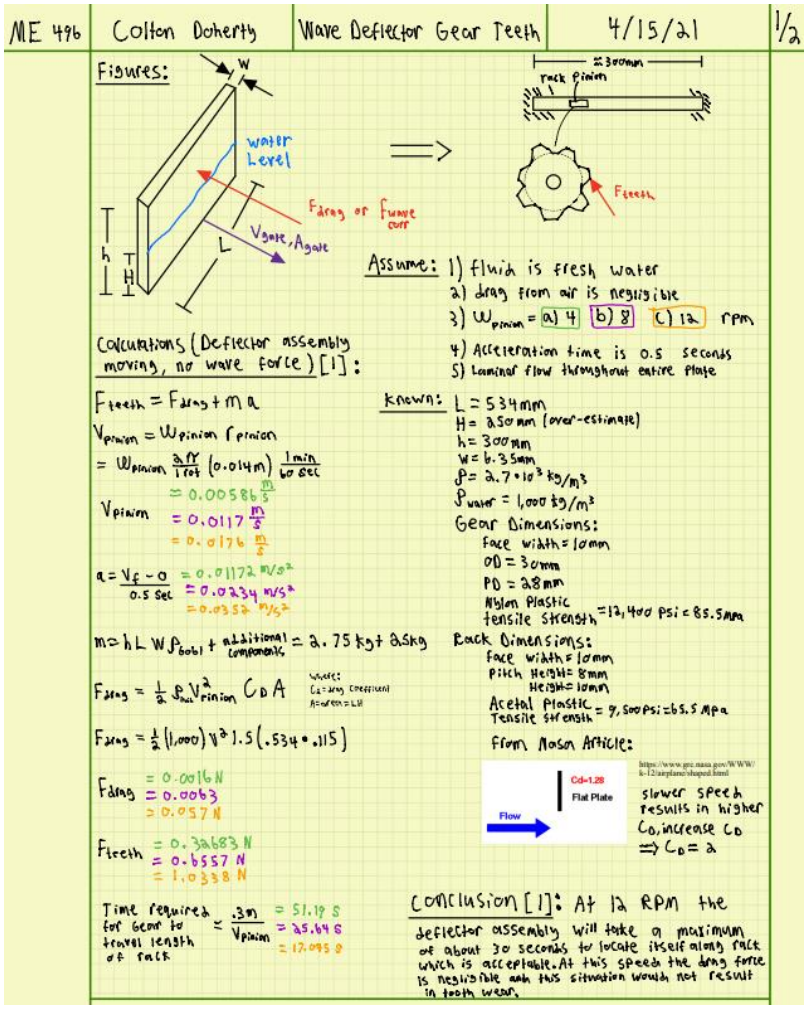

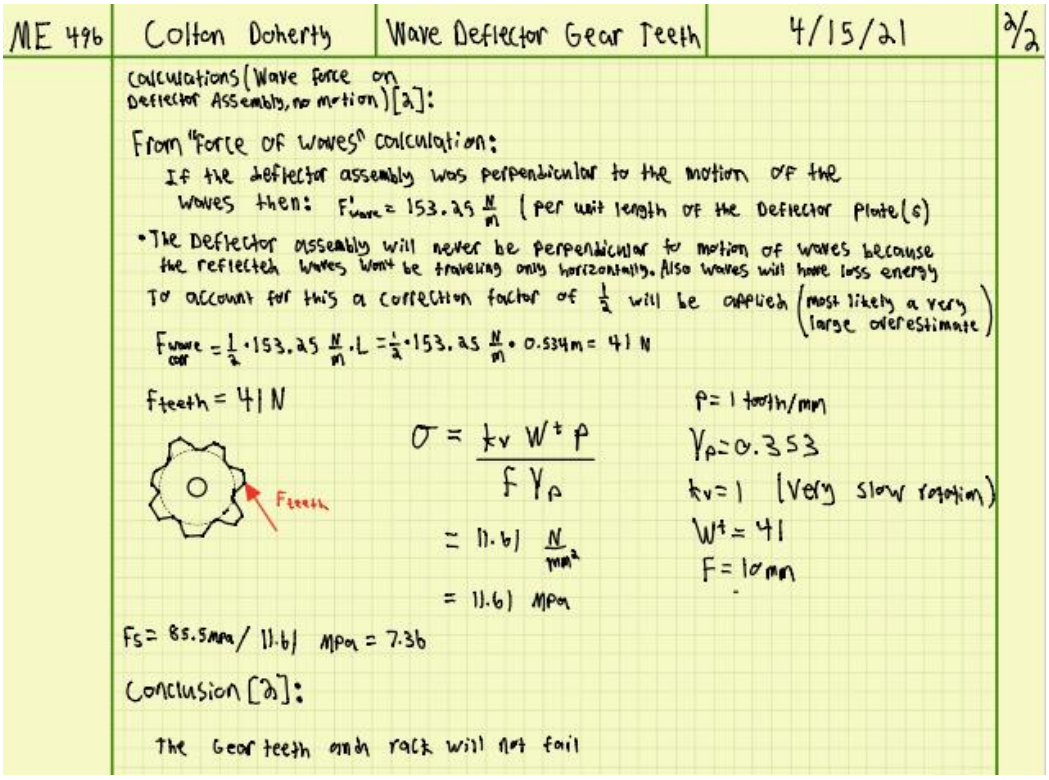

Figure 61: Hand Calculations for Force on Rack and Pinion Gear Teeth

Another important note from Figure 61 above, is that if the worm gear is run at 12RPM, then the deflector assembly will be able to travel the length of the rack in about 17 seconds. This relatively slow linear velocity is not too much of a hinderance on the user and results in very little drag as the plates move through the water and the importance of this will be shown later.

Iterative Design Spreadsheet

Table 14 below uses equations derived from Figure 58, Figure 59, Figure 60, and Figure 61. The equations used to derive initial estimates were placed in this spreadsheet in order to be able to iterate design parameters like dimensions and material selections and easily see how it would affect the failure analysis of the device. Using this spreadsheet, it was decided to reduce the length of the wave gates to 0.3m to ensure the worm gear motor would not fail when static and facing the forces of the waves.

Design Parameters		
Parameter		**Value**
Length of Gate, L_gate (m)		0.3
Width of Gate, W_gate (m)		0.00635
Height of Gate, h_gate (m)		0.3
Height of Submerged Gate, H_gate (m)		0.14
Length of deflector, L_defl (m)		0.15
Width of deflector, W_defl (m)		0.00635
Height of deflector, h_defl (m)		0.3
Height of Submerged Deflector, H_defl (m)		0.14
Estimated Length of combined delfector plates, L_est (m)		0.53
Worm Gear Motor Rated Torque (Nm)		5.88
Worm Gear Max Torque (Nm)		6.86
Aluminum 6061 Density, ρ (kg/m^3)		8000
Aluminum 6061 Yield Strength (MPa)		290
Pinion Nylon Plastic Yield Strength (Mpa)		85.5
Rack Acetal Plastic Yield Strength (MPa)		65.5
Calculated Stresses		
Description	**Wave Gate**	**Wave Deflectors**
Maximum Required Torque (Nm)	0.28	0.03
Maximum Back Force (N)	45.94	27.56
Maximum Back Torque (Nm)	6.89	2.07
Maximum Stress on Plates (N/m^2)	3417756.84	1025327.05
Maximum Force on combined deflector plate assembly (N)	N/A	73.04
Factors of Safety		
Factor of Safety	**Wave Gate**	**Wave Deflectors**
Driven Gear Motor FS	21.03	184.64
Bending of Wave Gate Plate FS	84.85	282.84
Stationary Gear Motor FS	1.04	3.32
Wave Deflector Rack Tooth Bending FS	N/A	3.17
Wave Deflector Pinion Tooth Bending FS	N/A	4.13

Table 14: Iterative Design Spreadsheet to allow for adjustment of dimensions and materials

This table also references: Equation 33, Equation 32, and Equation 31. The bottom section of Table 14 shows the factor of safety of different failure modes. All FS are above 3 and satisfactory besides the Stationary Gear Motor FS. This value of 1.04 although barely greater than 1 is not too concerning because this factory of safety references the max torque that the motor can output. In the applied scenario the worm gear would only need to lock in place and would not need to drive any motion. The actual motor would likely fail much sooner before the worm gear box. This assumption combined with the fact an overestimate of the wave forces was used, the low FS of 1.04 is not of great concern but would be closely monitored in actual testing.

Appendix I: Mechanical CAE

Input Conditions for FEA

To run FEA on the wave gate assembly, input conditions like boundary conditions and external forces needed to be applied. Figure 62 below shows the input conditions applied. The 100N is 5/3 of the estimated force of the waves from "Maximum Back Force (N)" of Wave Gates in Table 14. The 5/3 is meant to compensate for the uncertainty in the wave force calculations.

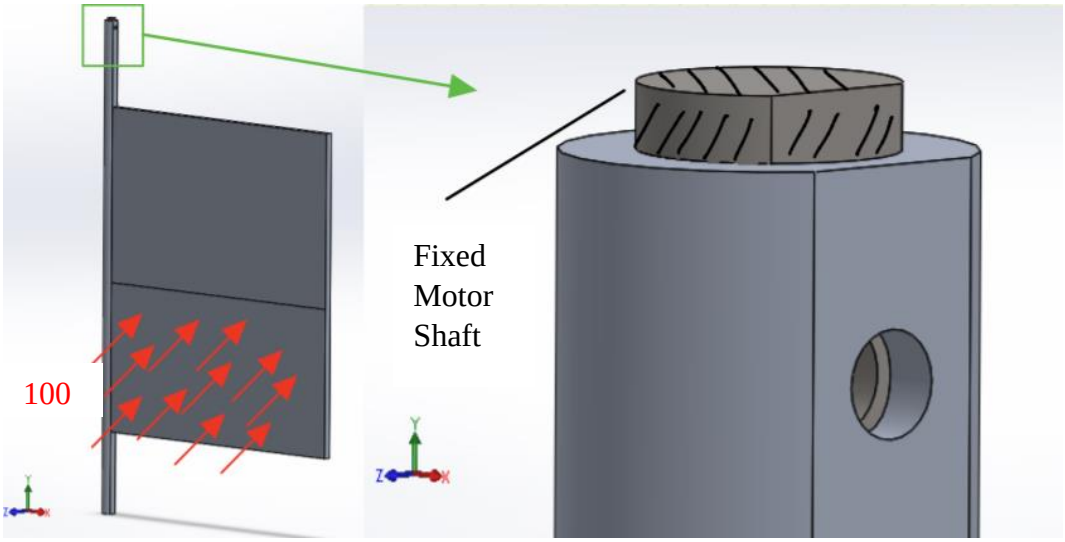

Figure 62: FEA Input Conditions of Wave Gate Assembly

Figure 63 below shows the FEA input conditions for the Overtopping Skeleton. The overtopping skeleton was bonded to the back plate and as a result the frame. The bottom of the frame was fixed since it would be fastened to the bottom of the wave pool. The estimated force of waves value of 60N from the calculations in Figure 59 was applied in both the y and z-axis on to the overtopping skeleton. The weight of the sheet metal and water was estimated to be 200N and was added to the force in the y-axis. The bottom of the frame was fixed since it would be mounted to the floor of the wave pool.

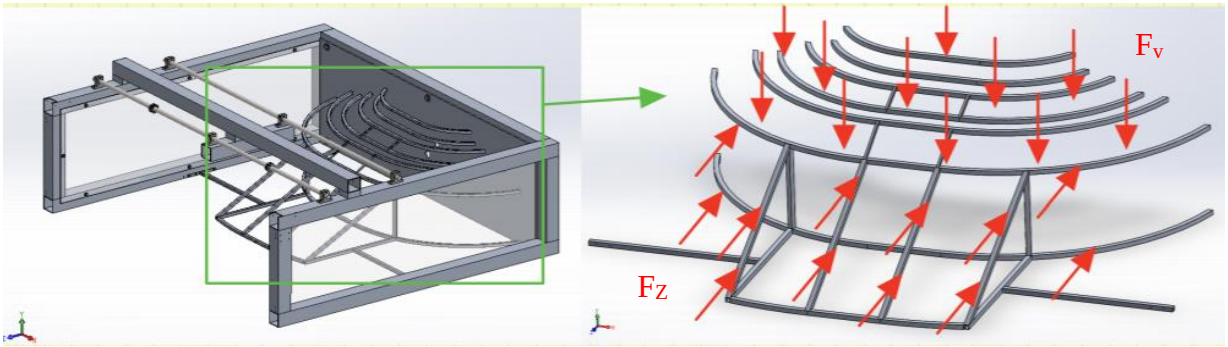

F_Z=60N, F_y=260N

Figure 63: FEA Input Conditions of Overtopping Skeleton

Figure 64 below shows the input conditions for the FEA analysis of the Frame and the shafts that support the wave deflector mechanisms. These conditions are for when the device is static and exposed to wave forces. Although there is uncertainty of the value and direction of some forces due to reflecting waves and complex geometry, asymmetric loading conditions and maximum possible forces were used to account for all possible scenarios.

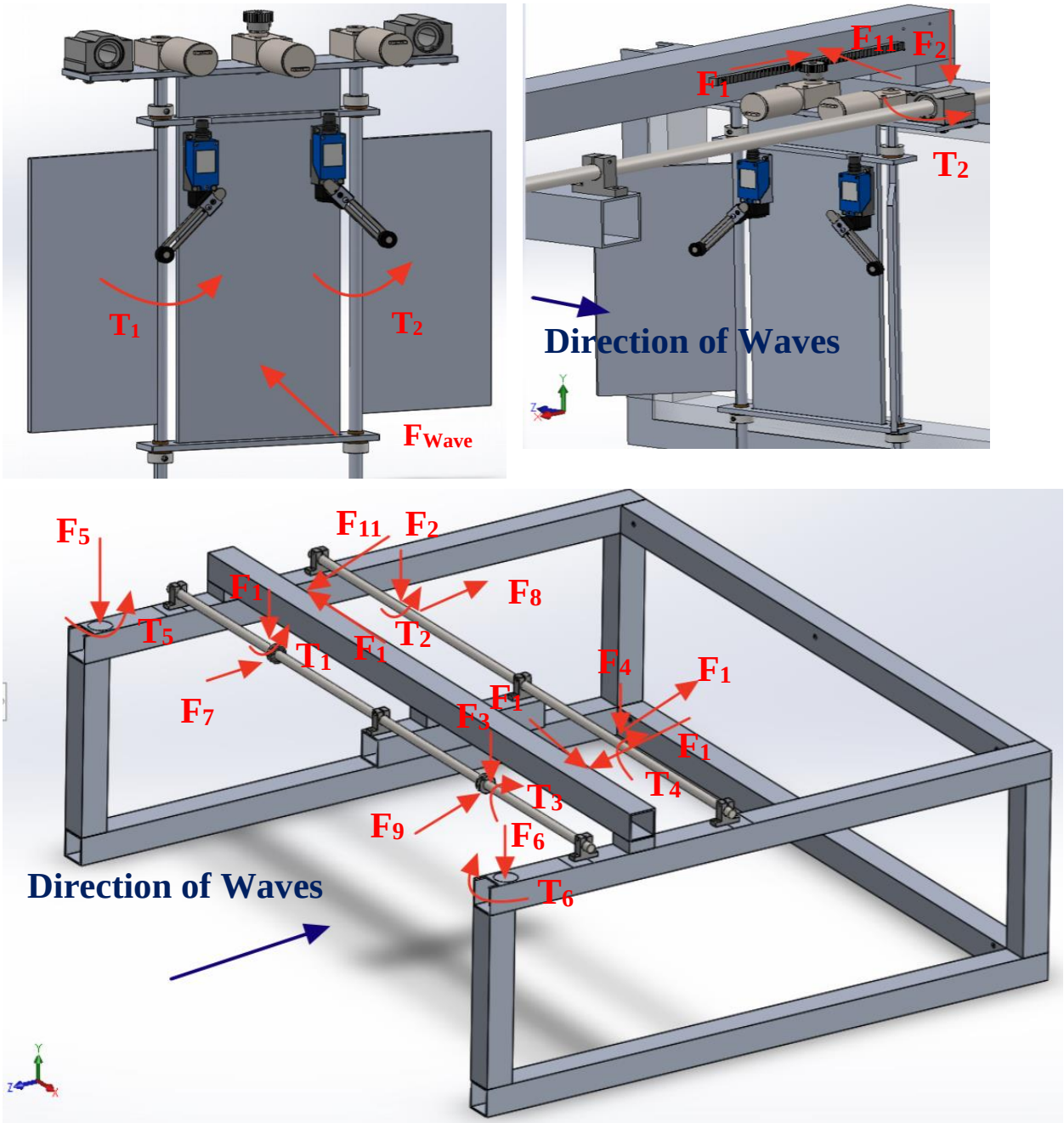

$F_1=F_2=F_3=F_4=200N$, $F_5=F_6=42N$, $F_7=F_8=F_9=F_{10}=25N$, $F_{11}=F_{12}=25N$, $F_{13}=F_{14}=70N$, $T_1=T_2=T_3=T_4=2Nm$, $T_5=T_6=6.9Nm$

Figure 64: FEA Input Conditions of Frame and Supporting Shafts for Static Conditions

$F_{1\text{-}4}$ were calculated by adding the weight of the deflector mechanism, shown in top left of Figure 64, and the resulting force in the negative y-axis that the linear bearings apply to the supporting shafts due to the torque applied to the linear bearings by the force F_{Wave}, see "Maximum Force on combined deflector plate assembly (N)" in Table 14, to the bottom of the deflector mechanism in the x-direction. This force could also have been applied as a torsion about the z-axis, but in a worst-case scenario only one side of the linear bearing would contact the shaft and cause a shear force that would result in bending instead of pure bending/torsion. $F_{5\text{-}6}$ were simply the weight of the wave gate assemblies. $F_{7\text{-}10}$ were calculated using the maximum wave back force applied to the wave deflectors found in "Maximum Back Force (N)" of Table 14. $F_{11\text{-}12}$ and $F_{13\text{-}14}$ are from the back force of the wave deflectors applied to the rack and pinion, see Figure 65 for derivation of these forces. $T_{1\text{-}4}$ comes from the torsion applied on the wave deflectors, see "Maximum Back Torque (Nm)" in Table 14. $T_{5\text{-}6}$ comes from the torsion applied on waves gates, see "Maximum Back Torque (Nm)" in Table 14.

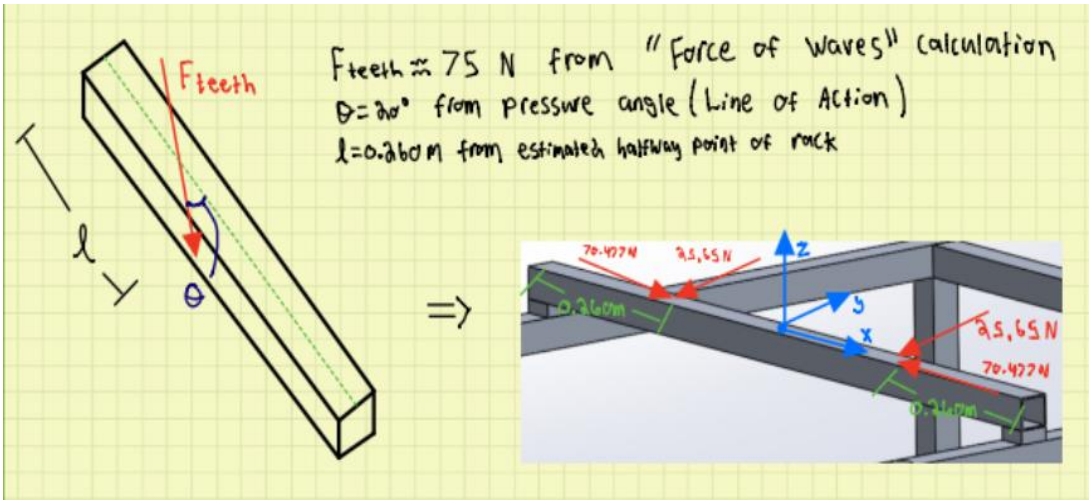

Figure 65: Calculation of Forces Transferred Through Rack and Pinion

Figure 66 below shows the input conditions for the FEA analysis of the Frame and the shafts that support the wave deflector mechanisms. These conditions are for when the device is dynamic and would not be exposed to wave forces. All the forces and torques experienced are due to the drag in the water. Note that the image in the left of Figure 66 shows how the frame and rods will experience no applied torques about the y-axis due to symmetry. The torsion about the z-axis shown in the left image is negligible and is not included in the image on the right.

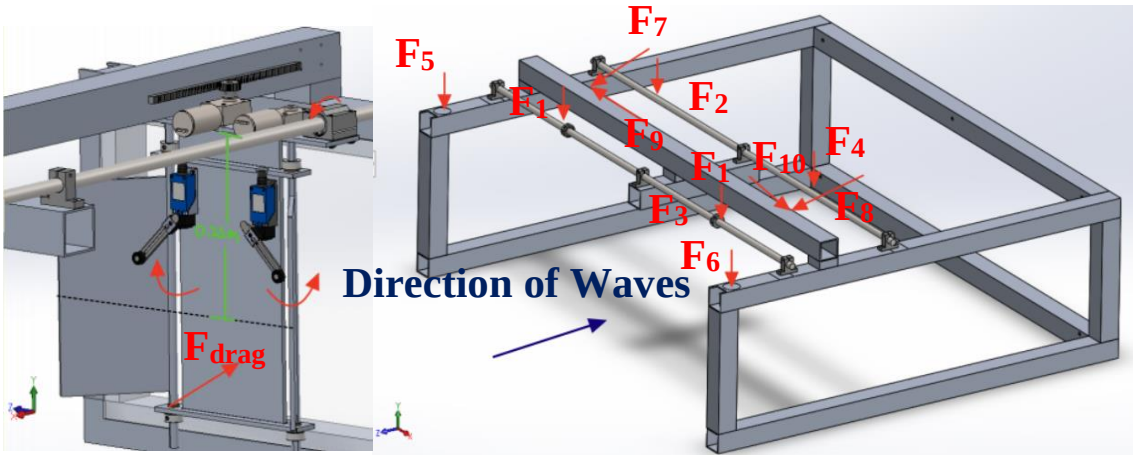

$F_1=F_2=F_3=F_4=60N$, $F_5=F_6=42N$, $F_7=F_8=25N$, $F_9=F_{10}=70N$

Figure 66: FEA Input Conditions of Frame and Supporting Shafts for Dynamic Conditions

$F_{1\text{-}4}$ distribute the weights of the deflector mechanisms, while $F_{5\text{-}6}$ are the weights of the wave gate assemblies. $F_{7\text{-}10}$ are the forces transferred through the rack and pinion, the same values from Figure 65 will be used, although they are overestimates it does not change the results any significant amount.

SolidWorks FEA

FEA was performed on various wave-gate assembly components and the contour plots are shown below in Figure 67 and Figure 68. For the input conditions of this analysis see Figure 62. For the wave gates, the yield strength of the material, Aluminum 6061, is 290Mpa. The maximum stress value on the chart is 145Mpa which would result in a factor of safety of 2. Since no stress value on the contour plot exceeds 145Mpa, the wave gate shaft and plate have a factor of safety larger than 2 which is acceptable. The maximum deflection of the plate is 1.5mm which is 0.5% of the length of the plate. This, along with the plate not being attached to another mechanism gives good reason to assume it is negligible. The wave gate length was shortened to reduce the deflection. The plate is deflected while the shafts show very little deflection. The wave gate shaft and plates will be subjected to worse conditions then the wave deflectors, so this analysis is sufficient to validate the predicted success of the shaft and plates in both sub-assemblies. Further dynamic FEA analysis may be analyzed in the future but would require much more complex CFD analysis to develop semi-accurate dynamic force estimates.

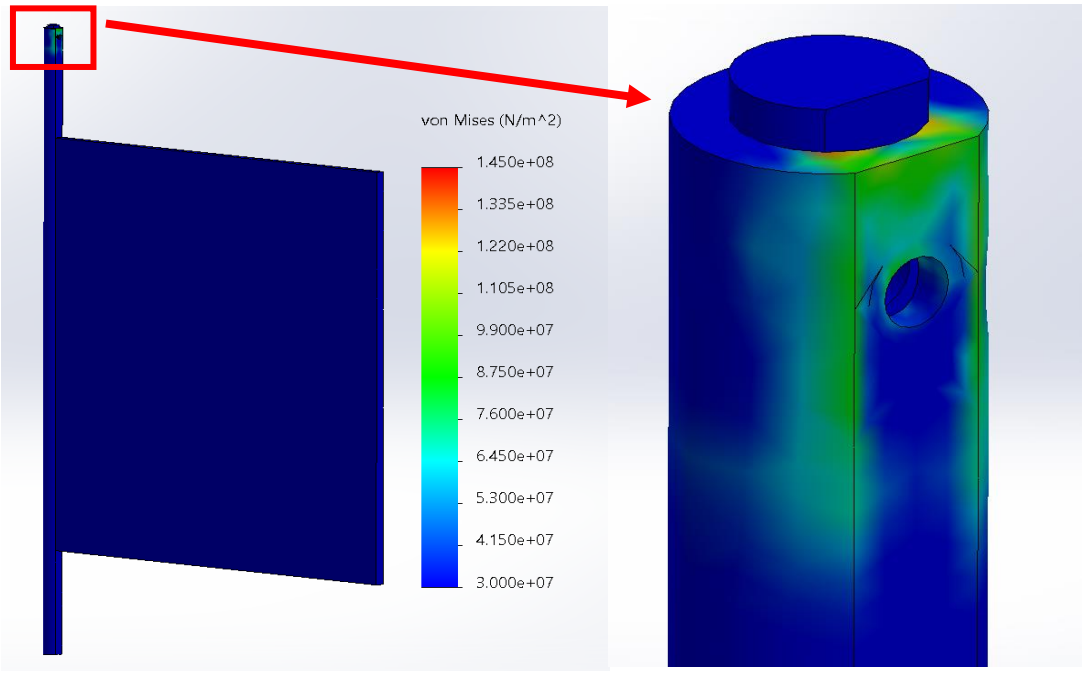

Figure 67: Worse Case Stress on Wave Gate Shafts and Plates

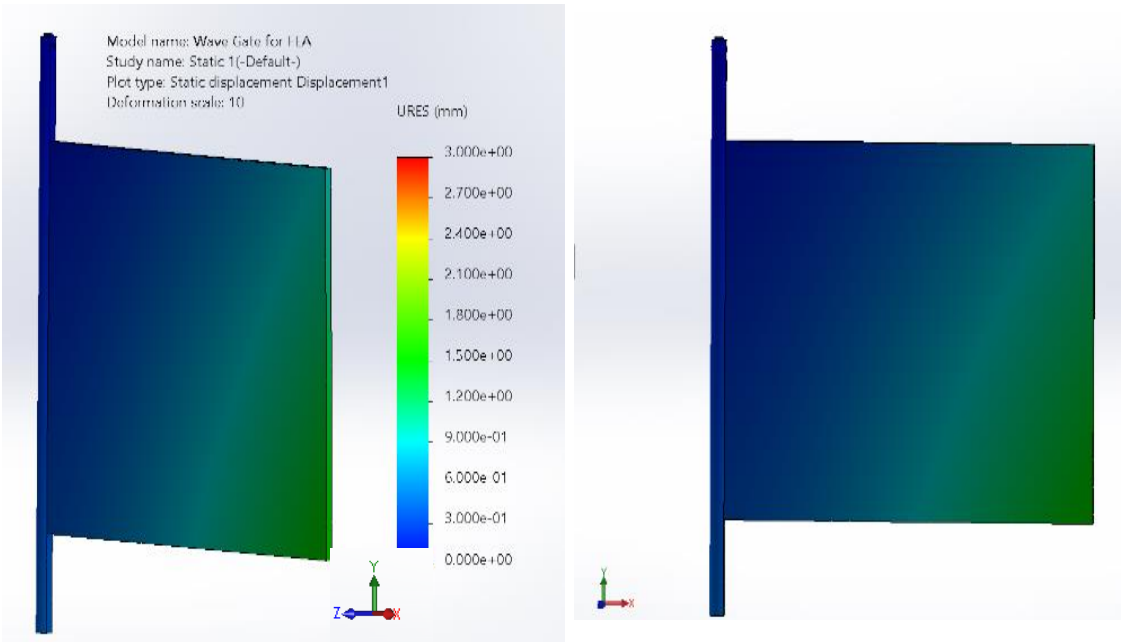

Figure 68: Worse Case Deflection of Wave Gate Shafts and Plates

FEA was performed on the overtopping device and the results are shown below. For the input conditions of this analysis see Figure 63. Figure 69 shows the experienced stress and Figure 70 shows the displacement. For the overtopping device, the yield strength of the material, Aluminum 6061, is 290 MPa. The maximum stress value on the chart is 145 MPa which would

result in a factor of safety of 2. Since no stress value on the contour plot exceeds or reaches anywhere near that value, the overtopping device is assumed to be structurally sound. Although this simulation does not show the sheet metal plates on top, their weights are accounted for using external loads. The maximum displacement of the overtopping device occurs in the upper curved supports and is a value slightly larger than 1mm. This deflection is only 0.1% of the height of the overtopping device so it has been deemed negligible.

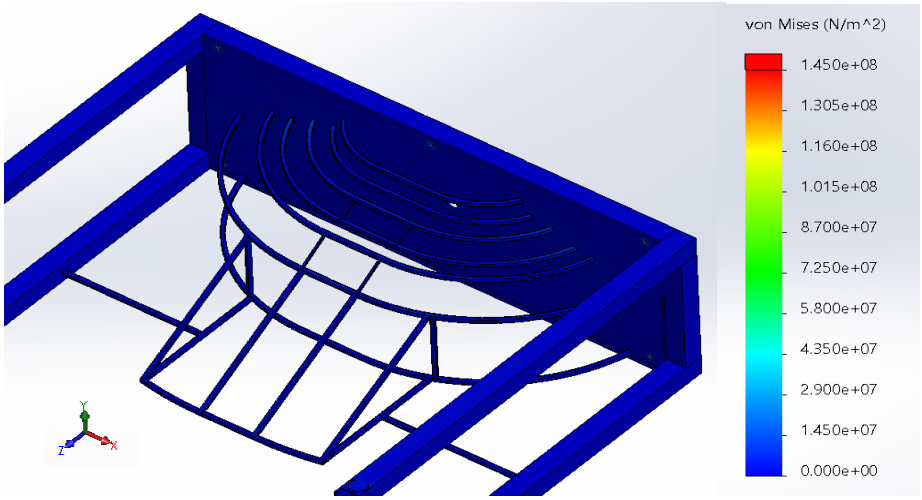

Figure 69: Stress on Overtopping Frame when Subjected to Wave Forces

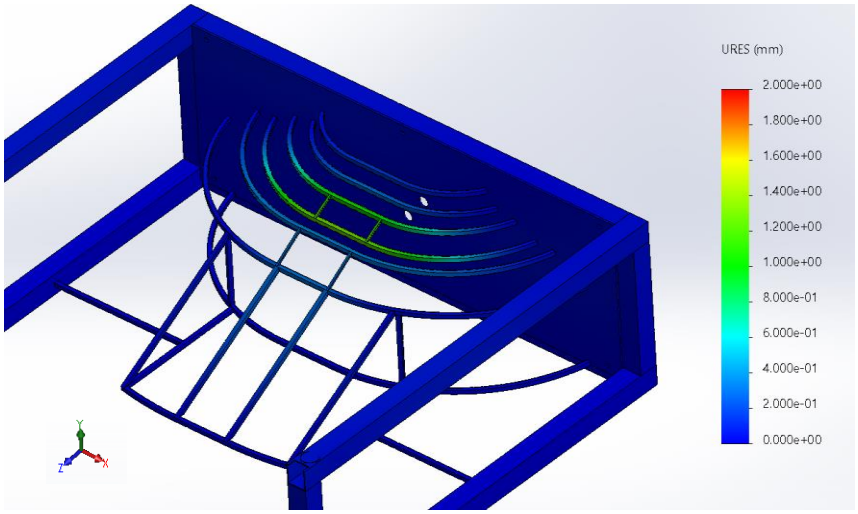

Figure 70: Displacement of Overtopping Device when subjected to Wave Forces

FEA analysis was performed on the frame and the shafts that support the wave deflector mechanisms. These conditions are for when the device is static and exposed to wave forces. For the input conditions of this analysis see Figure 64. The results are shown in Figure 71, Figure 72, Figure 73 below.

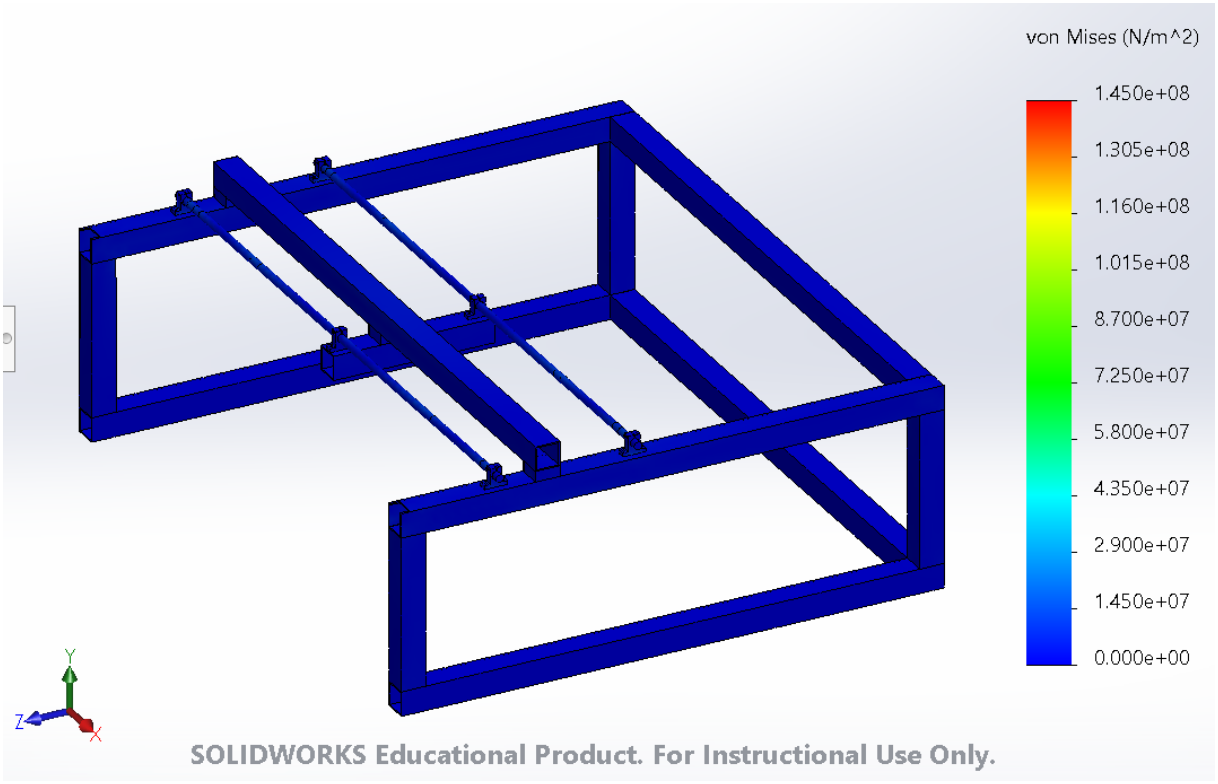

Figure 71: Stress on Frame and Supporting Shafts in Static Conditions When Exposed to Wave Forces

There is no stress near the yield strength of aluminum 6061, the weakest material in this analysis, so these results in Figure 71 are satisfactory.

Below, Figure 72 shows the displacement in the Y-axis and Figure 73 shows the displacement in the Z-axis of the same study as Figure 71.

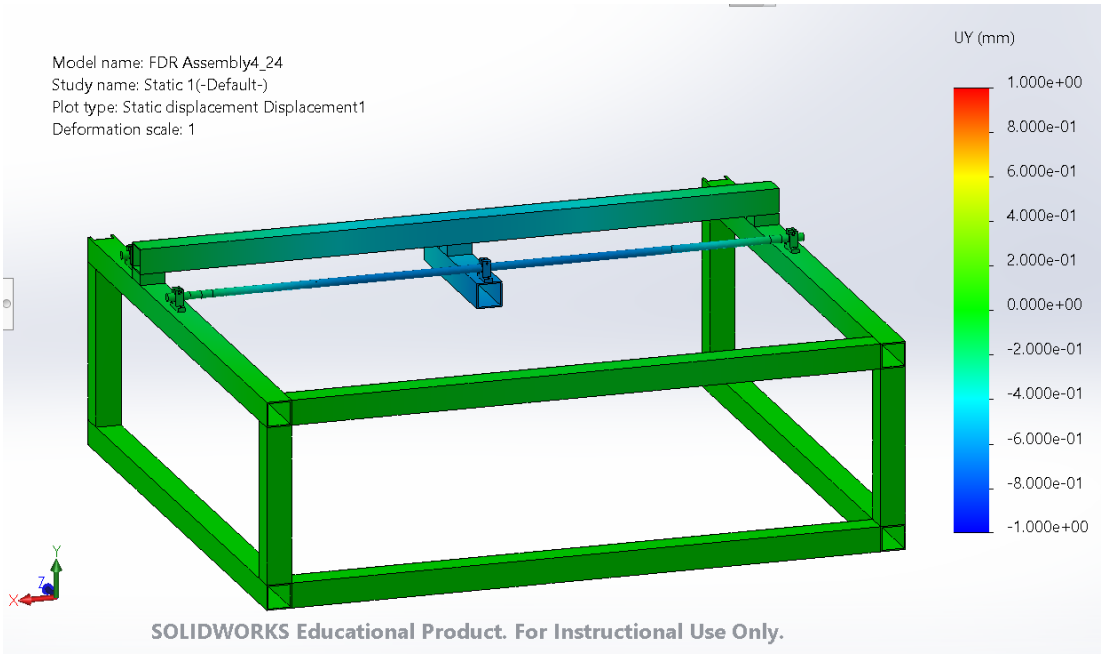

Figure 72: Y-Axis Displacement of Frame and Supporting Shafts in Static Conditions Exposed to Wave Forces

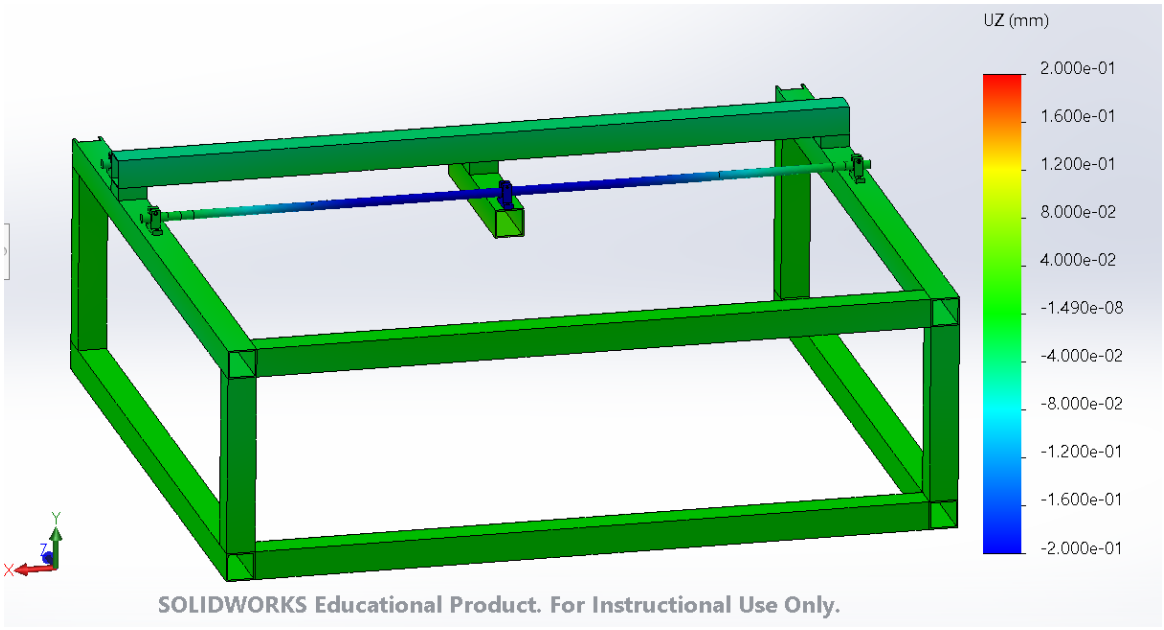

Figure 73: Z-Axis Displacement of Frame and Supporting Shafts in Static Conditions Exposed to Wave Forces

The key results of Figure 72 is that the square bar support beam and supporting shafts deflect in the same direction along the y-axis. Assuming worse case, where the center square bar and supporting shafts do not deflect together, the maximum displacement in the y-axis positions between the original positions of the square bar and supporting shafts is about 0.5mm. This value will be used in Displacement Analysis Appendix in which deflection stack up analysis is

performed. The key results of Figure 73 is that the center square essential does not deflect in the z-axis and the supporting shafts deflect a small amount of about 0.16mm at the farthest point towards the center that the rack extends. These results will also be shown in Displacement Analysis Appendix of the deflection analysis.

FEA analysis was performed on the frame and the shafts that support the wave deflector mechanisms. These conditions are for when the device is dynamic but not exposed to wave forces. This analysis is simulating the forces when the wave deflectors would be moving linearly, no other mechanisms will be moving at this time. For the input conditions of this analysis see Figure 66. The results are shown in below in Figure 74, Figure 75, and Figure 76.

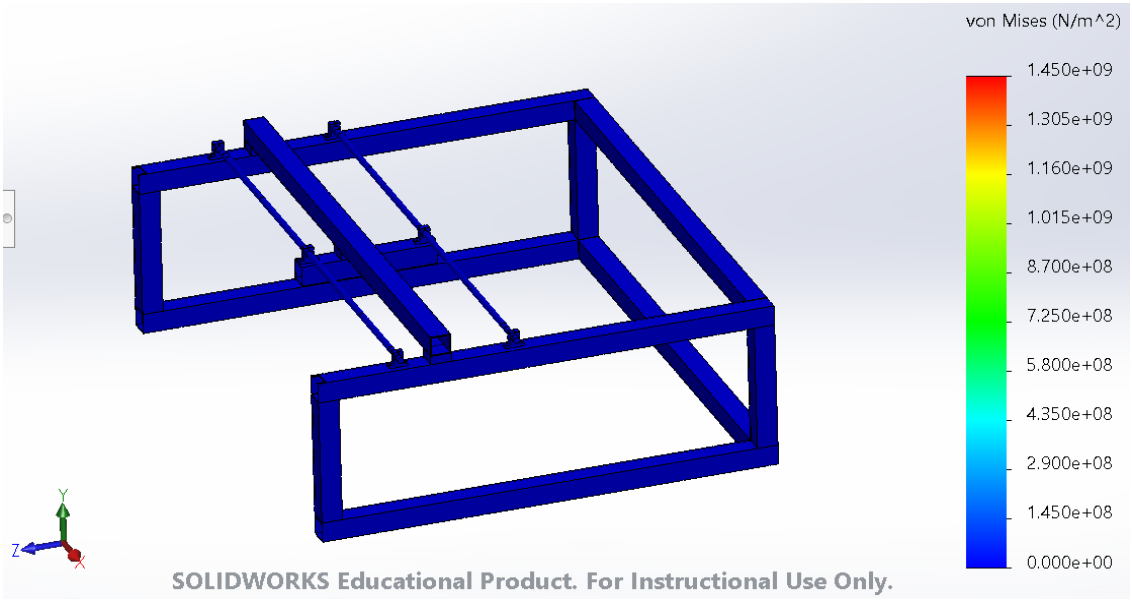

Figure 74: FEA Analysis of Frame and Supporting Shafts for Dynamic Conditions

There is no stress near the yield strength of aluminum 6061, the weakest material in this analysis, so these results in Figure 74 are satisfactory.

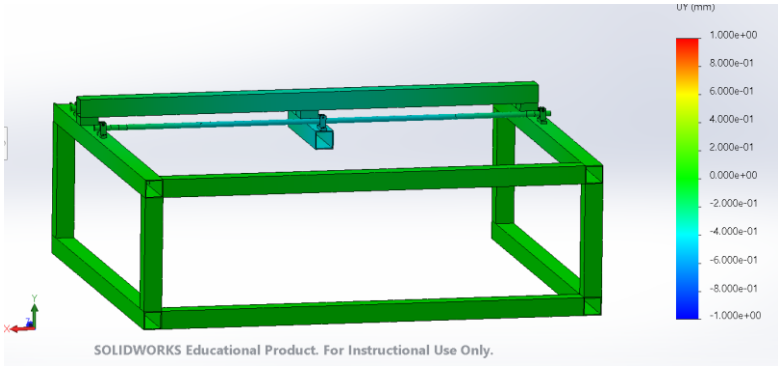

Figure 75: Y-Axis Displacement of Frame and Supporting Shafts in Dynamic Conditions

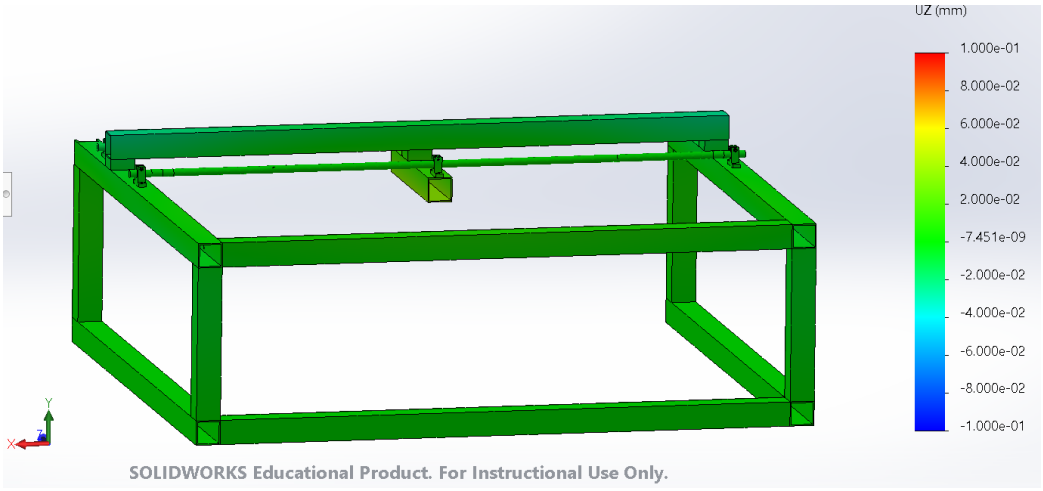

Figure 76: Z-Axis Displacement of Frame and Supporting Shafts in Dynamic Conditions

From Figure 75, the maximum displacement in the y-axis positions between the original positions of the square bar and supporting shafts is about 0.4mm. This value will be used in Displacement Analysis Appendix in which deflection stack up analysis is performed. The key results of Figure 76 is that the center square essential does not deflect in the z-axis and the supporting shafts deflect a small amount of about 0.02mm at the farthest point towards the center that the rack extends. These results will also be shown in Displacement Analysis Appendix.

Displacement Analysis from FEA Results

When analyzing the function of the rack and pinion it is critical to evaluate the deflection of the supporting shafts and the square bar that holds the piston. Another factor that contributes to the alignment of the rack and pinion is the rotation of the linear bearings about the supporting shaft. In Figure 77 the red arrow represents the torque that would be caused by either the force of the waves perpendicular to the center deflector pate or the drag on the wave deflector mechanism as it moves. The 0.25mm in Figure 77 is the worst case (loose) clearance between the linear bearing and the supporting shaft. This clearance would cause the deflector mechanism to slightly rotate and offset the gear at an angle, this motion is represented by the orange arrows.

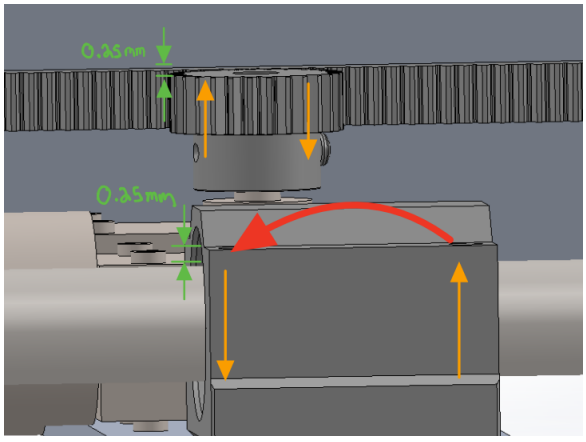

Figure 77: Linear Bearing Displacement Analysis

Since the angle of rotation is very small and can be assumed as negligible, the resulting displacement of this phenomenon would be 0.25mm in the y-axis. See Figure 78 below for axis orientation reference.

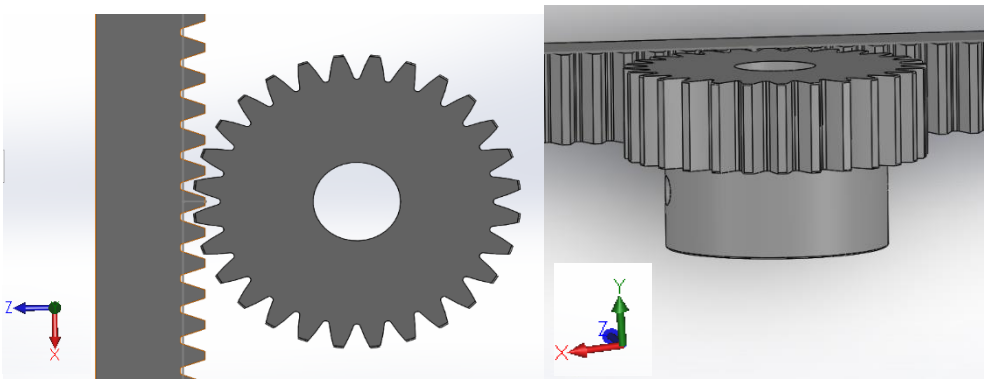

Figure 78: Orientation Reference of Rack and Pinion

The total, worst case, displacement in the y-axis for the static mechansim exposed to waves is calcualted with Equation 34. This equation includes the value from the phenomon in Figure 77 and the y-axis displcament value from Figure 72. It also shows the displacement as a percentage of the total face width.

Equation 34

$$dy(displacement) = 0.25mm + 0.5mm = 0.75mm, Face\ Width = 10mm, \frac{0.75}{10} = 7.5\%$$

For the static mechanism, the pinion does not have to run smoothly, it simply just needs to hold its position and not jump teeth. Since 92.5% of the pinion (along the y-axis) will still be in contact with the rack the deflection in y-axis is deemed negligible.

The total, worst case, displacement in the z-axis between the pinion and the rack in static conditions is 0.16mm, which was derived from the analysis shown in Figure 73. Equation 35 below shows the displacement as a percentage of the teeth depth. The ideal tooth depth of the pinion into the rack would be 2mm but to account for tolerances a tooth depth of 1.5mm will be used.

Equation 35

$$dz(displacement) = 0.16mm, Tooth\ Depth = 1.5mm, \frac{0.16}{1.5} = 10.6\%$$

Since 89.4% of the tooth depth is still engaged, and the pinion does not need to run smoothly, just hold its position, the deflection in the z-axis is deemed negligible. If that same displacement occurred in which the pinion would get closer to the rack it would assist in locking the mechanism so that is not a concern.

The total, worst case, displacement in the y-axis for the dynamic mechansim exposed only to drag is calcualted with Equation 36. This equation includes the value from the phenomon in Figure 77 and the y-axis displcament value from Figure 75. It also shows the displacement as a percentage of the total face width.

Equation 36

$$dy(displacement) = 0.25mm + 0.4mm = 0.65mm, Face\ Width = 10mm, \frac{0.65}{10} = 6.5\%$$

93.5% of the face width of pinion will be activated against the rack, this should be sufficient for the pinion to run smoothly on the rack. This is again the absolute worst-case scenario.

The total, worst case, displacement in the z-axis between the pinion and the rack in dynamic conditions is 0.02mm which was derived from the analysis shown in Figure 76. Equation 37 below shows the displacement as a percentage of the teeth depth.

Equation 37

$$dz(displacement) = 0.02mm, Teeth\ Depth = 1.5mm, \frac{0.02}{1} = 1.3\%$$

Since 98.7% of the tooth depth is still engaged, the pinion should be able to run smoothly on the rack. If this displacement pushed the pinion closer to the gear, than there would still be plenty of clearance between the teeth and base circle to run smoothly since worse case there would be 0.5mm of clearance.

Finally, when considering the displacement of the rack and pinion and the motion of the linear bearing on the supporting shaft, it is important to consider the forces on the linear bearing. When the wave deflector mechanisms are moving linearly, the drag creates the phenomenon shown in Figure 77 which results in the bearing applying forces to the shaft. Figure 79 below calculates what forces the bearing would apply to the shaft.

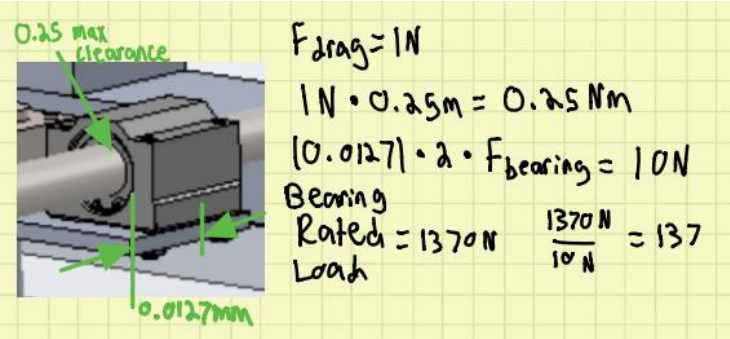

Figure 79: Linear Bearing Force Analysis

Since the wave deflector mechanism will move slowly through the water and result in very little drag, the linear bearing will experience only small amounts of torsion and induce 137 times less than rated load of the bearing.

These analyses give us good reason to believe that the rack and pinion will holds its position in the static state and run smoothly in the dynamic state. For future considerations, it might be beneficial to flip the bar and pinion to the other side of the rack and pinion so that deflection from the force of the waves would most likely push the teeth closer together and assist in locking it.

Dimensional Analysis for Wave Parameters

For hydrodynamic experiments, the wave scale factors were derived from Froude scaling laws (Islam, Jahra, & Hiscock, 2016). These were then modified to convert wave characteristics from actual ocean size to the smaller test pool conditions (Table 15). Wave conditions were scaled from actual size to prototype size based on conditions at the Port of Garibaldi in Oregon. Applying a scale factor of 1:32 resulted in the wave conditions in Table 16.

Table 15: Scaling Factors based on Froude Scaling Laws

Signal Type	Unit	Scale Factor
Acceleration	m/s^2	λ^0
Area	m^2	λ^{-2}
Density	kg/m^3	λ^0
Force	N	λ^{-3}
Frequency	s^{-1}	$\lambda^{0.5}$
Length	m	λ^{-1}
Mass	kg/m^3	λ^{-3}
Moment	N-m	λ^{-4}
Pressure	N/m^2	λ^{-1}
Speed	m/s	$\lambda^{-0.5}$
Time	s	$\lambda^{-0.5}$

Table 16: Prototype-Scaled Wave Characteristics

Wave Characteristic	Actual Size	Test Pool	Unit
Wavelength	61.61	1.925	m
Period	8.291	1.466	s
Height	3.685	0.115	m
Frequency	0.121	0.682	s^{-1}

To evaluate the accuracy of the Froude scaling method, two non-dimensional wave parameters developed by Le Méhauté and later used by the USACE were also calculated based on the full-scale model. Based on our calculations, the waves are Stokes 2nd Order, Intermediate Depth Waves (seen in Figure 80). These non-dimensional numbers were then used with the USACE method to scale the three key wave parameters for CFD simulations: average water depth (d), wave height (H), and wave period (T). Since there are three wave parameters and two non-dimensional numbers, one of the parameters must be defined by user. First, the period for USACE was set to match the period of the Froude scale. As seen in Table 17, the two scaling

methods agree, and therefore the USACE method was used to determine suitable wave parameters for the simulations.

Since the full-scale parameters are based on a buoy at sea (not on shore where the overtopping device will be placed), the initial USACE parameters are not the correct parameters for the simulation. The shore will slope upwards, decreasing the average water depth and wave height. Ideally, the high tide would have an average water depth the same height as the ramp to maximize power output. However, a more realistic average water depth would be near the top of the ramp, but slightly lower due to changing tides and imperfect real-world conditions. Because of this, the simulations were run based on the USACE Initial Modification as shown in Table 17. For future simulations, the ideal case (USACE Future Modification) or a low tide case (lower average water depth than the initial modification) should be run for comparison.

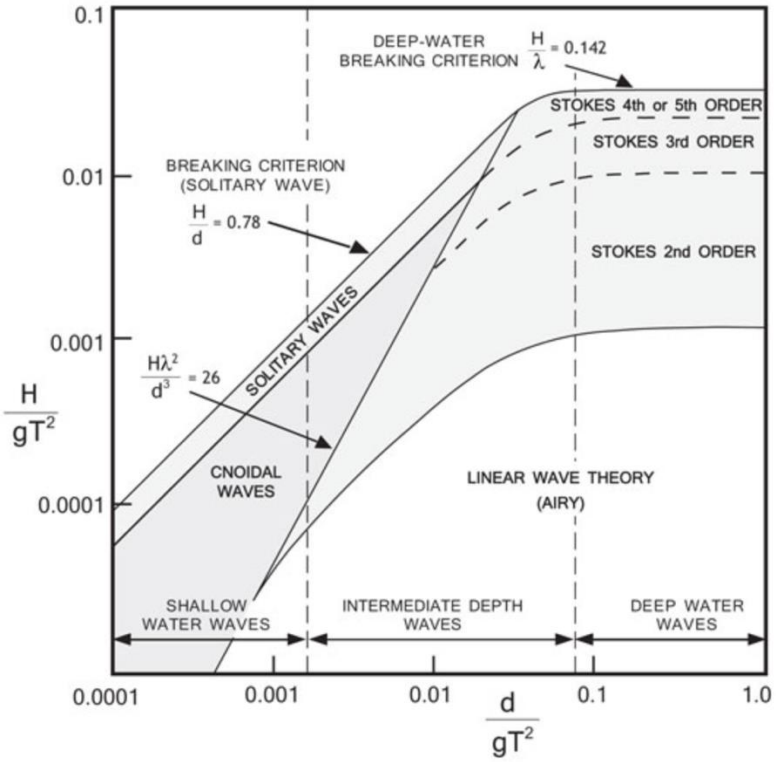

Figure 80: USACE Dimensionless Wave Parameters

Table 17: Comparison of Dimensionless Wave Parameters

Parameters	Full Scale	Froude Scaling	USACE	USACE Initial Modification	USACE Future Modification
H [m]	3.685	0.1152	0.1150	0.0433	0.0475
d [m]	19	0.5938	0.5927	0.2234	0.2450
T [s]	8.3	1.466	1.466	0.9	0.9425
g [m/s^2]	9.81	9.81	9.81	9.81	9.81
d/(gT^2)	0.0281	0.0282	0.0281	0.0281	0.0281
H/(gT^2)	0.0055	0.0055	0.0055	0.0055	0.0055

CFD Software & Process

To further analyze the flow and forces, the CFD software Flow3D-Hydro was used. This software is specifically designed for analysis on large energy producing structures and has built in wave features. This software was used to simulate the flow through the test rig when the deflectors are set in a variety of configurations to better inform physical testing. These simulations also provide valuable force data for the forces and torques acting on different components of the testing rig. This allowed for further analyzation of the test rig using FEA to iterate on the material selection process.

As seen in Table 18, five different simulation configurations were run. The first two simulations compared just the overtopping device to the initial test rig configuration. After this, different parameters were individually changed to see the impact on the wave height. Simulations 3 and 4 changed the gate angle to 15 and 75 degrees, respectively. Simulation 5 changed the deflector angles with the same gate angle as the first simulation.

For all simulations, 3 history probes, 2 flux planes, and 1 volume of fluid were used to capture various measurements. A history probe was placed near the top of the ramp, as well as one in each channel. These probes were used to determine the free surface elevation at those specific points. One flux plane was placed at the front of the ramp, and one at the outflow of the overtopping device. These flux planes were used to capture volume flow rate in and out of the overtopping device, however, based on the initial simulations, the overtopping outflow should be redesigned with downward sloping reservoirs and larger outflow holes to better simulate the results. The volume of fluid was a cube placed around the overtopping device. This proved to be misleading as it accidentally captured some of the volume outside of the overtopping device. Therefore, a volume of fluid should be specifically modeled to fit inside the overtopping reservoirs (one for each) to provide the most accurate results.

To finalize the setup for the simulations, more initial/boundary conditions are required, as well as appropriate meshing. The mesh was generated to fit the sides of the frame in the y direction. There was an additional 0.25 m behind the overtopping device in the x direction to allow appropriate outflow conditions and spans to 3 m in the positive x direction, allowing sufficient space for the waves to develop before entering the test rig. A cell size of 0.01 m was used as it provided an accurate model of the test rig, without being computationally over-demanding. The remaining parameters are shown in Table 19 and Figure 82 shows an example of the setup conditions of the simulation in the Flow-3D Hydro user interface.

Table 18: CFD Test Sets

Simulation Number	Gate Angle (deg)	Deflector Y Position [cm]	Top Deflector Angle	Bottom Deflector Angle	Measurements	Simulation Workspace	Simulation Name	Status	Notes
1	30	20	45	45	3 history probes (both channels and ramp), 2 flux planes (top of ramp and outflow), 1 VOF of overtopping	OvertoppingV1 Test	Test Setup	C	Testing functionality of probes and flux planes. Simulation ran as planned. Need to decrease time step in simulation to allow for better videos. Simulation stopped short for unknown reason but still post processed so unsure what happened there.
2	None	None	None	None	3 history probes (both channels and ramp), 2 flux planes (top of ramp and outflow), 1 VOF of overtopping	OvertoppingV1 Test	Test Setup no Frame	C	Purpose: Test the wave height at the top of the ramp without the frame to compare with future results
3	15	20	45	45	3 history probes (both channels and ramp), 2 flux planes (top of ramp and outflow), 1 VOF of overtopping	OvertoppingV1 Test	Sim3_15_20_45_45	C	Purpose: Test same setup as sim1 since it appeared succesful just with an altered gate angle
4	75	20	45	45	3 history probes (both channels and ramp), 2 flux planes (top of ramp and outflow), 1 VOF of overtopping	OvertoppingV1 Test	Sim4_75_20_45_45	C	Purpose: Test same setup as sim1 since it appeared succesful just with an altered gate angle
5	30	20	30	30	3 history probes (both channels and ramp), 2 flux planes (top of ramp and outflow), 1 VOF of overtopping	OvertoppingV1 Test	Sim5_30_20_30_30	C	Purpose: Test same setup as sim1 since it appeared succesful just with an altered deflector angle

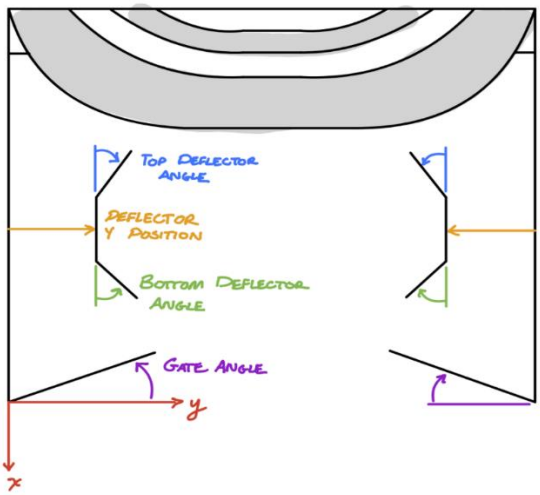

Figure 81: Gate and Deflector Angle and Position Definitions

Table 19: Key CFD Simulation Parameters

Parameter	
Referemce Pressure [atm]	1
Finish Time [s]	10
Density [kg/m^3]	1030
X-min Boundary Condition	Outflow (with 0.2 m wave absorbing layer)
X-max Boundary Condition	Wave (with previously mentioned wave parameters)
Y-min Boundary Condition	Symmetry
Y-max Boundary Condition	Symmetry
Z-min Boundary Condition	Symmetry
Z-max Boundary Condition	Pressure
Initial Conditions	Based on wave boundary condition

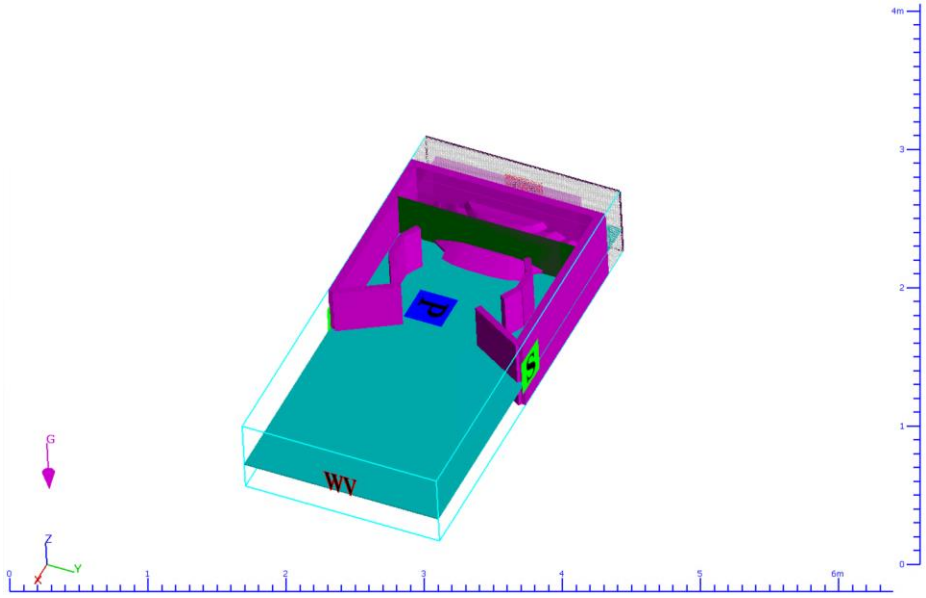

Figure 82: Example CFD model in Flow3D User Interface

CFD Results

For this projects purposes, the results of the CFD can best be shown in 3 different plots: the wave height on the ramp, the volume flow rate at the top of the ramp (the flow rate into the overtopping device/backwash that occurs), and the wave height in the left and right channels. All heights are in m, and the volume flow rate is in cu-m/s. In the graphs with left and right channels the left is represented by the blue line and right by the red line. Cases for all the simulations can be seen in Figure 83 - Figure 87 below.

Based on these results, both simulations 1 and 5 showed ~20% increase in wave height compared to the only the overtopping device (simulation 2), proving the functionality of the

device. Additionally, the volume flow rate at the top of the ramp in simulations 1, 3, and 5 show a decrease in backwash (the negative flow rate decreases and approaches 0). Additionally, the simulations show that the left and right channels are nearly symmetric in terms of wave height, which was expected and helps prove the merit of the CFD model. These channel graphs also approach a sinusoidal function that could be used in future work to better control the wave period of the reflected waves to perfectly align for constructive interference.

Simulation 4 shows a unique test case that would not normally be physically run. This test case had the gate inside of the deflectors, which was assumed to not work any better than the standalone overtopping device. The beginning of this simulation justifies this assumption as the wave height does not increase. There appears to be a significant wave height increase at the end of the simulation, however, this was due to the CFD software not being able to handle this configuration and a diverging solution at the end. This test case was run to prove the initial assumption as well as to assert that CFD is a good tool to use to eliminate certain test cases from physical testing.

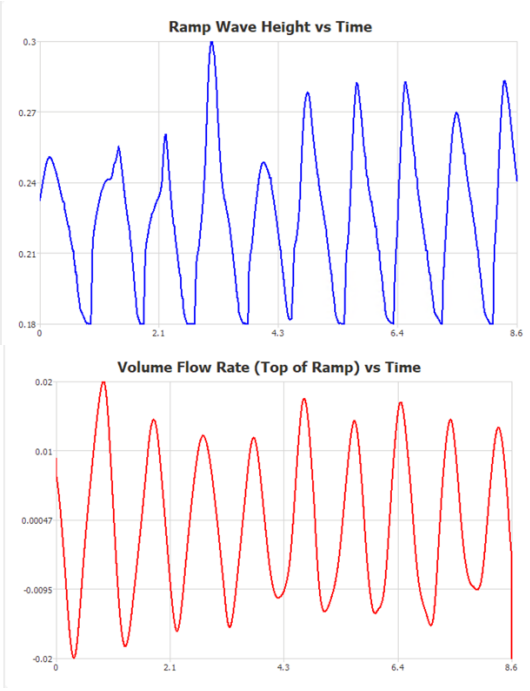

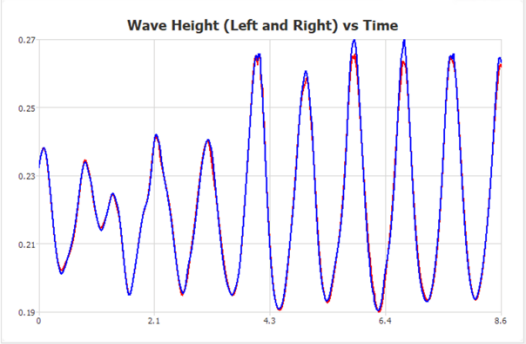

Figure 83: Simulation 1 Results

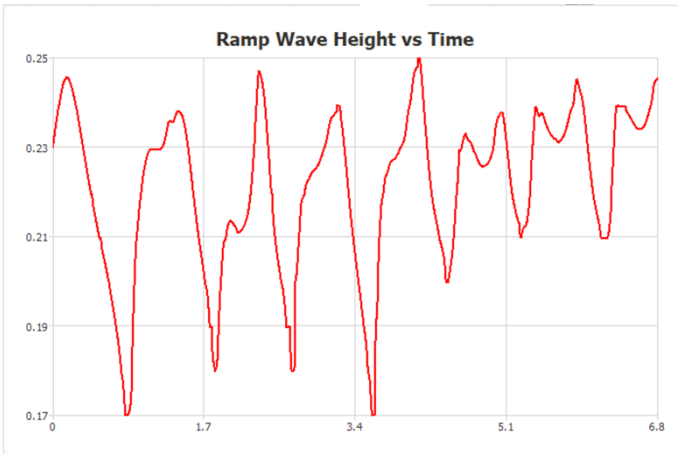

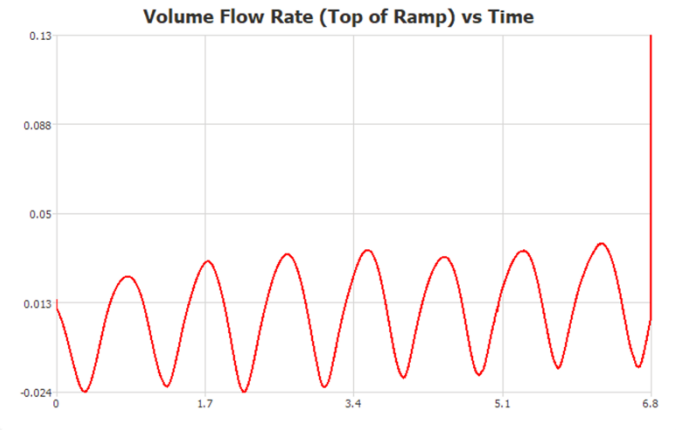

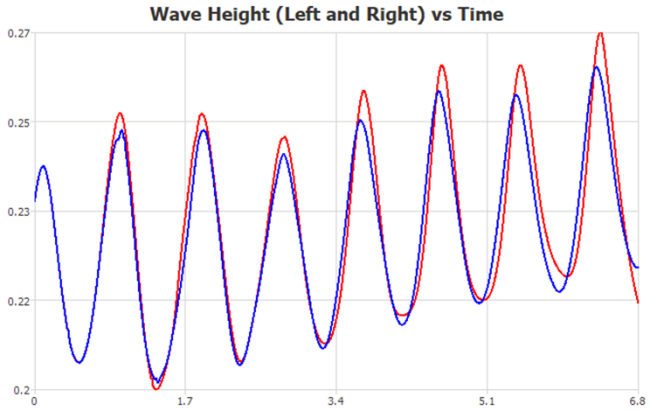

Figure 84: Simulation 2 Results

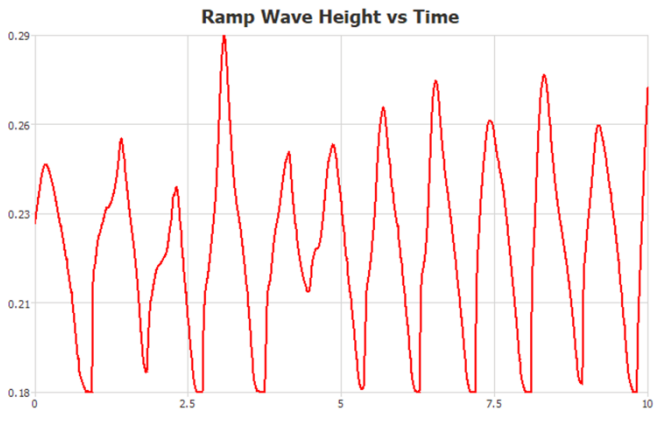

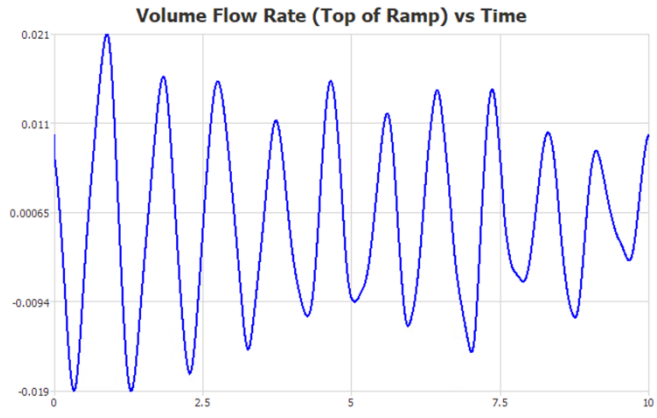

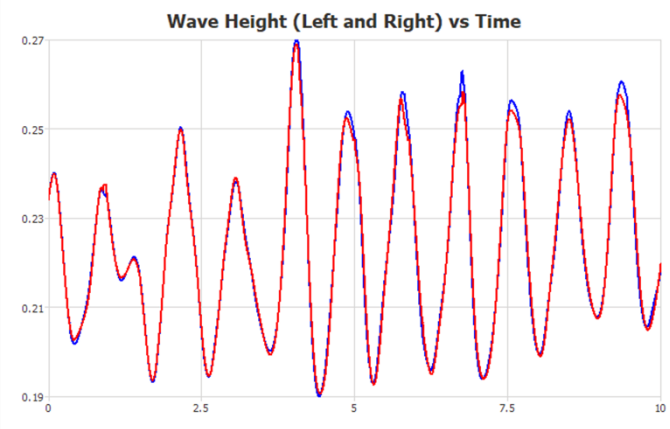

Figure 85: Simulation 3 Results

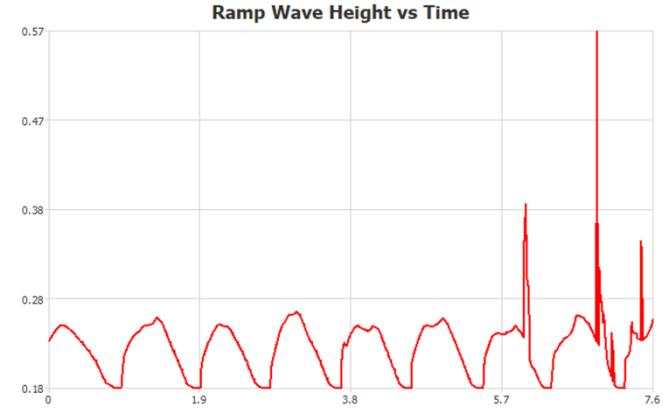

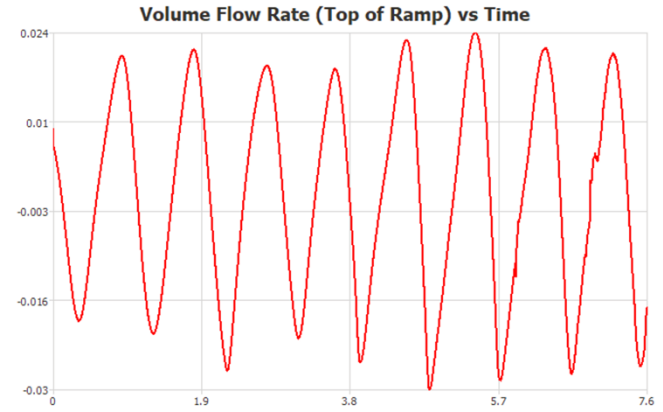

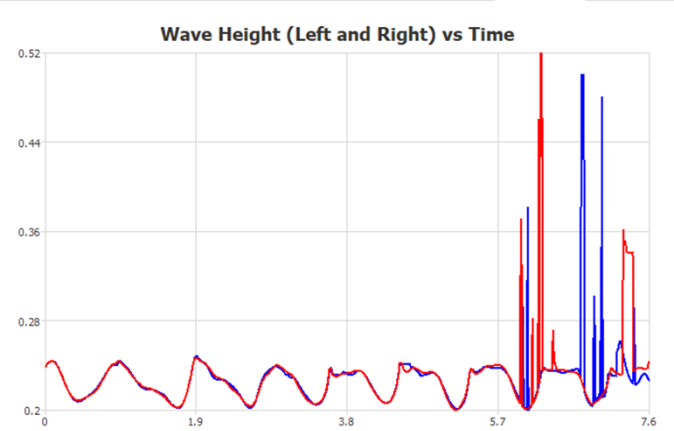

Figure 86: Simulation 4 Results

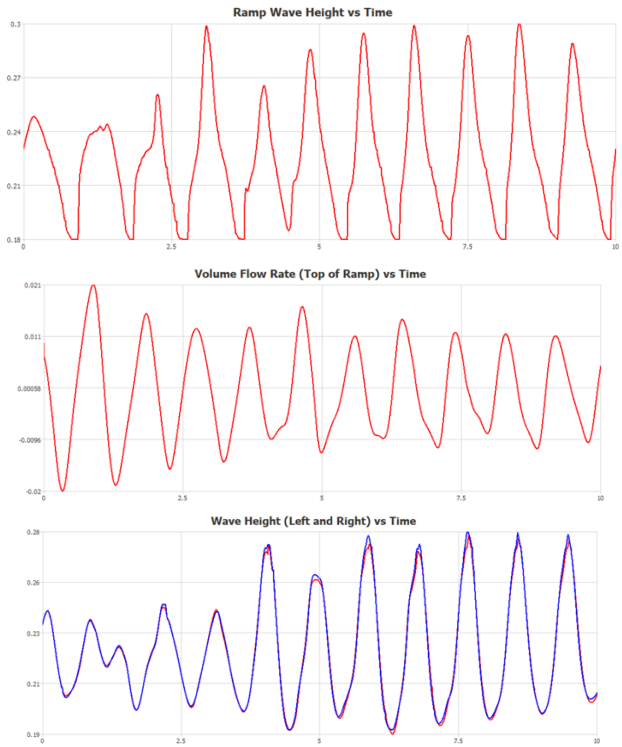

Figure 87: Simulation 5 Results

Future CFD & Testing

Based on these initial CFD simulations, there is proof that creating constructive interference is possible. Because of these initial results, more cases of the test rig should be simulated to better inform physical testing and eliminate any unnecessary cases. The future testing should only change one parameter at a time (either deflector angles, linear distance, or gate angles) to see the effects of the change. Since there are thousands of different cases that could be run, many extremes should be tested first to gage what works and then iterate from there.

Additionally, verification and validation of this CFD should be done to ensure that the model accurately depicts the real-world problem and that the model is correctly implemented and has a low error between several runs. The validation can be done within Flow3D by running several of the same test case, however, verification of the model's accuracy to the real-world problem is more difficult. This will be done with the physical test rig and could additionally be coupled with calculations to see how the wave parameters change as the wave approaches the shore.

Appendix J: Electronic Schematics and Controls

The electronics and controls for the overtopping test device are centered around a National Instruments myRIO system. This microcontroller was selected for its rapid and robust data acquisition on multiple input channels at a time. The myRIO is also easily programmed in LabVIEW which is taught in the Purdue mechanical engineering curriculum and a standard in lab spaces, making future work easier to complete and troubleshoot.

The full wiring diagram (Figure 89) shows all the connections necessary for this design. As shown in Appendix G: Mechanical CAD in the Wiring section, this wiring schematic as well as all the electrical components were drawn in CAD to fully plan their implementation. The control of the motors is completed with two digital pins to select whether all the motors should be moving towards or away from their default positions and eight PWM (pulse width modulation) pins to control motor power. These pins are wired to the L298N dual H-bridges that control two motors each with a supplied 24V. This setup limits the ability to control all the motors individually at once but the test procedure to be used with this device will not requires that functionality. The hall effect encoder signals from each motor are delivered through two data lines for an A and B pulse that are 90° out of phase. These encoder pulses have a resolution of 16 pulses per revolution each allowing a measurement precision of 64 counts per revolution of the DC motor. The gear ratio for the worm gear attached to the DC motor is 1/500 so the measurement resolution that can be obtained for the output shaft is 32000 counts per revolution or ±0.01125°. The myRIO has four dedicated encoder port pairs which allows measurements to be read from half of the motors at a time. With the use of the ADG436 digital switch IC, the myRIO can use a single digital output to select between which half of the motors are being measured currently. The test procedure is designed around this measurement limitation such that this is not an issue.

To acquire accurate and low noise signals from the pressure sensors, a separate 4-20mA current loop was implemented for each sensor using the XTR105 and RCV420 integrated circuits. The diagram of the current loop setup can be seen in Figure 88 below with the leads labeled to use this setup in the overall wiring diagram. This circuit has a direct voltage out that will be read by an analog pin on the myRIO to determine the instantaneous static pressure the sensor is experiencing.

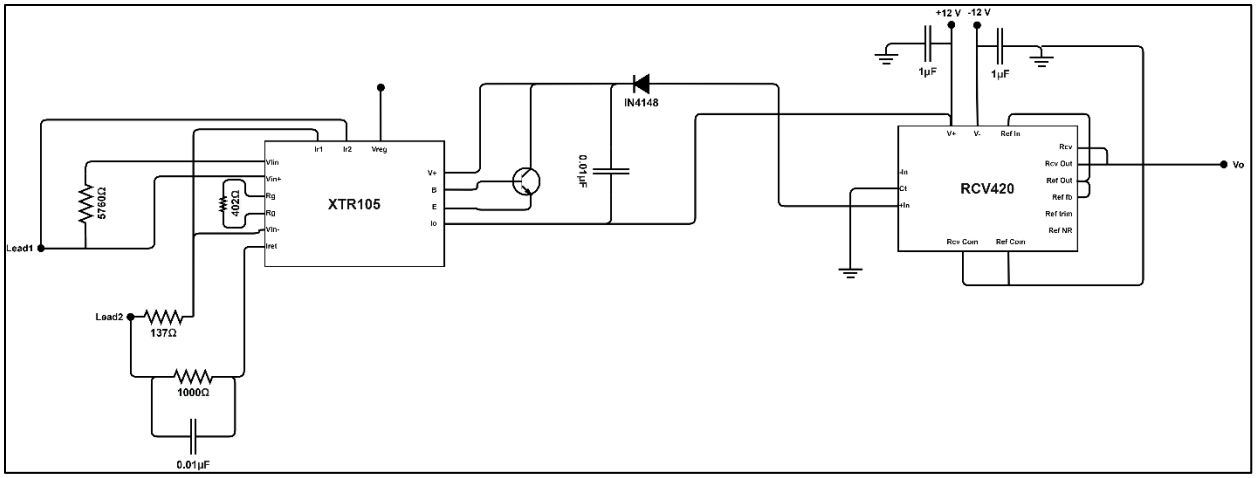

Figure 88: 4-20mA Current Loop Schematic

The flow sensors used at the back of the overtopping device use a ground and 5V connection to generate a voltage output that can be read by an analog pin on the myRIO to determine the time variable volume of liquid flowing out of the overtopping reservoir and directly analyze the performance of the present test scenario.

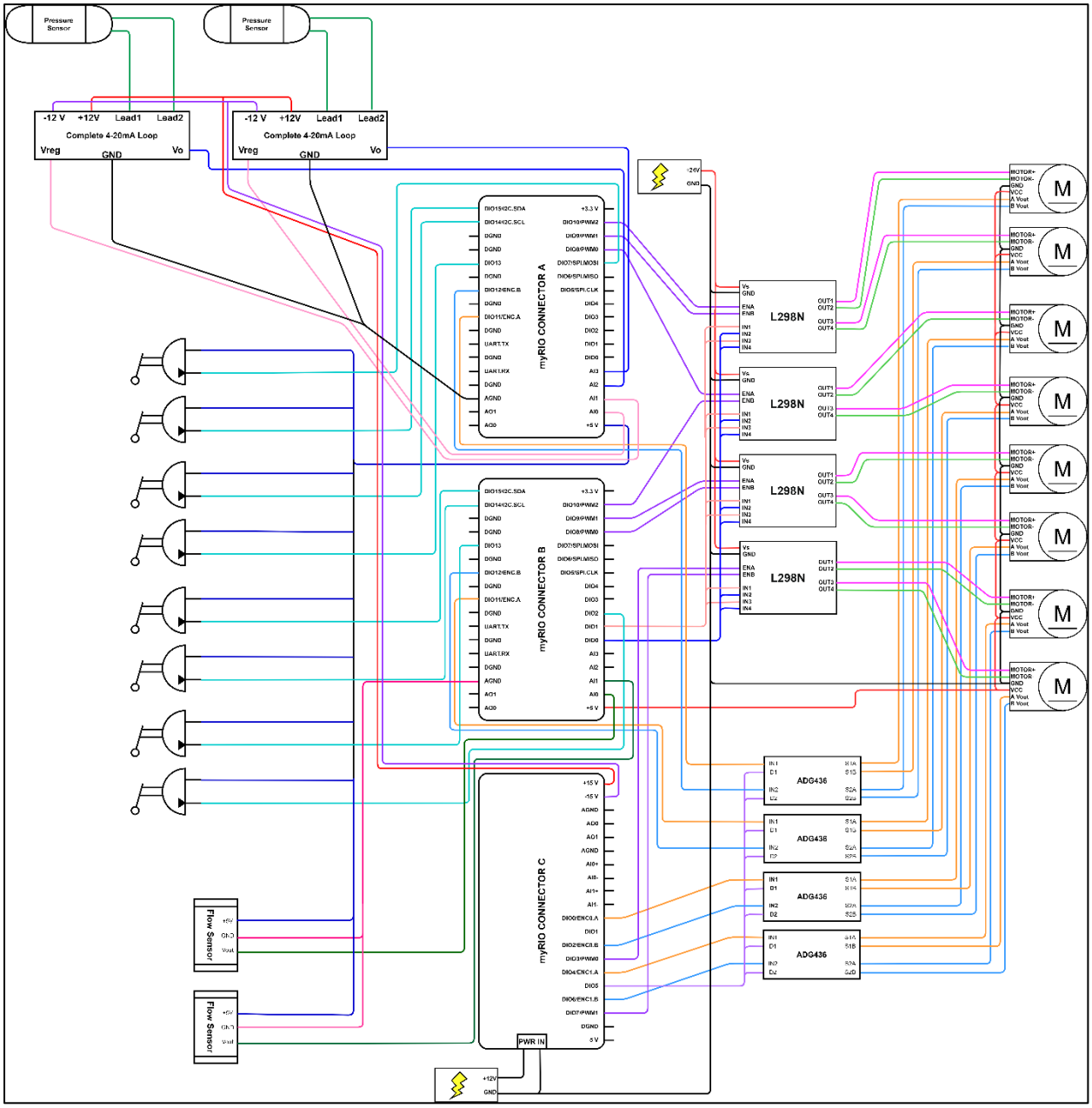

Figure 89: Full Device Wiring Diagram

The first step in the overall control scheme (shown in Figure 91) is to check if the water in the wave pool is motionless. This can be visually inspected and does not require a perfectly still pool. This inspection is to ensure most of the residual waves have stopped before moving the device.

Once the wave pool is still, the "Set Deflector Settings" function is run. This process begins with the "Begin at Home Position Process" outlined in Figure 90. This process will use a limit switch to detect when the linear actuators of the deflectors have reached their home positions. This will be run before the rest of the functions to ensure that the deflectors are set in

the desired testing location (specified by the testing plan). Once the home position is reached, the linear actuators will move the deflectors to the correct horizontal location. Then the motors will drive the deflectors to the correct angle. After the deflector settings are set, the "Set Gate Settings" function is run. This function follows the same process that the deflector settings follow, however, only rotation of the wave gates is required.

After all the settings for the gate and deflectors are set, the wave pool conditions are manually set to the desired specifications (wave period, amplitude, etc.). Once again, the wave pool is visually inspected to ensure that the water is relatively motionless before the test begins. Once the water is still, the wave pool is turned on. Two flow sensors, one for each reservoir, will read in, store, and display flow data to the user. This will be done for the duration of the test period, here set to 5 minutes. Throughout the duration of the test, an emergency stop function will run in the background to stop the test immediately if there is undesired motion in the gates or deflectors.

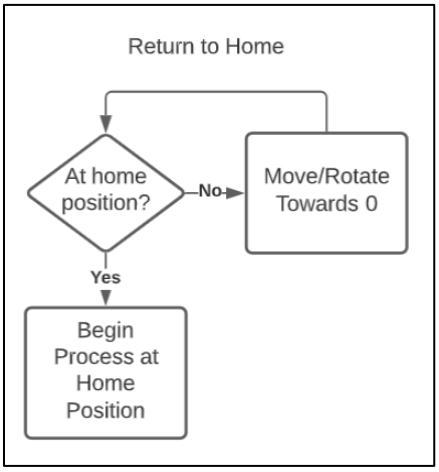

Figure 90: Control for Return to Home Mechanism

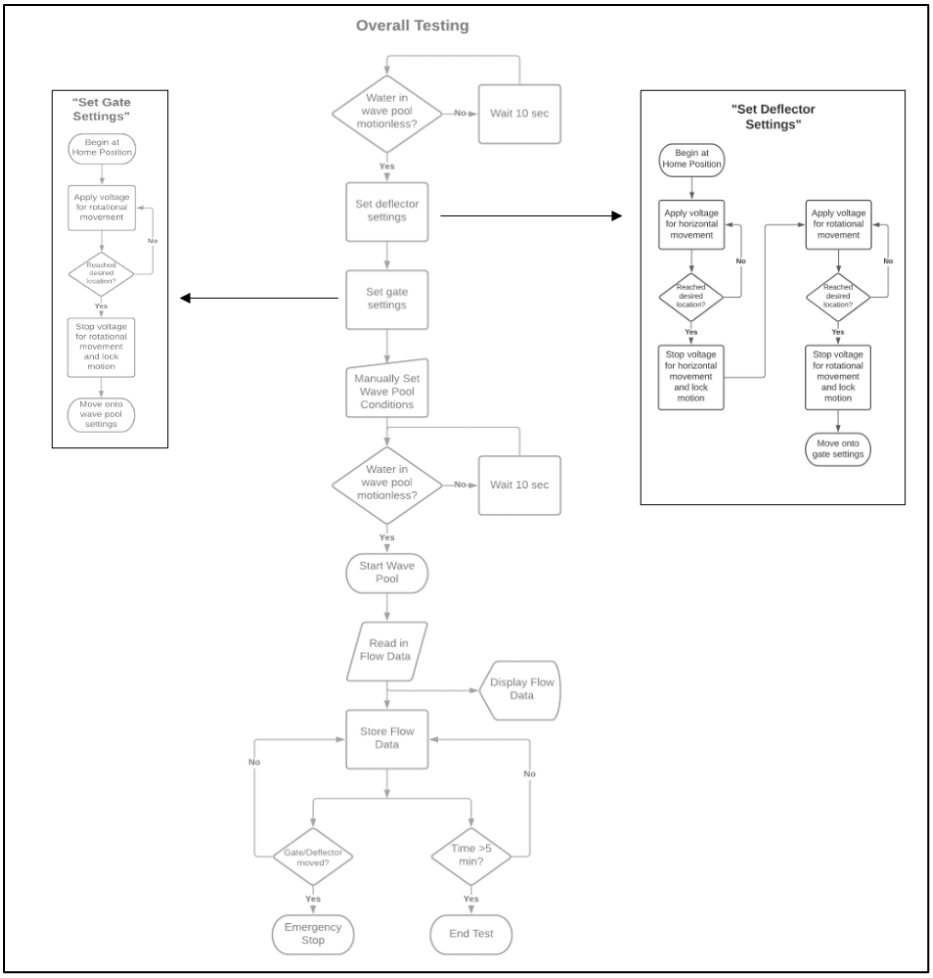

Figure 91: Control Scheme for Overall Testing Process

Appendix K: Manufacturing Drawings & Process

Bar Cuts

The frame and overtopping skeleton bar will be cut to length from stock. If the prototype is built at Purdue, the vertical bandsaw located in the Bechtel Innovation and Design Center (BIDC) can be used, which is what the tolerances for the bar cuts were based around. The amount of 0.5” and 0.25” Aluminum 6061 square bar stock required for the skeleton was determined by first flattening each of the curved pieces and measuring the flattened length. The frame is made from 2.5” Aluminum 6061 square bar stock. An excel sheet was used to determine the best combination of parts to be cut from the 6ft and 3ft stock bar for the frame and overtopping skeleton to create the least amount of waste possible. The resulting cut lists are seen in Table 20 and Table 21 below. The skeleton bar will need to be bent to appropriate dimensions once cut which will need to be outsourced to a professional.

	0.5"x 0.5" Bar								0.25" x 0.25" Bar
Stock Bar	1	2	3	4	5	6	7	8	1
Purchased Length (ft)	6	6	6	6	6	6	6	6	3
Cut 1 Length (ft)	1.49	1.49	1.98	1.69	3.16	4.49	5.56	5.56	0.40
Cut 2 Length (ft)	0.76	0.76	1.69	3.87	2.53				0.40
Cut 3 Length (ft)	1.63	1.63	2.23						0.26
Cut 4 Length (ft)	1.44	1.44							0.26
Total Used Length (ft)	5.32	5.32	5.90	5.56	5.69	4.49	5.56	5.56	1.32
Remaining Length (ft)	0.68	0.68	0.10	0.44	0.31	1.51	0.44	0.44	1.68

Table 20: Overtopping Stock Bar Cuts

	2.5" x 2.5" Stock Bar							
Stock Bar	1	2	3	4	5	6	7	8
Purchased Stock Length (ft)	6	6	6	6	6	6	6	2
Cut 1 Length (ft)	4.64	4.64	4.64	4.64	4.92	4.92	5.34	1.38
Cut 2 Length (ft)	1.31	1.31	1.31	1.31	0.10	0.10	0.10	
Total Used Length (ft)	5.95	5.95	5.95	5.95	5.02	5.02	5.44	1.38
Remaining Length (ft)	0.05	0.05	0.05	0.05	0.98	0.98	0.56	0.62

Table 21: Frame Stock Bar Cuts

Water Jet Cuts

The overtopping sheet metal plates will be precisely cut from a sheet of 3003 aluminum using water jet cutter, such as the one in the BIDC. Each of the sheet metal parts was flattened and fit onto the size of sheet metal stock that was the largest and had the lowest unit cost. The intended purchase sheet metal stock is 4 feet by 8 feet. The parts are oriented in such a way to ensure that they all fit on the sheet and that no part is closer than three times the 0.13mm tolerance width for a laser cutting on sheet metal (Protocase, 2019). The water jet cutter will also

be used to cut the various plates and parts for the wave deflectors and gates. These parts will be cut from a 2’ x 2’ aluminum 6061. The layouts for the water jet cuts can be seen in the manufacturing drawings Sheet Metal Cuts 1, Sheet Metal Cuts 2, Wave Gate and Deflector Cuts 1, and Wave Gate and Deflector Cuts 2.

Critical Fits and Tolerances

Proper tolerances are critical to ensure that each part fits well enough to function. Tolerances for bushing fits on shafts are detailed in Figure 92.

LC 6 Fit	Image		Bracket Hole	Size/Tolerance	Bushing	Size/Tolerance
	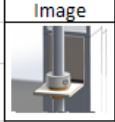	MMC	0.6396 in	0.638 + 0.0016 in	0.626 in	0.626 - 0.006 in
		LMC	0.638 in		0.62 in	

LC11 Fit	Image		Bushing	Size/Tolerance	Shaft	Size/Tolerance
	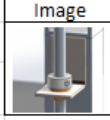	MMC	0.510 in	0.500 + 0.010 in	0.5 in	0.500 - 0.008 in
		LMC	0.500 in		0.492 in	

	Image		Linear Bearing	Size/Tolerance	Shaft	Size/Tolerance
	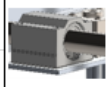	MMC	0.792 in	0.787 + 0.005 in	0.787 in	0.787 - 0.003 in
		LMC	0.787 in		0.784 in	

Figure 92: Table of fits and tolerances for the gate/deflector shaft assembly

When multiple joined parts have dimensional tolerances, it is necessary to analyze the propagation of these tolerances though the assembly to ensure correct fit and function. The wave gates and deflectors rely on straight supporting shafts to function properly. Maximum deflection for any shaft was 1/8”. Further analysis or physical study would determine whether tolerances should be tightened to reduce shaft deflection.

Gate Shaft Tolerance Stack Analysis				
Component	Image	Horizontal Displacement Tolerance	Worst Case Scenario	Max. Shaft Runout
Gate Shaft Bracket (Upper)		± 0.03 in	+ 0.03 in	0.12 in (1/8 in)
Gate Shaft Bracket (Lower)		± 0.03 in	- 0.03 in	
Worm Gear Mounting Plate	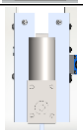	± 0.03 in	- 0.03 in	
Shaft Hole in Bracket (Upper)	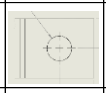	± 0.03 in	+ 0.03 in	
Shaft Hole in Bracket (Lower)	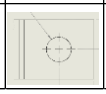	± 0.03 in	- 0.03 in	

Figure 93: Gate Shaft Tolerance Stack Analysis

Deflector Rail Tolerance Stack Analysis				
Component	Image	Horizontal Displacement Tolerance	Worst Case Scenario	Max. Shaft Runout
Shaft Bearing (Deflector)	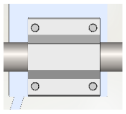	± 0.03 in	+ 0.03 in	0.06 in (1/16 in)
Shaft End Bearing (Frame)	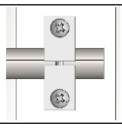	± 0.03 in	- 0.03 in	
Shaft Middle Bearing (Frame)	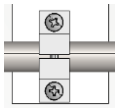	± 0.03 in	- 0.03 in	

Figure 94: Deflector Rail Tolerance Stack Analysis

Deflector Shaft Tolerance Stack Analysis				
Component	Image	Horizontal Displacement	Worst Case Scenario	Max. Shaft Runout
Deflector Gate Motor (Rear)	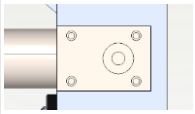	± 0.03 in	+ 0.03 in	0.12 in (1/8 in)
Top Deflector Shaft Bushing Hole		± 0.03 in	- 0.03 in	
Bottom Deflector Bushing Hole		± 0.03 in	+ 0.03 in	
Top Deflector Plate Slot	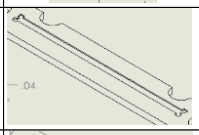	± 0.03 in	+ 0.03 in	
Bottom Deflector Plate Slot		± 0.03 in	- 0.03 in	

Figure 95: Deflector Shaft Tolerance Stack Analysis

Tolerance stacking was also studied to ensure the rack and pinion that translates the deflectors would mesh. The tooth depth is 2.5 mm and the maximum separation of the rack from the pinion is 0.06” or 1.5 mm (Figure 96). All tolerances are based on mounting screw locations for the rail bearings and pinion motor, so tightening these tolerances would result in a better mesh. Adding spacers between the rack and the frame would be an easier way to correct for an incomplete mesh.an incomplete mesh.

Gear Mesh Tolerance Stack Analysis						
Component	Image	Horizontal Displacement	Worst Case Scenario (Loose)	Max. Gear Separation	Worst Case Scenario (Tight)	Theoretical Gear Overlap
Deflector Rail Bearing (Front)	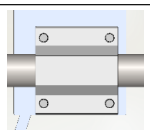	± 0.03 in	+ 0.03 in	0.06 in (1/16 in)	- 0.03 in	0.03 in (1/32 in)
Deflector Rail Bearing (Rear)	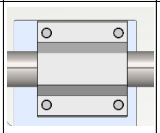	± 0.03 in	+ 0.03 in		- 0.03 in	
Pinon Motor	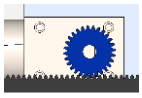	- 0.03 in	- 0.03 in		- 0.00 in	

Figure 96: Gear Mesh Tolerance Stack Analysis

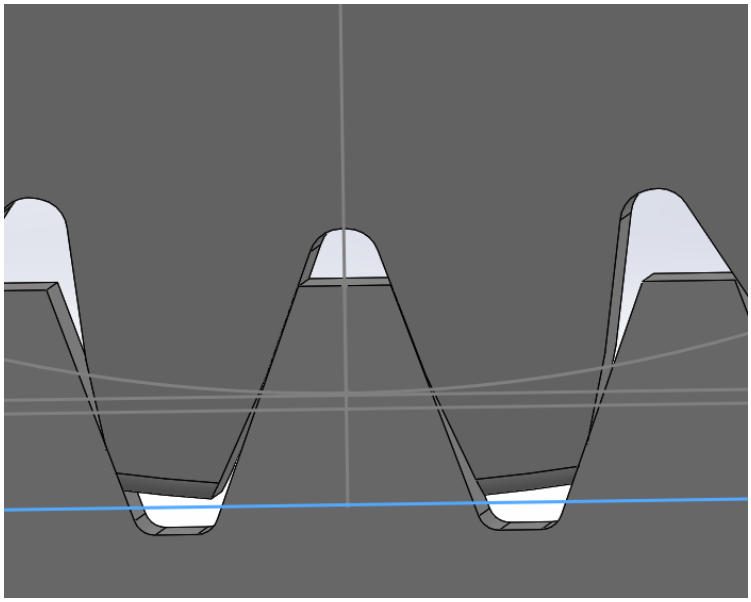

Figure 97: Ideal Gear Mesh

Ideally the gears will mesh so that the pitch circle of the rack aligns with addendum of pinion (Figure 97). In the worst-case tolerance scenario, the gears will either mesh loosely or too tightly. If they mesh too loosely, there is a chance that the pinion could skip teeth during operation. If the mesh is too tight, binding could occur. This is a worse scenario because it could hinder operation entirely. The machinist should take care to drill screw holes for the bearing and motor mounts in the correct locations.

Assembly Steps

The full detailed assembly steps for the device are listed below. Preprocesses to be done before assembly include water jet cuts, bandsaw cuts, bar bends, and machining processes for all the various parts. The assembly is then broken up into the 4 subassemblies: frame, overtopping,

wave gates, and wave deflectors. The "– [number]" following each step corresponds to the number of times the specific step should be completed.

1. Pre-processes
    a. BIDC Water jet cuts:
        i. Overtopping Sheet Metal 1 – 1
        ii. Overtopping Sheet Metal 2 – 1
        iii. Deflectors & Gates 1 – 1
        iv. Deflectors & Gates 2 – 1
        v. Frame acrylic plates – 2
    b. BIDC Vertical Bandsaw:
        i. Frame Bar (Table 21) – 1
        ii. Overtopping Skeleton Bar (Table 20) – 1
        iii. Wave Gate Shaft – 2
        iv. Deflector Shaft – 4
        v. Support Shaft – 2
        vi. Worm Gear Mount – 2
    c. Bends:
        i. Overtopping Skeleton Bar – 1
        ii. Overtopping sheet metal – 1
    d. Machining (milling and boring):
        i. Wave Gate Shaft - 2
        ii. Wave Gate Shaft Brackets – 4
        iii. Worm Gear Mount – 2
        iv. Back Plate – 1
        v. Deflector Shaft – 4
        vi. Deflector Base – 1
        vii. Frame Top Bar – 2
2. Overtopping Subassembly
    a. Assemble flow sensor components - 2
    b. Weld skeleton base
    c. Weld skeleton reservoir 2
    d. Weld corresponding sheet metal to skeleton base, reservoir 2, and crest bars
    e. Weld the two flow sensors to the reservoir 2 subsystem and base subsystem
    f. Apply waterproof Silicone sealant to the 3 welded systems: base, reservoir 2, and crest
    g. Weld overtopping base, reservoir 2, and crest to back plate
    h. Apply waterproof Silicone sealant to remaining weld locations
    i. Bolt Pressure Sensor to front of Overtopping
3. Frame Subassembly
    a. Weld 2.5" aluminum bar
    b. Secure Plexiglas Plates to Frame with ¼" bolts and washers
    c. Bolt Pressure Sensor to side
4. Wave Gates Subassembly - 2

a. Wave gate welded to Wave Gate Shaft
b. Shaft Sleeve Bearings into Shaft Brackets
c. Shaft Sleeve Bearings onto Wave Gate Shaft
d. Collars onto Wave Gate Shaft
e. Worm Gear Motor mounted to Worm Gear Mount with 4 M4 10mm Screws
f. Wave Gate Shaft secured with 4-40 0.5in Screw to Worm Gear Motor

5. Wave Deflectors Subassembly
    a. Weld Deflector Base – 2
    b. Deflector Sides Assembly – 2
        i. Deflector Shafts through holes – 2
        ii. Weld Deflector Plate to Deflector shafts – 2
        iii. Top Sleeve Bearings and Shaft Collars on and tightened with the Deflector Shaft all the way down – 2
        iv. Bottom Sleeve Bearings and Shaft Collars on and tightened to Deflector Shaft – 2
        v. Limit Switches mounted to Deflector Base – Tall Vertical with 4 M5 16mm Screws – 2
        vi. Support Shaft Sleeve Bearings mounted to Deflector Base with 4 M6 14mm Screws– Large Horizontal – 2
        vii. Worm Gear Motors mounted to Deflector Base – Large Horizontal with 4 M4 10mm Screws – 3
        viii. Deflector Shafts secured with 4-40 0.5in Screw to Worm Gear Motors - 2
        ix. Plastic Gear secured with 4-40 0.5in Screw to Worm Gear Motor - 1
6. Device Assembly
    a. Bolt Overtopping back plate to Frame
    b. Bolt Overtopping angle brackets to Frame
    c. Deflectors:
        i. Mount 6 Support Bearings to Frame – 6
        ii. Slide Support Shafts through Support Bearings just past the Frame Middle Support
        iii. Align first Deflector Side onto Support Shafts
        iv. Slide Support Shafts and Wave Deflector Side farthest possible before Frame Middle Support
        v. Align second Deflector Side onto Support Shafts
        vi. Align Support Shafts with Support Bearings and secure in place
        vii. Align Rack with Gear and mount to Frame – 2
        viii. Mount Wave Deflector Limit Switches – 2
    d. Wave Gates: 2
        i. Secure Worm Gear Mount to Frame
        ii. Secure L brackets to Frame – 2
        iii. Mount Wave Gate Limit Switches to Frame

Manufacturing Drawings

Drawing	Page #
Overtopping Device	
Back Plate	108
Skeleton Bar	
Base Semi Circle	109
Ramp Front	110
Reservoir 1 - Top	111
Reservoir 2 - Bottom	112
Reservoir 2 - Top	113
Crest - Bottom	114
Crest - Top	115
Sheet Metal	
Sheet Metal Cuts 1	116
Sheet Metal Cuts 2	117
Base Semi-Circle	118
Ramp - Left	119
Ramp - Right	120
Reservoir 1 - Left Outer	121
Reservoir 1 - Left Inner	122
Reservoir 1 - Right Outer	123
Reservoir 1 - Right Inner	124
Reservoir 2 - Left Outer	125
Reservoir 2 - Left Inner	126
Reservoir 2 - Right Outer	127
Reservoir 2 - Right Inner	128
Crest - Left	129
Crest - Right	130
Overtopping Skeleton	
Skeleton Base	131
Skeleton Reservoir 2	132
Exploded Overtopping Skeleton	133
Assembly	
Base Welds 1	134
Base Welds 2	135
Reservoir 2 Welds	136
Crest Welds	137
Overtopping Device	138
Overtopping Device Exploded	139
Overtopping Device BOM	140
Flow Sensor Piping	141

Drawing	Page #
Frame Subassembly	
Plexiglass Plate	142
Side Top	143
Frame Welds	144
Frame	145
Frame BOM	146
Wave Gates Subassembly	
Wave Gate and Deflector Cuts 1	147
Wave Gate and Deflector Cuts 2	148
Wave Gate Shaft	149
Worm Gear Mount	150
Shaft Bracket	151
Wave Gates Assembly	152
Exploded Assembly and BOM	153
Wave Deflectors Subassembly	
Deflector Shaft	154
Deflector Base - Large Horizontal	155
Deflector Base - Tall Vertical	156
Deflector Base - Small Horizontal Top	157
Deflector Base - Small Horizontal Bottom	158
Deflector Base Welds	159
Deflector Side	160
Deflector Side Exploded	161
Deflector Assembly	162
Full Assembly	163

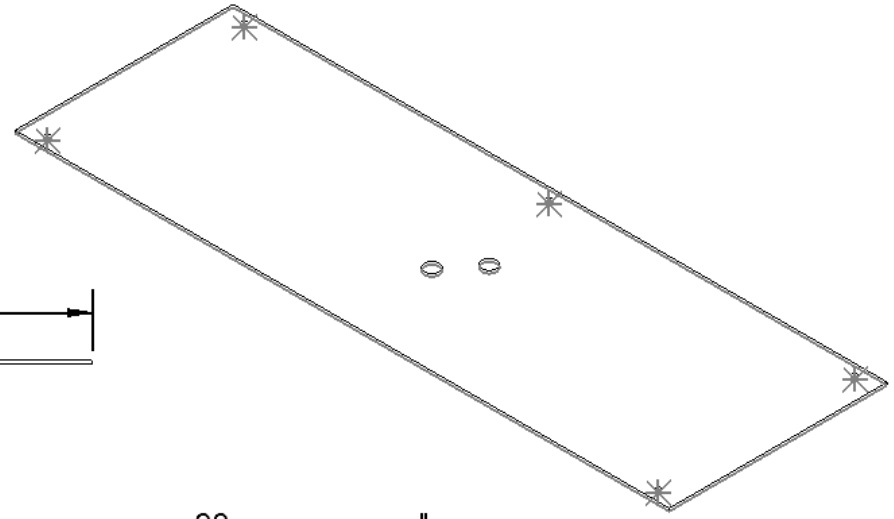

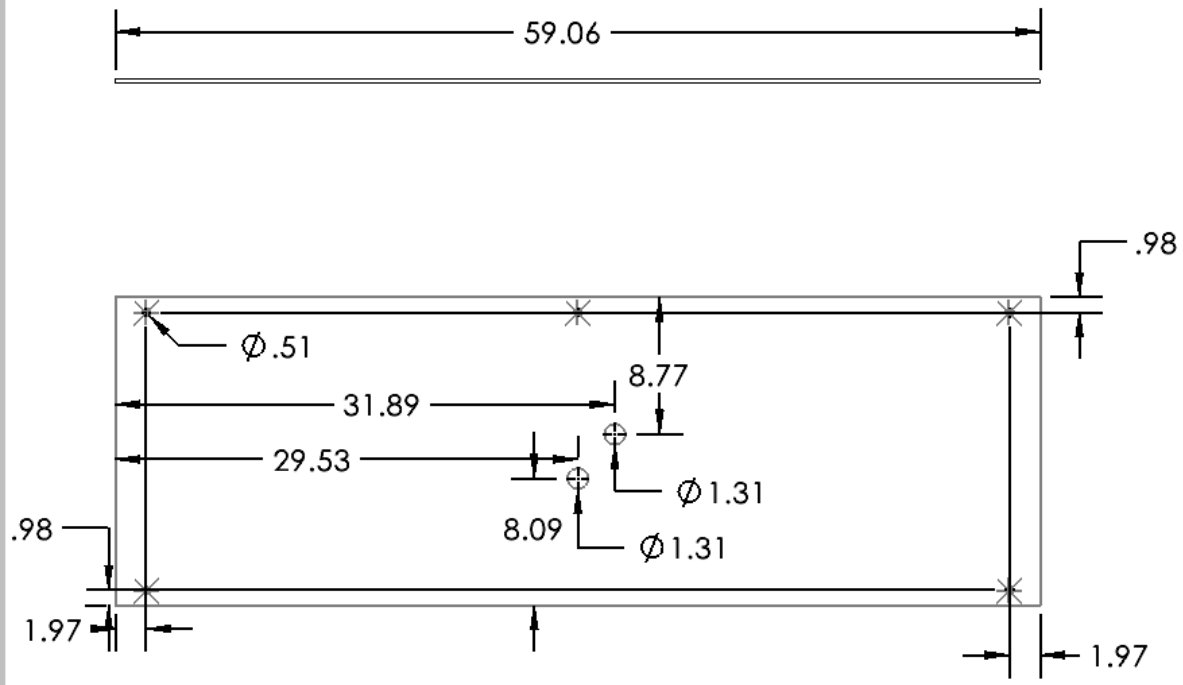

General Tolerances
X.X ± 0.1
X.XX ± 0.03
X° ± 0.5°

		NAME	DATE
UNLESS OTHERWISE SPECIFIED:	DRAWN		
DIMENSIONS ARE IN INCHES TOLERANCES: FRACTIONAL ± ANGULAR: MACH ± BEND ± TWO PLACE DECIMAL ± THREE PLACE DECIMAL ±	CHECKED		
	ENG APPR.		
	MFG APPR.		
	COMMENTS:		
MATERIAL AL 6061-T6	WEIGHT:		
FINISH			
DO NOT SCALE DRAWING			

COASTAL CURRENT

TITLE:
Back Plate

SIZE	DWG. NO.	REV
A	Overtopping Device - 1	

SCALE: 1:12 SHEET 1 OF 8

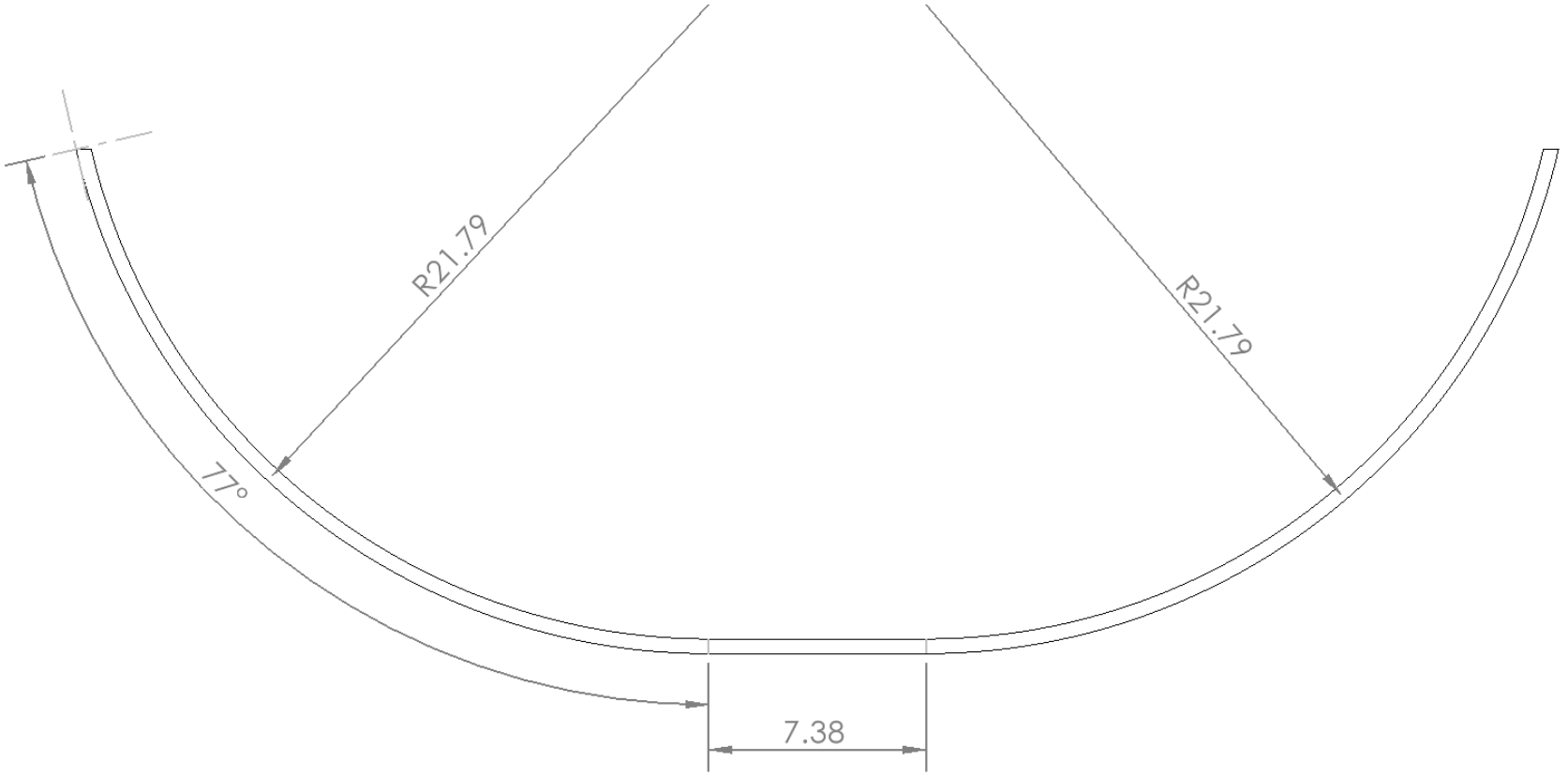

General Tolerances
X.X ± 0.1
X.XX ± 0.03
X° ± 0.5°

UNLESS OTHERWISE SPECIFIED:		NAME	DATE
DIMENSIONS ARE IN INCHES TOLERANCES: FRACTIONAL ± ANGULAR: MACH ± BEND ± TWO PLACE DECIMAL ± THREE PLACE DECIMAL ±	DRAWN		
	CHECKED		
	ENG APPR.		
	MFG APPR.		
MATERIAL Aluminum 6061-T6	COMMENTS: WEIGHT: Bar Stock: Cross Section: 0.5 in Wall Thickness: 0.0625 in		
FINISH 63µin			
DO NOT SCALE DRAWING			

COASTAL CURRENT

TITLE:
Base Semi Circle

SIZE	DWG. NO.	REV
A	Bar Stock Metal Bending - 1	

SCALE: 1:6 | SHEET 1 OF 7

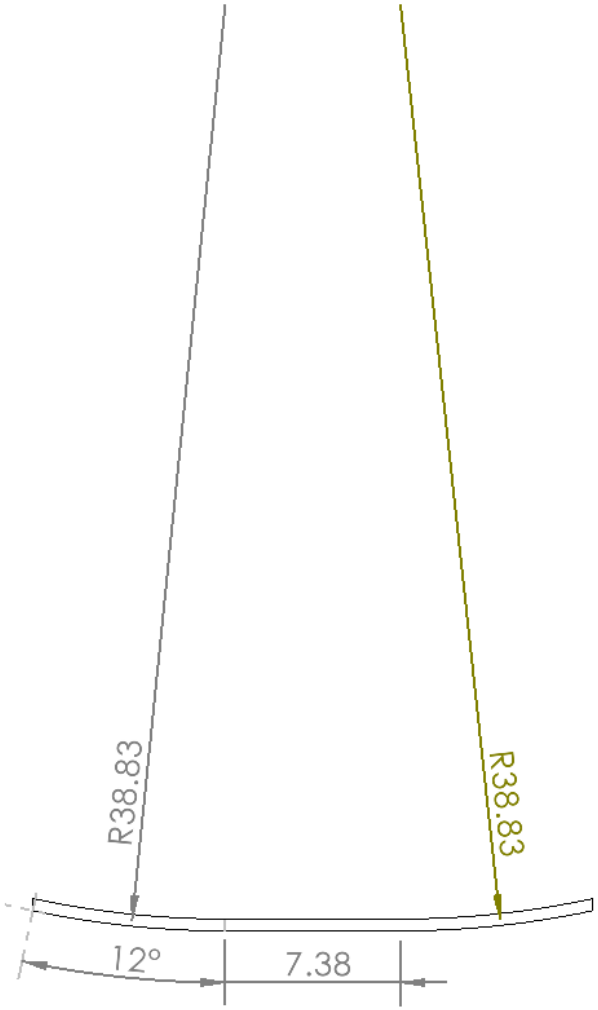

General Tolerances
X.X ± 0.1
X.XX ± 0.03
X° ± 0.5°

UNLESS OTHERWISE SPECIFIED:		NAME	DATE
DIMENSIONS ARE IN INCHES TOLERANCES: FRACTIONAL ± ANGULAR: MACH ± BEND ± TWO PLACE DECIMAL ± THREE PLACE DECIMAL ±	DRAWN		
	CHECKED		
	ENG APPR.		
	MFG APPR.		
MATERIAL Aluminum 6061-T6	COMMENTS: WEIGHT: Bar Stock: Cross Section: 0.5 in Wall Thickness: 0.0625 in		
FINISH 63µin			
DO NOT SCALE DRAWING			

COASTAL CURRENT

TITLE:
Ramp Front

SIZE	DWG. NO.	REV
A	Bar Stock Metal Bending - 2	

SCALE: 1:8 | SHEET 2 OF 7

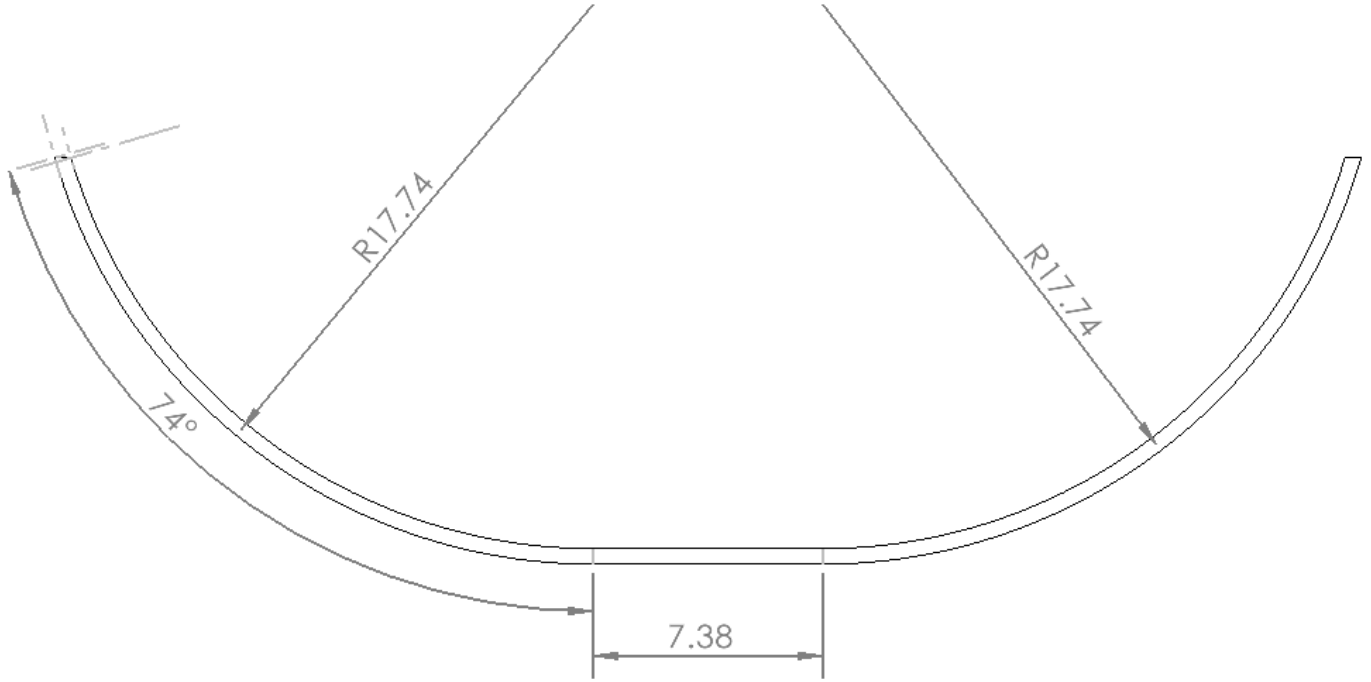

General Tolerances
X.X ± 0.1
X.XX ± 0.03
X° ± 0.5°

UNLESS OTHERWISE SPECIFIED:		NAME	DATE
DIMENSIONS ARE IN INCHES TOLERANCES: FRACTIONAL ± ANGULAR: MACH ± BEND ± TWO PLACE DECIMAL ± THREE PLACE DECIMAL ±	DRAWN		
	CHECKED		
	ENG APPR.		
	MFG APPR.		
MATERIAL Aluminum 6061-T6	COMMENTS: WEIGHT: Bar Stock: Cross Section: 0.5 in Wall Thickness: 0.0625 in		
FINISH 63µin			
DO NOT SCALE DRAWING			

COASTAL CURRENT		
TITLE: Reservoir 1 - Top		
SIZE A	DWG. NO. Bar Stock Metal Bending - 3	REV
SCALE: 1:6		SHEET 3 OF 7

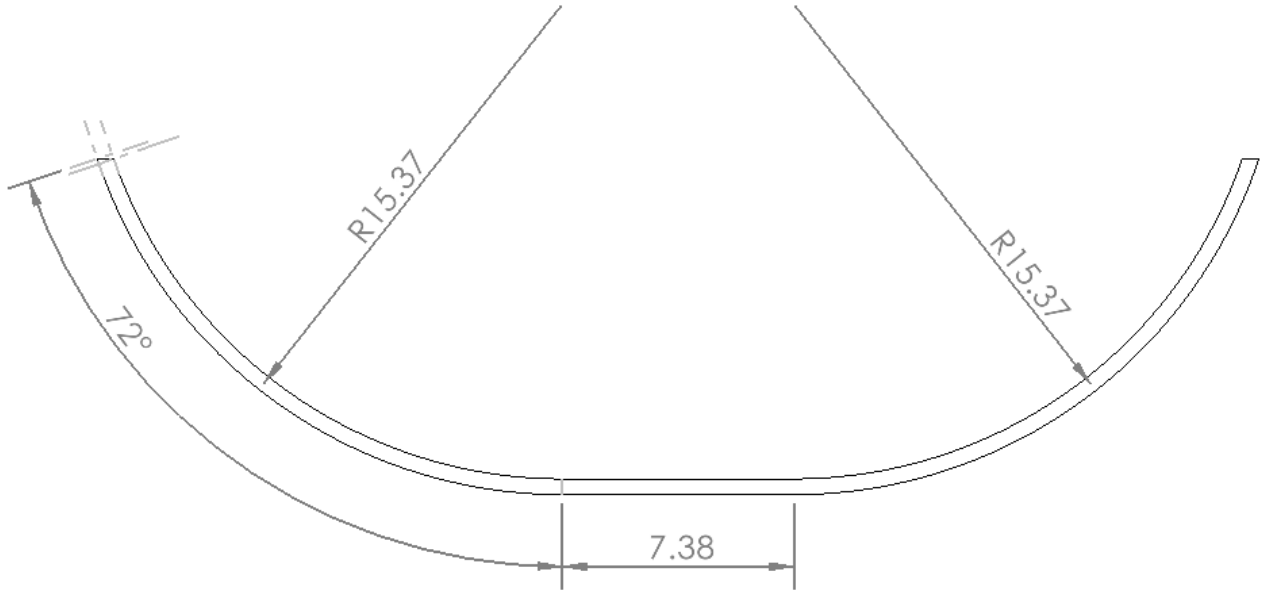

General Tolerances
X.X ± 0.1
X.XX ± 0.03
X° ± 0.5°

UNLESS OTHERWISE SPECIFIED:		NAME	DATE
DIMENSIONS ARE IN INCHES TOLERANCES: FRACTIONAL ± ANGULAR: MACH ± BEND ± TWO PLACE DECIMAL ± THREE PLACE DECIMAL ±	DRAWN		
	CHECKED		
	ENG APPR.		
	MFG APPR.		
MATERIAL Aluminum 6061-T6	COMMENTS: WEIGHT: Bar Stock: Cross Section: 0.5 in Wall Thickness: 0.0625 in		
FINISH 63µin			
DO NOT SCALE DRAWING			

COASTAL CURRENT

TITLE:
Reservoir 2 - Bottom

SIZE	DWG. NO.	REV
A	Bar Stock Metal Bending - 4	

SCALE: 1:6 | SHEET 4 OF 7

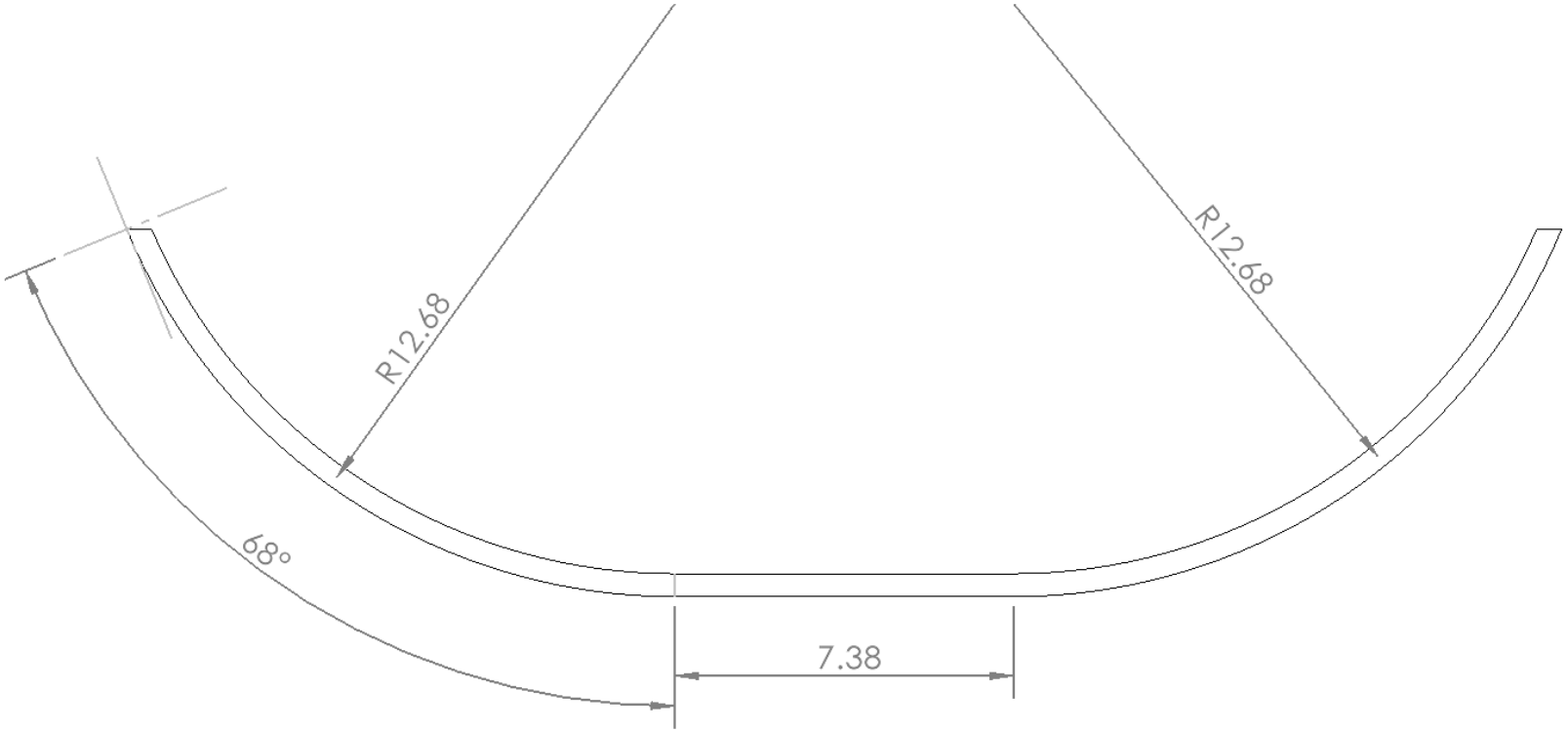

General Tolerances
X.X ± 0.1
X.XX ± 0.03
X° ± 0.5°

UNLESS OTHERWISE SPECIFIED:		NAME	DATE
DIMENSIONS ARE IN INCHES TOLERANCES: FRACTIONAL ± ANGULAR: MACH ± BEND ± TWO PLACE DECIMAL ± THREE PLACE DECIMAL ±	DRAWN		
	CHECKED		
	ENG APPR.		
	MFG APPR.		
MATERIAL Aluminum 6061-T6	COMMENTS: WEIGHT: Bar Stock: Cross Section: 0.5 in Wall Thickness: 0.0625 in		
FINISH 63µin			
DO NOT SCALE DRAWING			

COASTAL CURRENT		
TITLE: Reservoir 2 - Top		
SIZE A	DWG. NO. Bar Stock Metal Bending - 5	REV
SCALE: 1:4		SHEET 5 OF 7

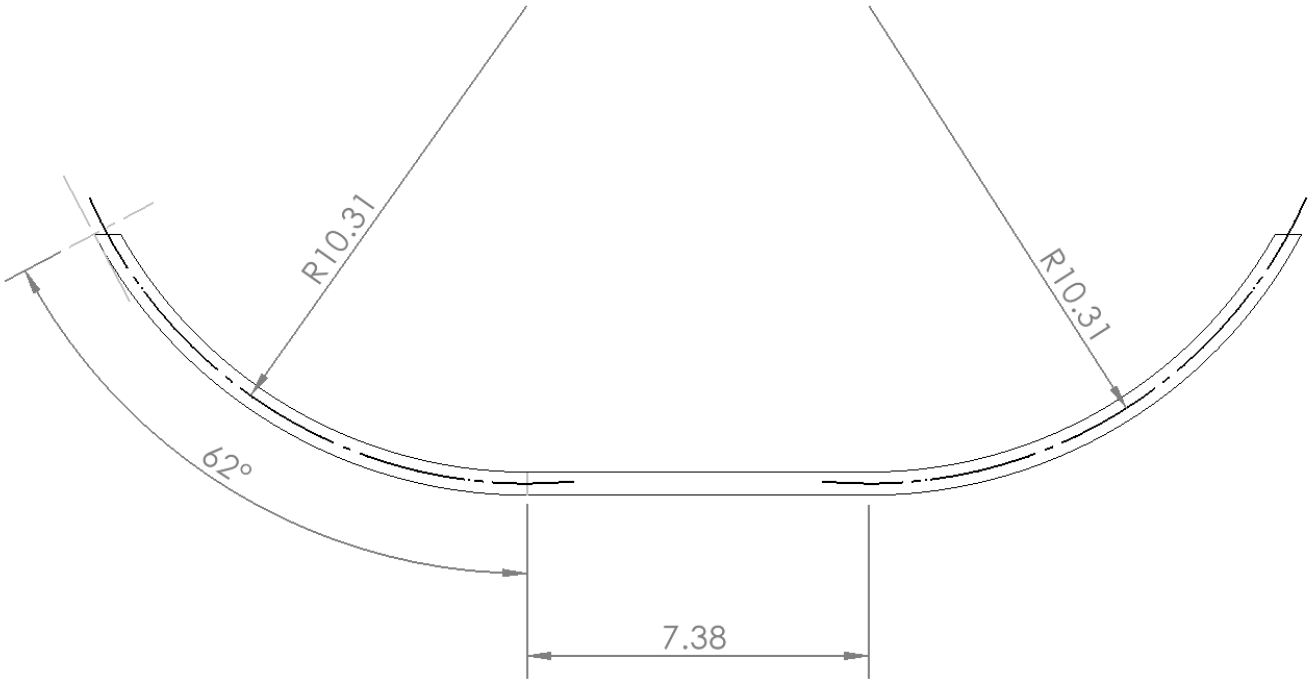

General Tolerances
X.X ± 0.1
X.XX ± 0.03
X° ± 0.5°

		NAME	DATE
UNLESS OTHERWISE SPECIFIED:	DRAWN		
DIMENSIONS ARE IN INCHES TOLERANCES: FRACTIONAL ± ANGULAR: MACH ± BEND ± TWO PLACE DECIMAL ± THREE PLACE DECIMAL ±	CHECKED		
	ENG APPR.		
	MFG APPR.		
	COMMENTS:		
MATERIAL: Aluminum 6061-T6	WEIGHT:		
FINISH: 63µin	Bar Stock: Cross Section: 0.5 in Wall Thickness: 0.0625 in		
DO NOT SCALE DRAWING			

COASTAL CURRENT

TITLE: Crest - Bottom

SIZE	DWG. NO.	REV
A	Bar Stock Metal Bending - 6	

SCALE: 1:4 | SHEET 6 OF 7

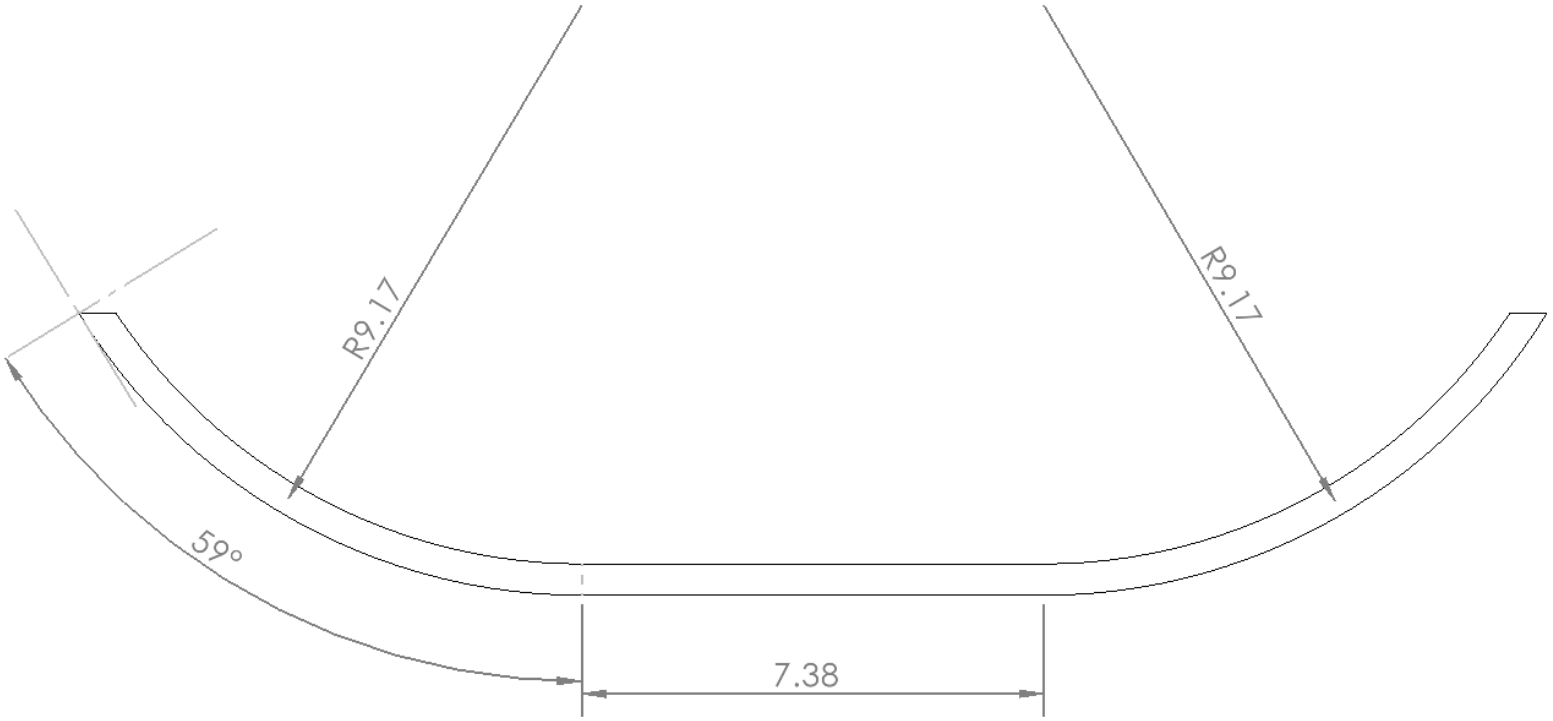

General Tolerances
X.X ± 0.1
X.XX ± 0.03
X° ± 0.5°

UNLESS OTHERWISE SPECIFIED:		NAME	DATE
DIMENSIONS ARE IN INCHES TOLERANCES: FRACTIONAL ± ANGULAR: MACH ± BEND ± TWO PLACE DECIMAL ± THREE PLACE DECIMAL ±	DRAWN		
	CHECKED		
	ENG APPR.		
	MFG APPR.		
MATERIAL: Aluminum 6061-T6	COMMENTS:		
FINISH: 63µin	WEIGHT: Bar Stock: Cross Section: 0.5 in Wall Thickness: 0.0625 in		
DO NOT SCALE DRAWING			

COASTAL CURRENT

TITLE: Crest - Top

SIZE	DWG. NO.	REV
A	Bar Stock Metal Bending - 7	

SCALE: 1:3 | SHEET 7 OF 7

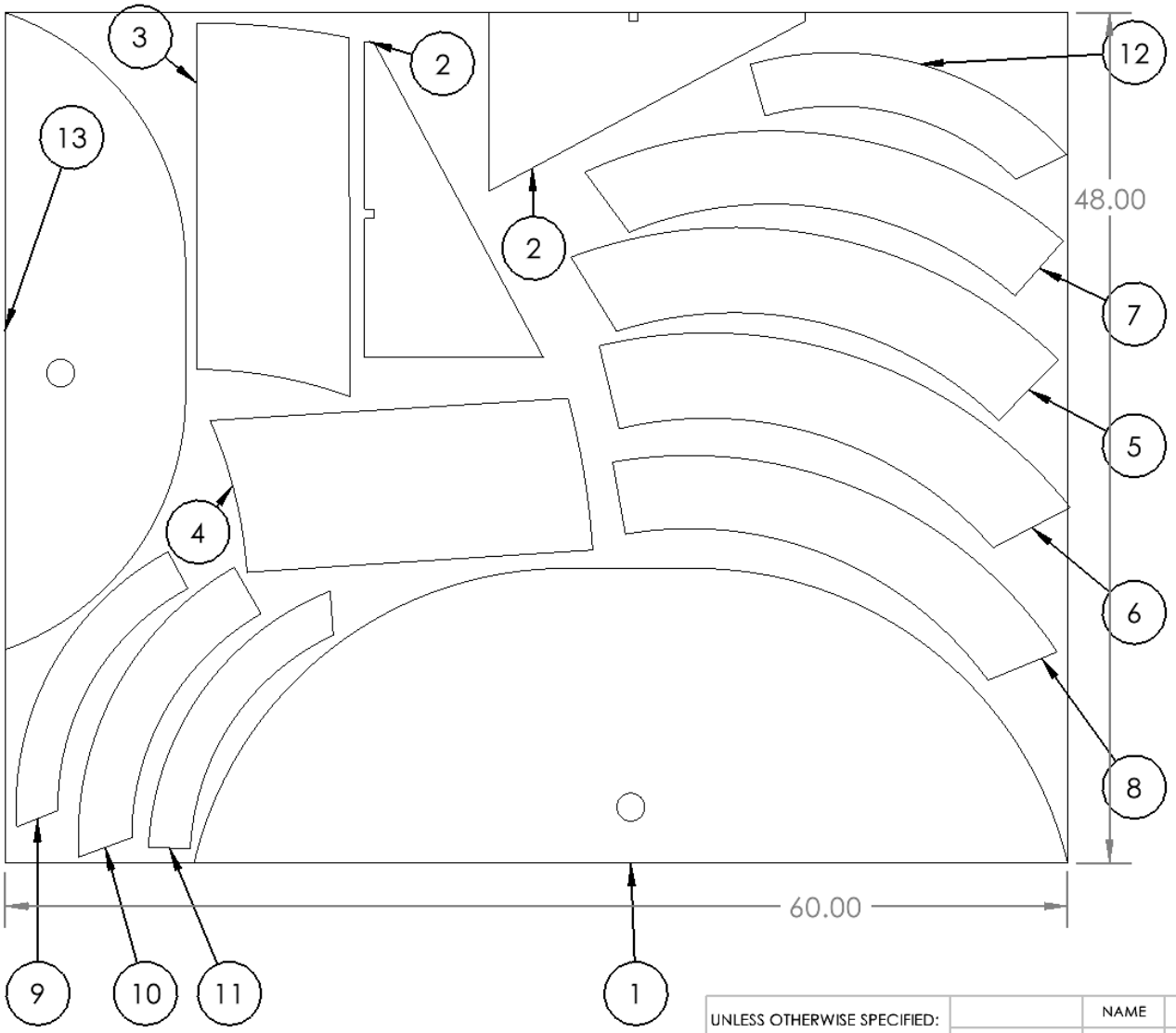

ITEM NO.	PART NUMBER	QTY.
1	Reservoir1_Base	1
2	Ramp_triagnle sides	2
3	Ramp Right_flat	1
4	Ramp Left._flatSLDPRT	1
5	Reservoir1_Curve_Left_Outer_flat	1
6	Reservoir1_Curve_Right_Outer_flat	1
7	Reservoir1_CurvePart_Left_inner_flat	1
8	Reservoir1_CurvePart_Right_inner_flat	1
9	Reservoir2_CurvePart_Left_inner_flat	1
10	Reservoir2_CurvePart_Left_Outer_flat	1
11	Reservoir2_CurvePart_Right_inner_flat	1
12	Reservoir2_CurvePart_Right_Outer_Flat	1
13	Reservoir2_Base	1
14	4x5	1

		NAME	DATE
UNLESS OTHERWISE SPECIFIED:	DRAWN		
DIMENSIONS ARE IN INCHES TOLERANCES: FRACTIONAL ± ANGULAR: MACH ± BEND ± TWO PLACE DECIMAL ± THREE PLACE DECIMAL ±	CHECKED		
	ENG APPR.		
	MFG APPR.		
MATERIAL	COMMENTS:		
FINISH	WEIGHT:		
DO NOT SCALE DRAWING			

COASTAL CURRENT

TITLE: Sheet Metal Cuts

SIZE	DWG. NO.	REV
A	Sheet Metal Cuts - 1	

SCALE: 1:10 SHEET 1 OF 2

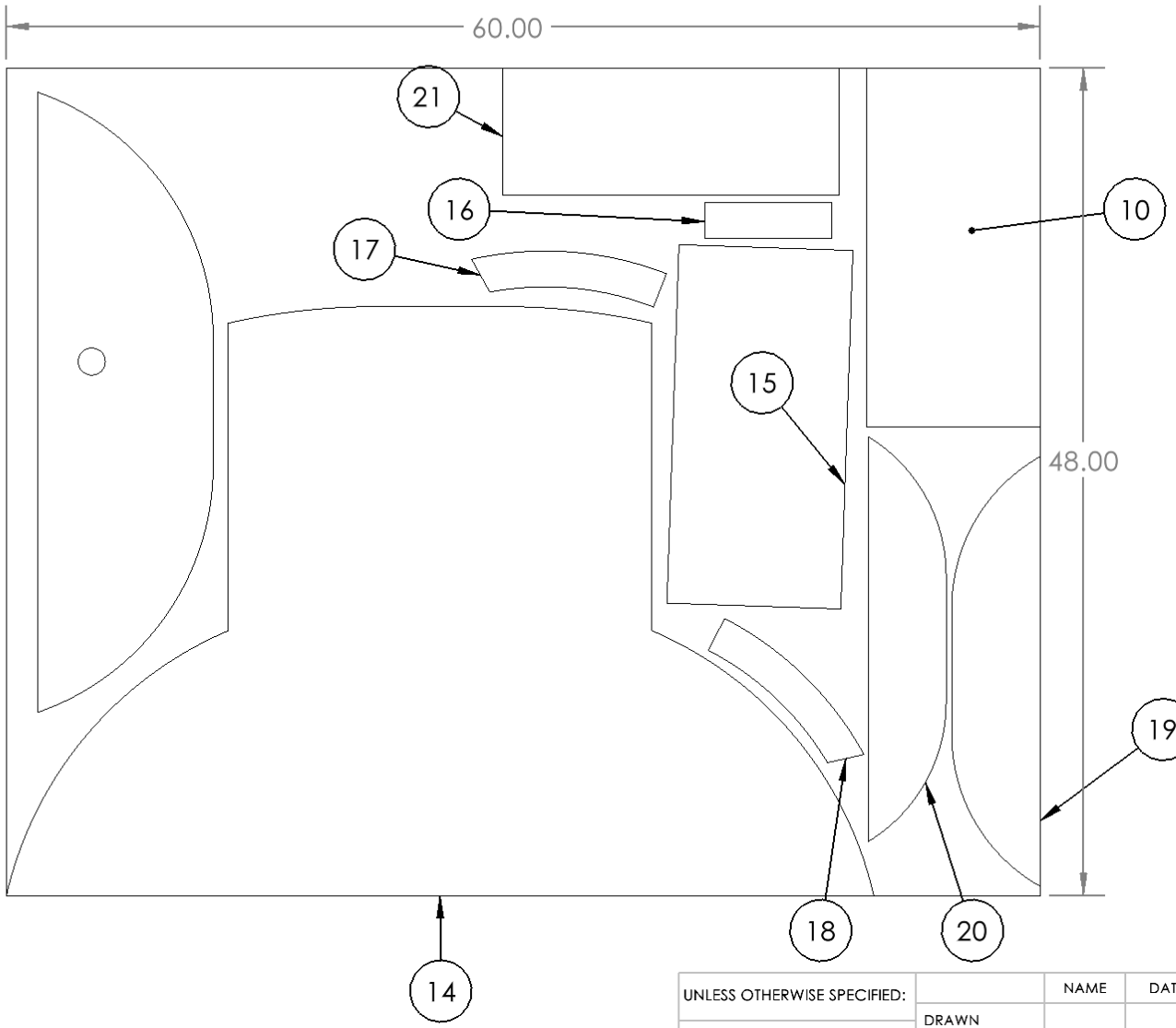

ITEM NO.	PART NUMBER	QTY.
14	Base_bottom plate	1
15	Base_outersemi_cricle_flat	2
16	Crest_Front	1
17	Crest_Left_flat	1
18	Crest_Right_flat	1
19	TopCrest_bottom	1
20	TopCrest_top	1
21	Ramp Front	1
13	Reservoir2_Base	1
10	4x5	1

		NAME	DATE
UNLESS OTHERWISE SPECIFIED:	DRAWN		
DIMENSIONS ARE IN INCHES TOLERANCES: FRACTIONAL ± ANGULAR: MACH ± BEND ± TWO PLACE DECIMAL ± THREE PLACE DECIMAL ±	CHECKED		
	ENG APPR.		
	MFG APPR.		
MATERIAL	COMMENTS:		
FINISH	WEIGHT:		
DO NOT SCALE DRAWING			

COASTAL CURRENT

TITLE: Sheet Metal Cuts

SIZE	DWG. NO.	REV
A	Sheet Metal Cuts - 2	

SCALE:1:10 SHEET 2 OF 2

Top View

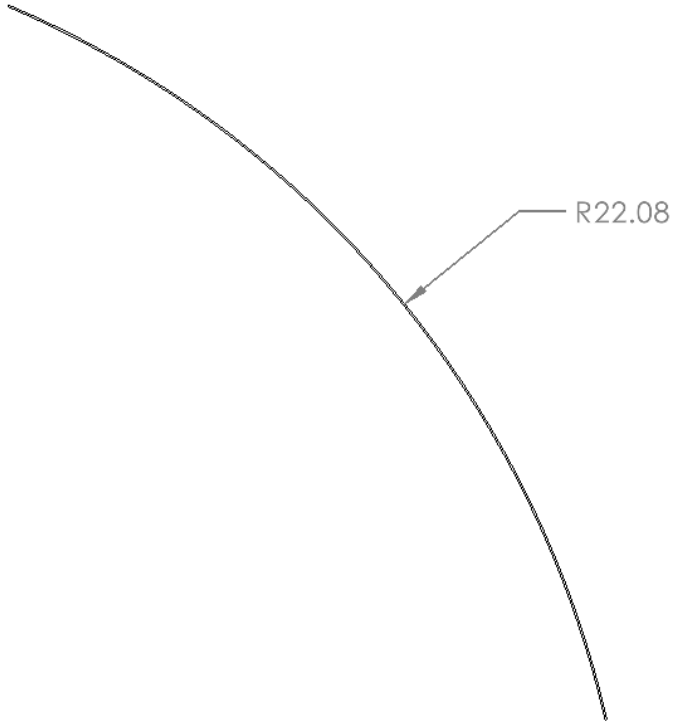

Isometric View

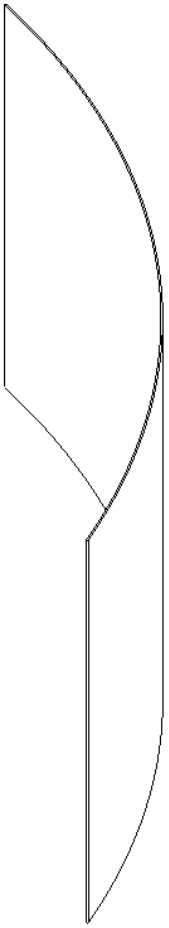

General Tolerances
X.X ± 0.1
X.XX ± 0.03
X° ± 0.5°

UNLESS OTHERWISE SPECIFIED:		NAME	DATE
DIMENSIONS ARE IN INCHES TOLERANCES: FRACTIONAL ± ANGULAR: MACH ± BEND ± TWO PLACE DECIMAL ± THREE PLACE DECIMAL ±	DRAWN		
	CHECKED		
	ENG APPR.		
	MFG APPR.		
MATERIAL: Aluminum 3003 Alloy	COMMENTS:		
FINISH: 94µin	WEIGHT:		
DO NOT SCALE DRAWING			

COASTAL CURRENT

TITLE: Base Semi-Circle

SIZE	DWG. NO.	REV
A	Sheet Metal Bending - 1	

SCALE: 1:4 SHEET 1 OF 13

Front View

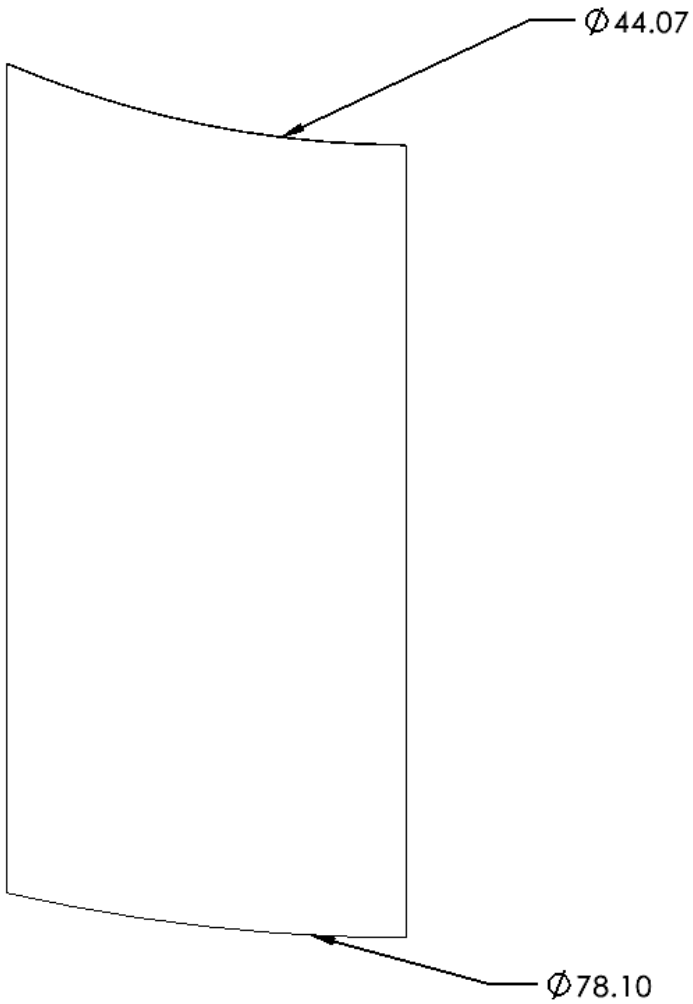

General Tolerances
X.X ± 0.1
X.XX ± 0.03
X° ± 0.5°

UNLESS OTHERWISE SPECIFIED:		NAME	DATE
	DRAWN		
DIMENSIONS ARE IN INCHES TOLERANCES: FRACTIONAL ± ANGULAR: MACH ± BEND ± TWO PLACE DECIMAL ± THREE PLACE DECIMAL ±	CHECKED		
	ENG APPR.		
	MFG APPR.		
	COMMENTS:		
MATERIAL Aluminum 3003 Alloy	WEIGHT:		
FINISH 94µin			
DO NOT SCALE DRAWING			

COASTAL CURRENT

TITLE:
Ramp-Left

SIZE	DWG. NO.	REV
A	Sheet Metal Bending - 2	

SCALE: 1:4 | SHEET 2 OF 13

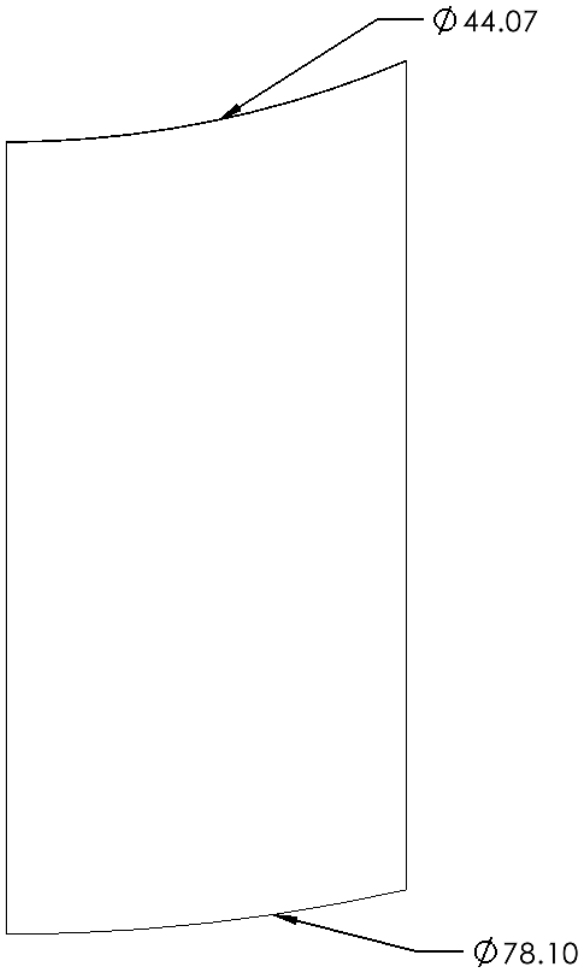

General Tolerances
X.X ± 0.1
X.XX ± 0.03
X° ± 0.5°

UNLESS OTHERWISE SPECIFIED:		NAME	DATE
DIMENSIONS ARE IN INCHES TOLERANCES: FRACTIONAL ± ANGULAR: MACH ± BEND ± TWO PLACE DECIMAL ± THREE PLACE DECIMAL ±	DRAWN		
	CHECKED		
	ENG APPR.		
	MFG APPR.		
	COMMENTS:		
MATERIAL Aluminum 3003 Alloy	WEIGHT:		
FINISH 94µin			
DO NOT SCALE DRAWING			

COASTAL CURRENT

TITLE:
Ramp-Right

SIZE	DWG. NO.	REV
A	Sheet Metal Bending - 3	

SCALE: 1:4 SHEET 3 OF 13

Top View

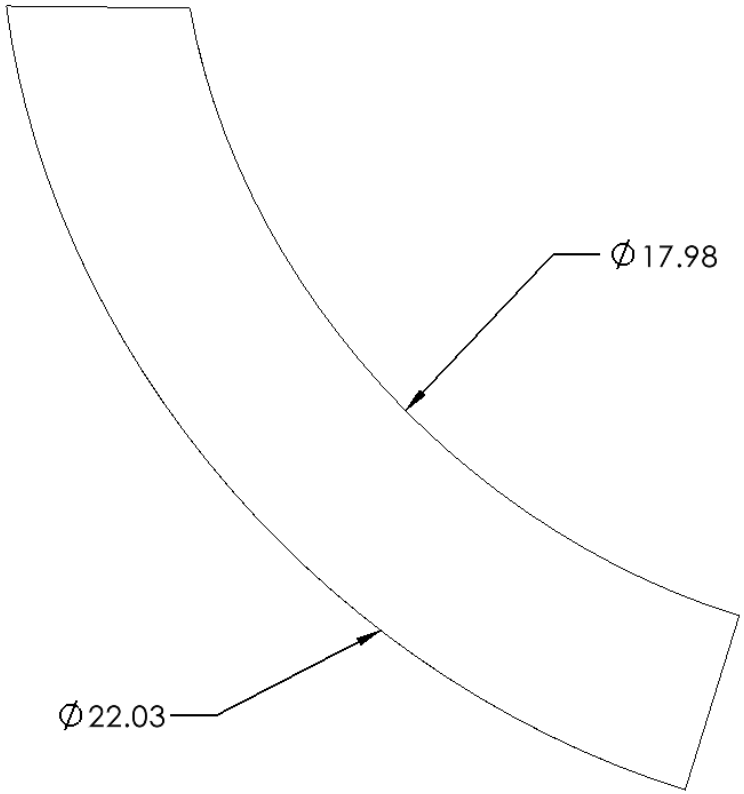

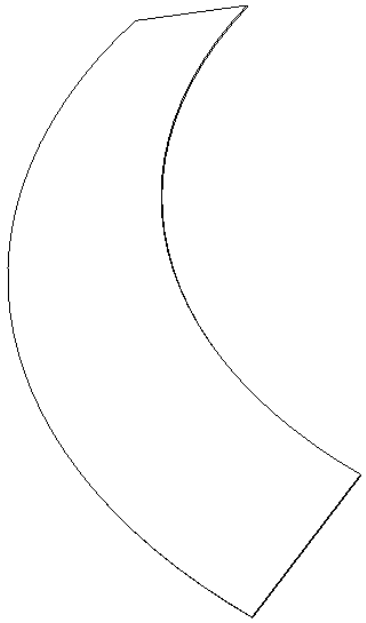

Isometric View

General Tolerances
X.X ± 0.1
X.XX ± 0.03
X° ± 0.5°

UNLESS OTHERWISE SPECIFIED:		NAME	DATE
DIMENSIONS ARE IN INCHES TOLERANCES: FRACTIONAL ± ANGULAR: MACH ± BEND ± TWO PLACE DECIMAL ± THREE PLACE DECIMAL ±	DRAWN		
	CHECKED		
	ENG APPR.		
	MFG APPR.		
MATERIAL Aluminum 3003 Alloy	COMMENTS: WEIGHT:		
FINISH 94µin			
DO NOT SCALE DRAWING			

COASTAL CURRENT

TITLE:
Reservoir 1 - Left Outer

SIZE	DWG. NO.	REV
A	Sheet Metal Bending - 4	

SCALE: 1:5 SHEET 4 OF 13

Top View

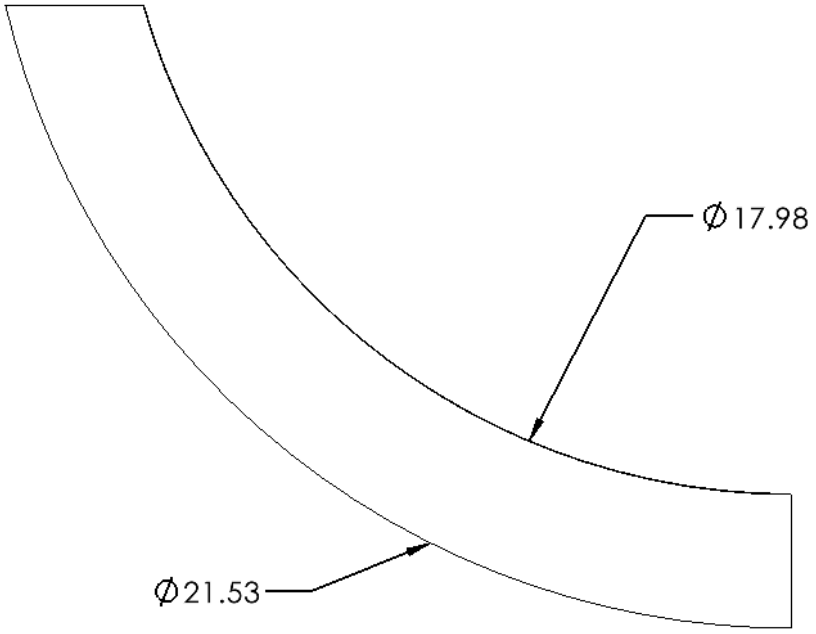

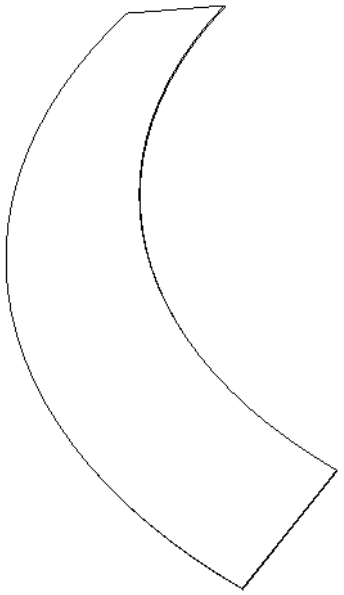

Isometric View

General Tolerances
X.X ± 0.1
X.XX ± 0.03
X° ± 0.5°

UNLESS OTHERWISE SPECIFIED:		NAME	DATE
	DRAWN		
DIMENSIONS ARE IN INCHES TOLERANCES: FRACTIONAL ± ANGULAR: MACH ± BEND ± TWO PLACE DECIMAL ± THREE PLACE DECIMAL ±	CHECKED		
	ENG APPR.		
	MFG APPR.		
	COMMENTS:		
MATERIAL Aluminum 3003 Alloy	WEIGHT:		
FINISH 94µin			
DO NOT SCALE DRAWING			

COASTAL CURRENT

TITLE:
Reservoir 1 - Left Inner

SIZE	DWG. NO.	REV
A	Sheet Metal Bending - 5	

SCALE: 1:5 | SHEET 5 OF 13

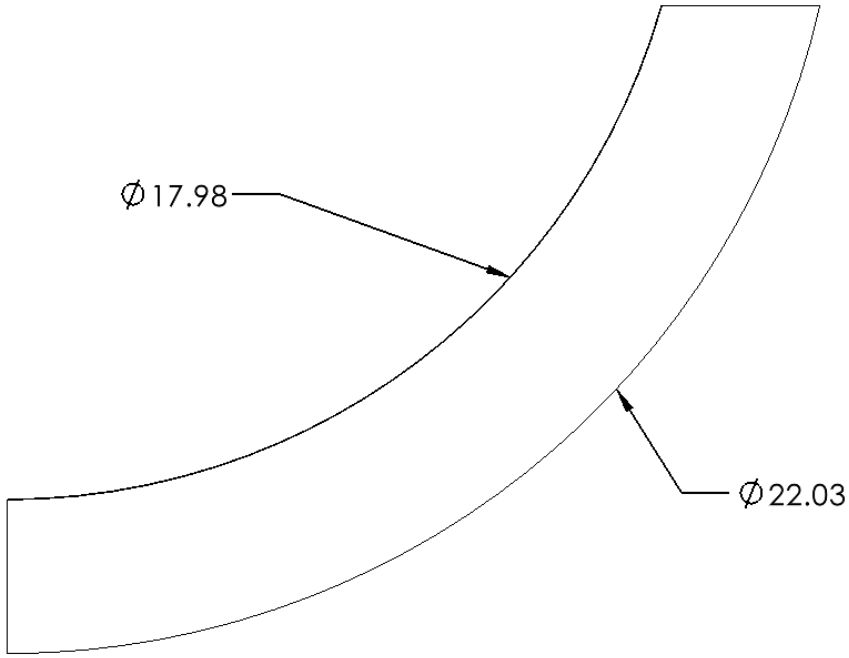

Top View

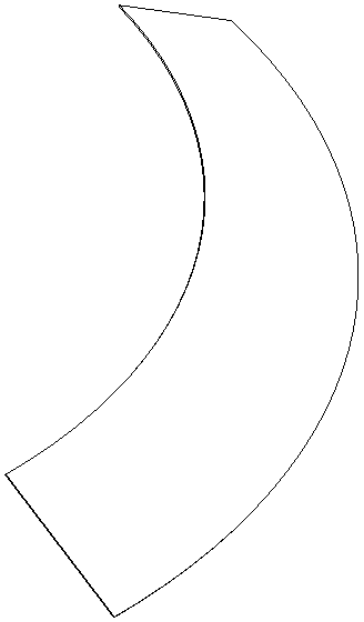

Isometric View

General Tolerances
X.X ± 0.1
X.XX ± 0.03
X° ± 0.5°

UNLESS OTHERWISE SPECIFIED:		NAME	DATE
DIMENSIONS ARE IN INCHES TOLERANCES: FRACTIONAL ± ANGULAR: MACH ± BEND ± TWO PLACE DECIMAL ± THREE PLACE DECIMAL ±	DRAWN		
	CHECKED		
	ENG APPR.		
	MFG APPR.		
	COMMENTS:		
MATERIAL Aluminum 3003 Alloy	WEIGHT:		
FINISH 94µin			
DO NOT SCALE DRAWING			

COASTAL CURRENT		
TITLE: Reservoir 1 - Right Outer		
SIZE A	DWG. NO. Sheet Metal Bending - 6	REV
SCALE: 1:5		SHEET 6 OF 13

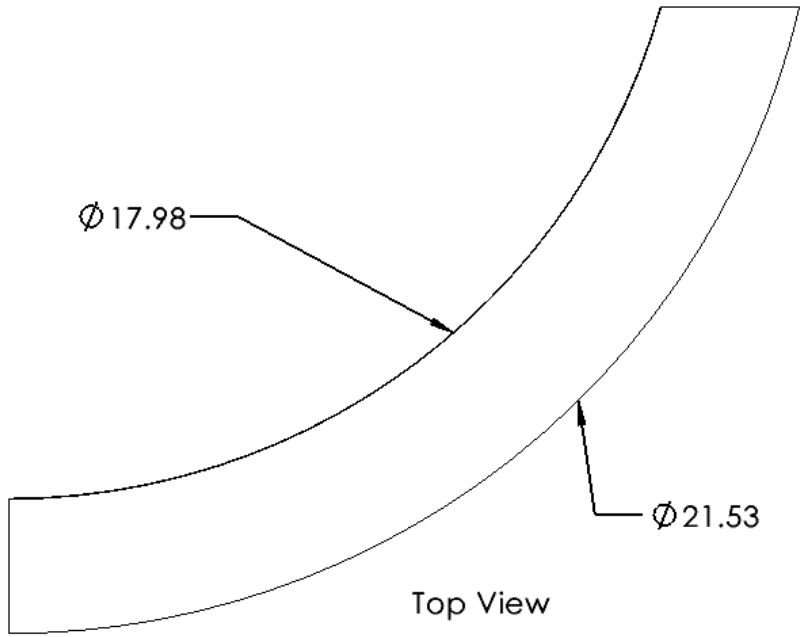

Top View

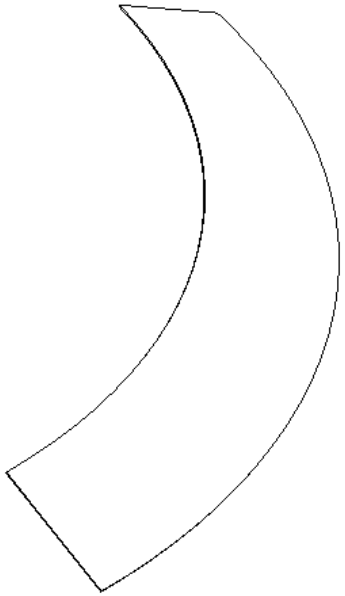

Isometric View

General Tolerances
X.X ± 0.1
X.XX ± 0.03
X° ± 0.5°

UNLESS OTHERWISE SPECIFIED:		NAME	DATE
DIMENSIONS ARE IN INCHES TOLERANCES: FRACTIONAL ± ANGULAR: MACH ± BEND ± TWO PLACE DECIMAL ± THREE PLACE DECIMAL ±	DRAWN		
	CHECKED		
	ENG APPR.		
	MFG APPR.		
MATERIAL Aluminum 3003 Alloy	COMMENTS: WEIGHT:		
FINISH 94µin			
DO NOT SCALE DRAWING			

COASTAL CURRENT

TITLE:
Reservoir 1 - Right Inner

SIZE	DWG. NO.	REV
A	Sheet Metal Bending - 7	

SCALE: 1:5 | SHEET 7 OF 13

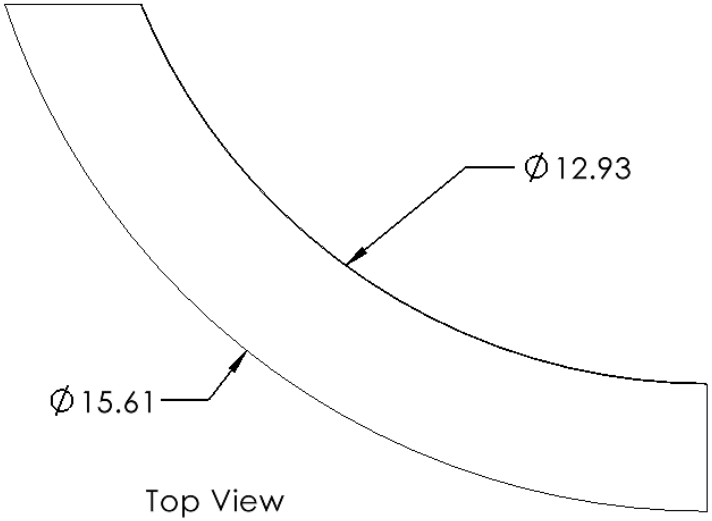

Top View

Isometric View

General Tolerances
X.X ± 0.1
X.XX ± 0.03
X° ± 0.5°

UNLESS OTHERWISE SPECIFIED:		NAME	DATE
DIMENSIONS ARE IN INCHES TOLERANCES: FRACTIONAL ± ANGULAR: MACH ± BEND ± TWO PLACE DECIMAL ± THREE PLACE DECIMAL ±	DRAWN		
	CHECKED		
	ENG APPR.		
	MFG APPR.		
	COMMENTS:		
MATERIAL Aluminum 3003 Alloy	WEIGHT:		
FINISH 94µin			
DO NOT SCALE DRAWING			

COASTAL CURRENT		
TITLE: Reservoir 2 - Left Outer		
SIZE A	DWG. NO. Sheet Metal Bending - 8	REV
SCALE: 1:4		SHEET 8 OF 13

Isometric View

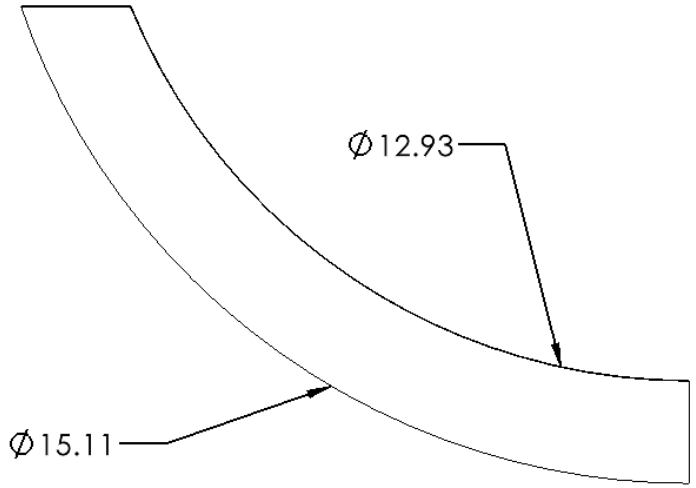

Top View

General Tolerances
X.X ± 0.1
X.XX ± 0.03
X° ± 0.5°

UNLESS OTHERWISE SPECIFIED:		NAME	DATE
DIMENSIONS ARE IN INCHES TOLERANCES: FRACTIONAL ± ANGULAR: MACH ± BEND ± TWO PLACE DECIMAL ± THREE PLACE DECIMAL ±	DRAWN		
	CHECKED		
	ENG APPR.		
	MFG APPR.		
MATERIAL: Aluminum 3003 Alloy	COMMENTS: WEIGHT:		
FINISH: 94µin			
DO NOT SCALE DRAWING			

COASTAL CURRENT

TITLE: Reservoir 2 - Left Inner

SIZE	DWG. NO.	REV
A	Sheet Metal Bending - 9	

SCALE: 1:4 SHEET 9 OF 13

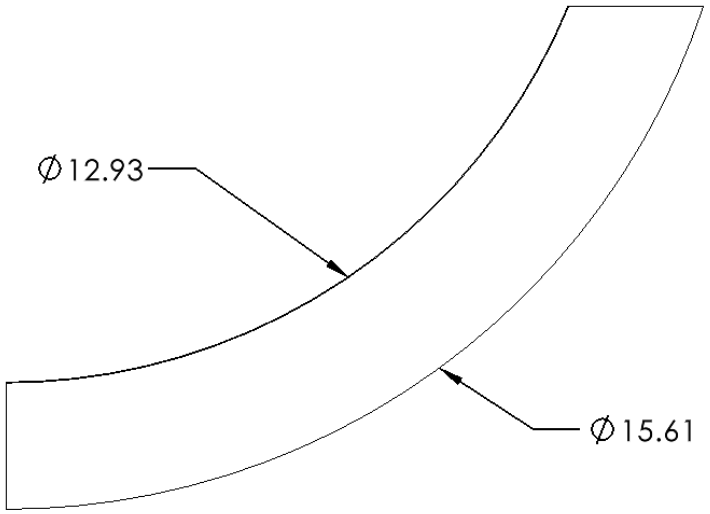

Top View

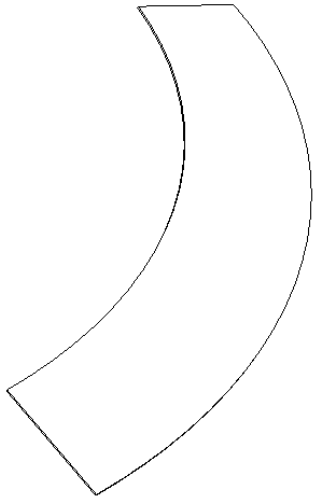

Isometric View

General Tolerances
X.X ± 0.1
X.XX ± 0.03
X° ± 0.5°

		NAME	DATE
UNLESS OTHERWISE SPECIFIED:	DRAWN		
DIMENSIONS ARE IN INCHES TOLERANCES: FRACTIONAL ± ANGULAR: MACH ± BEND ± TWO PLACE DECIMAL ± THREE PLACE DECIMAL ±	CHECKED		
	ENG APPR.		
	MFG APPR.		
	COMMENTS:		
MATERIAL: Aluminum 3003 Alloy	WEIGHT:		
FINISH: 94µin			
DO NOT SCALE DRAWING			

COASTAL CURRENT

TITLE: Reservoir 2 - Right Outer

SIZE	DWG. NO.	REV
A	Sheet Metal Bending - 10	

SCALE: 1:4 SHEET 10 OF 13

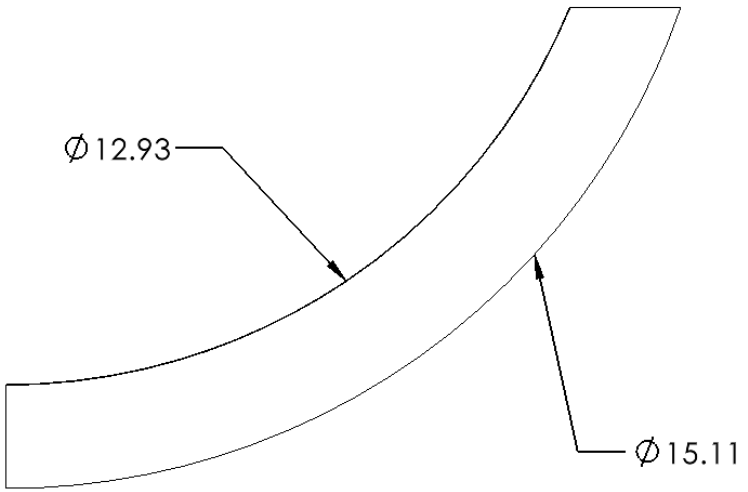

Top View

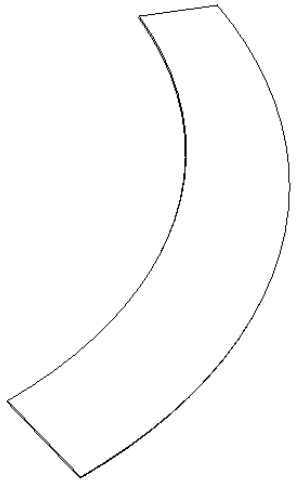

Isometric View

General Tolerances
X.X ± 0.1
X.XX ± 0.03
X° ± 0.5°

UNLESS OTHERWISE SPECIFIED:		NAME	DATE
DIMENSIONS ARE IN INCHES TOLERANCES: FRACTIONAL ± ANGULAR: MACH ± BEND ± TWO PLACE DECIMAL ± THREE PLACE DECIMAL ±	DRAWN		
	CHECKED		
	ENG APPR.		
	MFG APPR.		
	COMMENTS:		
MATERIAL: Aluminum 3003 Alloy	WEIGHT:		
FINISH: 94µin			
DO NOT SCALE DRAWING			

COASTAL CURRENT

TITLE: Reservoir 2 - Right Inner

SIZE	DWG. NO.	REV
A	Sheet Metal Bending - 11	

SCALE: 1:4 | SHEET 11 OF 13

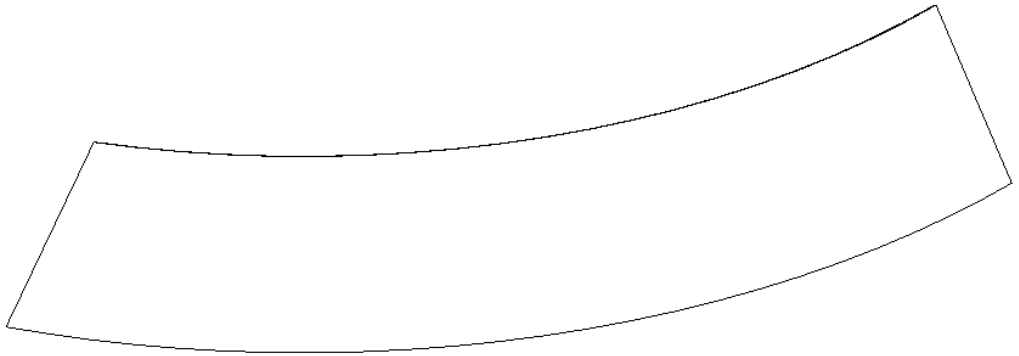

Isometric View

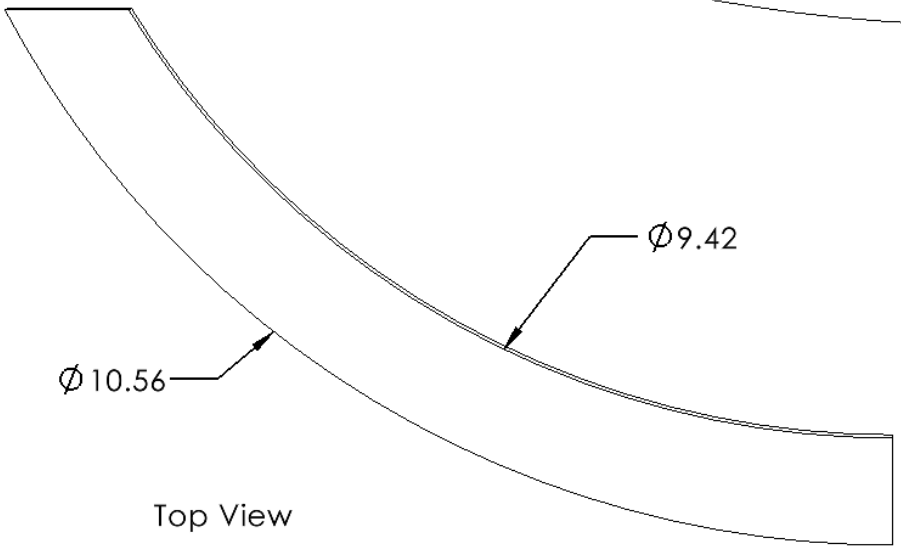

Top View

General Tolerances
X.X ± 0.1
X.XX ± 0.03
X° ± 0.5°

		NAME	DATE
UNLESS OTHERWISE SPECIFIED:	DRAWN		
DIMENSIONS ARE IN INCHES TOLERANCES: FRACTIONAL ± ANGULAR: MACH ± BEND ± TWO PLACE DECIMAL ± THREE PLACE DECIMAL ±	CHECKED		
	ENG APPR.		
	MFG APPR.		
	COMMENTS:		
MATERIAL: Aluminum 3003 Alloy	WEIGHT:		
FINISH: 94µin			
DO NOT SCALE DRAWING			

COASTAL CURRENT

TITLE: Crest - Left

SIZE	DWG. NO.	REV
A	Sheet Metal Bending - 12	

SCALE: 1:2 | SHEET 12 OF 13

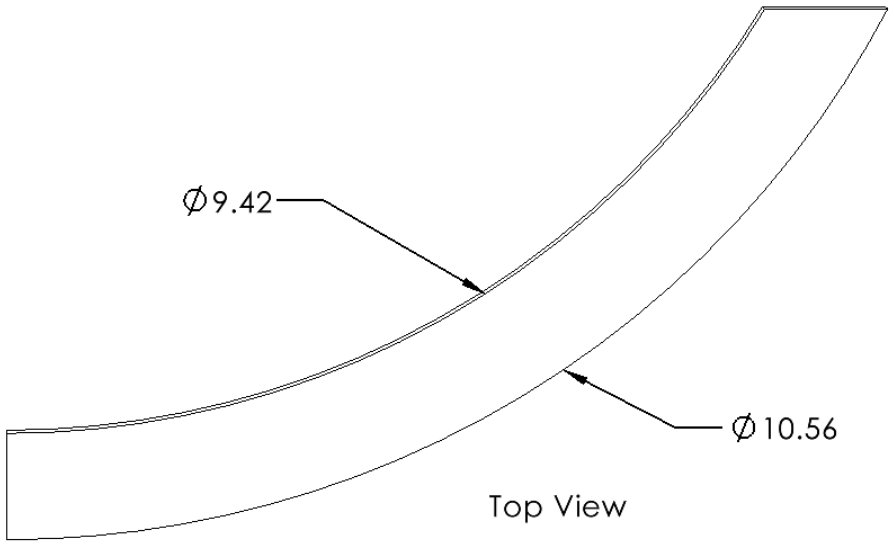

Top View

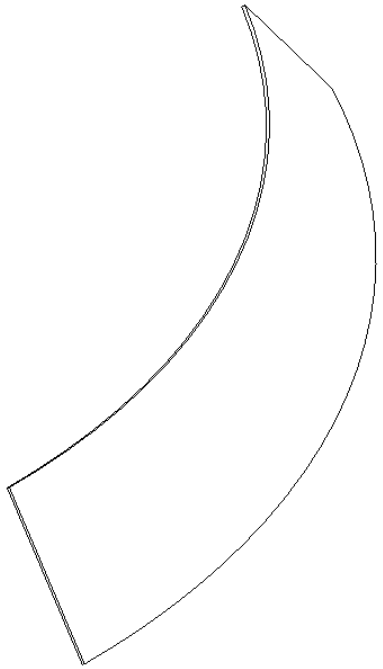

Isometric View

General Tolerances
X.X ± 0.1
X.XX ± 0.03
X° ± 0.5°

UNLESS OTHERWISE SPECIFIED:		NAME	DATE
DIMENSIONS ARE IN INCHES TOLERANCES: FRACTIONAL ± ANGULAR: MACH ± BEND ± TWO PLACE DECIMAL ± THREE PLACE DECIMAL ±	DRAWN		
	CHECKED		
	ENG APPR.		
	MFG APPR.		
MATERIAL Aluminum 3003 Alloy	COMMENTS: WEIGHT:		
FINISH 94µin			
DO NOT SCALE DRAWING			

COASTAL CURRENT

TITLE:
Crest - Right

SIZE	DWG. NO.	REV
A	Sheet Metal Bending - 13	

SCALE: 1:2 SHEET 13 OF 13

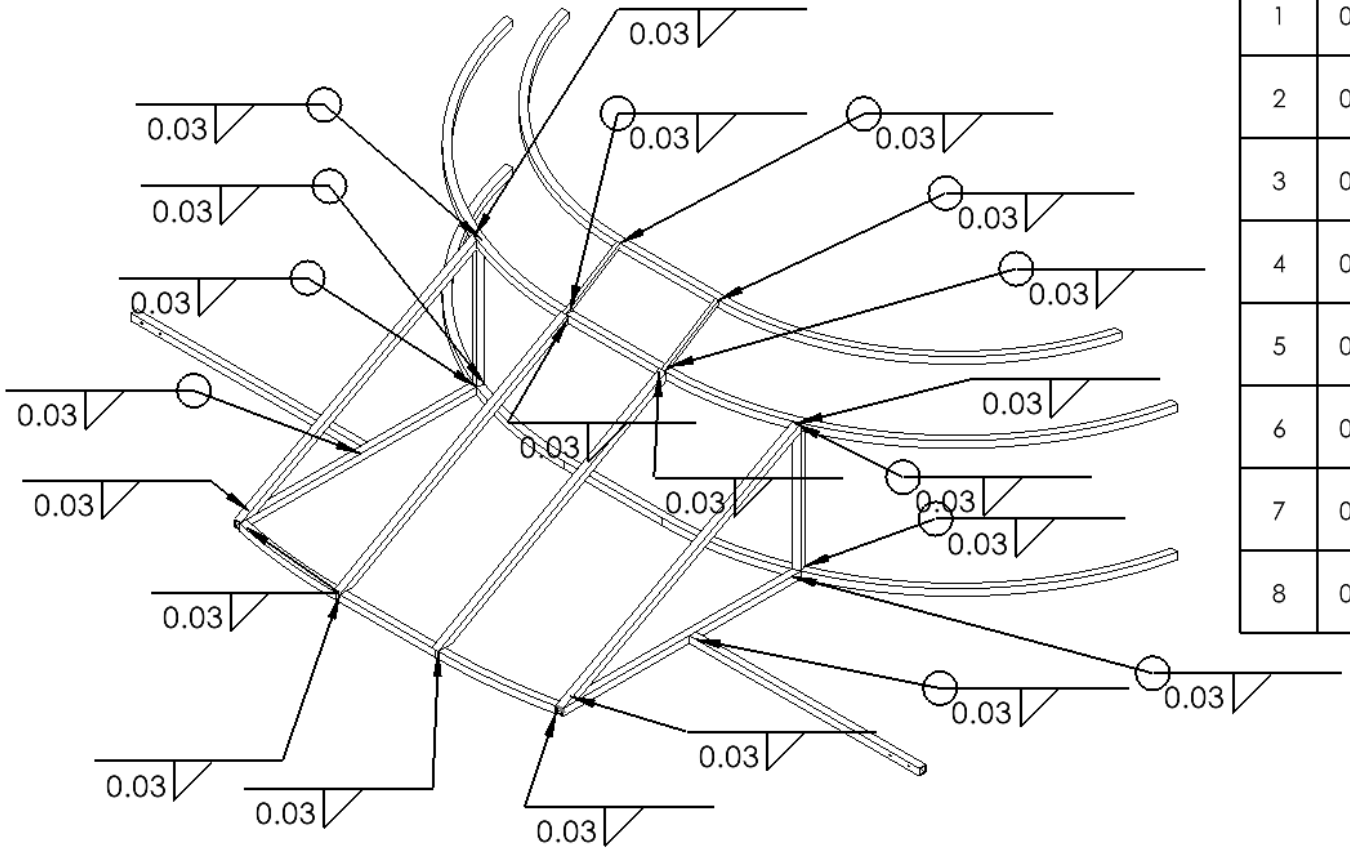

ITEM NO.	WELD SIZE	SYMBOL	WELD LENGTH	WELD MATERIAL	QTY.
1	0.03	◺	2.09	AI 4043	2
2	0.03	◺	3.11	AI 4043	2
3	0.03	◺	2	AI 4043	8
4	0.03	◺	1.44	AI 4043	2
5	0.03	◺	1.5	AI 4043	2
6	0.03	◺	1.43	AI 4043	2
7	0.03	◺	1.09	AI 4043	2
8	0.03	◺	1.82	AI 4043	2

		NAME	DATE
UNLESS OTHERWISE SPECIFIED:	DRAWN		
DIMENSIONS ARE IN INCHES TOLERANCES: FRACTIONAL ± ANGULAR: MACH ± BEND ± TWO PLACE DECIMAL ± THREE PLACE DECIMAL ±	CHECKED		
	ENG APPR.		
	MFG APPR.		
MATERIAL	COMMENTS:		
FINISH	WEIGHT:		
DO NOT SCALE DRAWING			

COASTAL CURRENT

TITLE:
Overtopping Skeleton Base

SIZE	DWG. NO.	REV
A	Overtopping Skeleton - 1	

SCALE: 1:10 | SHEET 1 OF 3

ITEM NO.	WELD SIZE	SYMBOL	WELD LENGTH	WELD MATERIAL	QTY.
1	0.03	◺	1.5	AI 4043	2
2	0.03	◺	1.06	AI 4043	2

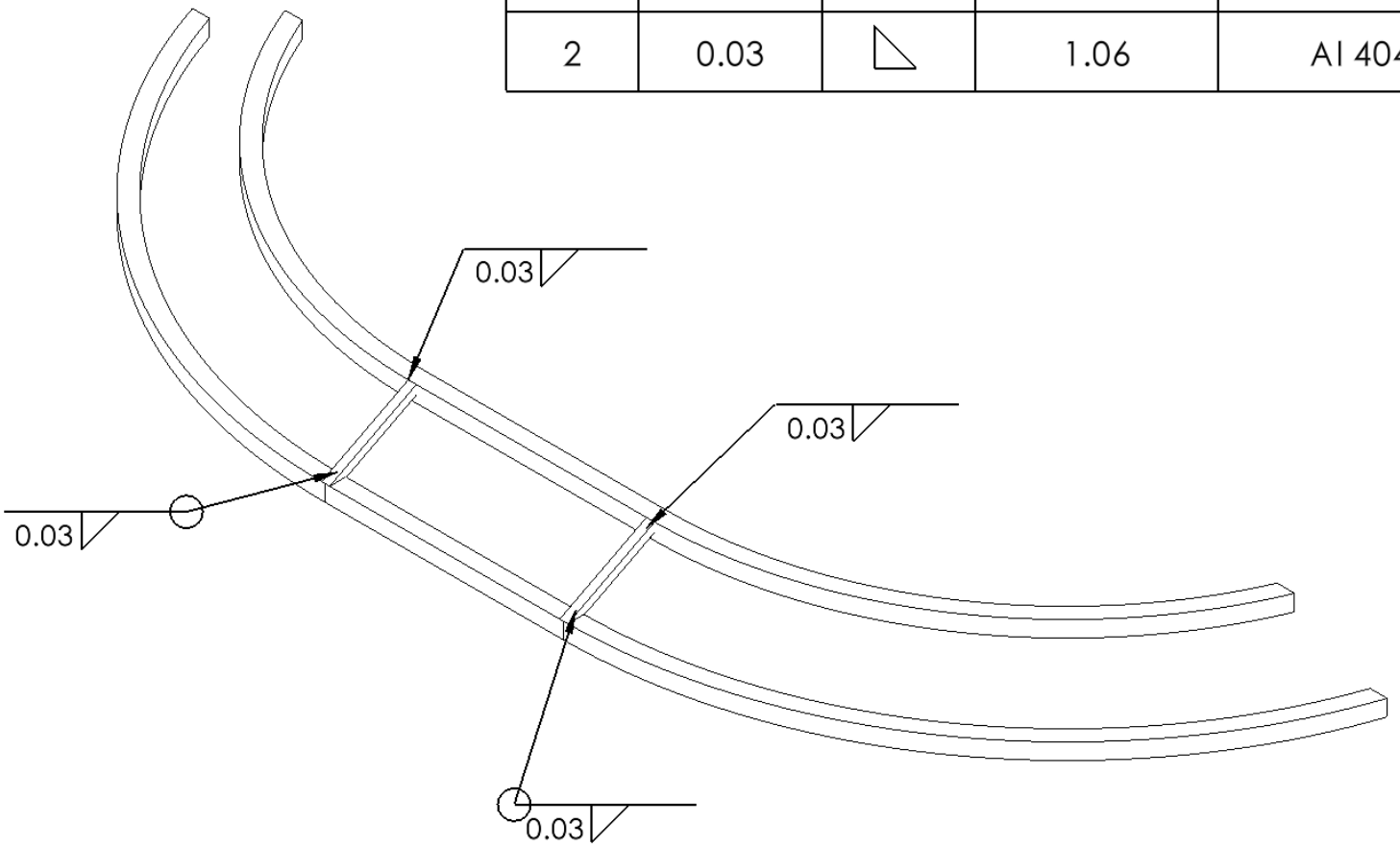

		NAME	DATE
UNLESS OTHERWISE SPECIFIED:	DRAWN		
DIMENSIONS ARE IN INCHES TOLERANCES: FRACTIONAL ± ANGULAR: MACH ± BEND ± TWO PLACE DECIMAL ± THREE PLACE DECIMAL ±	CHECKED		
	ENG APPR.		
	MFG APPR.		
MATERIAL	COMMENTS:		
FINISH	WEIGHT:		
DO NOT SCALE DRAWING			

COASTAL CURRENT

TITLE: Overtop. Skeleton Reservoir 2

SIZE	DWG. NO.	REV
A	Overtopping Skeleton - 2	

SCALE: 1:4 | SHEET 2 OF 3

ITEM NO.	PART NUMBER	QTY.
1	1 - Base Semi-Circle	2
2	2 - Ramp Sides	2
3	3 - Ramp Front	1
4	4 - Vertical Ramp Supports	2
5	5 - Left Outside Slanted Ramp Supports	1
6	6 - Right Outside Slanted Ramp Support	1
7	7 - Inner Slanted Ramp Support	2
8	8 - Reservoir 1 Top	1
9	9 - Reservoir 1 Slanted Support	2
10	10 - Reservoir 2 Bottom	1
11	11 - Reservoir 2 Top	1
12	12 - Reservoir 2 Slanted Support	2
13	13 - Crest Bottom	1
14	14 - Crest Top	1
15	15 - Frame Support	2

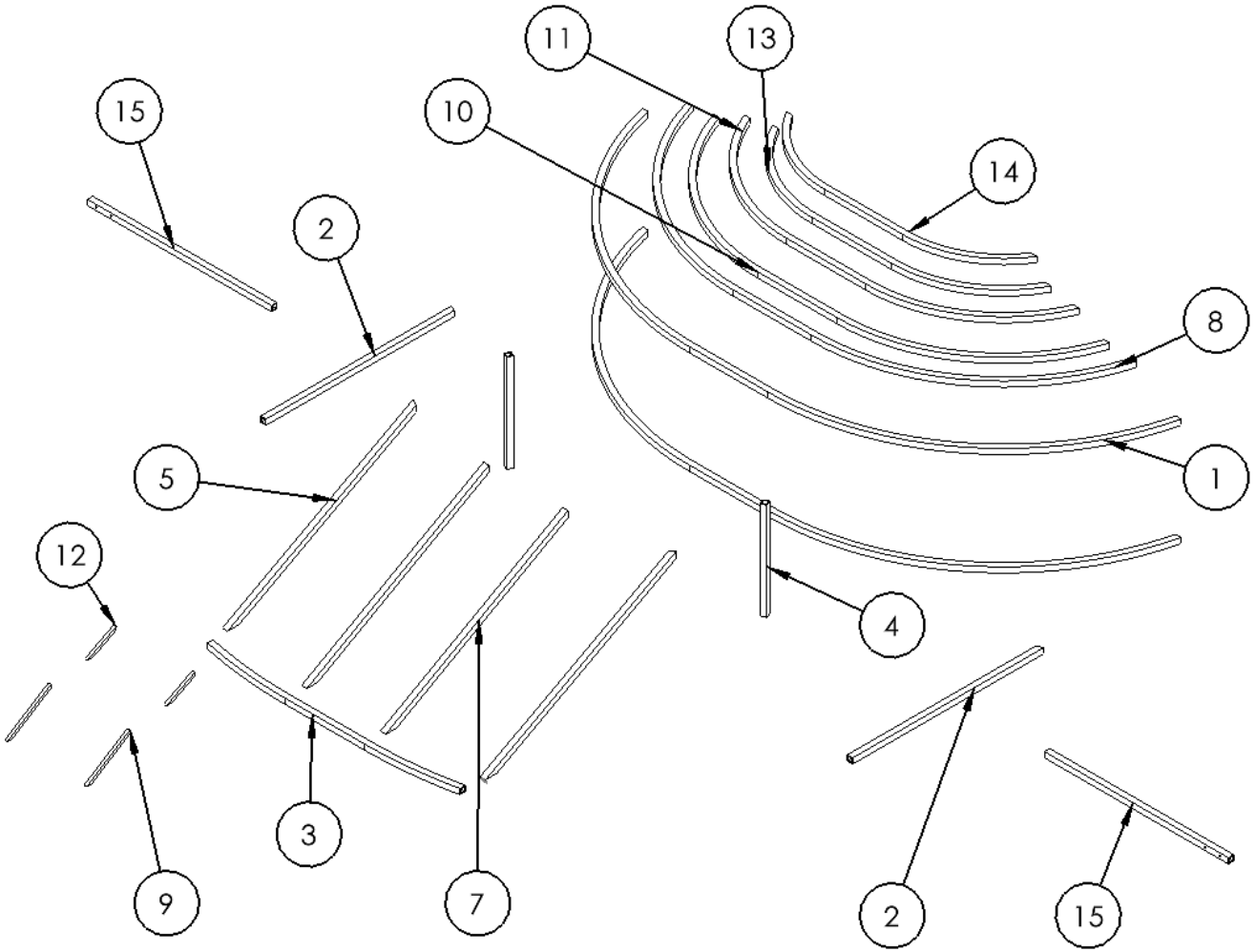

UNLESS OTHERWISE SPECIFIED:		NAME	DATE
DIMENSIONS ARE IN INCHES TOLERANCES: FRACTIONAL ± ANGULAR: MACH ± BEND ± TWO PLACE DECIMAL ± THREE PLACE DECIMAL ±	DRAWN		
	CHECKED		
	ENG APPR.		
	MFG APPR.		
MATERIAL	COMMENTS: WEIGHT: 3.80		
FINISH			
DO NOT SCALE DRAWING			

COASTAL CURRENT

TITLE:
Exploded Overtopping Skeleton

SIZE	DWG. NO.	REV
A	Overtopping Skeleton - 3	

SCALE: 1:12 | SHEET 3 OF 3

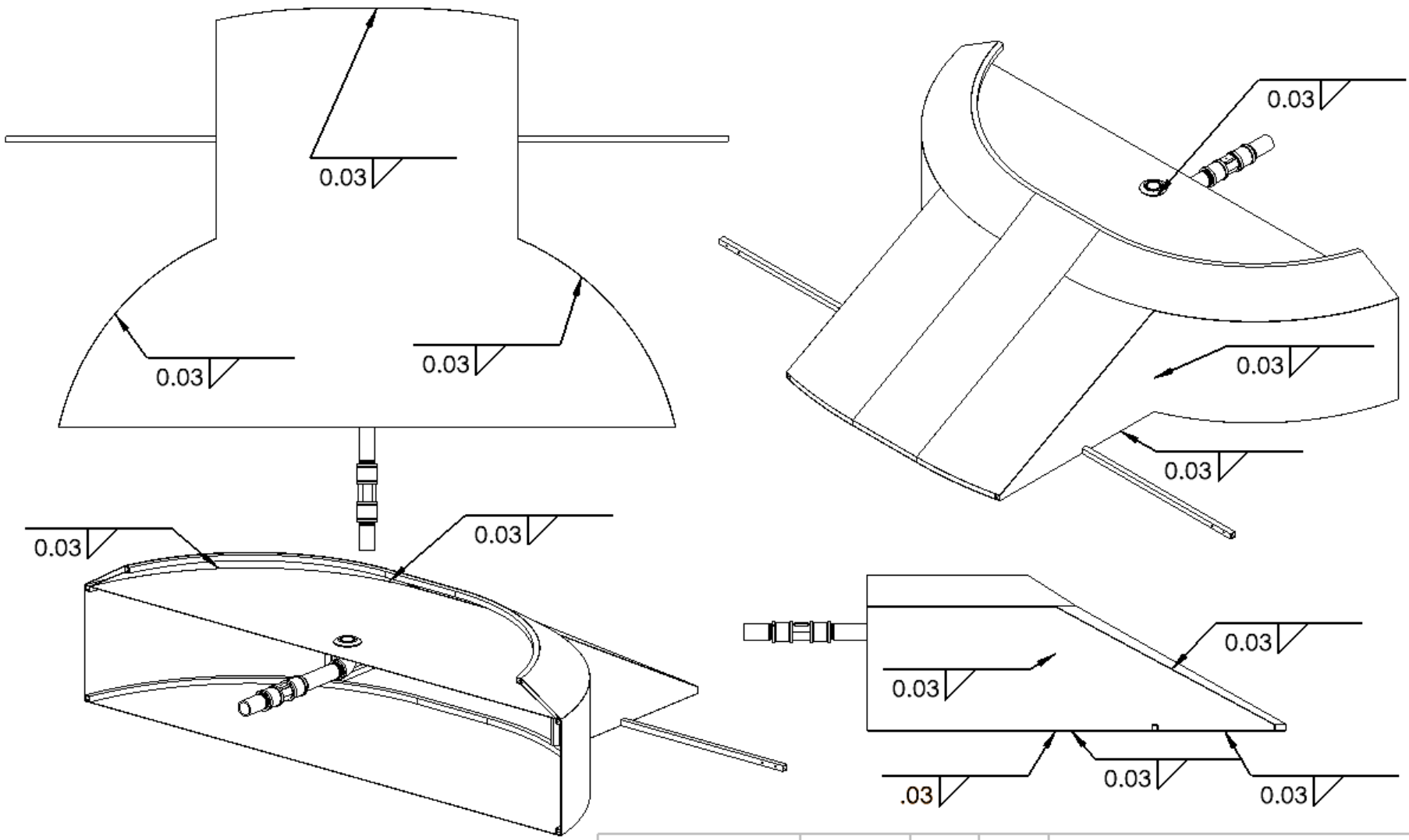

UNLESS OTHERWISE SPECIFIED:		NAME	DATE
DIMENSIONS ARE IN INCHES TOLERANCES: FRACTIONAL ± ANGULAR: MACH ± BEND ± TWO PLACE DECIMAL ± THREE PLACE DECIMAL ±	DRAWN		
	CHECKED		
	ENG APPR.		
	MFG APPR.		
MATERIAL	COMMENTS:		
FINISH	WEIGHT:		
DO NOT SCALE DRAWING			

COASTAL CURRENT

TITLE:
Overtopping Base Welds 1

SIZE	DWG. NO.	REV
A	Overtopping Device - 2	

SCALE: 1:12 SHEET 2 OF 8

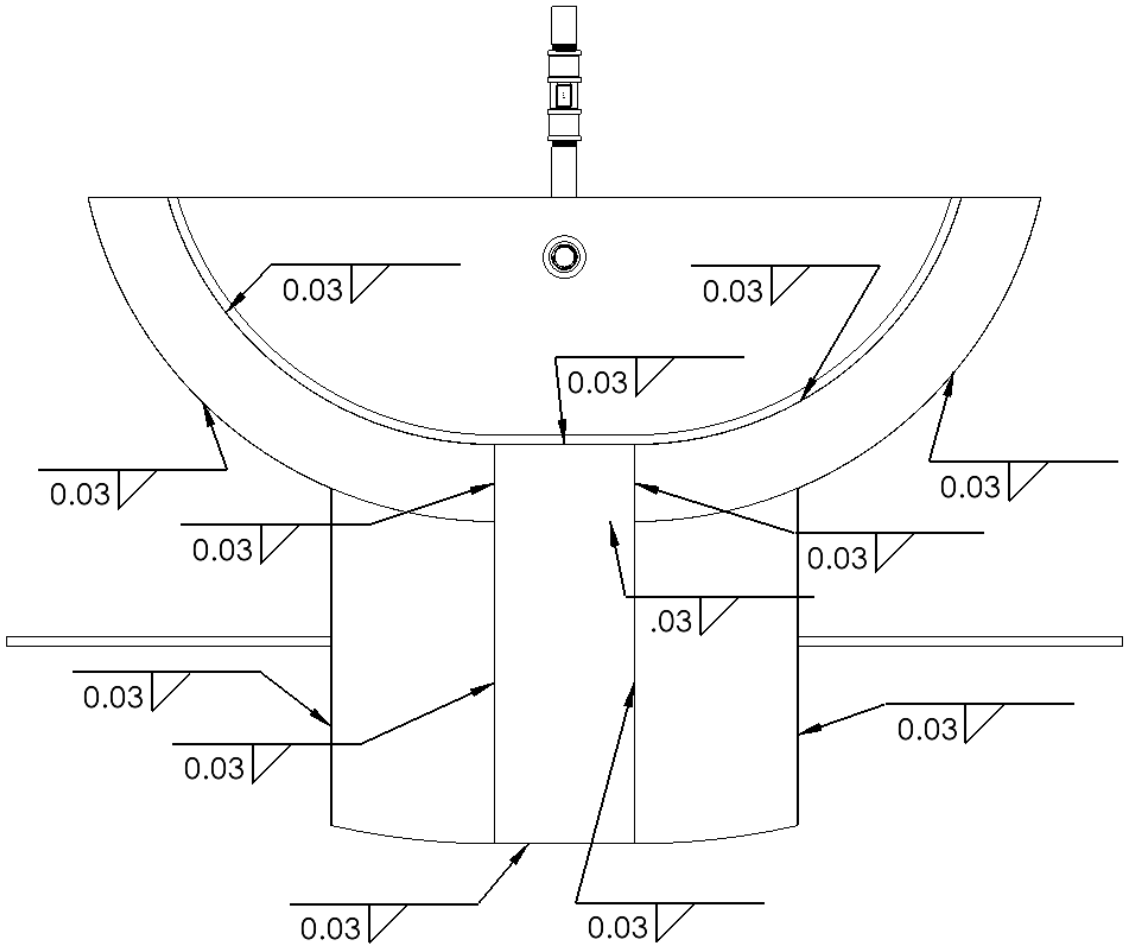

ITEM NO.	WELD SIZE	SYMBOL	WELD LENGTH	WELD MATERIAL	QTY.
1	0.03	◺	60.43	AI 4043	1
2	0.03	◺	20.8	AI 4043	6
3	0.03	◺	30.22	AI 4043	2
4	0.03	◺	9.09	AI 4043	4
5	0.03	◺	7.87	AI 4043	2
6	0.03	◺	56.84	AI 4043	1
7	0.03	◺	57.34	AI 4043	1
8	0.03	◺	7.38	AI 4043	5
9	0.03	◺	19.56	AI 4043	2
10	0.03	◺	56.26	AI 4043	2
11	0.03	◺	28.08	AI 4043	2
12	0.03	◺	29.66	AI 4043	2
13	0.03	◺	4.82	AI 4043	2
14	0.03	◺	65.15	AI 4043	1
15	0.03	◺	7.07	AI 4043	1

UNLESS OTHERWISE SPECIFIED:

DIMENSIONS ARE IN INCHES
TOLERANCES:
FRACTIONAL ±
ANGULAR: MACH ± BEND ±
TWO PLACE DECIMAL ±
THREE PLACE DECIMAL ±

MATERIAL

FINISH

DO NOT SCALE DRAWING

	NAME	DATE
DRAWN		
CHECKED		
ENG APPR.		
MFG APPR.		

COMMENTS:

WEIGHT:

COASTAL CURRENT

TITLE:

Overtopping Base Welds 2

SIZE	DWG. NO.	REV
A	Overtopping Device - 3	

SCALE: 1:10 SHEET 3 OF 8

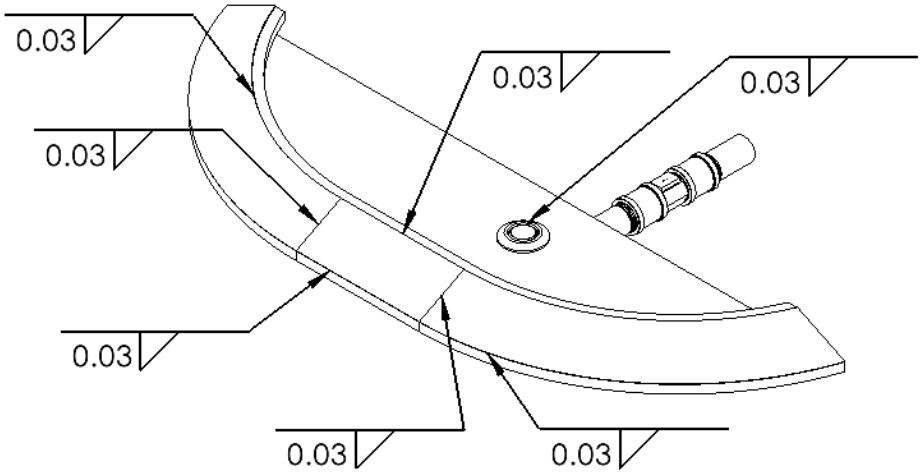

ITEM NO.	WELD SIZE	SYMBOL	WELD LENGTH	WELD MATERIAL	QTY.
1	0.03		15.26	Al 4043	2
2	0.03		18.74	Al 4043	2
3	0.03		7.38	Al 4043	4
4	0.03		2.36	Al 4043	2
5	0.03		37.81	Al 4043	2
6	0.03		3.02	Al 4043	2
7	0.03		89.79	Al 4043	2
8	0.03		7.07	Al 4043	1

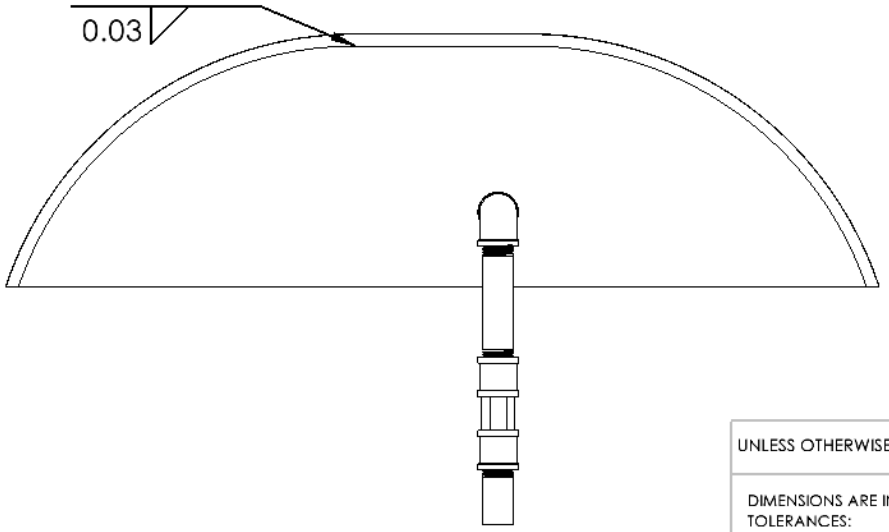

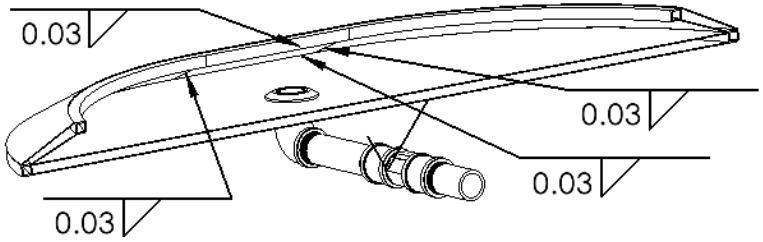

		NAME	DATE
UNLESS OTHERWISE SPECIFIED:	DRAWN		
DIMENSIONS ARE IN INCHES TOLERANCES: FRACTIONAL ± ANGULAR: MACH ± BEND ± TWO PLACE DECIMAL ± THREE PLACE DECIMAL ±	CHECKED		
	ENG APPR.		
	MFG APPR.		
	COMMENTS:		
MATERIAL	WEIGHT:		
FINISH			
DO NOT SCALE DRAWING			

COASTAL CURRENT

TITLE: Reservoir 2 Welds

SIZE	DWG. NO.	REV
A	Overtopping Device - 4	

SCALE: 1:8 | SHEET 4 OF 8

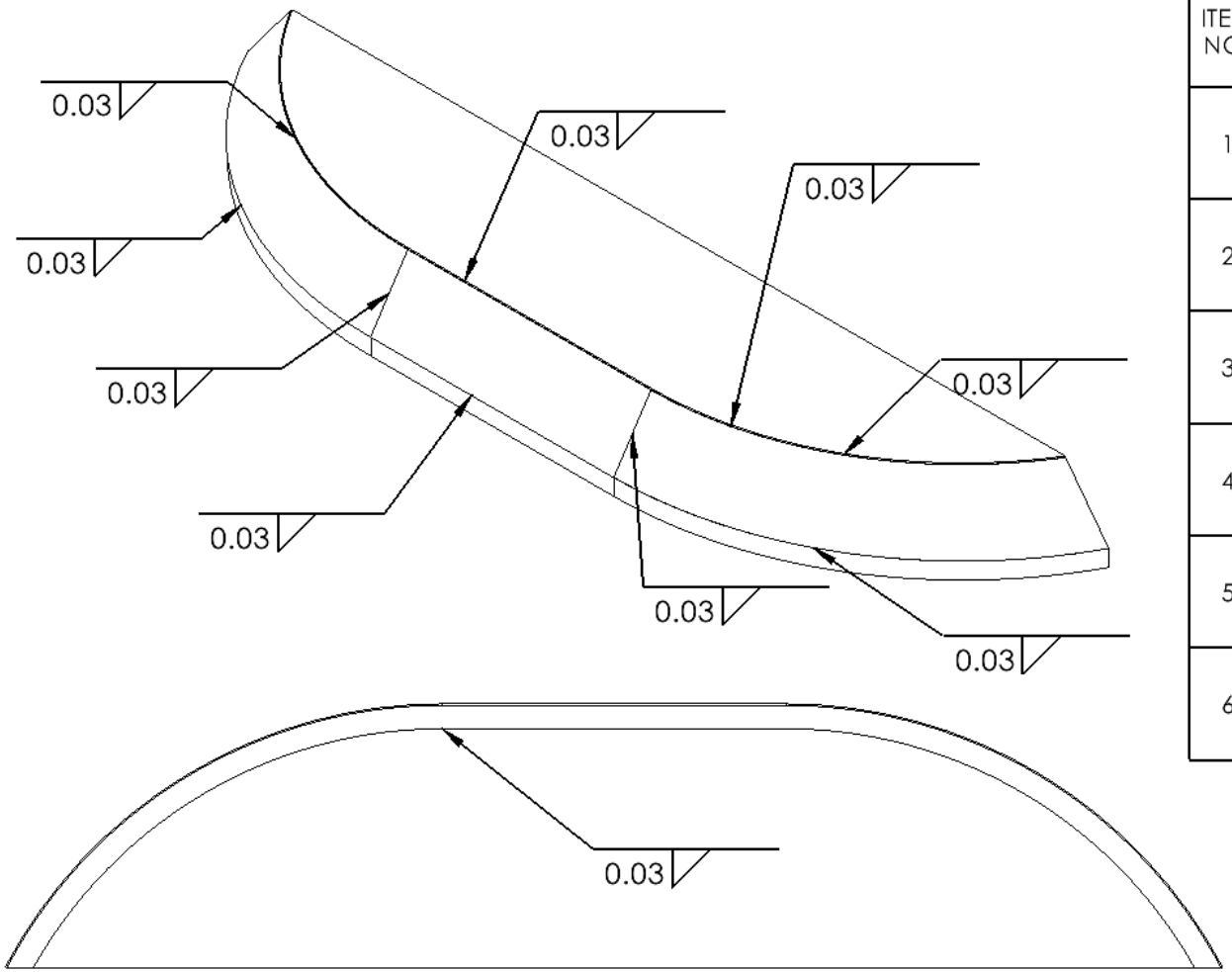

ITEM NO.	WELD SIZE	SYMBOL	WELD LENGTH	WELD MATERIAL	QTY.
1	0.03	◺	9.62	AI 4043	2
2	0.03	◺	11.46	AI 4043	2
3	0.03	◺	7.38	AI 4043	2
4	0.03	◺	2.07	AI 4043	2
5	0.03	◺	57.47	AI 4043	1
6	0.03	◺	26.63	AI 4043	1

		NAME	DATE
UNLESS OTHERWISE SPECIFIED:	DRAWN		
DIMENSIONS ARE IN INCHES TOLERANCES: FRACTIONAL ± ANGULAR: MACH ± BEND ± TWO PLACE DECIMAL ± THREE PLACE DECIMAL ±	CHECKED		
	ENG APPR.		
	MFG APPR.		
MATERIAL	COMMENTS:		
FINISH	WEIGHT:		
DO NOT SCALE DRAWING			

COASTAL CURRENT

TITLE: Crest Welds

SIZE	DWG. NO.	REV
A	Overtopping Device - 5	

SCALE: 1:4 | SHEET 5 OF 8

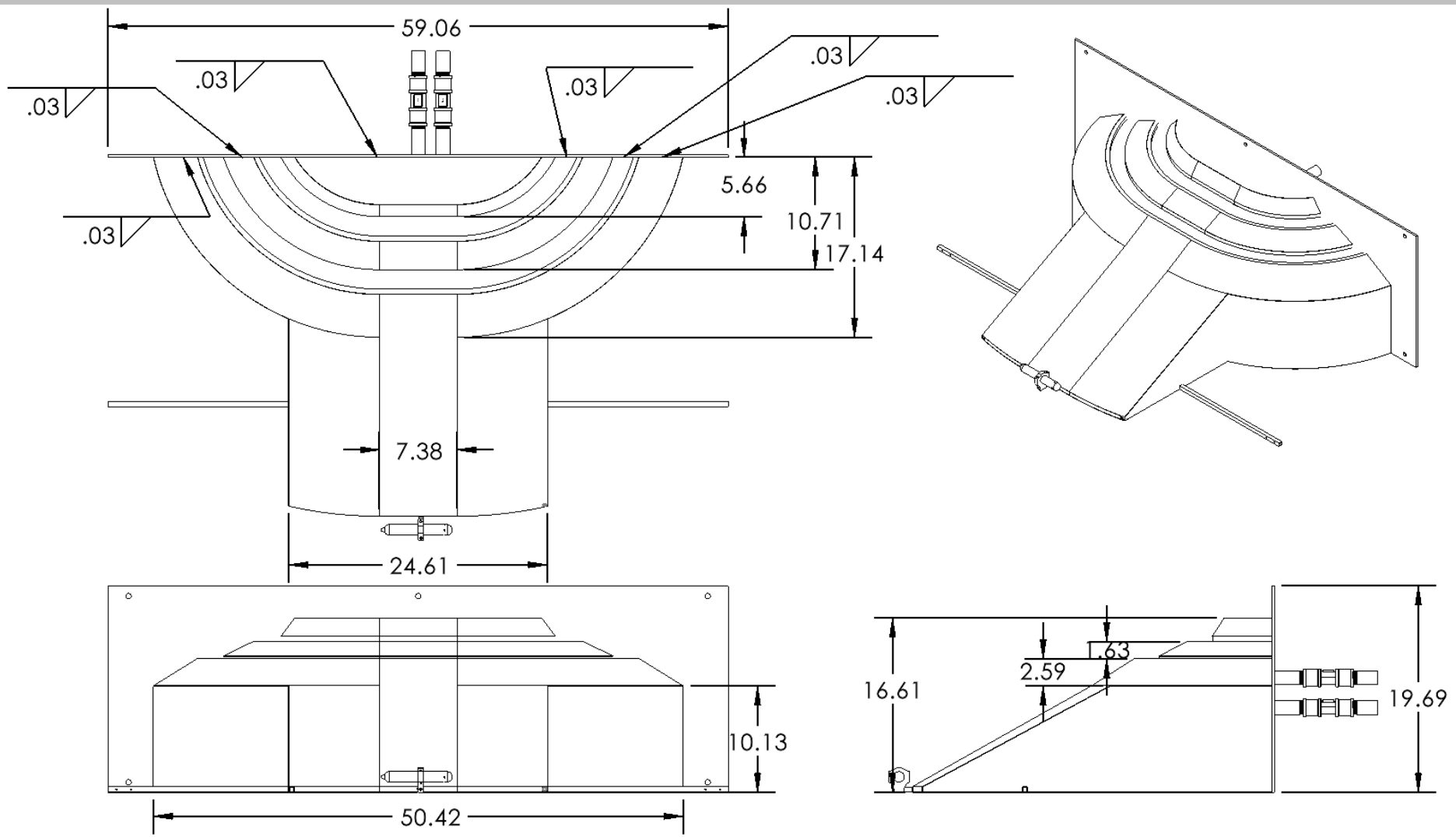

General Tolerances
X.X ± 0.1
X.XX ± 0.03
X° ± 0.5°

		NAME	DATE
UNLESS OTHERWISE SPECIFIED:	DRAWN		
DIMENSIONS ARE IN INCHES TOLERANCES: FRACTIONAL ± ANGULAR: MACH ± BEND ± TWO PLACE DECIMAL ± THREE PLACE DECIMAL ±	CHECKED		
	ENG APPR.		
	MFG APPR.		
MATERIAL	COMMENTS:		
FINISH	WEIGHT:		
DO NOT SCALE DRAWING			

COASTAL CURRENT

TITLE:
Overtopping Device

SIZE	DWG. NO.	REV
A	Overtopping Device - 6	

SCALE: 1:14 SHEET 6 OF 8

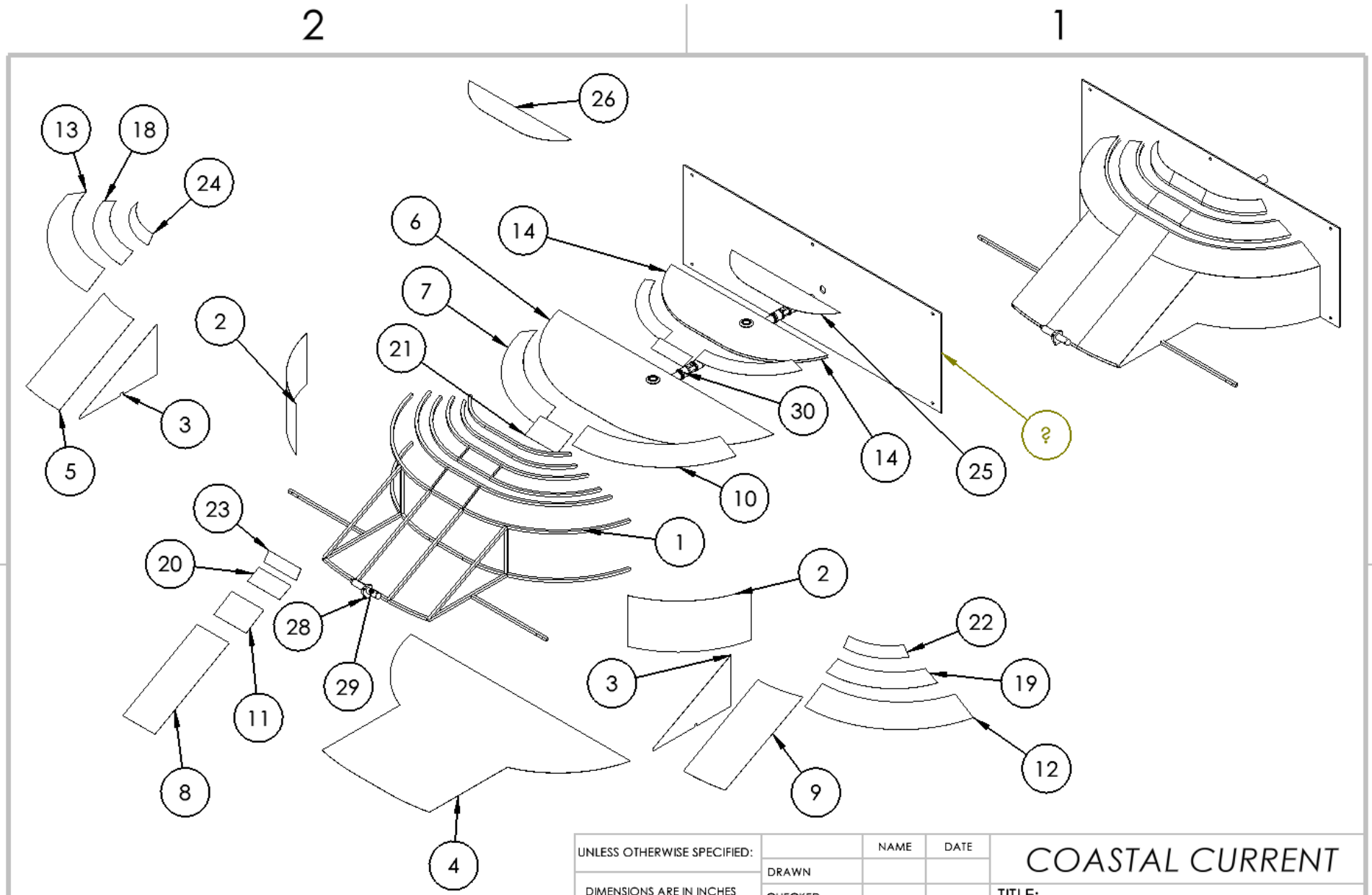

UNLESS OTHERWISE SPECIFIED:		NAME	DATE
DIMENSIONS ARE IN INCHES TOLERANCES: FRACTIONAL ± ANGULAR: MACH ± BEND ± TWO PLACE DECIMAL ± THREE PLACE DECIMAL ±	DRAWN		
	CHECKED		
	ENG APPR.		
	MFG APPR.		
MATERIAL	COMMENTS:		
FINISH	WEIGHT:		
DO NOT SCALE DRAWING			

COASTAL CURRENT

TITLE:
Overtopping Device Exploded

SIZE	DWG. NO.	REV
A	Overtopping Device - 7	

SCALE: 1:22 SHEET 7 OF 8

ITEM NO.	PART NUMBER	QTY.
1	Overtopping Skeleton	1
2	Base_outersemi_cricle	2
3	Ramp_triagnle sides	2
4	Base_bottom plate	1
5	Ramp Left	1
6	Reservoir1_Base	1
7	Reservoir1_CurvePart_Left_inner	1
8	Ramp Front	1
9	Ramp Right	1
10	Reservoir1_CurvePart_Right_inner	1
11	Reservoir1_Front_Outer	1
12	Reservoir1_Curve_Right_Outer	1
13	Reservoir1_Curve_Left_Outer	1
14	Reservoir2_Base	2
15	Reservoir2_CurvePart_Left_inner	1
16	Reservoir2_CurvePart_Right_inner	1
17	Reservoir2_Front_Inner	1
18	Reservoir2_CurvePart_Left_Outer	1
19	Reservoir2_CurvePart_Right_Outer	1
20	Reservoir2_Front_Outer	1
21	Reservoir1_Front_Inner	1
22	Crest_Right	1
23	Crest_Front	1
24	Crest_Left	1
25	TopCrest_bottom	1
26	TopCrest_top	1
27	Back Plate	1
28	Pressure Sensor Mount	1
29	Pressure Sensor	1
30	Flow Sensor and Piping	2

TITLE: Overtopping Device BOM

SIZE	DWG. NO.	REV
A	Overtopping Device -8	

SCALE: 1:22 | WEIGHT: | SHEET 8 OF 8

ITEM NO.	PART NUMBER	QTY.
1	4429K165	1
2	4568K231	1
3	4429K115	2
4	Flowmeter	1
5	9580K45	1
6	8694T46	1
7	4568K221	1

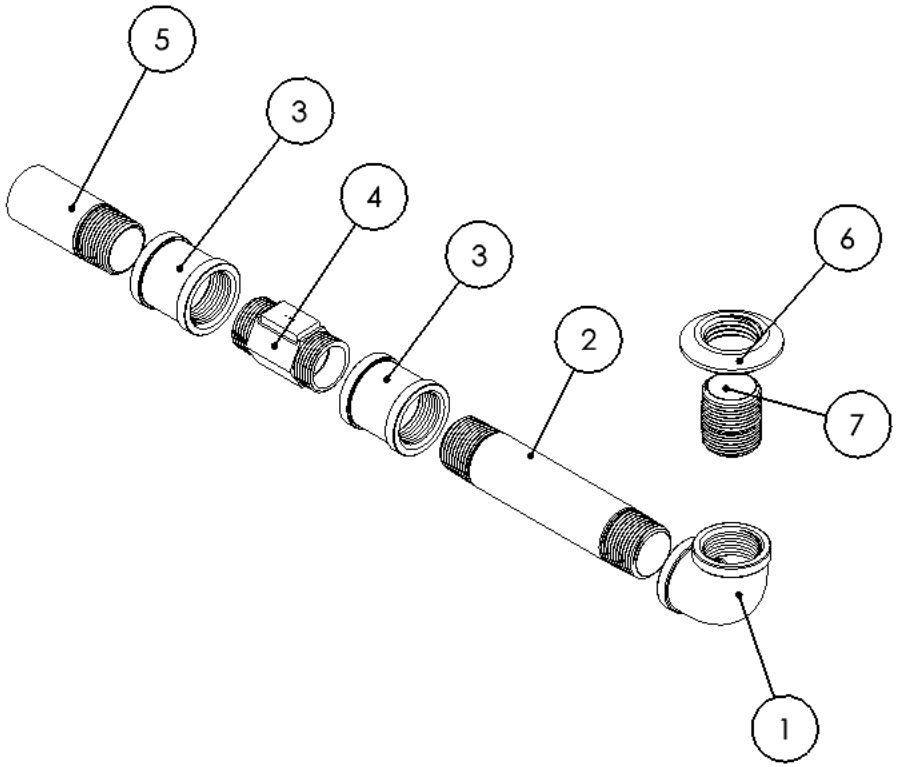

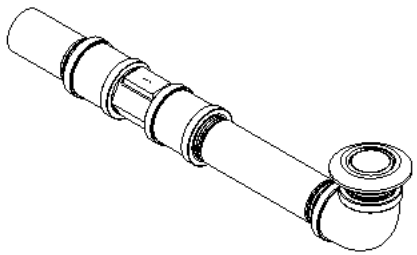

UNLESS OTHERWISE SPECIFIED:		NAME	DATE
DIMENSIONS ARE IN INCHES TOLERANCES: FRACTIONAL ± ANGULAR: MACH ± BEND ± TWO PLACE DECIMAL ± THREE PLACE DECIMAL ±	DRAWN		
	CHECKED		
	ENG APPR.		
	MFG APPR.		
	COMMENTS:		
MATERIAL	WEIGHT:		
FINISH			
DO NOT SCALE DRAWING			

COASTAL CURRENT

TITLE:
Flow Sensor Piping

SIZE	DWG. NO.	REV
A	Flow Sensor Piping - 1	

SCALE: 1:4 | SHEET 1 OF 1

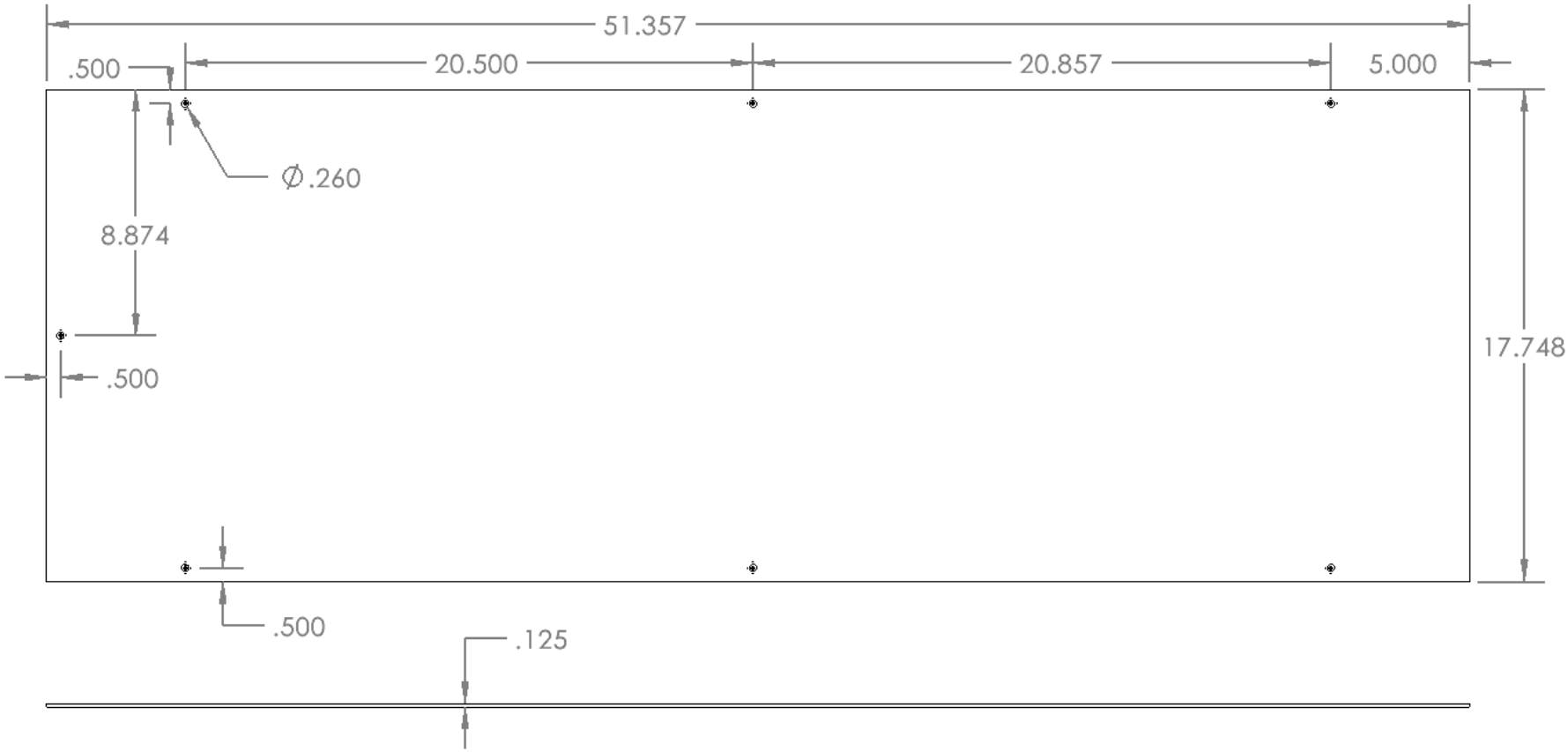

General Tolerances
X.X ± 0.1
X.XX ± 0.03
X° ± 0.5°

		NAME	DATE
UNLESS OTHERWISE SPECIFIED:	DRAWN		
DIMENSIONS ARE IN INCHES TOLERANCES: FRACTIONAL ± ANGULAR: MACH ± BEND ± TWO PLACE DECIMAL ± THREE PLACE DECIMAL ±	CHECKED		
	ENG APPR.		
	MFG APPR.		
MATERIAL	COMMENTS:		
FINISH	WEIGHT:		
DO NOT SCALE DRAWING			

COASTAL CURRENT

TITLE: Plexiglass Plate

SIZE	DWG. NO.	REV
A	Frame - 1	

SCALE: 1:6 | SHEET 1 OF 5

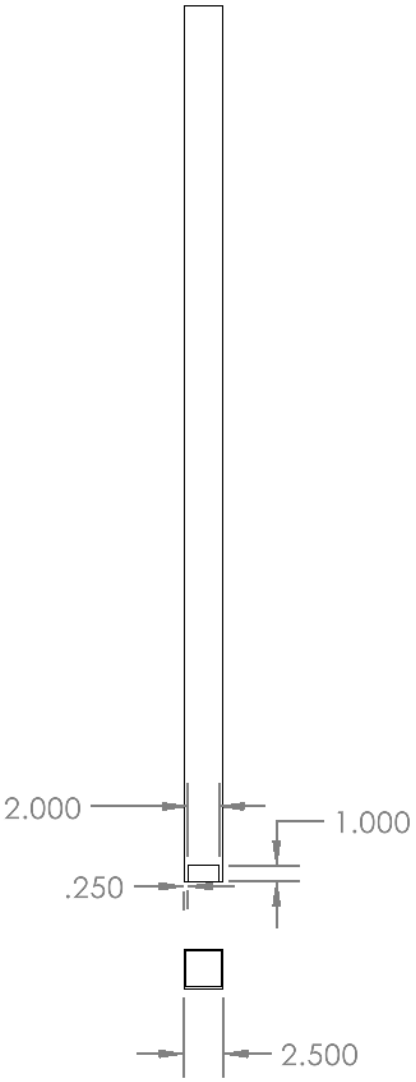

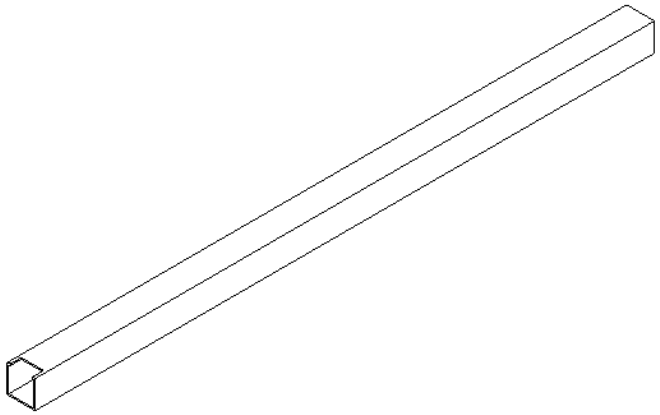

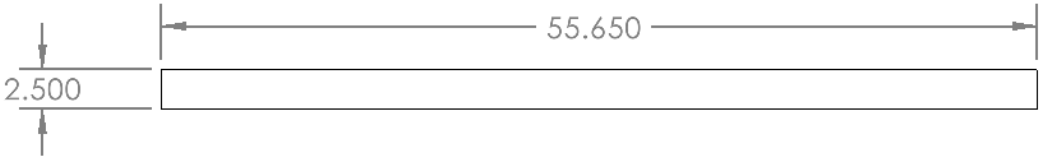

General Tolerances
X.X ± 0.1
X.XX ± 0.03
X° ± 0.5°

UNLESS OTHERWISE SPECIFIED:		NAME	DATE
DIMENSIONS ARE IN INCHES TOLERANCES: FRACTIONAL ± ANGULAR: MACH ± BEND ± TWO PLACE DECIMAL ± THREE PLACE DECIMAL ±	DRAWN		
	CHECKED		
	ENG APPR.		
	MFG APPR.		
MATERIAL	COMMENTS:		
FINISH	WEIGHT:		
DO NOT SCALE DRAWING			

COASTAL CURRENT

TITLE: Side Top

SIZE	DWG. NO.	REV
A	Frame - 2	

SCALE: 1:12 | SHEET 2 OF 5

ITEM NO.	WELD SIZE	SYMBOL	WELD LENGTH	WELD MATERIAL	QTY.
1	0.047	◺	10	AL 4043	18

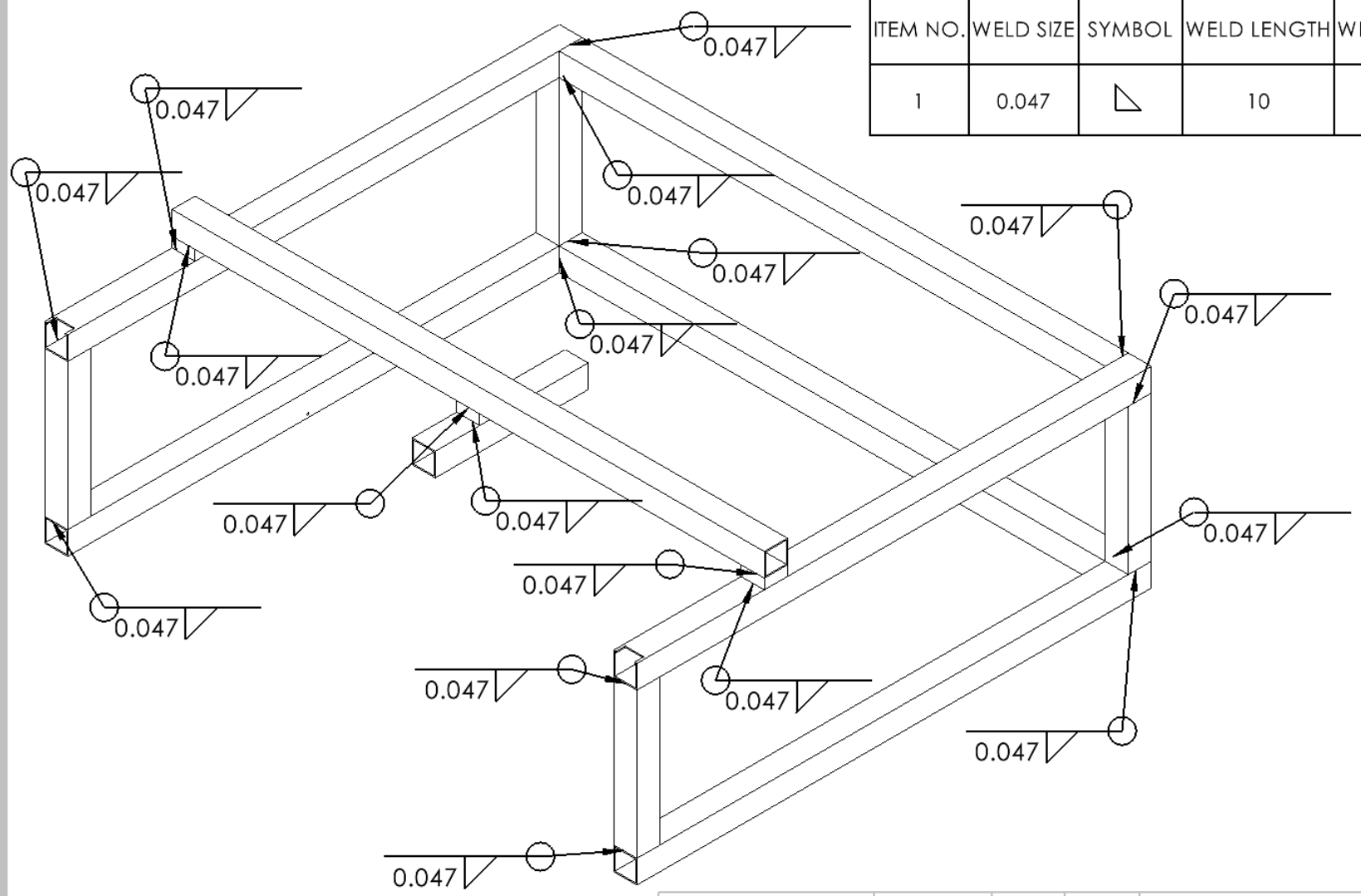

UNLESS OTHERWISE SPECIFIED:		NAME	DATE	COASTAL CURRENT
DIMENSIONS ARE IN INCHES TOLERANCES: FRACTIONAL ± ANGULAR: MACH ± BEND ± TWO PLACE DECIMAL ± THREE PLACE DECIMAL ±	DRAWN			TITLE: Frame Welds
	CHECKED			
	ENG APPR.			
	MFG APPR.			
MATERIAL	COMMENTS: WEIGHT:			SIZE A | DWG. NO. Frame - 3 | REV
FINISH				SCALE: 1:12 | SHEET 3 OF 5
DO NOT SCALE DRAWING				

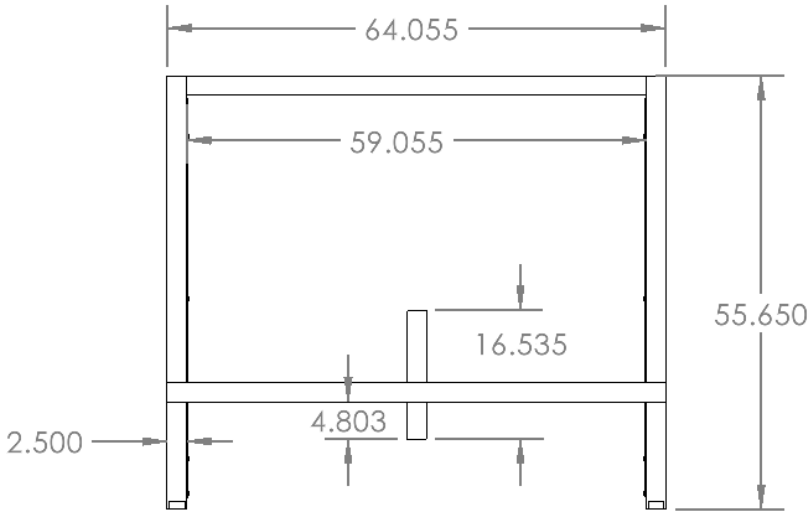

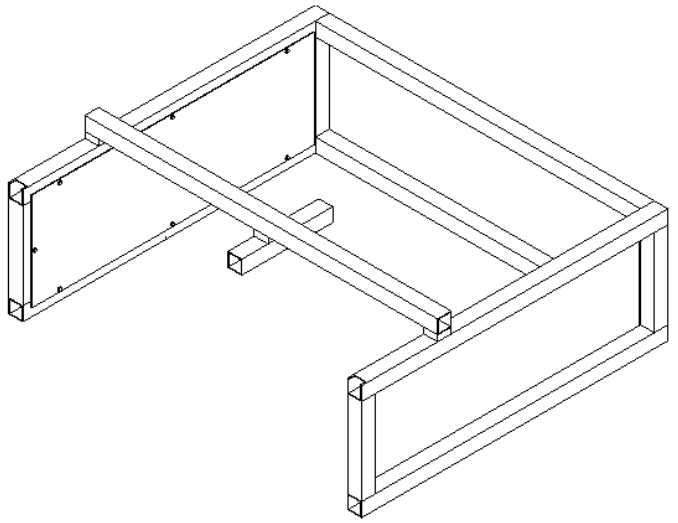

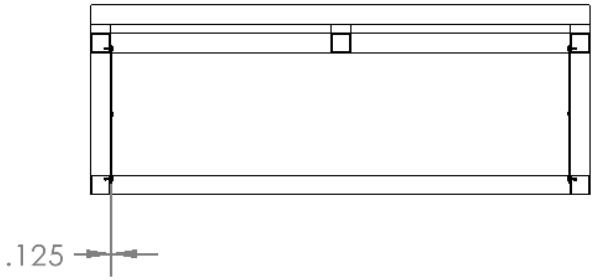

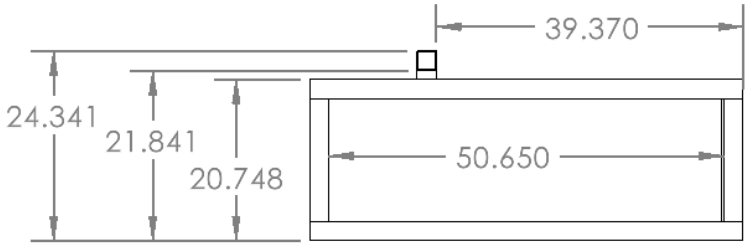

General Tolerances
X.X ± 0.1
X.XX ± 0.03
X° ± 0.5°

		NAME	DATE
UNLESS OTHERWISE SPECIFIED:	DRAWN		
DIMENSIONS ARE IN INCHES TOLERANCES: FRACTIONAL ± ANGULAR: MACH ± BEND ± TWO PLACE DECIMAL ± THREE PLACE DECIMAL ±	CHECKED		
	ENG APPR.		
	MFG APPR.		
MATERIAL	COMMENTS:		
	WEIGHT:		
FINISH			
DO NOT SCALE DRAWING			

COASTAL CURRENT

TITLE: Frame

SIZE	DWG. NO.	REV
A	Frame - 4	

SCALE: 1:24 | SHEET 4 OF 5

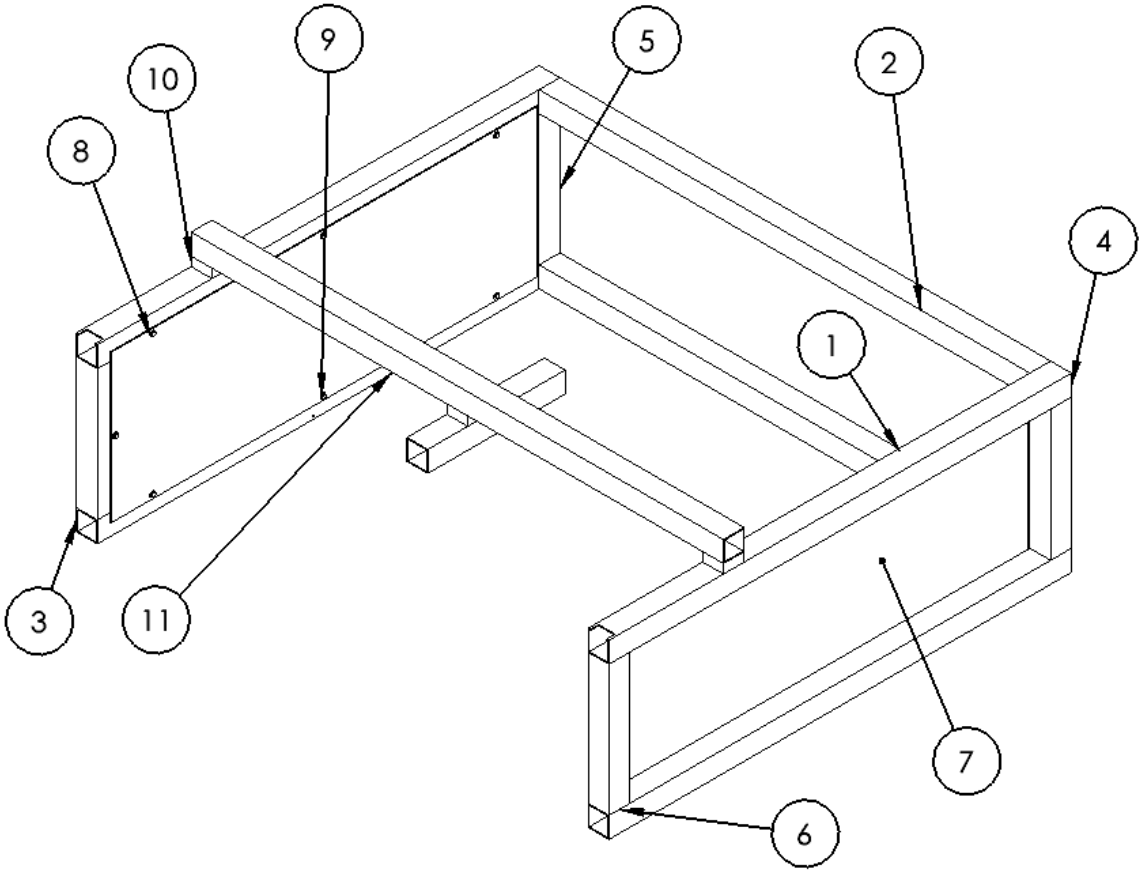

ITEM NO.	PART NUMBER	QTY.
1	Back Bottom^Frame	1
2	Back Top^Frame	1
3	Side Bottom^Frame	2
4	Side Top	2
5	Back Vertical^Frame	2
6	Front Vertical^Frame	2
7	Pexiglass Plate	2
8	90107A029	14
9	93190A542	14
10	Deflector Rack Bar Support	3
11	Deflector Rack Bar	1
12	Deflector Middle Support	1

		NAME	DATE
UNLESS OTHERWISE SPECIFIED:	DRAWN		
DIMENSIONS ARE IN INCHES TOLERANCES: FRACTIONAL ± ANGULAR: MACH ± BEND ± TWO PLACE DECIMAL ± THREE PLACE DECIMAL ±	CHECKED		
	ENG APPR.		
	MFG APPR.		
	COMMENTS:		
MATERIAL	WEIGHT:		
FINISH			
DO NOT SCALE DRAWING			

COASTAL CURRENT

TITLE: Frame BOM

SIZE	DWG. NO.	REV
A	Frame - 5	

SCALE: 1:16 | SHEET 5 OF 5

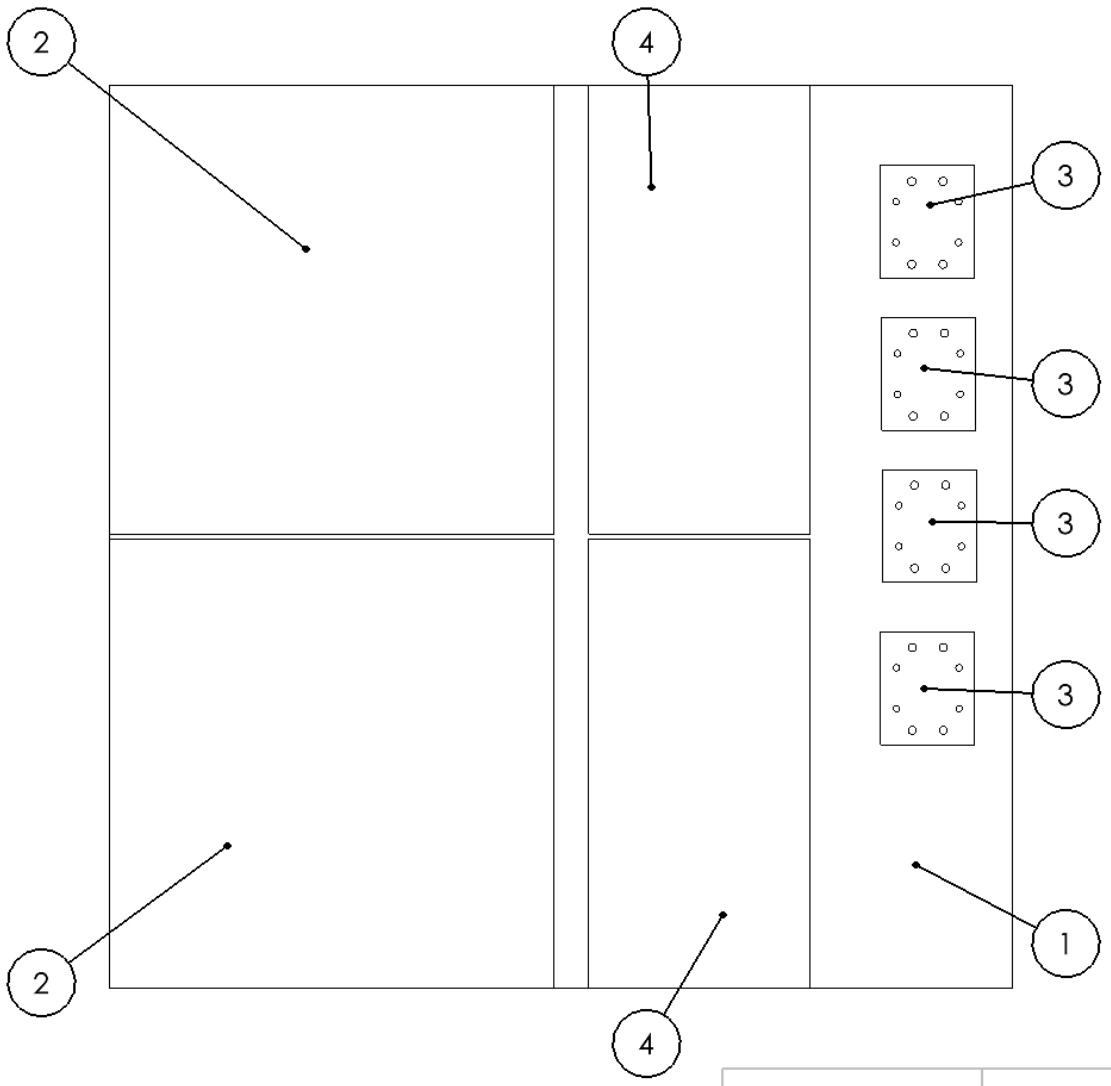

ITEM NO.	PART NUMBER	QTY.
1	24_24 Stock	1
2	Wave Gate Plate	2
3	Limit Switch Mount	4
4	Deflector Plate	2

General Tolerances
X.X ± 0.1
X.XX ± 0.03
X° ± 0.5°

		NAME	DATE
UNLESS OTHERWISE SPECIFIED:	DRAWN		
DIMENSIONS ARE IN INCHES TOLERANCES: FRACTIONAL ± ANGULAR: MACH ± BEND ± TWO PLACE DECIMAL ± THREE PLACE DECIMAL ±	CHECKED		
	ENG APPR.		
	MFG APPR.		
MATERIAL	COMMENTS:		
FINISH	WEIGHT:		
DO NOT SCALE DRAWING			

COASTAL CURRENT

TITLE:
Gate and Deflector Cuts 1

SIZE	DWG. NO.	REV
A	Wave Gate and Deflector Cuts - 1	

SCALE: 1:5 | SHEET 1 OF 2

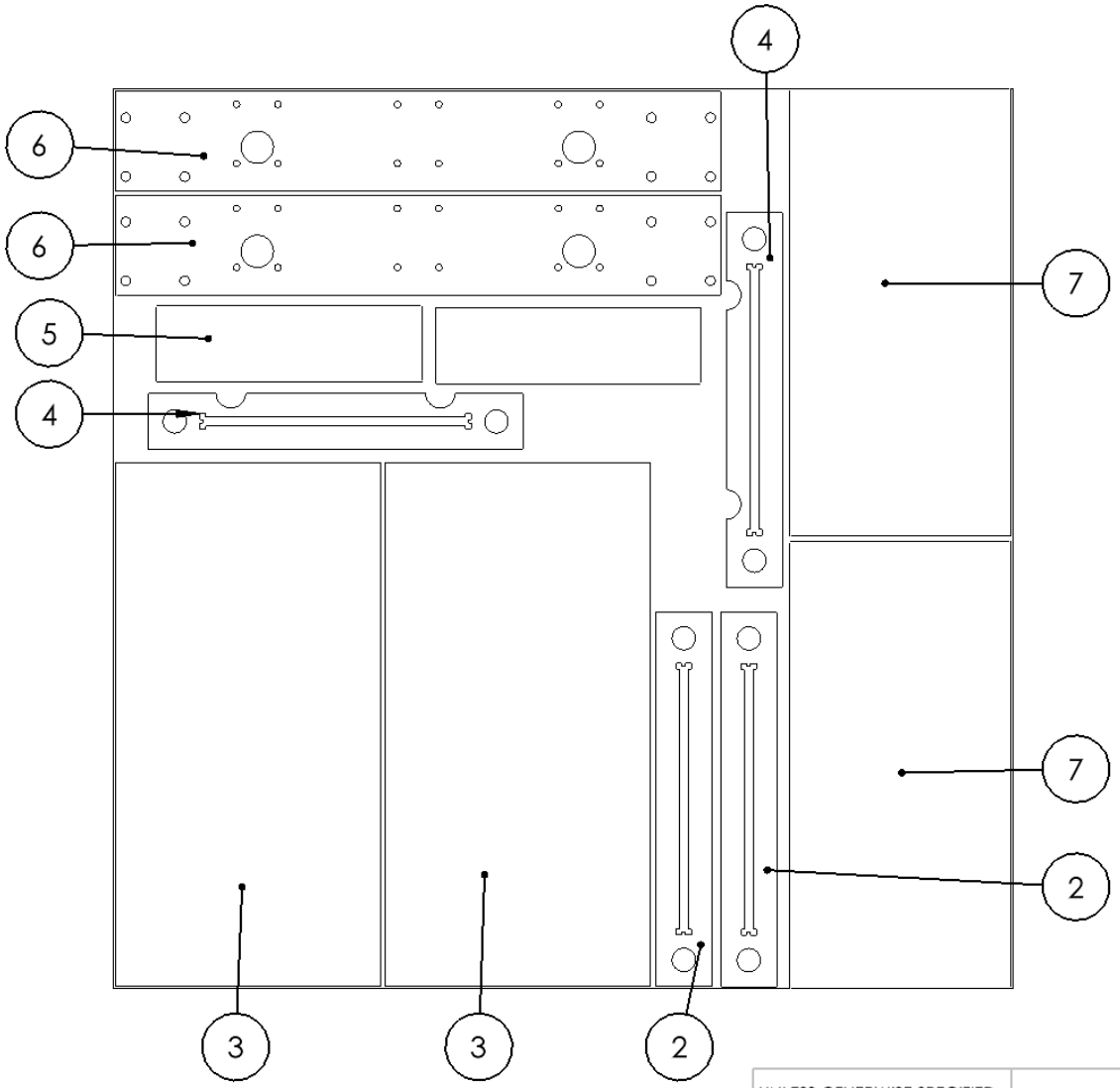

ITEM NO.	PART NUMBER	QTY.
1	24_24 Stock	1
2	Deflector Base - Small Horizontal Bottom	2
3	Deflector Base - Tall Vertical	2
4	Deflector Base - Small Horizontal Top	2
5	Deflector Base - Short Vertical	2
6	Deflector Base - Large Horizontal	2
7	Deflector Plate	2

General Tolerances
X.X ± 0.1
X.XX ± 0.03
X° ± 0.5°

		NAME	DATE
UNLESS OTHERWISE SPECIFIED:	DRAWN		
DIMENSIONS ARE IN INCHES TOLERANCES: FRACTIONAL ± ANGULAR: MACH ± BEND ± TWO PLACE DECIMAL ± THREE PLACE DECIMAL ±	CHECKED		
	ENG APPR.		
	MFG APPR.		
MATERIAL	COMMENTS:		
FINISH	WEIGHT:		
DO NOT SCALE DRAWING			

COASTAL CURRENT

TITLE:
Gates and Deflector Cuts 2

SIZE	DWG. NO.	REV
A	Wave Gate and Deflector Cuts - 2	
SCALE: 1:5		SHEET 2 OF 2

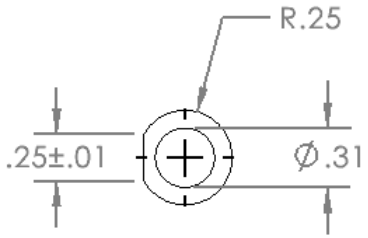

Scale 1:1

General Tolerances
X.X ± 0.1
X.XX ± 0.03
X° ± 0.5°

UNLESS OTHERWISE SPECIFIED:		NAME	DATE
DIMENSIONS ARE IN INCHES TOLERANCES: FRACTIONAL ± ANGULAR: MACH ± BEND ± TWO PLACE DECIMAL ± THREE PLACE DECIMAL ±	DRAWN		
	CHECKED		
	ENG APPR.		
	MFG APPR.		
MATERIAL	COMMENTS:		
FINISH	WEIGHT:		
DO NOT SCALE DRAWING			

COASTAL CURRENT

TITLE:
Wave Gate Shaft

SIZE	DWG. NO.	REV
A	Wave Gate Subassembly - 1	

SCALE: 1:3 | SHEET 1 OF 5

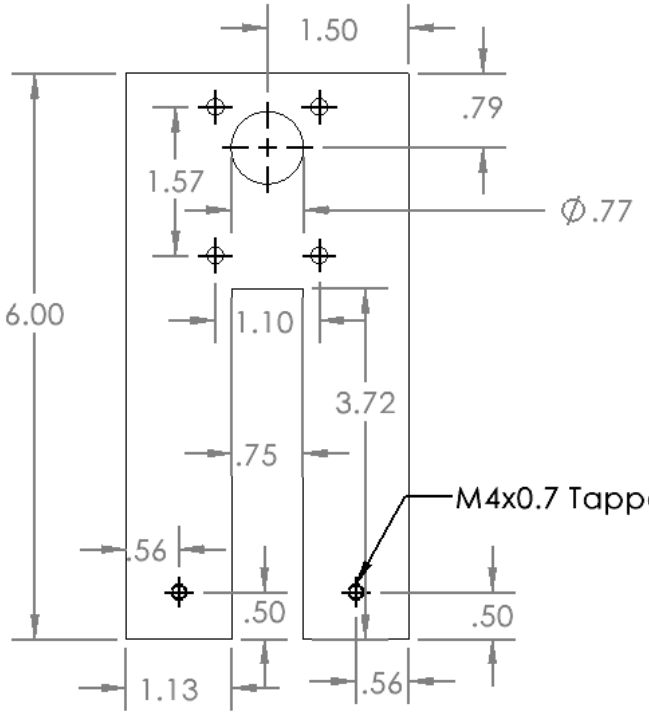

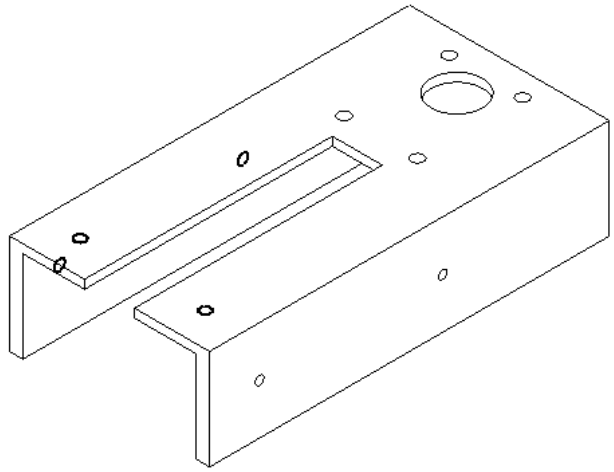

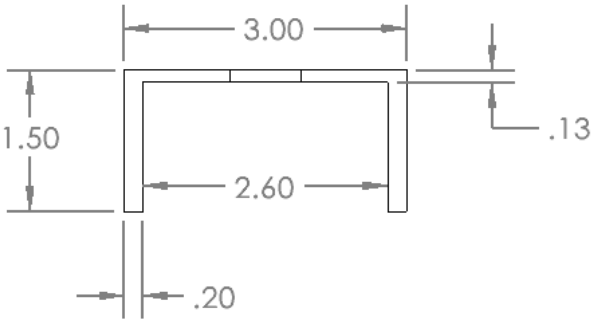

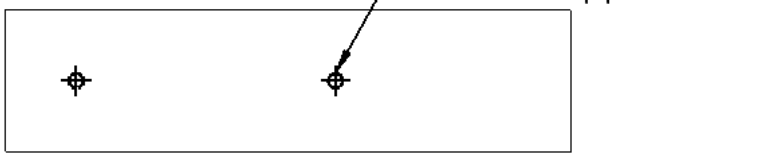

General Tolerances
X.X ± 0.1
X.XX ± 0.03
X° ± 0.5°

UNLESS OTHERWISE SPECIFIED:		NAME	DATE
DIMENSIONS ARE IN INCHES TOLERANCES: FRACTIONAL ± ANGULAR: MACH ± BEND ± TWO PLACE DECIMAL ± THREE PLACE DECIMAL ±	DRAWN		
	CHECKED		
	ENG APPR.		
	MFG APPR.		
MATERIAL	COMMENTS:		
FINISH	WEIGHT:		
DO NOT SCALE DRAWING			

COASTAL CURRENT

TITLE:
Worm Gear Mount

SIZE	DWG. NO.	REV
A	Wave Gate Subassembly - 2	

SCALE: 1:2 SHEET 2 OF 5

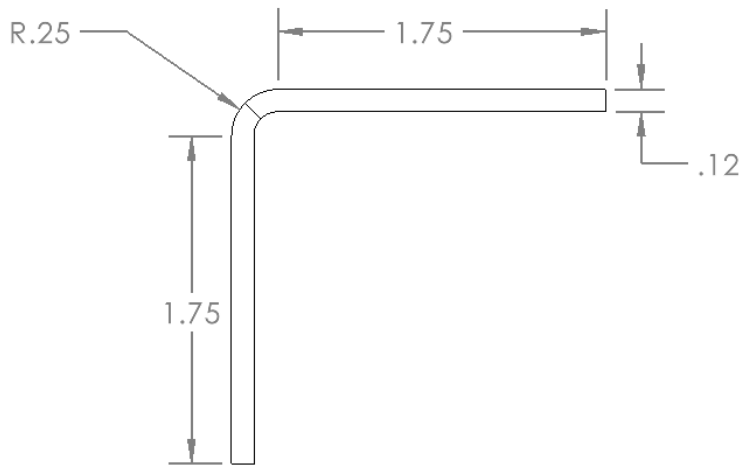

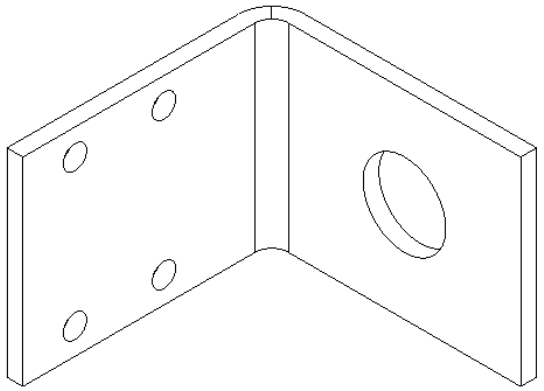

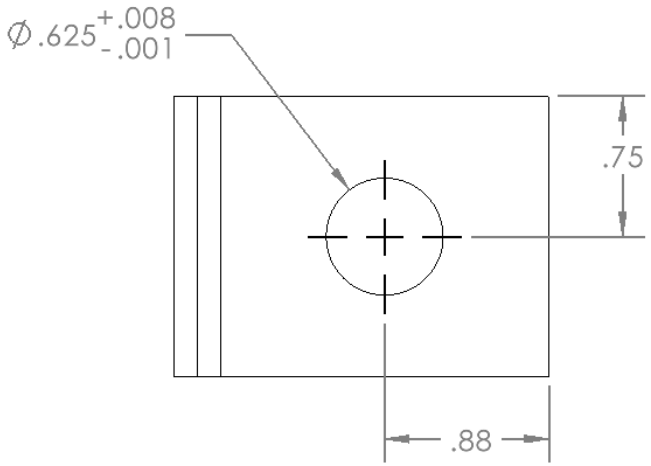

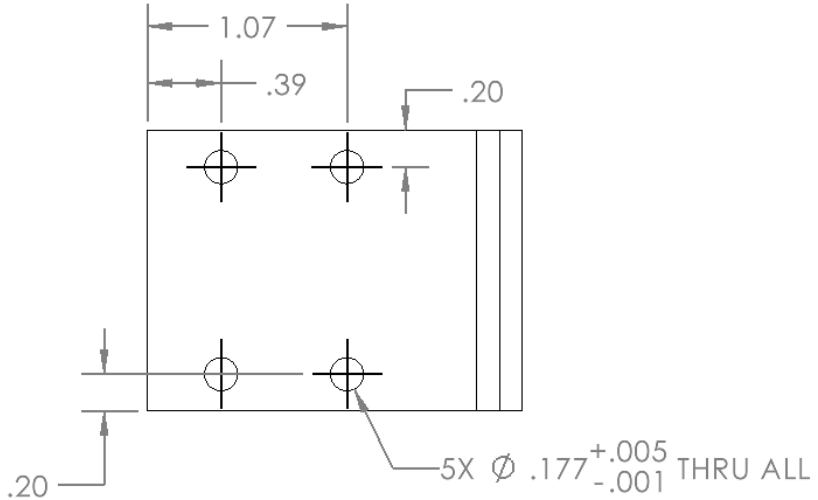

General Tolerances
X.X ± 0.1
X.XX ± 0.03
X° ± 0.5°

UNLESS OTHERWISE SPECIFIED:		NAME	DATE
DIMENSIONS ARE IN INCHES TOLERANCES: FRACTIONAL ± ANGULAR: MACH ± BEND ± TWO PLACE DECIMAL ± THREE PLACE DECIMAL ±	DRAWN		
	CHECKED		
	ENG APPR.		
	MFG APPR.		
MATERIAL	COMMENTS:		
	WEIGHT:		
FINISH			
DO NOT SCALE DRAWING			

COASTAL CURRENT

TITLE: Shaft Bracket

SIZE	DWG. NO.	REV
A	Wave Gate Subassembly - 3	

SCALE: 1:1 SHEET 3 OF 5

ITEM NO.	WELD SIZE	SYMBOL	WELD LENGTH	WELD MATERIAL	QTY.
1	0.03		24.36	AI 4043	1

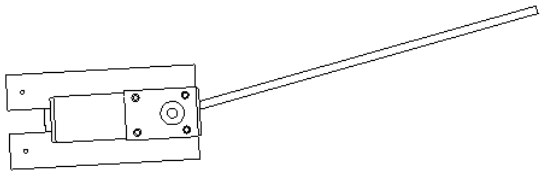

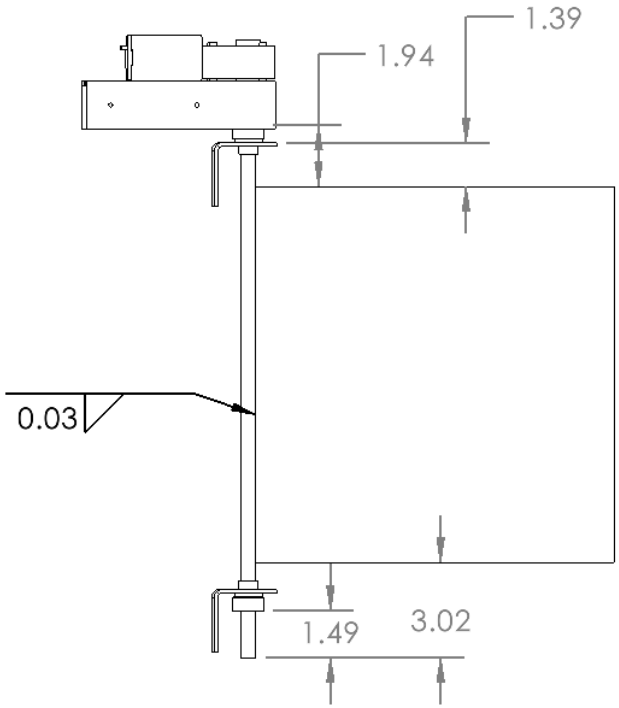

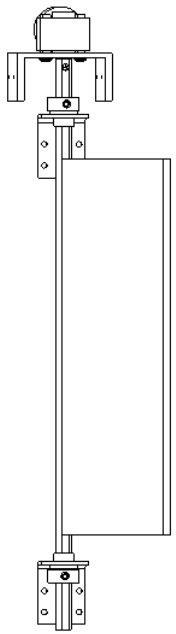

General Tolerances
X.X ± 0.1
X.XX ± 0.03
X° ± 0.5°

		NAME	DATE
UNLESS OTHERWISE SPECIFIED:			
DIMENSIONS ARE IN INCHES TOLERANCES: FRACTIONAL ± ANGULAR: MACH ± BEND ± TWO PLACE DECIMAL ± THREE PLACE DECIMAL ±	DRAWN		
	CHECKED		
	ENG APPR.		
	MFG APPR.		
MATERIAL	COMMENTS:		
FINISH	WEIGHT:		
DO NOT SCALE DRAWING			

COASTAL CURRENT

TITLE:
Wave Gate Assembly

SIZE	DWG. NO.	REV
A	Wave Gate Subassembly - 4	

SCALE: 1:6 | SHEET 4 OF 5

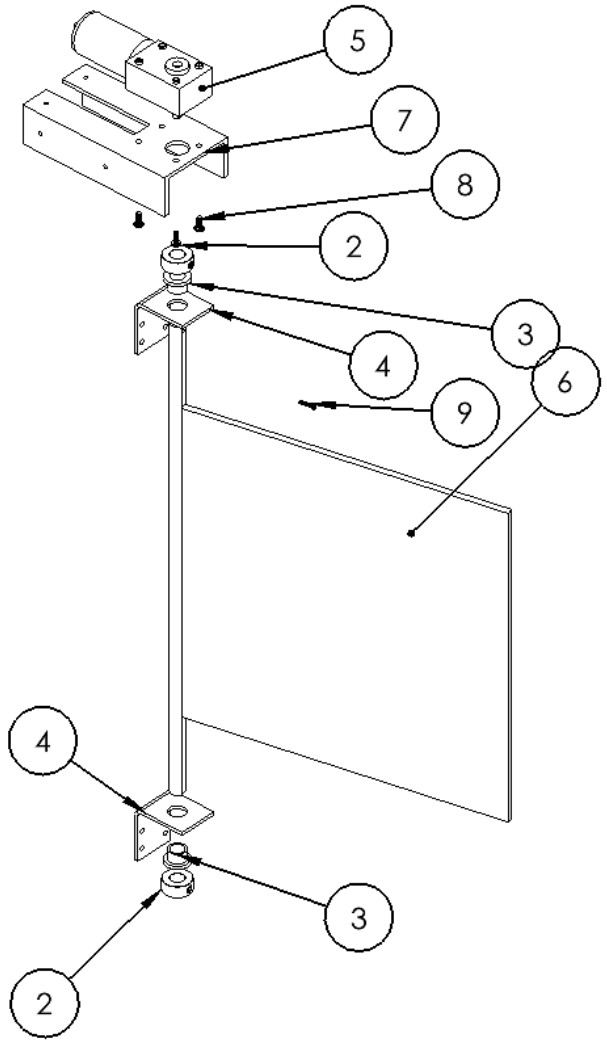

ITEM NO.	PART NUMBER	QTY.
1	Wave Gate Shaft	1
2	Shaft Collar	2
3	Shaft Sleeve Bearing	2
4	Shaft Bracket	2
5	Worm Gear Motor	1
6	Wave Gate Plate	1
7	Worm Gear Mount	1
8	M4 10mm Screw	4
9	4-40 .5in Screw	1

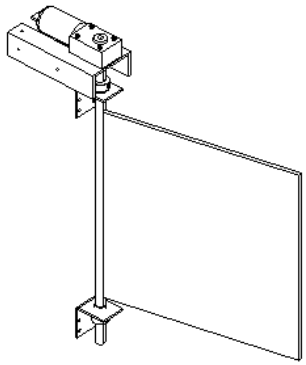

		NAME	DATE
UNLESS OTHERWISE SPECIFIED:	DRAWN		
DIMENSIONS ARE IN INCHES TOLERANCES: FRACTIONAL ± ANGULAR: MACH ± BEND ± TWO PLACE DECIMAL ± THREE PLACE DECIMAL ±	CHECKED		
	ENG APPR.		
	MFG APPR.		
MATERIAL	COMMENTS:		
FINISH	WEIGHT:		
DO NOT SCALE DRAWING			

COASTAL CURRENT

TITLE:
Wave Gate Exploded Views

SIZE	DWG. NO.	REV
A	Wave Gate Subassembly - 5	

SCALE: 1:6 | SHEET 5 OF 5

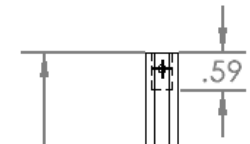

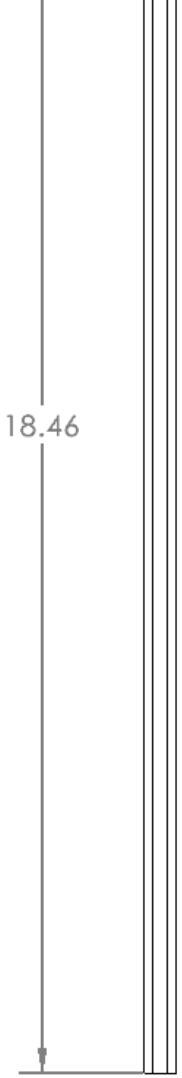

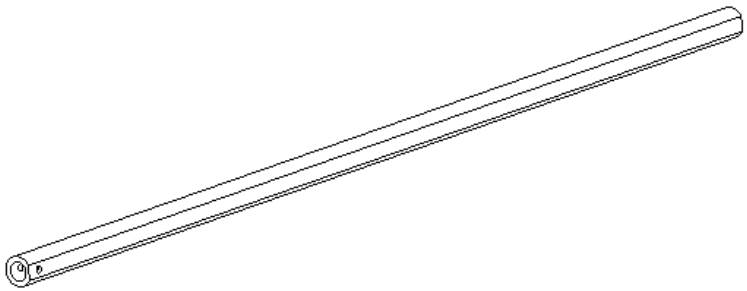

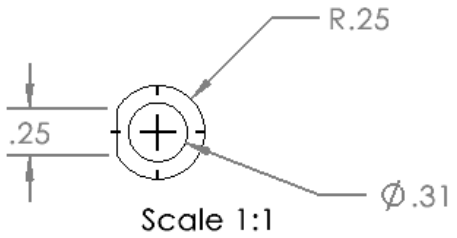

Scale 1:1

General Tolerances
X.X ± 0.1
X.XX ± 0.03
X° ± 0.5°

		NAME	DATE
UNLESS OTHERWISE SPECIFIED:	DRAWN		
DIMENSIONS ARE IN INCHES TOLERANCES: FRACTIONAL ± ANGULAR: MACH ± BEND ± TWO PLACE DECIMAL ± THREE PLACE DECIMAL ±	CHECKED		
	ENG APPR.		
	MFG APPR.		
	COMMENTS:		
MATERIAL 6061 Alloy	WEIGHT:		
FINISH			
DO NOT SCALE DRAWING			

COASTAL CURRENT

TITLE: Deflector Shaft

SIZE	DWG. NO.	REV
A	Wave Deflector Subassembly - 1	

SCALE: 1:3 | SHEET 1 OF 9

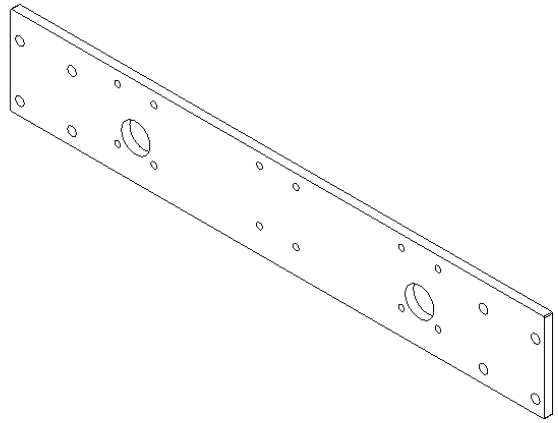

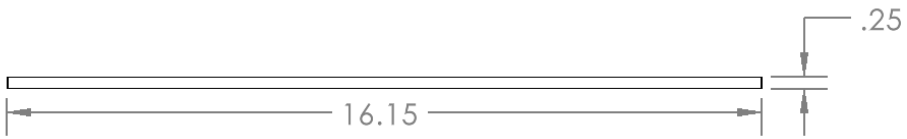

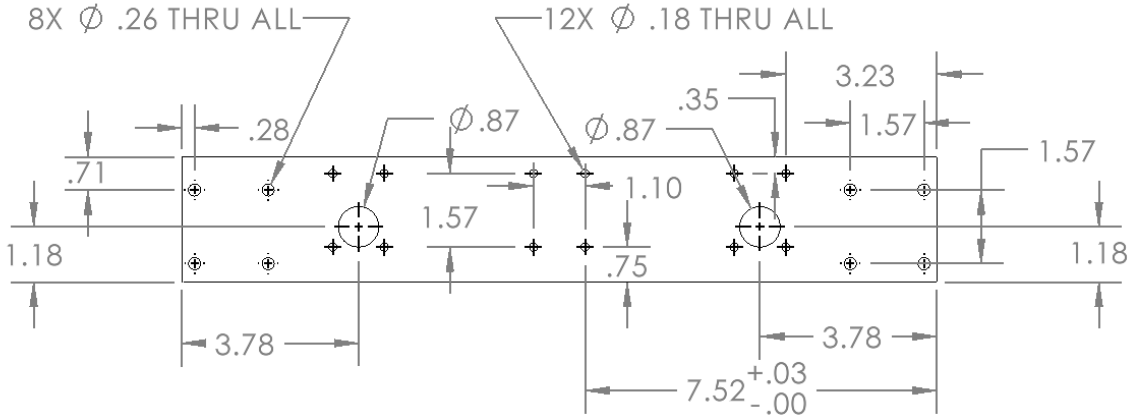

General Tolerances
X.X ± 0.1
X.XX ± 0.03
X° ± 0.5°

UNLESS OTHERWISE SPECIFIED:		NAME	DATE
DIMENSIONS ARE IN INCHES TOLERANCES: FRACTIONAL ± ANGULAR: MACH ± BEND ± TWO PLACE DECIMAL ± THREE PLACE DECIMAL ±	DRAWN		
	CHECKED		
	ENG APPR.		
	MFG APPR.		
MATERIAL 6061 Alloy	COMMENTS:		
FINISH	WEIGHT:		
DO NOT SCALE DRAWING			

COASTAL CURRENT

TITLE:
Deflector Base - Large Horiz

SIZE	DWG. NO.	REV
A	Wave Deflector Subassembly - 2	

SCALE: 1:4 SHEET 2 OF 9

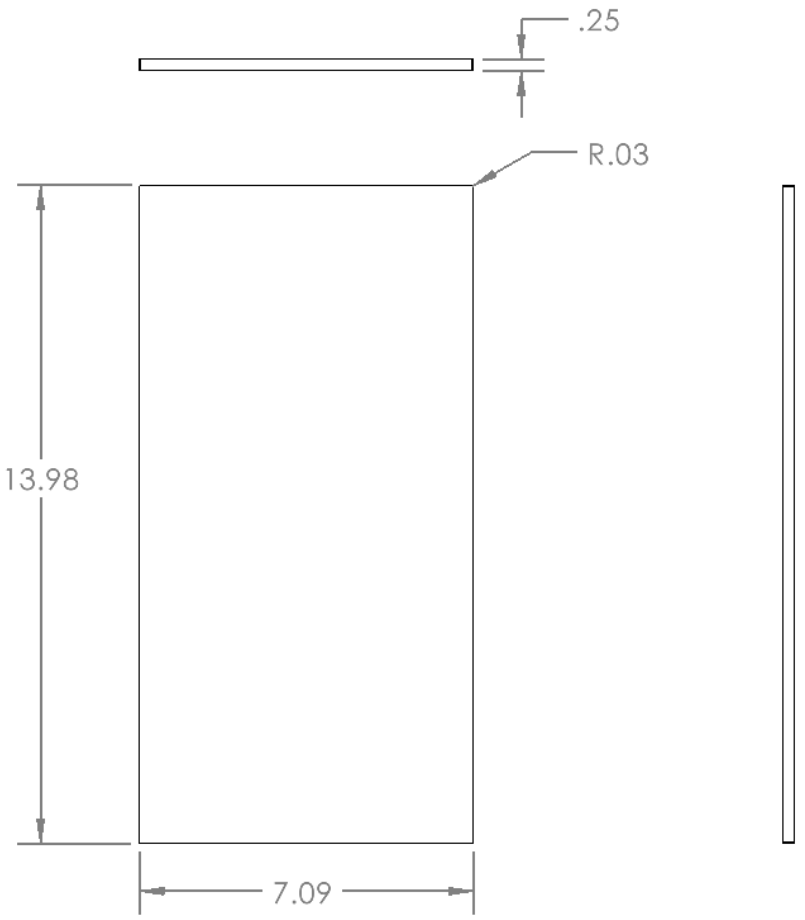

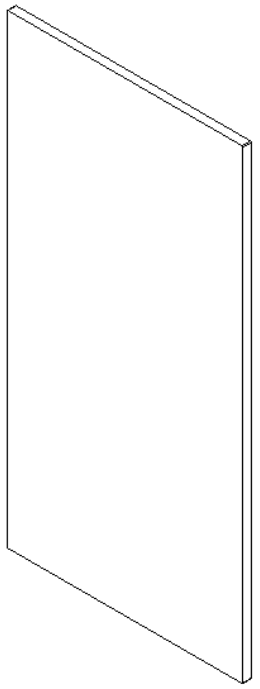

General Tolerances
X.X ± 0.1
X.XX ± 0.03
X° ± 0.5°

		NAME	DATE
UNLESS OTHERWISE SPECIFIED:	DRAWN		
DIMENSIONS ARE IN INCHES TOLERANCES: FRACTIONAL ± ANGULAR: MACH ± BEND ± TWO PLACE DECIMAL ± THREE PLACE DECIMAL ±	CHECKED		
	ENG APPR.		
	MFG APPR.		
MATERIAL 6061 Alloy	COMMENTS:		
FINISH	WEIGHT:		
DO NOT SCALE DRAWING			

COASTAL CURRENT

TITLE: Deflector Base - Tall Vertical

SIZE	DWG. NO.	REV
A	Wave Deflector Subassembly - 3	

SCALE: 1:4 | SHEET 3 OF 9

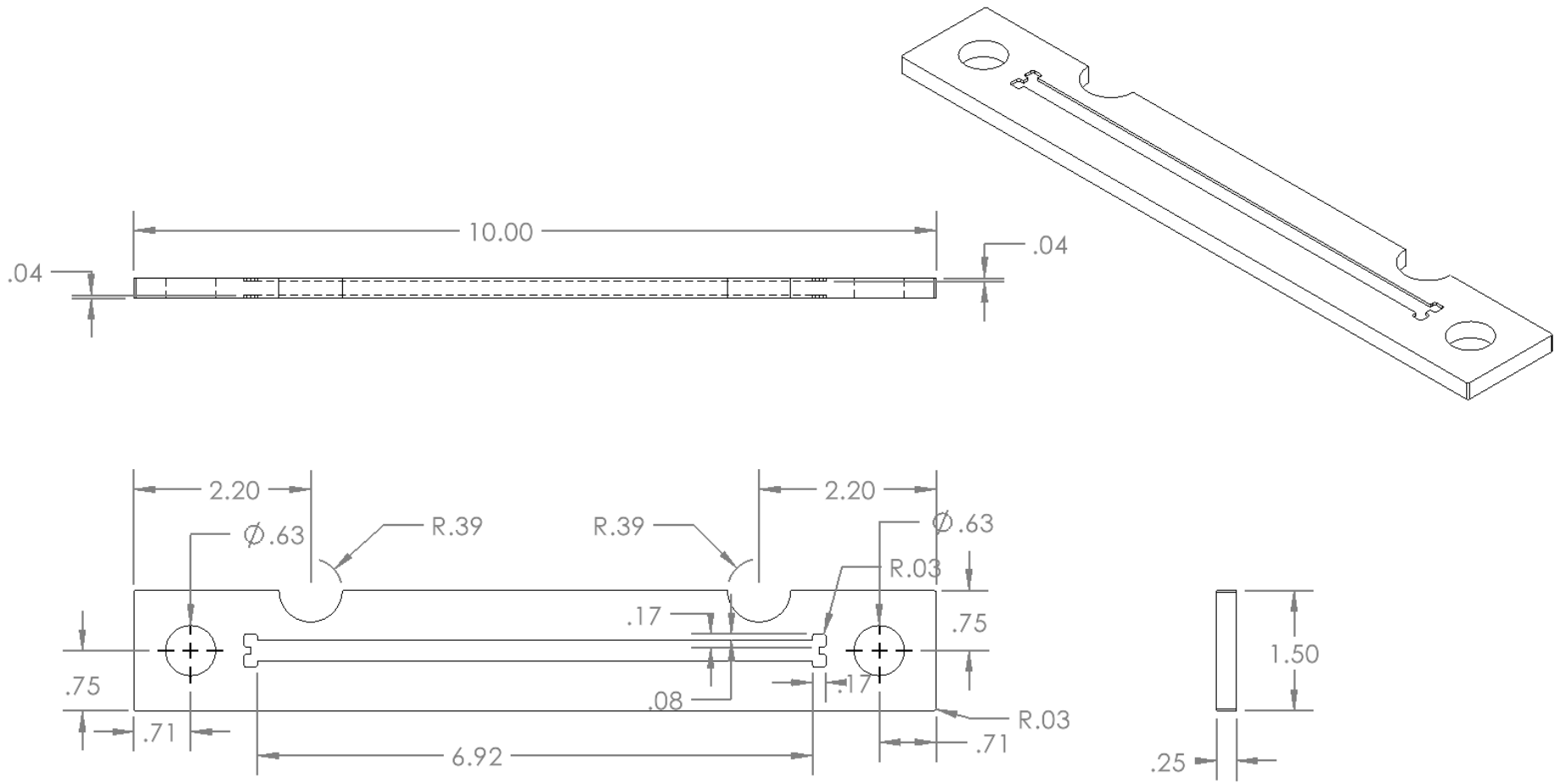

General Tolerances
X.X ± 0.1
X.XX ± 0.03
X° ± 0.5°

		NAME	DATE
UNLESS OTHERWISE SPECIFIED:	DRAWN		
DIMENSIONS ARE IN INCHES TOLERANCES: FRACTIONAL ± ANGULAR: MACH ± BEND ± TWO PLACE DECIMAL ± THREE PLACE DECIMAL ±	CHECKED		
	ENG APPR.		
	MFG APPR.		
	COMMENTS:		
MATERIAL 6061 Alloy	WEIGHT:		
FINISH			
DO NOT SCALE DRAWING			

COASTAL CURRENT

TITLE: Deflector Base - Sm Horiz Top

SIZE	DWG. NO.	REV
A	Wave Deflector Subassembly - 4	

SCALE: 1:2 SHEET 4 OF 9

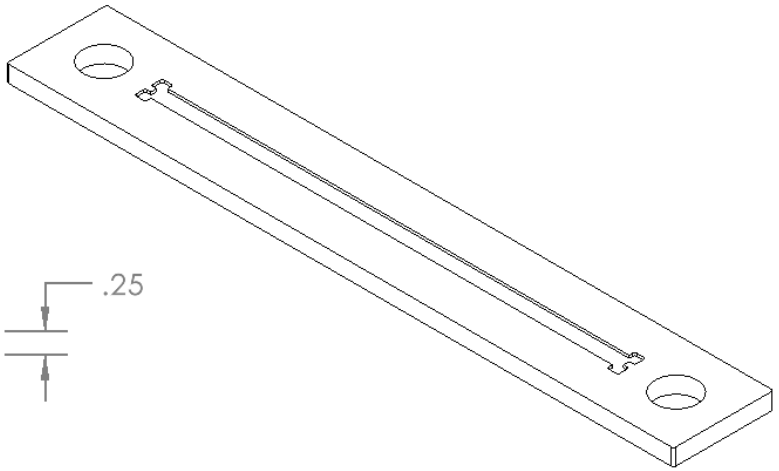

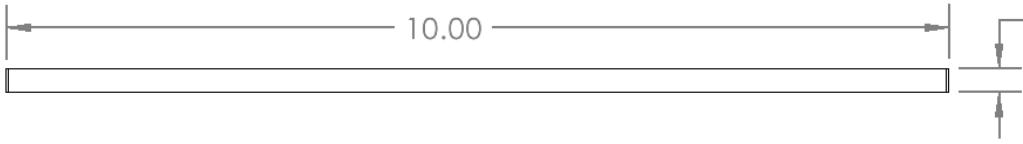

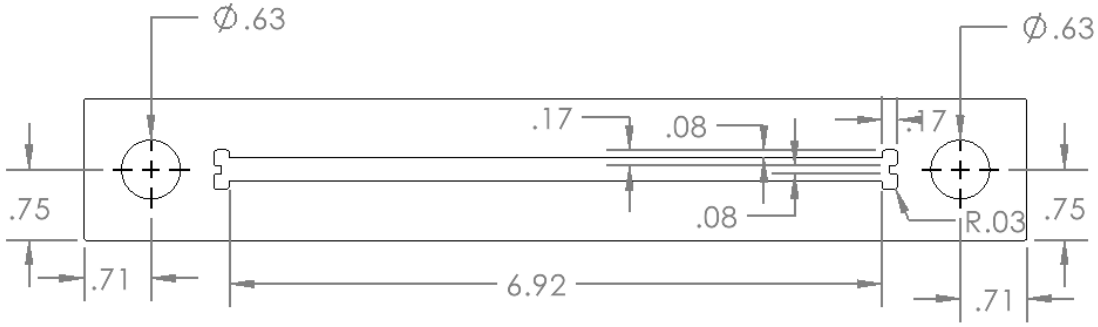

General Tolerances
X.X ± 0.1
X.XX ± 0.03
X° ± 0.5°

UNLESS OTHERWISE SPECIFIED:		NAME	DATE
DIMENSIONS ARE IN INCHES TOLERANCES: FRACTIONAL ± ANGULAR: MACH ± BEND ± TWO PLACE DECIMAL ± THREE PLACE DECIMAL ±	DRAWN		
	CHECKED		
	ENG APPR.		
	MFG APPR.		
MATERIAL 6061 Alloy	COMMENTS: WEIGHT:		
FINISH			
DO NOT SCALE DRAWING			

COASTAL CURRENT

TITLE: Deflector Base - Sm Horiz Bot

SIZE	DWG. NO.	REV
A	Wave Deflector Subassembly - 5	

SCALE: 1:2 | SHEET 5 OF 9

ITEM NO.	PART NUMBER	QTY.
1	Deflector Base - Large Horizontal	1
2	Deflector Base - Short Vertical	1
3	Deflector Base - Tall Vertical	1
4	Deflector Base - Small Horizontal Top	1
5	Deflector Base - Small Horizontal Bottom	1

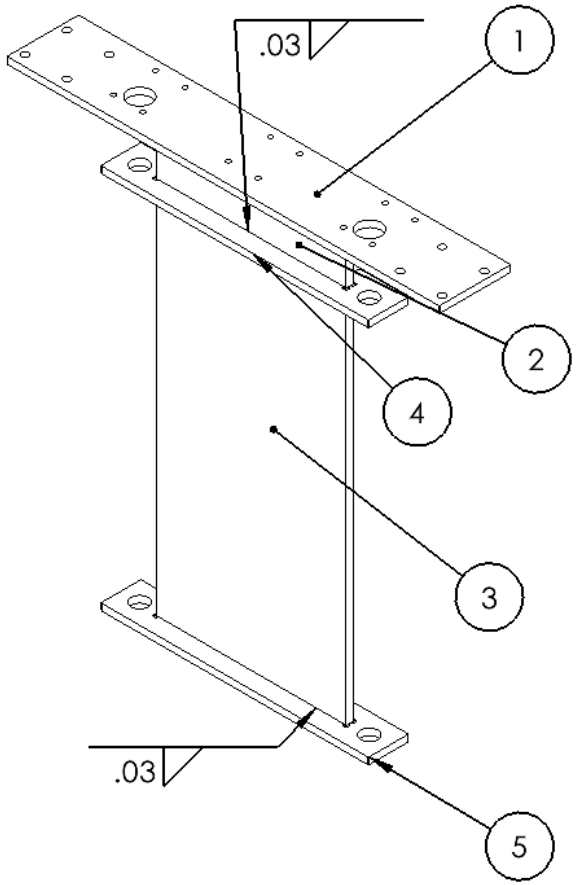

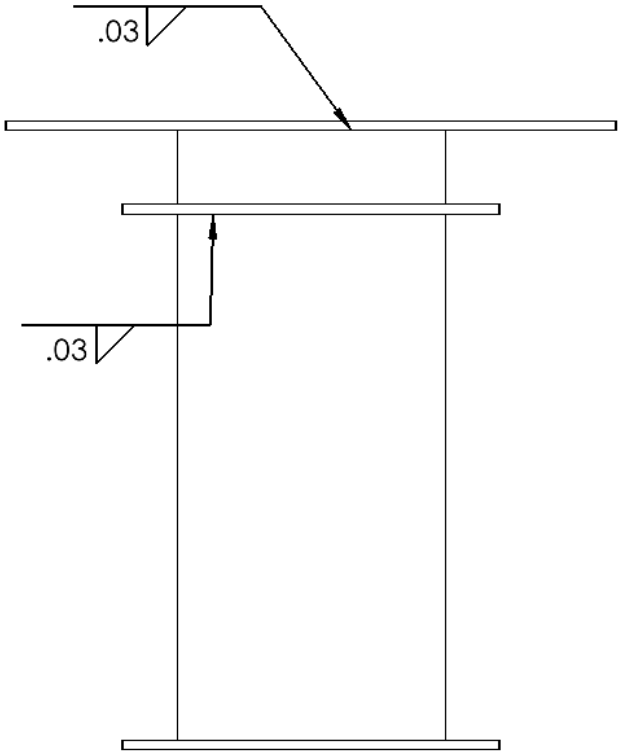

		NAME	DATE
UNLESS OTHERWISE SPECIFIED:	DRAWN		
DIMENSIONS ARE IN INCHES TOLERANCES: FRACTIONAL ± ANGULAR: MACH ± BEND ± TWO PLACE DECIMAL ± THREE PLACE DECIMAL ±	CHECKED		
	ENG APPR.		
	MFG APPR.		
	COMMENTS:		
MATERIAL	WEIGHT:		
FINISH			
DO NOT SCALE DRAWING			

COASTAL CURRENT

TITLE:
Deflector Base Welds

SIZE	DWG. NO.	REV
A	Wave Deflector Subassembly - 6	

SCALE: 1:5 | SHEET 6 OF 9

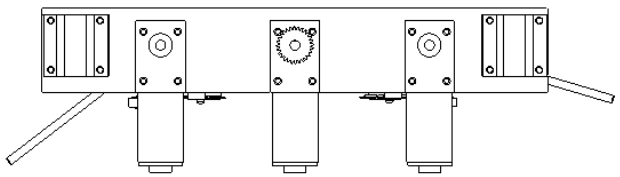

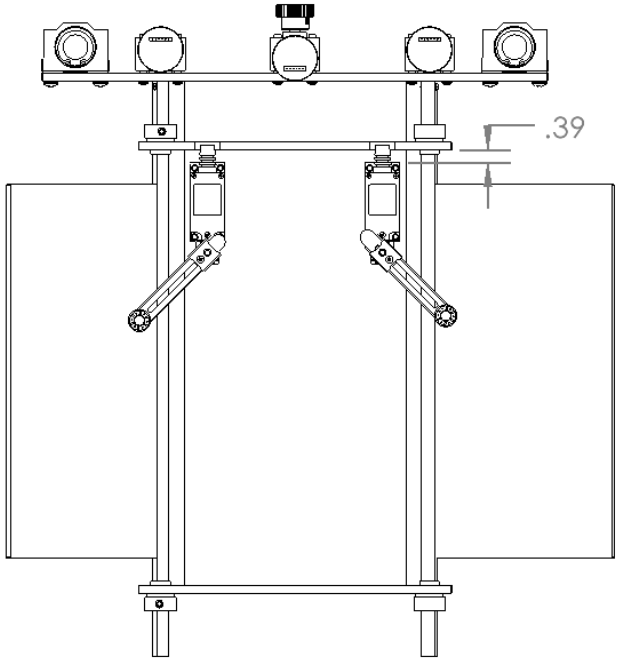

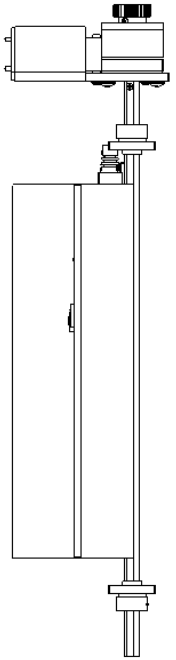

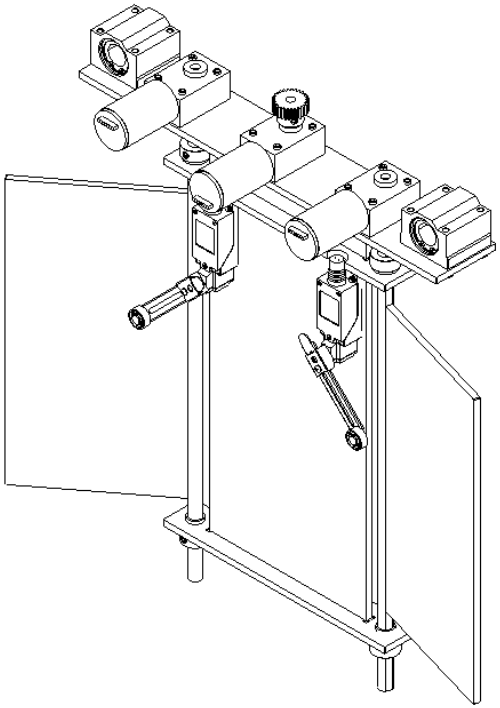

UNLESS OTHERWISE SPECIFIED:		NAME	DATE
DIMENSIONS ARE IN INCHES TOLERANCES: FRACTIONAL ± ANGULAR: MACH ± BEND ± TWO PLACE DECIMAL ± THREE PLACE DECIMAL ±	DRAWN		
	CHECKED		
	ENG APPR.		
	MFG APPR.		
MATERIAL	COMMENTS:		
	WEIGHT:		
FINISH			
DO NOT SCALE DRAWING			

COASTAL CURRENT

TITLE: Deflector Side

SIZE	DWG. NO.	REV
A	Wave Deflector Subassembly - 7	

SCALE: 1:6 SHEET 7 OF 9

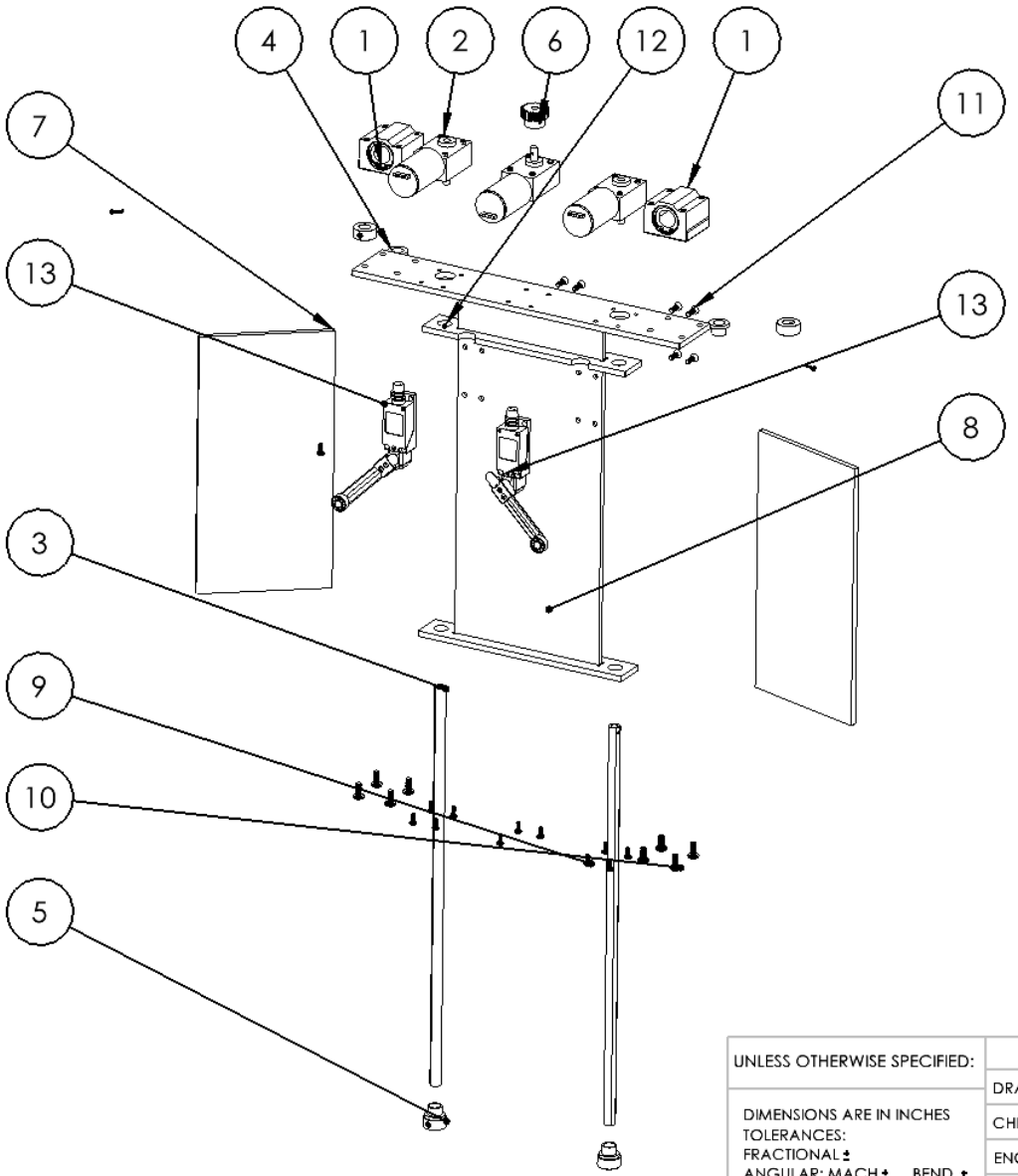

ITEM NO.	PART NUMBER	QTY.
1	LHBB20H	2
2	Worm Gear Motor	3
3	Deflector Shaft	2
4	3083K14	4
5	60475K72	4
6	2662N424	1
7	Deflector Plate	2
8	Deflector Base	1
9	90116A207	12
10	92000A210	8
11	92010A326	8
12	91772A110	3
13	Limit switch ME-8108	2

		NAME	DATE
UNLESS OTHERWISE SPECIFIED:			
DIMENSIONS ARE IN INCHES TOLERANCES: FRACTIONAL ± ANGULAR: MACH ± BEND ± TWO PLACE DECIMAL ± THREE PLACE DECIMAL ±	DRAWN		
	CHECKED		
	ENG APPR.		
	MFG APPR.		
	COMMENTS:		
MATERIAL	WEIGHT:		
FINISH			
DO NOT SCALE DRAWING			

COASTAL CURRENT

TITLE:

Deflector Side Exploded

SIZE	DWG. NO.	REV
A	Wave Deflector Subassembly - 8	

SCALE: 1:8 | SHEET 8 OF 9

ITEM NO.	PART NUMBER	QTY.
1	SHA2030	6
2	Wave Deflector Support Shaft	2
3	2662N57	2
4	91772A110	4
5	6063K19	2
6	Wave Deflector Side	2

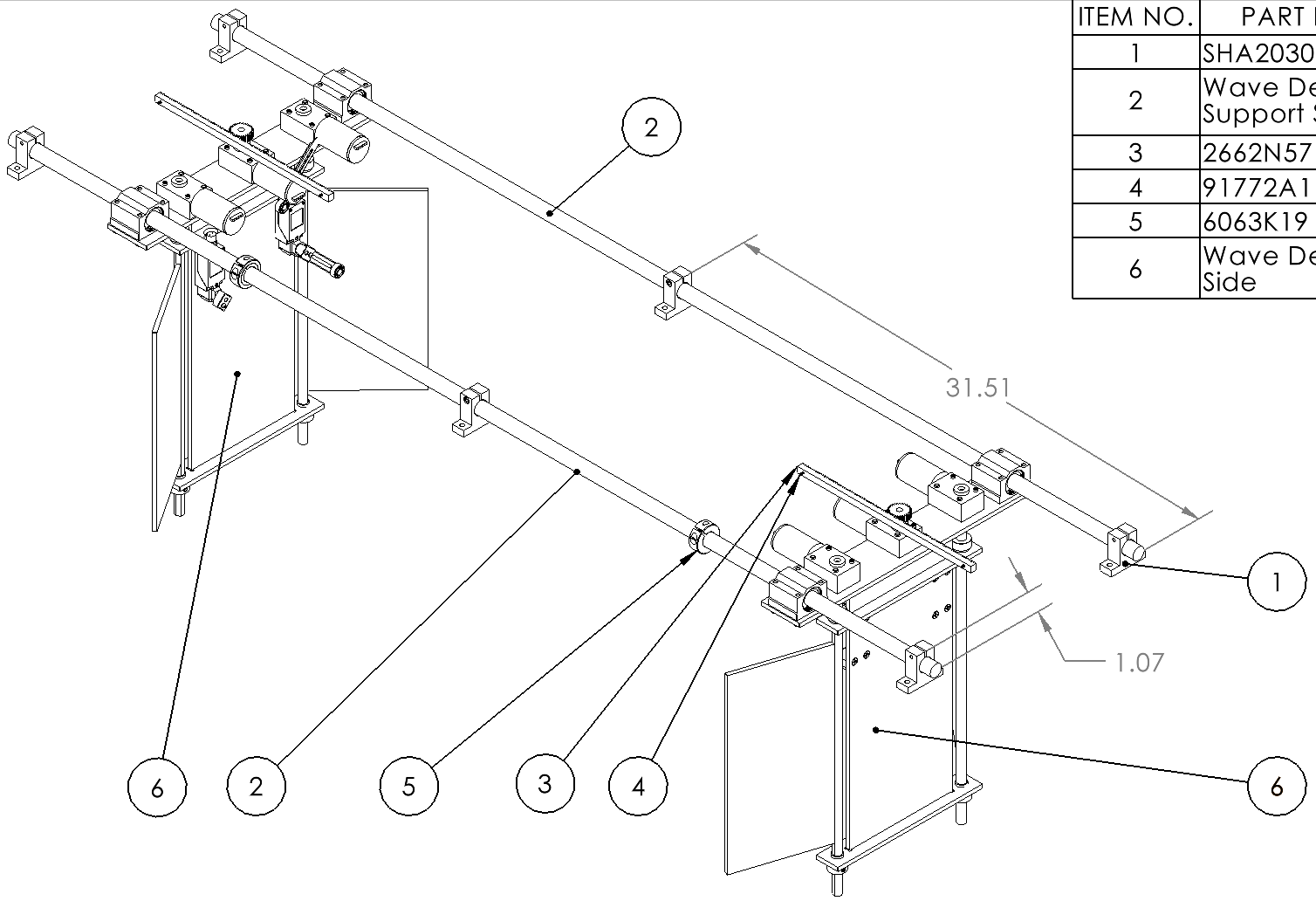

		NAME	DATE
UNLESS OTHERWISE SPECIFIED:	DRAWN		
DIMENSIONS ARE IN INCHES TOLERANCES: FRACTIONAL ± ANGULAR: MACH ± BEND ± TWO PLACE DECIMAL ± THREE PLACE DECIMAL ±	CHECKED		
	ENG APPR.		
	MFG APPR.		
MATERIAL	COMMENTS:		
FINISH	WEIGHT:		
DO NOT SCALE DRAWING			

COASTAL CURRENT

TITLE:
Deflector Assembly

SIZE	DWG. NO.	REV
A	Wave Deflector Subassembly - 9	

SCALE: 1:8 SHEET 9 OF 9

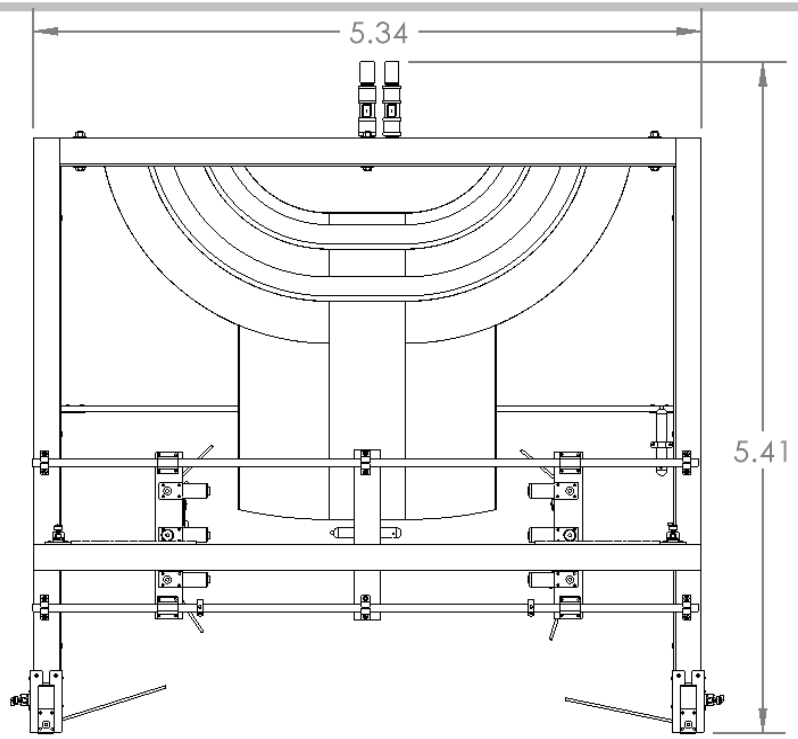

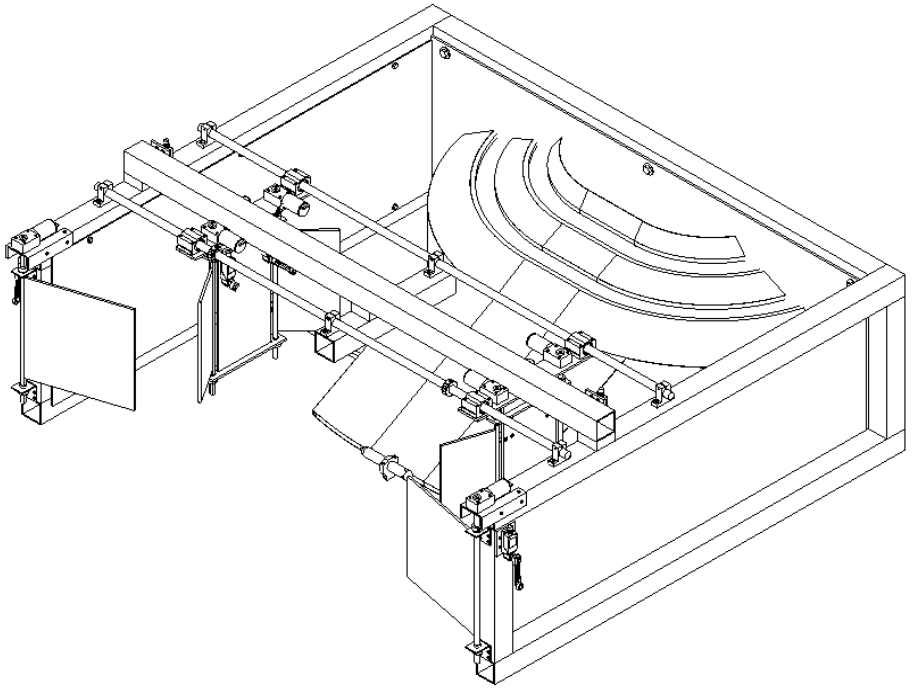

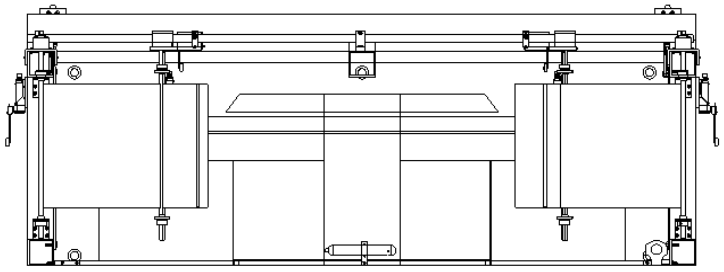

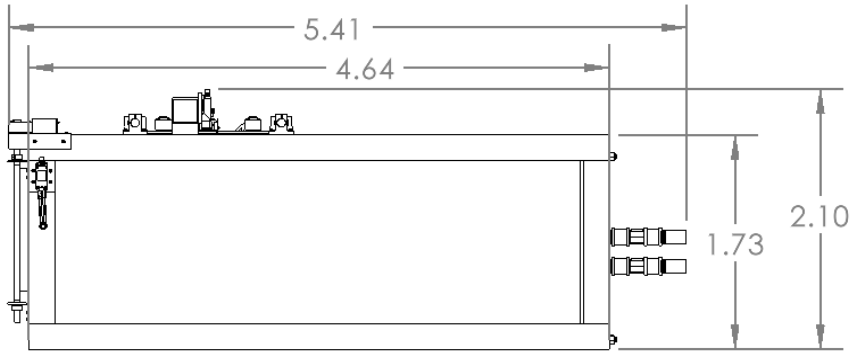

UNLESS OTHERWISE SPECIFIED:		NAME	DATE
DIMENSIONS ARE IN INCHES TOLERANCES: FRACTIONAL ± ANGULAR: MACH ± BEND ± TWO PLACE DECIMAL ± THREE PLACE DECIMAL ±	DRAWN		
	CHECKED		
	ENG APPR.		
	MFG APPR.		
MATERIAL	COMMENTS:		
FINISH	WEIGHT:		
DO NOT SCALE DRAWING			

COASTAL CURRENT

TITLE: Final Assembly

SIZE	DWG. NO.	REV
A	Full Assembly - 1	

SCALE: 1:18 | SHEET 1 OF 1

Appendix L: Validation Plan & Results

The main focus for validation of Coastal Current's design is the effects of constructive interference of waves in an overtopping WEC. The success of the virtual prototype was validated using engineering analysis (Appendix H) and mechanical CAE (Appendix I.) However, the virtual prototype contains various components for future validation if the physical test rig is built. A physical prototype will be partially evaluated based on how much water it collects in its reservoirs. To measure this, a flow sensor connected to a myRio is employed in each of the two reservoirs for data acquisition. Additionally, two pressure sensors mounted to the front of the overtopping device and to the side of the frame measure the wave parameters of the incoming waves and waves through the channels. The measurements taken from these sensors will guide the engineers in determining the optimal geometry of the wave deflectors and gates. To measure the positions of the deflectors and the gates for use in the control system, a total of eight encoders will be employed. Two of these will measure linear position and the remaining six will measure angular position.

Two different types of sensors are employed to measure the results of the analysis. Flow sensors on each reservoir will measure the amount of water that moves through the overtopping device. This is the most important performance metric because the volume of collected water directly correlates with the amount of electricity generated by a real overtopping device. There will also be pressure sensors mounted at the bottom of the ramp and in a wave channel. These will measure wave height so researchers can better understand if and where wave interference is occurring.

The flow and pressure sensors operate differently. The flow sensors output a range of voltages depending on their readings. These voltages are read by the myRio controller and interpreted as flow or pressure values. The pressure sensors output a range of currents depending on the depth of the water. These must be read by the 4-20mA receiver before being fed as voltage values into the myRio. Both types of sensors must be calibrated to ensure that the voltage readings reflect the correct physical values – this is done in the controller.

Table 22: Sensor Specifications

Liquid Level Sensor Specifications	
Measurement Range (ft)	0-3
Accuracy (%FSD)	±0.25%
Temperature Range (°F)	-10 to 175
DC Input Voltage	10-35
Output Current (mA)	4-20
Flow Sensor Specifications	
Measurement Range (L/min)	2-50
Accuracy (%FSD)	±3%
DC Input Voltage	5-15

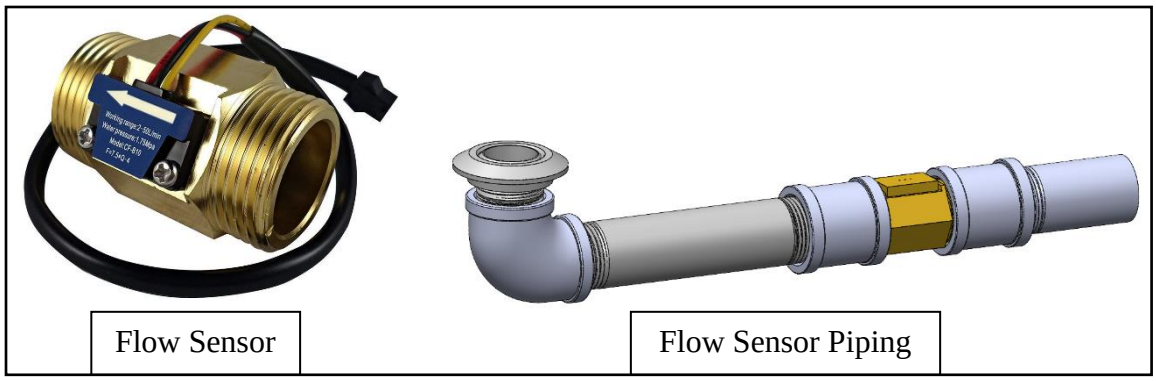

Figure 98: Flow Sensor

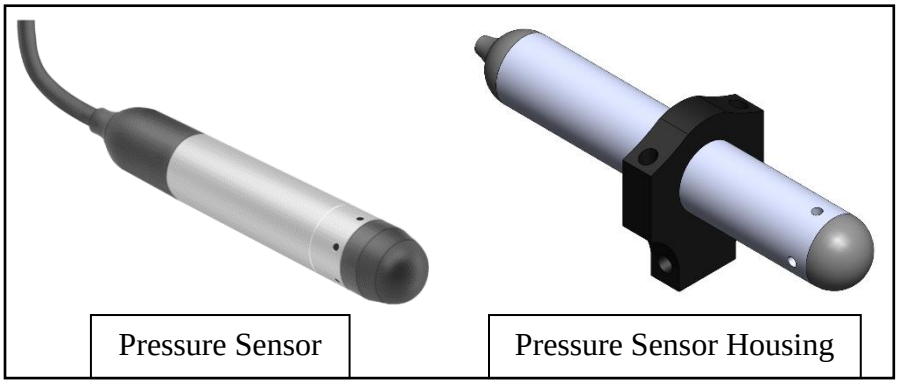

Figure 99: Pressure Sensor

The ideal testing location is the Lyles Burke Lab Wave Pool at Purdue. This is a well-established wave pool commonly used for research. Since gaining access to the wave pool is difficult and a physical prototype was not built this semester, a mid-fidelity prototype utilizing a bathtub as a rough wave pool was used to demonstrate the function of the design and the constructive interference principle.

The mid-fidelity prototype (Figure 100) is based around a 1:90 scale model of the full-size overtopping device so that it fits in a bathtub. The wave-producing mechanism hinges from the bottom so that it produces waves mostly on the surface of the water. The entire structure of the prototype is built of epoxy-coated plywood fastened with screws. The “overtopping device” is a plastic dog cone that was cut to fit against the bathtub. Waterproof tape was used to hold the cone in place and to seal the sides of the wave gates against the bathtub. Finally, stones were used to make sure the wooden prototype did not float.

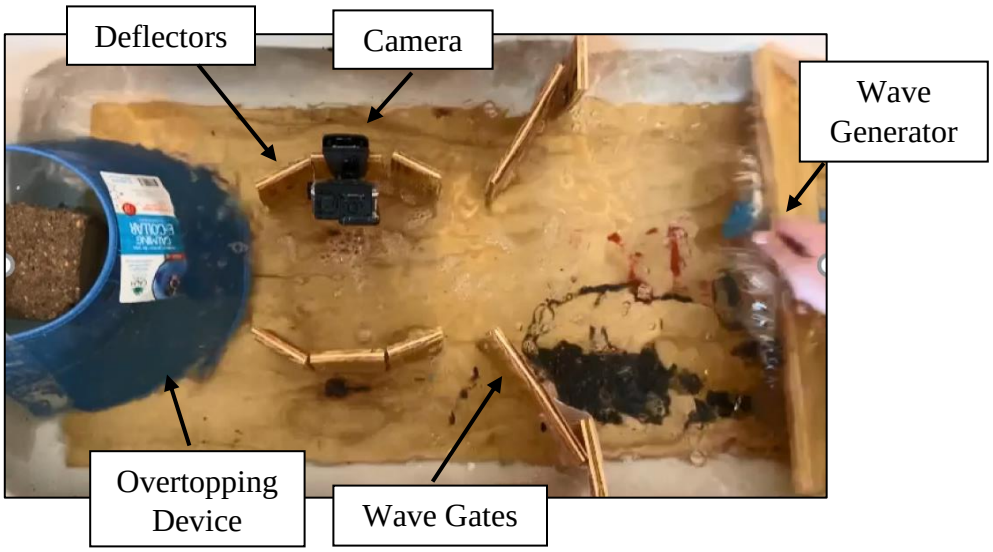

Figure 100: Mid-Fidelity Prototype

Appendix M: What was learned from the prototypes and validation

Low-fidelity Prototype

Through creation of the low-fidelity prototype, various lessons were learned and important observations were made. First, the size of the overtopping device, and therefore the presented constructive interference design additions, are highly dependent on the wave properties at the device location. Specifically, the wave height and tide climate heavily determine the number and size of reservoirs, and the water depth heavily influences the construction method and overall size (Vicinanza, 2012). Wave types also vary between location due to the shoreline's shape, see figure 29. Certain aspects and dimensions of the device will also be greatly affected by the wave type. Based on this, an important next step in the project is to determine a specific location to place the device to know the wave and tide climate. Further design developments will be based around this chosen location and its wave and tide climates to ensure optimal geometry and device efficiency.

From the analysis of the prototype, it became clear that the internal corner between the gate and channel wall would be critical for determining the direction of the reflected waves. The pieces circled in red in the figure below shows a proposed corner design to better direct reflected waves.

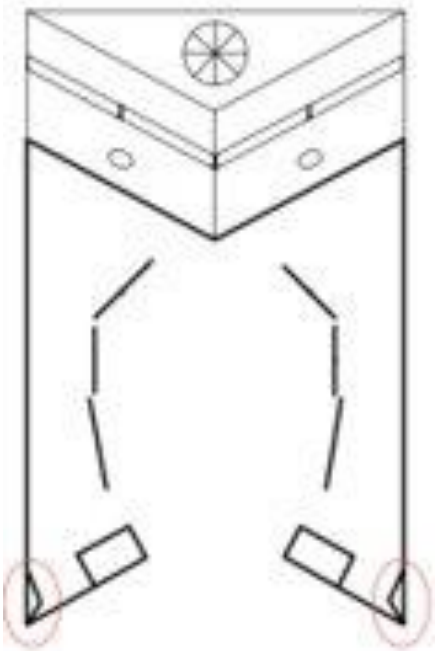

Figure 101: Proposed Corner Design

The prototype also allowed us to better envision gaps and fits for the wave deflectors and potential locations and positioning for servo motors to actuate the wave gates and ramps. These will be implemented in future design iterations.

Figure 102: Low-Fidelity Prototype

Mid-Fidelity Prototype

The mid-fidelity prototype required precise determination of physical dimensions, materials, and manufacturing techniques. The form and function of the final prototype is now easily understood. The budget of $1,000 was exceeded. However, since this prototype is being marketed towards research teams, the hope is that enough money to construct the prototype will be available through other means. Still, measures have been and will be taken to reduce costs. One area could be the wave deflectors – a slight redesign could allow for one actuator to be used instead of two. The $200 flowmeters specified initially were replaced with similar $20 models. The prototype design will continue to be refined leading up to the final design report.

High-Fidelity Prototype and Testing

The high-fidelity prototype incorporated several refinements and small design iterations over the mid-fidelity prototype. To make the prototype more attractive to potential adopters, pressure sensors were added to measure wave height in strategic locations. Costs were cut by removing the linear actuators in lieu of a cheaper rack-and-pinion setup to move the wave deflectors. While the prototype is projected to greatly exceed the team's budget, its ~$5500 cost is well within reach of a researcher at Purdue. Hopefully, someone with interest in wave mechanics and renewable energy will take interest in the idea of an enhanced overtopping device and develop the idea further.

Appendix N: List of Standards Referenced

Running and Sliding Limits and Fits For Cylindrical Parts [(ANSI B4.1-1967,R1987)]

		VALUES SHOWN BELOW ARE IN THOUSANDTHS OF AN INCHES											
Nominal (Basic) Size Ranges (Inches)		Class RC1			Class RC2			Class RC3			Class RC4		
		Clearance Limits	Standard Tolerance Limits		Clearance Limits	Standard Tolerance Limits		Clearance Limits	Standard Tolerance Limits		Clearance Limits	Standard Tolerance Limits	
Over	To		Hole H5	Shaft g4		Hole H6	Shaft g5		Hole H7	Shaft f6		Hole H8	Shaft f7
0	0.12	0.1 0.45	+0.2 0	-0.1 -0.25	0.1 0.55	+0.25 0	-0.1 -0.3	0.3 0.95	+0.4 0	-0.3 -0.55	0.3 1.3	+0.6 0	-0.3 -0.7
0.12	0.40	0.15 0.5	+0.2 0	-0.15 -0.3	0.15 0.65	+0.3 0	-0.15 -0.35	0.4 1.12	+0.5 0	-0.4 -0.7	0.4 1.6	+0.7 0	-0.4 -0.9
0.24	0.40	0.2 0.6	+0.25 0	-0.2 -0.35	0.2 0.85	+0.4 0	-0.2 -0.45	0.5 1.5	+0.6 0	-0.5 -0.9	0.5 2.0	+0.9 0	-0.5 -1.1
0.40	0.71	0.25 0.75	+0.3 0	-0.25 -0.45	0.25 0.95	+0.4 0	-0.25 -0.55	0.6 1.7	+0.7 0	-0.6 -1.0	0.6 2.3	+1.0 0	-0.6 -1.3
0.71	1.19	0.3 0.95	+0.4 0	-0.3 -0.55	0.3 1.2	+0.5 0	-0.3 -0.7	0.8 2.1	+0.8 0	-0.8 -1.3	0.8 2.8	+0.2 0	-0.8 -1.6
1.19	1.97	0.4 1.1	+0.4 0	-0.4 -0.7	0.4 1.4	+0.6 0	-0.4 -0.8	1.0 2.6	+1.0 0	-1.0 -1.6	1.0 3.6	+1.6 0	-1.0 -2.0
1.97	3.15	0.4 0.2	+0.5 0	-0.4 -0.7	0.4 1.6	+0.7 0	-0.4 -0.9	1.2 3.1	+1.2 0	-1.2 -1.9	1.2 4.2	+1.8 0	-1.2 -2.4
3.15	4.73	0.5 1.5	+0.6 0	-0.5 -0.9	0.5 2.0	+0.9 0	-0.5 -1.1	1.4 3.7	+1.4 0	-1.4 -2.3	1.4 5.0	+2.2 0	-1.4 -2.8
4.73	7.09	0.6 1.8	+0.7 0	-0.6 -1.1	0.6 2.3	+1.0 0	-0.6 -1.3	1.6 4.2	+1.6 0	-1.6 -2.6	1.6 5.7	+2.5 0	-1.6 -3.2
7.09	9.85	0.6 2.0	+0.8 0	-0.6 -1.2	0.6 2.6	+1.2 0	-0.6 -1.4	2.0 5.0	+1.8 0	-2.0 -3.2	2.0 6.6	+2.8 0	-2.0 -3.8
9.85	12.41	0.8 2.3	+0.9 0	-0.8 -1.4	0.8 2.9	+1.2 0	-0.8 -1.7	2.5 5.7	+2.0 0	-2.5 -3.7	2.5 7.5	+3.0 0	-2.5 -4.5
12.41	15.75	1.0 2.7	+1.0 0	-1.0 -1.7	1.0 3.4	+1.4 0	-1.0 -2.0	3.0 6.6	+2.2 0	-3.0 -4.4	3.0 8.7	+3.5 0	-3.0 -5.2
15.75	19.69	1.2 3.0	+1.0 0	-1.2 -2.0	1.2 3.8	+1.6 0	-1.2 -2.2	4.0 8.1	+2.5 0	-4.0 -5.6	4.0 10.5	+4.0 0	-4.0 -6.5

Figure 103: Fits and Tolerances for Cylindrical Parts

Locational Clearance Limits and Fits For Cylindrical Parts [(ANSI B4.1-1967,R1987)][Table LC1-LC5]

		VALUES SHOWN BELOW ARE IN THOUSANDTHS OF AN INCHES																	
Nominal (Basic) Size Ranges (Inches)		Class LC6			Class LC7			Class LC8			Class LC9			Class LC10			Class LC11		
		Clearance	Standard Tolerance Limits		Clearance	Standard Tolerance Limits		Clearance	Standard Tolerance Limits		Clearance	Standard Tolerance Limits		Clearance	Standard Tolerance Limits		Clearance	Standard Tolerance Limits	
Over	To	Limits	Hole H9	Shaft f8	Limits	Hole H10	Shaft e9	Limits	Hole H10	Shaft d9	Limits	Hole H11	Shaft c10	Limits	Hole H12	Shaft	Limits	Hole H13	Shaft
0	0.12	0. 1.9	+1.0 0	-0.3 -0.9	0.6 3.2	+1.6 0	-0.6 -1.6	1.0 2.0	+1.6 0	-1.0 -2.0	2.5 6.6	+2.5 0	-2.5 -4.1	4 12	+4 0	-4 -8	5 17	+6 0	-5 -11
0.12	0.24	0.4 2.3	+1.2 0	-0.4 -1.1	0.8 3.8	+1.8 0	-0.8 -2.0	1.2 4.2	+1.8 0	-1.2 -2.4	2.8 7.6	+3.0 0	-2.8 -4.6	4.5 14.5	+5 0	-4.5 -9.5	6 20	+7 0	-6 -13
0.24	0.40	0.5 2.8	+1.4 0	-0.5 -1.4	1.0 4.6	+2.2 0	-1.0 -2.4	1.6 5.2	+2.2 0	-1.6 -3.0	3.0 8.7	+3.5 0	-3.0 -5.2	5 17	+6 0	-5 -11	7 25	+9 0	-7 -16
0.40	0.71	0.6 3.2	+1.6 0	-0.6 -1.6	1.2 5.6	+2.8 0	-1.2 -2.8	2.0 6.4	+2.8 0	-2.0 -3.6	3.5 10.3	+4.0 0	-3.5 -6.3	6 20	+7 0	-6 -13	8 28	+10 0	-8 -18
0.71	1.19	0.8 4.0	+2.0 0	-0.8 -2.0	1.6 7.1	+3.5 0	-1.6 -3.6	2.5 8.0	+3.5 0	-2.5 -4.5	4.5 13.	+5.0 0	-4.5 -8.0	7 23	+8 0	-7 -15	10 34	+12 0	-10 -22
1.19	1.97	1.0 5.1	+2.5 0	-1.0 -2.6	2.0 8.5	+4.0 0	-2.0 -4.5	3.6 9.5	+4.0 0	-3.0 -5.5	5.0 15.0	+6.0 0	-5.0 -9.0	8 28	+10 0	-8 -18	12 44	+16 0	-12 -28
1.97	3.15	1.2 6.0	+3.0 0	-1.0 -3.0	2.5 10.0	+4.5 0	-2.5 -5.5	4.0 11.5	+4.5 0	-4.0 -7.0	6.0 17.5	+7 0	-6 -10.5	10 34	+12 0	-10 -22	14 50	+18 0	-14 -32
3.15	4.73	1.4 7.1	+3.5 0	-1.4 -3.6	3.0 11.5	+5.0 0	-3.0 -6.5	5.0 13.5	-5.0 0	-5.0 -8.5	7 21	+9 0	-7 -12	11 39	+14. 0	-11 -25	16 60	+22 0	-16 -38
4.73	7.09	1.6 8.1	+4.0 0	-1.6 -4.1	3.5 13.5	+6.0 0	-3.0 -7.5	6 16	+6 0	-6 -10	8 24	+10 0	-8 -14	12 44	+16 0	-12 -28	18 68	+25 0	-18 -43
7.09	9.85	2.0 9.3	+4.5 0	-2.0 -4.8	4.0 15.5	+7 0	-4.0 -8.5	7 18.5	+7 0	-7 -11.5	10 29	+12 0	-10 -17	16 52	+18 0	-16 -34	22 78	+28 0	-22 -50
9.85	12.41	2.2 10.2	+5.0 0	-2.2 -5.2	4.5 17.5	+8.0 0	-4.5 -9.5	7 20	-8 0	-7 -12	12 32	+12 0	-12 -20	20 60	+20 0	-20 -40	28 88	+30 0	-28 -58
12.41	15.75	2.5 12.0	+6.0 0	-2.5 -6.0	5.0 20.0	+9.0 0	-5 -11	8 23	+9 0	-8 -14	14 37	+14 0	-14 -23	22 66	+22 0	-22 -44	30 100	+35 0	-30 -65

Figure 104: Clearance Limits for Cylindrical Parts

Appendix O: Sources

Areva Inc. . (2014). *Constellation Energy Nuclear Group Flood Hazard Reevaluation Report for R.E. Ginna Nuclear Power Plant.* Areva.

B.G. Reguero, I. L. (2015). A global wave power resource and its seasonal, interannual and long-term variability. *Applied Energy*, 366-380.

Dalton, G., Madden, D., & Daly , M. (2014, June 24). *Lifecycle Assessment of the Wavestar*. Retrieved from IEEE Xplore: https://ieeexplore.ieee.org/abstract/document/6844034?casa_token=UFsuqsGSsGgAAAAA:02htUu8oD0Wu9c2qH0eopYwU2QotJXry_kMVdd9jBC8o_ua2u69fuTEqjVfNvu5wCdPbaT0G0g

Dane M. Wiebe, H. P. (2014). Application of the Goda Pressure Formulae for Horizontal Wave Loads on Elevated Structures. *KSCE Journal of Civil Engineering*, 1-24.

EMEC. (n.d.). *Wave Devices*. Retrieved from The European Marine Energy Centre LTD: http://www.emec.org.uk/marine-energy/wave-devices/

Fenton, J. D. (2006). *A note on two approximations to the linear dispersion relation.* Kaiserstrasse 12, 76131 Karlsruhe, Germany: Institut für Hydromechanik, Universität Karlsruhe.

Hagerman, G. (2011). *Mapping and Assesment of the United States Ocean Wave Energy Resource.* Palo Alto: Electric Power Research Institute. Retrieved from https://www1.eere.energy.gov/water//pdfs/mappingandassessment.pdf

Hall, N. (2015, May 05). *NASA*. Retrieved from Shape Effects on Drag: https://www.grc.nasa.gov/WWW/k-12/airplane/shaped.html

Hansen, R. H., Kramer, M. M., & Vidal, E. (2013). Discrete Displacement Hydraulic Power Take-Off System for the Wavestar Wave Energy Converter. *Energies*, 6, 4001-4044.

Hirt, D. T. (n.d.). *CFD-101*. Retrieved from Flow-3D: https://www.flow3d.com/resources/cfd-101/

Historical NDBC Data. (2020). Retrieved from National Data Buoy Center: https://www.ndbc.noaa.gov/historical_data.shtml#swden

Islam, M., Jahra, F., & Hiscock, S. (2016). Data Analysis Methodologies for Hydrodynamic Experiments in Waves. *Journal of Naval Architecture and Marine Engineering*.

Kofoed, J. P. (2002). *Wave Overtopping of Marine Structures - Utilization of Wave Energy.* Hydraulics & Coastal Engineering Laboratory Department of Civil Engineering Aalborg.

Lacasa, M. C. (2019). Feasibility Study of the Installation of Wave Energy Converters in Existing Breakwaters in the North of Spain. *Applied Sciences*.

Le Méhauté, B. (1976). An Introduction to Hydrodynamics and Water Waves. *Springer-Verlag*.

Levitan, D. (2014, April 28). *Why Wave Power Has Lagged Far Behind as Energy Source*. Retrieved from Yale Environement 360: https://e360.yale.edu/features/why_wave_power_has_lagged_far_behind_as_energy_source

Liu, Z., Shi, H., Zhao, H., Wang, D., Lv, X., Li, Y., . . . Song, J. (2016). *United Kingdom Patent No. GB2536071A.*

NASA. (2021, February 9). *Gloabl Climate Change - Vital Signs of the Plant* . Retrieved from The Effects of Climate Change: https://climate.nasa.gov/effects/

National Data Buoy Center. (2018, June 5). *How are significant wave height, dominant period, average period,, and wave steepness calculated?* Retrieved from National Data Buoy Center: https://www.ndbc.noaa.gov/wavecalc.shtml

O'Connor, M., Lewis, T., & Dalton, G. (n.d.). Techno-economic performance of the Pelamis P1 and Wavestar at different ratings and various locations in Europe. *hydraulics and Maritime Resesarch Centre (HMRC)*.

Protocase. (2019). Retrieved from Profile Cutting Tolerances: https://www.protocase.com/resources/tolerances/profile-cutting.php

School of Civil Engineering, Purdue University. (n.d.). *Facilities & Equipment at the Christopher and Susan Burke H2O Laboratory* . Retrieved from Hydraulic and Hydrology Research and Teaching Laboratory: https://engineering.purdue.edu/CE/H2O/facilities

Shallow-water Wave Thoery. (n.d.). Retrieved 02 07, 2021, from Coastal Wiki: http://www.coastalwiki.org/wiki/Shallow-water_wave_theory

Stevens, L. (2017). *The Footprint of Energy: Land use of U.S. Electricity Production* . Strata.

Tesla. (n.d.). *Tesla*. Retrieved from Solar for Existing Roofs: https://www.tesla.com/solarpanels

U.S Energy Information Administration. (2019). *Total Energy*. Retrieved from Energy Infromation Administration: https://www.eia.gov/totalenergy/data/browser/?tbl=T07.03B#/?f=A

U.S. Energy Information Administration . (2020, July). *Energy and the environment explained*. Retrieved from Energy Information Administration: https://www.eia.gov/energyexplained/energy-and-the-environment/where-greenhouse-gases-come-from.php#:~:text=Nearly%20half%20of%20U.S.%20energy,21%25%20came%20from%20burning%20coal

U.S. Energy Information Administration. (2020, December). *Hydropower explained*. Retrieved from https://www.eia.gov/energyexplained/hydropower/wave-power.php#:~:text=Ocean%20waves%20contain%20tremendous%20energy,U.S.%20electricity%20generation%20in%202018.

U.S. Energy Information Administration. (2020, June 22). *Renewable energy explained*. Retrieved from Energy Information Administration: https://www.eia.gov/energyexplained/renewable-sources/

U.S. Energy Information Administration. (2021). *Cost and Performance Characteristics of New Generating Technologies, Annual Energy Outlook 2021*. U.S. Energy Information Administration.

USACE. (2006). *Coastal Engineering Manual, EM 1110-2-1100.*

Vicinanza, D. (2012). The SSG Wave Energy Converter: Performance, Status, and Recent Developments. *Energies*.

World Nuclear Association . (2011). *Comparison of Lifecycle Greenhouse GAs Emissions of Various Electricity Generation Sources.* London, U.K.: Carlton House.

Appendix P: Acknowledgments

Simulation result courtesy of Flow Science, Inc., developer of the computational fluid dynamics (CFD) software, ***FLOW-3D®*** (https://www.flow3d.com).